

Dissertation zur Erlangung des Doktorgrades  
der Fakultät für Chemie und Pharmazie  
der Ludwig-Maximilians-Universität München

**Investigation of the Impact of Tumor  
Suppressors and Promoters on Oncogenesis**

vorgelegt von  
Nina Seitzer  
aus  
Eggenfelden/Rottal Inn  
2009

## Erklärung

Diese Dissertation wurde im Sinne von § 13 Abs. 4 der Promotionsordnung vom 29. Januar 1998 von Herrn Prof. Axel Ullrich betreut und von Herrn Prof. Domdey vor der Fakultät für Chemie und Pharmazie vertreten.

## Ehrenwörtliche Versicherung

Diese Dissertation wurde selbständig, ohne unerlaubte Hilfe erarbeitet.

München, am 18.11.2009

.....

Nina Seitzer

Dissertation eingereicht am 18.11.2009

1. Gutachter Prof. Axel Ullrich
2. Gutachter Prof. Horst Domdey

Mündliche Prüfung am 22. Januar 2010

<b>1</b>	<b>INTRODUCTION</b>	<b>1</b>
<b>1.1</b>	<b>Tumor suppressors</b>	<b>1</b>
1.1.1	The Tumor Protein 53 (TP53)	1
1.1.2	The retinoblastoma gene product (Rb)	3
1.1.3	Impact of p53 and Rb in human cancer	4
<b>1.2</b>	<b>Cancer barriers and neoplastic transformation of cells</b>	<b>6</b>
1.2.1	Cancer barriers of cells: limited life span, senescence and immortalisation	6
1.2.2	Cell transformation	8
1.2.3	<i>In vitro</i> transformation systems	8
<b>1.3</b>	<b>Receptor Tyrosine Kinases</b>	<b>9</b>
1.3.1	Fibroblast Growth Factor Receptors	10
1.3.1.1	<i>Signalling of Fibroblast Growth Factor Receptors and their implication in pathophysiological phenotypes</i>	11
1.3.1.2	<i>The Impact of the Fibroblast Growth Factor 4 and its variant Arg388 on human cancer</i>	13
<b>1.4</b>	<b>Human breast cancer and modelling mammary carcinoma in vivo</b>	<b>15</b>
1.4.1	The impact of the FGFR4 and its Arg388 variant on breast cancer	16
1.4.2	The TGF $\alpha$ -EGFR signalling cascade and its impact on human breast cancer	17
1.4.3	The WAP-TGF $\alpha$ mouse mammary carcinoma model	19
1.4.4	The MMTV-PymT model	19
<b>1.5</b>	<b>Liver Metabolism and Cancer</b>	<b>20</b>
1.5.1	The impact of FGFR4 signalling on the hepatic bile acid synthesis, hyperlipidemia, insulin resistance and hypercholesterolemia	20
1.5.2	The impact of FGFR4 on hepatic carcinogenesis	22
<b>2</b>	<b>SPECIFIC AIMS</b>	<b>23</b>
<b>3</b>	<b>MATERIALS AND METHODS</b>	<b>24</b>
<b>3.1</b>	<b>Materials</b>	<b>24</b>
3.1.1	Laboratory Chemicals	24
3.1.2	Radiochemicals	25
3.1.3	Enzymes	25
3.1.4	“Kits“and Other Materials	25
3.1.5	Growth factors and ligands	26
<b>3.2</b>	<b>Media</b>	<b>26</b>
3.2.1	Bacterial media	26
3.2.2	Cell culture media	27
<b>3.3</b>	<b>Stock solutions and commonly used buffers</b>	<b>27</b>
<b>3.4</b>	<b>Cells</b>	<b>29</b>
3.4.1	Eukaryotic cell lines	29
3.4.2	E. coli strains	30

<b>3.5</b>	<b>Antibodies.....</b>	<b>30</b>
3.5.1	Primary Antibodies.....	30
3.5.2	Secondary Antibodies.....	32
<b>3.6</b>	<b>Plasmids and oligonucleotides.....</b>	<b>32</b>
3.6.1	Primary Vectors and Constructs.....	32
3.6.2	Oligonucleotides.....	32
<b>3.7</b>	<b>Methods of Molecular Cloning.....</b>	<b>35</b>
3.7.1	Plasmid preparation.....	35
3.7.2	Enzymatic manipulation of DNA.....	35
3.7.2.1	Specific digestion of DNA samples by restriction endonucleases.....	35
3.7.2.2	Dephosphorylation of 5'-termini with calf intestine alkaline phosphatase (CIAP).....	35
3.7.2.3	Ligation of vector and insert DNA.....	35
3.7.2.4	Agarose gel electrophoresis.....	35
3.7.2.5	Isolation of DNA fragments from agarose gels.....	35
3.7.3	Introduction of plasmid DNA into E.coli.....	35
3.7.3.1	Preparation of competent cells.....	35
3.7.3.2	Transformation of competent bacteria.....	36
3.7.4	Enzymatic amplification of DNA by polymerase chain reaction (PCR).....	36
3.7.5	DNA sequencing.....	36
<b>3.8</b>	<b>Methods of mammalian cell culture.....</b>	<b>36</b>
3.8.1	Calcium-Phosphate transfection.....	36
3.8.2	Transfection of plasmid DNA using lipofectamine®.....	37
3.8.3	Transfection of siRNAs using oligofectamine®.....	37
3.8.4	Infection of cells.....	37
3.8.5	Stimulation of cells.....	37
<b>3.9</b>	<b>Methods of Biochemistry and Cell Biology.....</b>	<b>37</b>
3.9.1	Lysis of cells with Triton X-100 lysis buffer.....	37
3.9.2	Lysis of cells with RIPA lysis buffer.....	37
3.9.3	Determination of total protein concentration in lysates.....	38
3.9.4	Immunoprecipitation.....	38
3.9.5	SDS-polyacrylamide-gel electrophoresis (SDS-PAGE).....	38
3.9.6	Transfer of proteins on nitrocellulose membranes.....	38
3.9.7	Immunoblot detection.....	38
3.9.8	RNA isolation and RT-PCR analysis.....	39
3.9.9	Southern Blot analysis.....	39
3.9.10	Proliferation assay.....	39
3.9.11	Migration assay.....	39
3.9.12	Anchorage independent growth.....	39
3.9.13	Focus formation assay.....	40
3.9.14	Karyotyping.....	40
3.9.15	Cell branching assay.....	40
3.9.16	Apoptosis assay and cell cycle analysis by propidium Iodide staining.....	40
3.9.17	Senescence assay.....	40
3.9.18	Indirect flow cytometry.....	40
3.9.19	Stable isotope labelling by amino acids <i>in vivo</i> and <i>in vitro</i> (SILAC) and mass spectrometry.....	41
<b>3.10</b>	<b>Methods of mouse genetics.....</b>	<b>41</b>
3.10.1	Mice and gene targeting.....	41

3.10.2	Genotyping and intercrosses to oncomice .....	41
3.10.3	Isolation of mouse embryonic fibroblasts (MEFs).....	42
3.10.4	Tumor analysis .....	42
3.10.5	Analysis of lung metastases .....	42
3.10.6	Immunohistochemistry on murine organs and tumor sections.....	42
3.10.7	Injection of nude mice .....	42
<b>4</b>	<b>RESULTS .....</b>	<b>43</b>
<b>4.1</b>	<b>Establishment of an in vitro transformation system.....</b>	<b>43</b>
4.1.1	Knockdown strategy of p53 and Rb; physiological output on proliferation and G2 Arrest upon p53 and Rb reduction in non-cancerous human primary cells .....	43
4.1.2	Reduction of p53 and Rb in primary normal human dermal fibroblasts (NHDF) ...	46
4.1.2.1	Increased proliferation, morphological changes and decreased senescence in NHDF cells deficient for p53 and Rb .....	46
4.1.2.2	Reduction of contact inhibition, anchorage independence and invasion in NHDF deficient for p53 and Rb .....	51
4.1.2.3	NHDFdk cells display karyotypic abnormalities and tolerate extended telomere shortening .....	55
4.1.2.4	NHDFdk cells do not establish a stem cell-like cancer cell subpopulation.....	59
4.1.2.5	The malignancy of NHDF cells deficient for p53 and Rb is not potent enough to induce tumor growth in nude mice .....	60
<b>4.2</b>	<b>The impact of the FGFR4 and its variant Arg385 on tumor progression.....</b>	<b>62</b>
4.2.1	Characterisation of the <i>FGFR4 Arg385 KI</i> mouse .....	64
4.2.2	The impact of the FGFR4 and its variant Arg385 <i>in vitro</i> .....	67
4.2.2.1	The impact of the FGFR4 Arg385 on fibroblast transformation.....	67
4.2.2.2	Impact of FGFR4 Arg385 on proliferation, life span, migration and apoptosis of MEFs .....	69
4.2.2.3	Impact of FGFR4 Arg385 on proliferation, migration, invasion and apoptosis in transformed MEFs .....	74
4.2.3	The impact of the FGFR4 and its variant Arg385 on tumor progression <i>in vivo</i> .....	83
4.2.3.1	The <i>FGFR4 Arg385</i> allele promotes tumor mass and size of <i>WAP-TGF<math>\alpha</math></i> but not <i>MMTV -PymT</i> derived tumors .....	83
4.2.3.2	The impact of FGFR4 Arg385 on tumor mass and size of <i>WAP-TGF<math>\alpha</math></i> derived tumors over time .....	89
4.2.3.3	Molecular characterisation of <i>WAP-TGF<math>\alpha</math></i> derived tumors with different <i>FGFR4</i> genotypes .....	92
4.2.3.4	The impact of the <i>FGFR4 Arg385</i> allele on lung metastasis of <i>WAP-TGF<math>\alpha</math></i> derived tumors .....	97
<b>4.3</b>	<b>Investigation of new FGFR4 interaction partners .....</b>	<b>100</b>
4.3.1	Investigation of new FGFR4 binding partners in MDA-MB-231 cells .....	100
4.3.2	Validation of the EGFR/FGFR4 interaction .....	102
4.3.3	The FGFR4 Arg385 influences the migratory behavior and the sensitivity towards Gefitinib in MDA-MB-231 cells.....	107
4.3.4	Investigation of new interaction partners of the hepatic FGFR4 <i>in vivo</i> .....	111
4.3.5	Quantitative analysis of hepatic FGFR4 binding partners and their differences regarding the <i>FGFR4</i> isotypes .....	111
<b>5</b>	<b>DISCUSSION .....</b>	<b>117</b>
<b>5.1</b>	<b>Loss of p53 and Rb in human primary cells as a model of oncogenesis in vitro</b>	<b>117</b>

Contents

<b>5.2</b>	<b>FGFR4 Arg385 promotes MEF transformation in vitro and accelerates tumor growth and metastasis in the WAP-TGF<math>\alpha</math> mouse mammary tumor model .....</b>	<b>123</b>
<b>5.3</b>	<b>Investigation of new FGFR4 binding partners in vitro and in vivo .....</b>	<b>130</b>
<b>6</b>	<b>SUMMARY .....</b>	<b>139</b>
<b>7</b>	<b>ZUSAMMENFASSUNG.....</b>	<b>141</b>
<b>8</b>	<b>APPENDIX.....</b>	<b>143</b>
<b>8.1</b>	<b>Abbreviations.....</b>	<b>143</b>
<b>8.2</b>	<b>Acknowledgements.....</b>	<b>147</b>
<b>9</b>	<b>REFERENCES .....</b>	<b>148</b>

## 1 Introduction

Cancer is the leading cause of death world wide where it accounts of approximately 13 % of all deaths. Amongst others lung, stomach, liver, colorectal and breast cancer cause the most cancer deaths world wide. Next to biological carcinogens like infectious agents, physical and chemical carcinogens are potent effectors of cellular transformation. Although most of these carcinogens like tobacco smoke could be avoided and education towards prevention of cancer increases yearly, 30% of all cancer death still occurs because of environmental factors and lifestyle influence. Therefore, the scientific understanding of the development of this disease is the most important basis in fighting cancer.

### 1.1 Tumor suppressors

Tumor suppressors either have a dampening or repressive effect on the regulation of the cell cycle or promote apoptosis, and sometimes do both. The functions of tumor suppressor proteins fall into several categories including the following (Sherr, 2004):

1. **Repression of genes that are essential for cell cycle progression.** If these genes are not expressed, the cell cycle will not continue, effectively inhibiting cell division.
2. **Maintenance of genomic integrity.** As long as there is damaged DNA in the cell, it should not divide. If the damage can be repaired, the cell cycle can continue.
3. **Initiation of cell death.** If the damage *cannot* be repaired, the cell should initiate apoptosis (programmed cell death) to remove the threat it poses for the greater good of the organism.
4. **Repression of metastasis.** Some proteins involved in cell adhesion prevent tumor cells from dispersing, block loss of contact inhibition, and inhibit metastasis. These proteins are known as metastasis suppressors (Hirohashi and Kanai, 2003; Yoshida et al., 2000).

#### 1.1.1 The Tumor Protein 53 (TP53)

The p53 gene, first described in 1979, was the first tumor-suppressor gene to be identified. The heterozygous loss of p53 in humans causes the Li-Fraumeni syndrome with an early onset of cancers in diverse tissues. Similarly, the ablation of p53 in mice results in tumors of various tissues. P53 is primarily activated under conditions of cellular stress or DNA damage. Here, the activation of the network is dependent on the ATM kinase (for ataxia telangiectasia

## Introduction

mutated), which is stimulated by the DNA strand breaks and Chk2, which is in turn stimulated by ATM (Carr, 2000).

Another route of p53 activation is triggered by aberrant growth signals, such as those resulting from the expression of oncogenes like Ras or Myc. In this case, activation of the p53 network in humans depends on the cell cycle inhibitor p14<sup>ARF</sup> (Lowe and Lin, 2000; Sherr and Weber, 2000). The last known p53 pathway is induced by a wide range of chemotherapeutic drugs, ultraviolet light, and protein-kinase inhibitors and is not dependent on intact ATM, Chk2 or p14<sup>ARF</sup>, and may instead involve kinases called ATR (ataxia telangiectasia related) and casein kinase (Meek, 1999). However, phosphorylated and thereby activated by these proteins, p53 can be released from its negative regulator MDM2, which binds p53 and marks it for ubiquitination. Activated p53 can then act as a transcription factor of a multitude of genes involved in cell cycle arrest/senescence, apoptosis and prevention of blood vessel formation as seen in Figure 1.

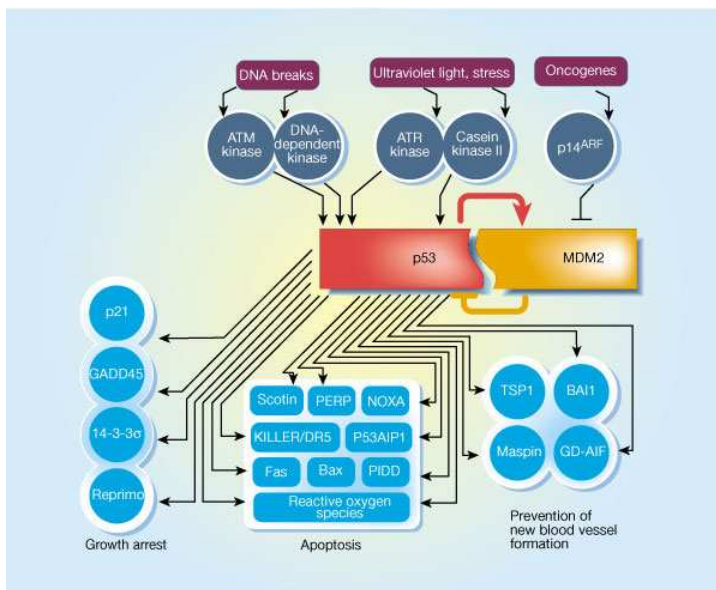


**Figure 1: Network of p53; p53 gets activated via ATM, ATR or p14 in response to DNA-damage, cellular stress or oncogenes; released from its negative regulator MDM2 that marks p53 for degradation, p53 activates the expression of its target genes to induce growth arrest, apoptosis or the prevention of new blood vessel formation (Vogelstein et al., 2000).**

All aforementioned processes shut down the multiplication of stressed cells, inhibiting progress through the cell cycle or cause apoptosis to defend the organism for a greater risk, that these cells become cancerous.

### 1.1.2 The retinoblastoma gene product (Rb)

The retinoblastoma gene product (Rb) was the first tumor suppressor identified to be significantly lost in human cancer. This loss of heterozygosity in humans causes retinoblastoma (Friend et al., 1986). In the mouse, the germline knockout of Rb results in embryonic lethality at mid-gestation (Maandag et al., 1994). However, its primary function is to prevent the unscheduled entry into the mitotic cell cycle (Classon and Harlow, 2002; Cobrinik, 2005; Liu et al., 2004). In the absence of mitogens, Rb inhibits cell-cycle progression by preventing the transcription of multiple genes required for S-phase-entry (Blais and Dynlacht, 2004; Blais and Dynlacht, 2007; Diehl, 2002; Nevins, 2001; Sherr, 2000; Wang et al., 1994). The best studied targets are regulated through the E2F transcription factor family, the main target of Rb. Unbiased gene expression analyses revealed, that the Rb-E2F pathway regulates and controls approximately 150-200 genes (Figure 2) (Knudsen and Knudsen, 2008).

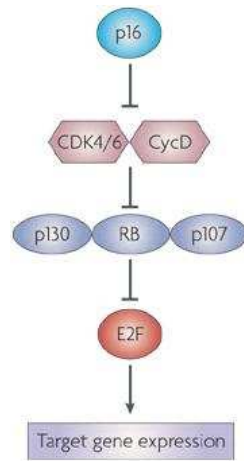


**Figure 2: Simplified scheme of Rb regulation; in cell cycle progression Rb gets inactivated via phosphorylation by CDK4/6; if the cell cycle is blocked by p16, Rb gets dephosphorylated and thereby activated to bind E2F. This binding inhibits E2F to activate the expression of its target genes to stimulate S-phase entry (Burkhart and Sage, 2008).**

For the cell cycle to progress, mitogens must counteract the action of Rb by activating cyclin-dependent kinases, which attenuate the capacity of Rb to induce transcriptional repression by phosphorylation of Rb (Mittnacht, 1998). Through the cell cycle, Rb remains in this inactive stage, until passage through mitosis, at which point it is re-engaged through phosphatases (Vietri et al., 2006).

Next to its main role in arresting cells in G1/S by inhibiting the transcription factor E2F (Riley et al., 1994; Weinberg, 1995), Rb is also associated in various other physiological processes

## Introduction

like differentiation, regulation of cell death, maintenance of permanent cell cycle arrest (senescence) and preservation of genomic stability (Figure 3) (Dannenberg and te Riele, 2006; Zheng and Lee, 2001).

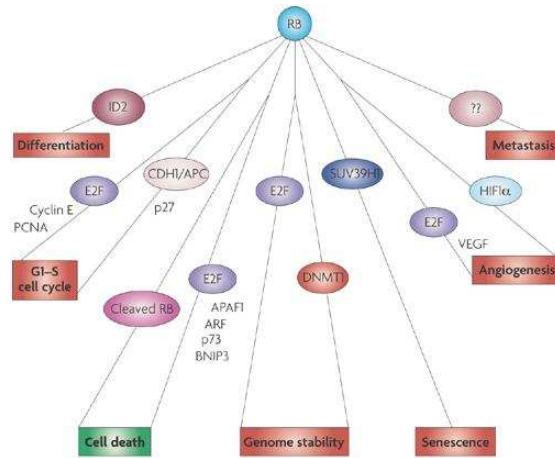


**Figure 3: Model of physiological processes that are regulated by Rb; Rb is not only involved in cell cycle arrest, senescence or apoptosis, but also regulates differentiation, the integrity of the genome, angiogenesis and metastasis (Burkhardt and Sage, 2008).**

### 1.1.3 Impact of p53 and Rb in human cancer

It is well accepted that tumor cells invoke multiple mechanisms to bypass proliferative control. As crucial regulators of the cell cycle, p53 and Rb confer a proliferative advantage to tumor cells via their perturbations.

Due to its frequent high expression in cancer the tumor suppressor p53 was originally believed to be an oncogene, but genetic and functional data obtained ten years after its discovery showed it to be a tumor suppressor. Moreover, it was found that the p53 protein does not function correctly in most human cancers (Table 1). In about half of these tumors, p53 is inactivated directly as a result of mutations in the p53 gene. In many others, it is inactivated indirectly through binding to viral proteins, or as a result of alterations in genes whose products interact with p53 or transmit information to or from p53. However, since 1989, 10.000 tumor associated -mutations were discovered, highlighting the impact and the importance of p53 inactivation in human cancers (Hollstein et al., 1999; Hussain and Harris, 1999). The importance of p53 in the inhibition of cellular transformation is pointed out in p53-restoration experiments in mice. Here, highly aggressive hepatocarcinoma, lymphoma and osteosarcoma start to regress if p53 is re-expressed (Xue et al., 2007)

Mechanism of inactivating p53	Typical tumours	Effect of inactivation
Amino-acid-changing mutation in the DNA-binding domain	Colon, breast, lung, bladder, brain, pancreas, stomach, oesophagus and many others	Prevents p53 from binding to specific DNA sequences and activating the adjacent genes
Deletion of the carboxy-terminal domain	Occasional tumours at many different sites	Prevents the formation of tetramers of p53
Multiplication of the MDM2 gene in the genome	Sarcomas, brain	Extra MDM2 stimulates the degradation of p53
Viral infection	Cervix, liver, lymphomas	Products of viral oncogenes bind to and inactivate p53 in the cell, in some cases stimulating p53 degradation
Deletion of the p14 <sup>ARF</sup> gene	Breast, brain, lung and others, especially when p53 itself is not mutated	Failure to inhibit MDM2 and keep p53 degradation under control
Mislocalization of p53 to the cytoplasm, outside the nucleus	Breast, neuroblastomas	Lack of p53 function (p53 functions only in the nucleus)

**Table 1: Status of the tumor suppressor p53 in various human cancers; next to genomic loss, p53 mostly gets inactivated via mutations or fractional deletions in human cancers. Furthermore, the deregulation of its negative regulator MDM2, viral infections or deletions of p53 target genes are found to dysregulate the p53-network. In breast or neuroblastomas p53 often gets mislocated to the cytoplasm and thereby lacks its function (Vogelstein et al., 2000).**

In the case of the retinoblastoma gene product several observations support the significant role of Rb –mediated cell cycle control and moreover the loss in human tumors. First, loss of heterozygosity of Rb results e.g. in tumor formation in the retina (retinoblastoma) (Cavenee et al., 1983). Second, mutations that are either inactivating or facilitate the phosphorylation of Rb are observed at high frequency like in small-cell lung cancer (Kaye, 2002) or moderate like in breast, bladder or prostate cancer (Diehl, 2002; Malumbres and Barbacid, 2001; Palmero and Peters, 1996; Sherr, 2000; Sherr and McCormick, 2002). Third, the inactivation of Rb is mediated by and cooperates with oncogenes that contribute to human cancers like HPV-E7 oncoprotein, that is involved in the aetiology of cervical cancer (Table 2) (Dyson et al., 1989; Munger, 2002; Munger et al., 2001).

Tumour type	Frequency of RB inactivation (genetic or epigenetic)	Presumed consequence of RB inactivation
Lung cancer	Germline RB mutations predispose to small cell lung carcinoma (SCLC), and RB is inactivated in >90% of sporadic SCLC cases. In contrast, RB is mutated in only 15–30% of non-SCLC cases.	SCLC initiation; progression to invasive forms of non-SCLC
Melanoma	RB inactivation is rare in sporadic cases, but inherited mutation predisposes to melanoma	Initiating event in familial cases
Prostate cancer	~20%	Progression to invasive carcinoma <sup>†</sup>
Breast cancer	~20%	Progression
Bladder cancer	20–50%	Progression to invasive tumours
Leukaemia	Reduced levels of expression are frequent, but mutations in RB are rare in leukaemias, except in 20% of chronic myeloid leukaemia (CML) cases	Progression (CML blast crisis)
Brain cancer	Rb-mutant mice develop pituitary tumours, but RB mutations are rare in human cases. 15–30% of advanced gliomas have RB mutations	Progression
Oesophageal cancer	RB deletion are found in 15–50% of adenocarcinomas or squamous cell carcinomas	Early progression
Liver cancer	Mutations in RB are found in 15–30% of the advanced hepatocellular carcinomas <sup>§</sup>	Progression

**Table 2: Inactivation of the RB gene in common human cancer types; Rb gets inactivated through genetic or epigenetic mechanism and its functional loss is a frequent event in human cancers. Via its inactivation cancers are either initiated or progressed early or to an invasive state (Burkhart and Sage, 2008).**

## 1.2 Cancer barriers and neoplastic transformation of cells

In organisms every cell is embedded and organized in its characteristic tissue with its specific duties. To maintain this organisation of an organism, cells are strictly confined in their cell-cell-interaction ability and behaviour. These restrictions are barriers to cancer and cells must overcome these barriers to escape the organized tissue and convert to a neoplastically transformed cell.

### 1.2.1 Cancer barriers of cells: limited life span, senescence and immortalisation

Primary cells display a restricted life span *in vitro*. These cells enter permanent growth arrest after a defined number of cell divisions, called replicative senescence (Harada et al., 2003; Hayflick, 1965). Senescent cells can be detected via different markers like the expression of  $\beta$ -galactosidase (Dimri et al., 1995), p16 and p21 or the activated of CHK1 and 2 (d'Adda di Fagagna et al., 2003; Suzuki et al., 2001). This permanent growth arrest is caused by different intrinsic or extrinsic stresses (Figure 4)(Priour and Peeper, 2008).

Formatiert: Englisch (USA)

Feldfunktion geändert

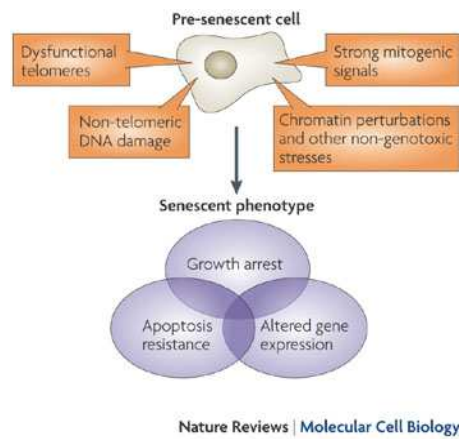


**Figure 4: Senescence in cultured cells; senescence can be triggered by different mechanisms including dysfunctional telomeres, DNA-damage, mitogenic signals or other stresses (Campisi and d'Adda di Fagagna, 2007).**

One of these stresses is the progressive shortening of telomeres. With each cell division telomeres are reduced by about 50-150 base pairs (bp) (Collado et al., 2007; Shay and Wright, 2000). The achievement of a critical telomere length triggers a DNA-damage response which most of the times moves the cells into irreversible growth arrest (d'Adda di Fagagna et al., 2003). This replicative senescence is finally driven by the activation of p53 and Rb (Campisi, 2005). If these gatekeepers of tumor suppression are inactivated, loss of telomere function contributes to oncogenic transformation (Chin et al., 1999).

Next to telomere-associated senescence, permanent growth arrest can be elicited by activation of oncogenes, a phenomenon that was firstly described in 1997 (Serrano et al., 1997). Here, the overexpression of the mutant H-Ras<sup>v12</sup> induces cellular senescence in human and rodent cells. Activated mutants of RAF, MEK and BRAF were also shown to induce cell cycle arrest (Lin et al., 1998; Michaloglou et al., 2005; Zhu et al., 1998). These oncogenes trigger senescence by induction of a DNA-damage response, which contributes to cell cycle arrest (Bartkova et al., 2006; Di Micco et al., 2006).

This permanent growth arrest is suggested as a tumor-suppressive mechanism and one of the main barriers to tumorigenesis (Reddel, 2000; Wright and Shay, 2001).

The first step to a malignant phenotype of cells is the ability to bypass this senescence, a process called immortalisation where cells acquire an indefinite life span. As telomeres act as a “molecular clock” of the cellular life span, immortalized cells have to stabilize their telomeres to escape the definite growth capacity. Therefore pre-cancerous cells have to reactivate the expression of telomerase or maintain them through alternative telomere lengthening (ATL) (Counter et al., 1992; Kim et al., 1994). Further processes that contribute to immortalisation

are DNA-damage, inactivation of cell cycle regulatory genes like p53 and Rb, epigenetic gene silencing or the overexpression of oncogenic or viral proteins (Figure 5) (Berube et al., 1998; Bringold and Serrano, 2000; Itahana et al., 2003; Lundberg et al., 2000; Neumeister et al., 2002).

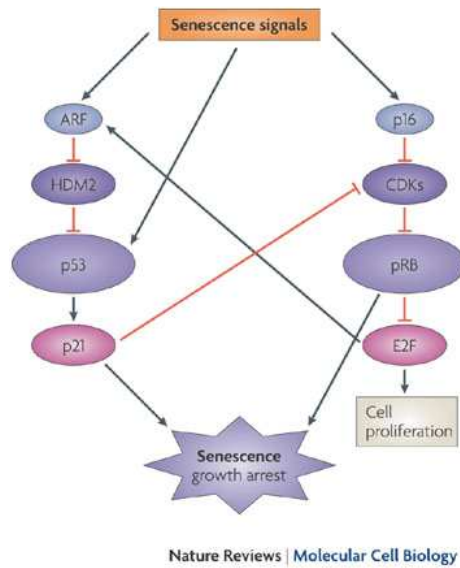


**Figure 5: Implication of p53 and Rb in cellular senescence; as the cell triggers senescence signals, p53 gets released from HDM2 and induces senescence via p21; Rb governs the cell into permanent growth arrest through the permanent inhibition of E2F (Campisi and d'Adda di Fagagna, 2007).**

### 1.2.2 Cell transformation

The basis of neoplastic cell transformation is the accumulation of genetic and epigenetic changes (Hanahan and Weinberg, 2000). These changes mainly apply to genes involved in the regulation of the cell cycle and proliferation such as proto-oncogenes and tumor suppressors. Large scale sequencing, transcriptional profiling and gene expression analysis have implicated thousands of genetic modifications to be involved in neoplastic transformation of human cells (Baylin and Bestor, 2002; Golub et al., 1999; Perou et al., 2000).

### 1.2.3 *In vitro* transformation systems

Although studies on alterations in human cancer deliver a never ending number of genetic changes or combinations of alterations that are involved in distinct steps of neoplastic transformation, experimental models of *in vitro* transformation indicate, that just a few disruptions or amplifications of pathways seem to be sufficient to steer cells into a cancerous phenotype. In the early eighties the malignant transformation of bird and rodent cells via either viral or human oncogenes were the first described models of oncogenesis of primary

cells (Land et al., 1983; Ruley, 1983). In human cells the introduction of viral oncoproteins like the papilloma simian virus 40 (SV 40) large T antigen (LT) or the human papilloma virus (HPV) E6 or E7 fail to induce immortalisation in cells although they extend their cellular lifespan via inhibitory binding to p53 or Rb and thereby perturbing their signalling pathways. Only the introduction of both tumor suppressors allows pre-senescent cells to overcome the permanent growth arrest. By a successful reactivation of telomerase or alternative mechanisms (ALT) to maintain stable telomere length, immortalisation and thereby the prerequisite of malignant transformation can be achieved. Further models develop immortalisation chemically, or with biological agents. Here, cells can be immortalized by addition of mutagens like aflatoxin B (Bond et al., 1999; Opitz et al., 2001; Shay et al., 1991). So far, some defined manipulations are necessary to completely transform cells. In normal human fibroblast the induction of the SV40 early region, expression of hTERT and oncogenic RAS cooperate to induce a malignant phenotype (Hahn et al., 2002; Yu et al., 2001). These genes are further sufficient to transform a wide range of primary cells like epithelial cells of the breast or lung, mesothelial cells, melanocytes and neuroectodermal cells (Elenbaas et al., 2001; Liu et al., 2004; Lundberg et al., 2002; Rich et al., 2001). Other combinations of introduced genes have shown to be successful without expression of hTERT. In keratinocytes, the coexpression of CDK4 and RAS appears to be sufficient for transformation. In fibroblasts the introduction of the adenoviral E1A oncoprotein, RAS and MDM2 transformed the cells without telomerase expression (Brookes et al., 2002; Seger et al., 2002). However, with few exceptions so far, the transformation of human cells requires the introduction of viral oncoproteins and thereby does not fully reflect the situation of malignant cell transformation *in vivo*.

### ***1.3 Receptor Tyrosine Kinases***

Protein tyrosine kinases are important regulators of intracellular signal transduction pathways mediating aspects of multicellular communication and development (Ullrich and Schlessinger, 1990). Tyrosine kinases play an important role in the control of most fundamental cellular processes including cell cycle, migration, metabolism and survival, as well as proliferation and differentiation. There are currently more than 90 known tyrosine kinase genes in the human genome; 58 encode transmembrane receptor tyrosine kinases (RTKs). The epidermal growth factor receptor (EGFR) was the first RTK to be cloned and characterized by Ullrich and colleagues in 1984 (Ullrich et al., 1984). Since then, RTKs have been distributed into 20 subfamilies based on their structural characteristics. RTKs are type I transmembrane proteins

and contain an extracellular ligand-binding domain that is usually glycosylated (Hubbard and Till, 2000). The structural diversity of RTK ectodomains is due to the presence of one or several copies of immunoglobulin-like domains, fibronectin type III-like domains, EGF-like domains, cysteine-rich domains, or other domains. The ligand binding domain is connected to the cytoplasmic domain by a single transmembrane helix. The cytoplasmic domain contains a highly conserved protein tyrosine kinase core and additional regulatory sequences that are subjected to autophosphorylation and phosphorylation by heterologous protein kinases (Blume-Jensen and Hunter, 2001).

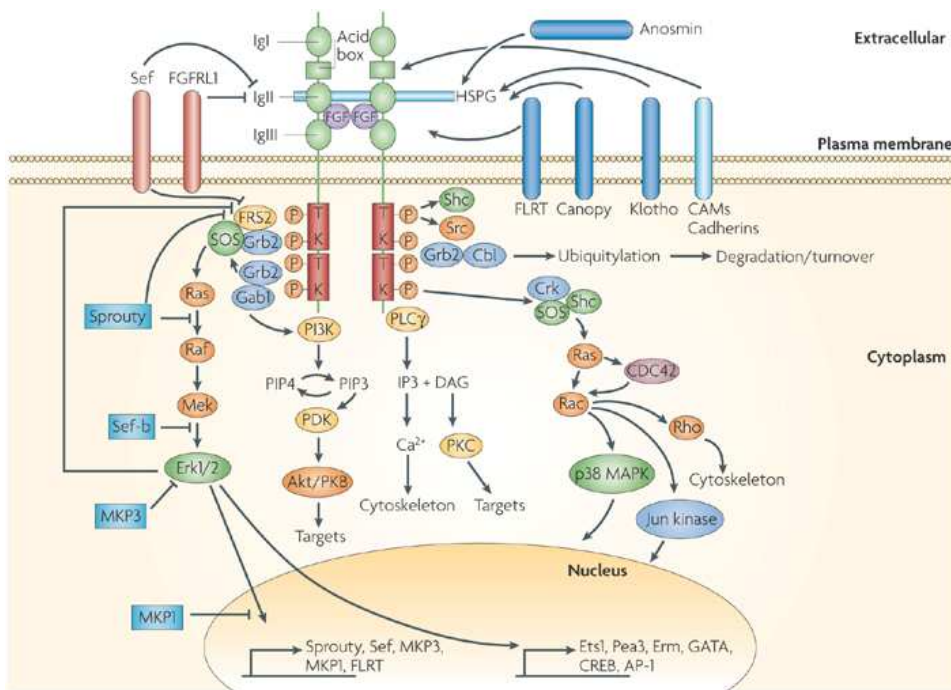
Beginning with the discovery that the EGFR and the oncogene *v-erbB* are directly related, RTKs were found to be frequently implicated in cancer development and progression by different mechanisms including activating mutations, gene fusions, overexpression or gene amplification (Ullrich et al., 1984). RTKs may also serve as excellent prognostic factors or targets of cancer therapy. The first and most prominent example for a RTK as an anticancer-target is the human epidermal growth factor receptor 2 (HER2). In 1985, the HER2 EGFR-like receptor gene was identified and its amplification in breast cancer was correlated with relapse and survival of breast cancer patients (Coussens et al., 1985; Slamon et al., 1987). Herceptin, the humanized monoclonal antibody that targets HER2 at the cell surface, is the first genomic-research based anti-cancer therapeutic. Herceptin is approved by the FDA for the treatment of locally advanced and metastatic breast cancer since 1998 (Fischer et al., 2003).

### **1.3.1 Fibroblast Growth Factor Receptors**

The fibroblast growth factor receptor (FGFR) family is composed of four receptors (FGFR1-4) and more than 20 known ligands and has been implicated in the regulation of various physiological processes including angiogenesis, mitogenesis, differentiation and development (Burke et al., 1998; Jeffers et al., 2002). FGFRs consist of an extracellular ligand-binding domain, a single transmembrane domain and a cytoplasmic domain containing the catalytic protein tyrosine kinase core as well as additional regulatory sequences (Hunter, 2000; Schlessinger, 2000). The extracellular ligand-binding domain of FGFRs is composed of three immunoglobulin like domains, designated D1-D3; a stretch of seven to eight acidic residues in the linker connecting D1 and D2, designated the “acid box” and a conserved positively charged region in D2 that serves as a binding site for heparin (Eswarakumar et al., 2005; Schlessinger et al., 2000).

**1.3.1.1 Signalling of Fibroblast Growth Factor Receptors and their implication in pathophysiological phenotypes**

Signalling via FGFRs is mediated via recruitment of several docking proteins after stimulation through FGFs. These docking-proteins, called FRS2 $\alpha$  and FRS2 $\beta$  bind to the auto-phosphorylation sites of the activated receptor (Dhalluin et al., 2000; Ong et al., 2000). Following recruitment of Grb-2 and Sos results in the activation of the Ras/MAP kinase signalling pathway (Kouhara et al., 1997). If Grb-2 recruits Gab-1, FGF stimulation results in the activation of the PI3-kinase leading to Akt dependent anti-apoptosis. Moreover, stimulation of FGFRs results in the expression of target genes that either trigger further cellular signals or result in a negative feedback loop of the respective FGFR (Figure 6).



Nature Reviews | Neuroscience

**Figure 6: Signalling pathways of FGF Receptors; FGFRs get stimulated and thereby phosphorylated via binding of their cognate ligands. Upon autophosphorylation FRS2 proteins are able to bind FGFRs in order to build signalling platforms that stimulate either the Erk1/2 or the Akt pathway resulting in the expression of target genes that trigger a physiological output or activate negative feedback loops of FGFR signalling (Mason, 2007).**

FGFs and FGFRs are implicated in a variety of cellular processes with diverse pathophysiological phenotypes as a result of the loss of function of either FGFs or FGFRs. Table 3 and 4 display the functions of different FGFs and FGFRs investigated in knock-out

## Introduction

mice. Here, the disruption of either FGFs or FGFRs results in diverse phenotypes ranging from developmental disorders, which cause embryonic lethality to no obvious phenotypes.

Gene	Survival	Phenotype
FGF1	Viable	No obvious phenotype
FGF2	Viable	Neuronal, skeletal and skin phenotypes
FGF3	Viable	Inner ear, tail outgrowth
FGF4	Lethal E5.5	Inner cell mass proliferation
FGF5	Viable	Long hair, "Angora" phenotype
FGF6	Viable	Muscle regeneration
FGF7	Viable	Hair follicle and kidney deficiency
FGF8	Lethal E8.5	Many phenotypes including gastrulation, brain, heart and craniofacial development
FGF9	Lethal Po	Lung, xy sex reversal
FGF10	Lethal Po	Many phenotypes including limbs, lungs, kidneys and others
FGF14	Viable	Neurological phenotype-ataxia and a paroxysmal hyperkinetic movement disorder
FGF15	Viable	No defect in inner ear development; poor survival rate
FGF17	Viable	Midline cerebral development
FGF18	Lethal P1	Delayed ossification and increased chondrocyte proliferation; decreased alveolar spaces in the lung
FGF23	Viable	Hyperphosphatemia, hypoglycemia, reduced bone density and infertility

**Table 3: Summary of phenotypes obtained from FGF knock-out mice; Phenotypes vary from developmental to regenerative to metabolic syndromes implicating the FGFs in variety of cellular processes (Eswarakumar et al., 2005).**

Receptor/isoform	Survival	Phenotype
<i>Fgfr1</i>	Lethal, E9.5-E12.5	Defective cell migration through primitive streak; posterior axis defect
<i>Fgfr1b</i>	Viable	No obvious phenotype
<i>Fgfr1c</i>	Lethal, E9.5	Defective cell migration through primitive streak; posterior axis defect
<i>Fgfr2</i>	Lethal, E10.5	Defect in placenta and limb bud formation
<i>Fgfr2b</i>	Lethal, P0	Agnesis of lungs, anterior pituitary, thyroid, teeth and limbs
<i>Fgfr2c</i>	Viable	Delayed ossification, proportionate dwarfism, synostosis of skull base (chondrocranium)
<i>Fgfr3</i>	Viable	Bone over growth; inner ear defect
<i>Fgfr4</i>	Viable	No obvious phenotype; growth retardation and lung defects in FGFR3 null background

**Table 4: Summary of phenotypes obtained from FGFR knock-out mice; Phenotypes vary from developmental to regenerative syndromes implicating the FGFRs in variety of cellular processes (Eswarakumar et al., 2005)**

In humans, the FGFR family is known to play a key role in skeletal development. Especially activating FGFR gene mutations are implicated in several skeletal disorders. Amongst others, an amino acid substitution from Tyrosine to Cystein mostly results in a hyperactivated receptor. This amino acid substitution is present in the FGFR2 (Y375C) and the FGFR3 (Y373C) and results in the Beare-Stevenson syndrome. Osteoglophomic dysplasia is linked to an Y372C mutation in the FGFR1. Furthermore, several other mutations in the FGFR1 and FGFR2 gene are linked to the Crouzon, Pfeiffer and Apert syndrome that all cause craniosynostosis. Dwarfing syndromes such as achondroplastic and hypochondroplastic dwarfism are associated with mutations in the FGFR3 gene. Table 5 summarizes the most frequent mutations in the FGFR 1-3 and the according syndromes (White et al., 2005; Wilkie et al., 2002).

Gene	AA-Substitution	Syndrome	Ref
FGFR 1	Y372C N330I	Osteoglophonic dysplasia	(White et al., 2005)
	P252R	Pfeiffer	(Roscioli et al., 2000)
FGFR 2	Y375C	Beare-Stevenson	(Krepelova et al., 1998)
	N331I S252W P253R	Crouzon	(Rutland et al., 1995)
	S252W P253R	Apert	(Cohen and Kreiborg, 1995)
	C342R W290C S351C	Pfeiffer	(Wilkie et al., 2002)
FGFR 3	Y373C	Beare-Stevenson	(White et al., 2005)
	P250R	Muenke	(White et al., 2005)
	P250R	Saethre-Chotzen	(White et al., 2005)
	N328I	Crouzon	(White et al., 2005)
	G380R	Achondroplastic dwarfism	(White et al., 2005)
	C1620A	Hypochondroplastic dwarfism	(Ramaswami et al., 1998)
	K650M	SADDAN	(Bellus et al., 1999)

**Table 5: Summary of FGFR 1-3 gene mutations and the according phenotypes: FGFR1-3 are implicated in several skeletal disorders via gene mutations that result in amino acid substitutions. According phenotypes include the Peiffer, Apert or Crouzon syndrome.**

### ***1.3.1.2 The Impact of the Fibroblast Growth Factor 4 and its variant Arg388 on human cancer***

In human cancer, the FGFRs are implicated either by overexpression like, pancreatic- or prostate carcinoma (Eswarakumar et al., 2005; Gowardhan et al., 2005; Morrison et al., 1994), or by activating mutations leading to abnormal fusion proteins or nucleotide substitutions (Cappellen et al., 1999; Fioretos et al., 2001; Jang et al., 2001; Macdonald et al., 1995) .

## Introduction

The human *FGFR4* is known to be involved in the progression of diverse cancers. In hepatocellular carcinoma (HCC), *FGFR4* promotes tumor growth by regulation cell proliferation and anti-apoptosis, suggesting that the *FGFR4* may represent a potential target for HCC therapy development (Ho et al., 2009). Ablation of *FGFR4* and the inhibition of FGF19, the specific ligand of *FGFR4*, in human colon cancer or liver cancer cell lines resulted in a reduced colony formation and tumor growth in nude mice by negatively affecting the  $\beta$ -catenin signalling pathway (Desnoyers et al., 2008; Pai et al., 2008; Xie et al., 1999). In pituitary tumors, the *FGFR4* promotes tumor progression as mutated truncated receptor. Here, the inactivation of the *FGFR4* with an inhibitor reduces the tumor volume with an additional less invasive behaviour in nude mice (Ezzat et al., 2006). In addition, in prostate and medullary thyroid cancer the *FGFR4* seems to promote tumor growth by its overexpression and is thought to be a valid target for prostate cancer therapy (Ezzat et al., 2005; Gowardhan et al., 2005; Shah et al., 2002).

Beside somatic mutations, it has become increasingly clear, that germline alterations like single nucleotide polymorphisms (SNP) have clinical significance for the development and progression of diseases like cancer as well as for the definition of a patients individual response to therapeutic agents (Ameyaw et al., 2002; Morimoto et al., 2003; Przybylowska et al., 2001).

In the human *FGFR4* gene a polymorphic nucleotide change in codon 388 converts Glycine (Gly) to Arginine (Arg) in the transmembrane region of the receptor, a hot spot in receptor tyrosine kinases (RTKs) for disease-relevant sequence variations (Bange et al., 2002). This single nucleotide substitution in the *FGFR4* was shown to be implicated in progression and poor prognosis of various types of human cancer (Bange et al., 2002; Spinola et al., 2005; Stadler et al., 2006; Streit et al., 2004; Streit et al., 2006; Wang et al., 2004). Here, Bange and colleagues could associate the *FGFR4 Arg388* allele with tumor progression in breast and colon cancer patients (Bange et al., 2002). Similarly, soft tissue sarcoma patients, who carried the *FGFR4 Arg388* allele had a poor clinical outcome (Morimoto et al., 2003). In melanoma the *Arg388* allele is associated with increased tumor thickness, while in head and neck squamous cell carcinoma the *FGFR4Arg388* allele correlates with reduced overall patient survival and advanced tumor stage. Furthermore, a recent study on prostate cancer patients strongly associated the *FGFR4 Arg388* allele not only with tumor progression but also with prostate cancer initiation.

## Introduction

The main conclusion of these studies was that the presence of one or two *Arg388* alleles in the genome of an individual does not initiate cancer development but predisposes the carrier to a more aggressive form if she or he is affected by the disease.

Furthermore, some studies focused on the molecular mechanism of *FGFR4 Arg388* allele. Studies on prostate cancer e.g. implicate the *Arg388* allele in *FGFR4* stability as the basis of its tumor promoting effect and further that the overexpression of Ehm-2 in the presence of the *FGFR4 Arg388* isotype results in the higher invasive potential of Arg-carrying prostate cancer patients (Wang et al., 2006; Wang et al., 2008).

In summary, the *FGFR4* is implicated in various cancers and the disruption of its signaling via inhibitors or reduction of the receptor seems to be a valid approach in cancer therapy. Moreover, the single nucleotide polymorphism in the *FGFR4*, which substitutes Glycine with Arginine at codon 388 is a promoter of aggressive cancer of various tissue origins and seems to be a more valid target and prognostic factor than the *FGFR4* itself.

### 1.4 Human breast cancer and modelling mammary carcinoma in vivo

Breast Cancer is the most frequently diagnosed cancer in women in the United States and Europe and the fifth leading cause of cancer death. Breast cancers have a huge histopathological and genetic diversity, that all result in a variety of clinical phenotypes (Table 6). This diversity is confronted by just a few prognostic markers that turn breast cancer into a difficult disease to be cured with a standard therapeutic strategy.

Histopathological type of invasive breast carcinoma	Frequency	10-year survival rate
Invasive ductal carcinoma, not otherwise specified	50–80%	35–50%
Invasive lobular carcinoma	5–15%	35–50%
Mixed type, lobular and ductal features	4–5%	35–50%
Tubular/invasive cribriform carcinoma	1–6%	90–100%
Mucinous carcinoma	<5%	80–100%
Medullary carcinoma	1–7%	50–90%
Invasive papillary carcinoma	<1–2%	Unknown
Invasive micropapillary carcinoma	<3%	Unknown
Metaplastic carcinoma	<5%	Unknown
Adenoid cystic carcinoma	0,1%	Unknown
Invasive apocrine carcinoma	0,3–4%	Unknown
Neuroendocrine carcinoma	2–5%	Unknown
Secretory carcinoma	0,01–0,15%	Unknown
Lipid-rich carcinoma	<1–6%	Unknown
Acinic-cell carcinoma	7 cases	Unknown
Glycogen-rich, clear-cell carcinoma	1–3%	Unknown
Sebaceous carcinoma	4 cases	Unknown

**Table 6: Histopathological type of invasive breast carcinoma its frequency and the estimated 10-year survival rate;**

Due to the high diversity of breast cancer traditional prognostic markers can identify approximately 30% of patients to have a favourable or bad prognosis. Table 7 lists the few factors out of a large number that so far fulfill the requirements of being a prognostic marker.

Marker	Use in clinic	Metastatic determinants	Details	References
Tumour size	Established	Tumours under 2 cm in diameter have a low risk of metastasis; tumours of 2–5 cm have a high risk of metastasis; tumours over 5 cm have a very high risk of metastasis	Independent prognosis marker	14–17
Axillary lymph-node status	Established	If there are no lymph-node metastases, the risk of metastasis is low; if lymph-node metastases are present, the risk of metastasis is high; the presence of over 4 lymph-node metastases is associated with very high metastasis risk	Related to tumour size	14,16,17
Histological grade	Established	Grade 1 tumours have a low risk of metastasis; grade 2 tumours have an intermediate risk of metastasis; grade 3 tumours have a high risk of metastasis	Related to tumour size	14,16,18
Angiolinvasion	Established in patients with lymph-node-negative tumours	The presence of tumour emboli in over 3 blood vessels is associated with metastasis	In patients with lymph-node-negative tumours	19,20
uPA/PAI1 protein level	Newly established marker	High protein levels of uPA and PAI1 are associated with high metastasis risk	Independent prognosis marker	55–60
Steroid-receptor expression	Established for adjuvant therapy decision	Low steroid-receptor levels are associated with metastasis	Short-term predictor of metastasis risk (5 years); related to histological grade	14
<i>ERBB2</i> gene amplification and protein expression	Established for adjuvant therapy decision	<i>ERBB2</i> amplification/overexpression is associated with metastasis	In patients with lymph-node-positive tumours	28,30,31
Gene-expression profiling	Currently being tested	A 'good signature' of 70 genes is associated with low metastasis risk; a 'poor signature' of 70 genes is associated with high metastasis risk	Tested in patients with lymph-node-negative tumours	7,8

PAI1, plasminogen activator inhibitor 1; uPA, urokinase-type plasminogen activator.

**Table 7: Summary of prognostic factors of breast cancer metastasis and outcome; the best established factors include tumor size, lymph node status and histological grade;**

Therefore, there is still an urgent need of novel prognostic factors to improve existing therapies and the expansion of the current understanding to identify novel therapeutics.

#### 1.4.1 The impact of the FGFR4 and its Arg388 variant on breast cancer

It is well known that the FGFR4 is frequently overexpressed in breast cancer and is therefore implicated in its progression (Jaakkola et al., 1993; Penault-Llorca et al., 1995). Further studies implicated the FGFR4 also in resistance to certain therapies. Here, breast cancer cell lines that were desensitized to doxorubicin or cyclophosphamid, overexpress the FGFR4 compared to the parental cell line. By specific knockdown of FGFR4, this apoptotic resistance can be rescued (Roidl et al., 2009). Besides that, overexpression of the FGFR4

ligand FGF8b promoted aggressiveness of MCF-7 breast cancer cells *in vitro* and *in vivo* (Ruohola et al., 2001). Moreover, high expression of the FGFR4 in patient mammary tumor samples is associated with a significantly higher rate of cancer relapse after usage of tamoxifen leading to a prognosis for breast cancer patients. These data involve the FGFR4 as a prediction marker of failure in tamoxifen treatment (Meijer et al., 2008). Above that, the single nucleotide polymorphism in the *FGFR4* gene that substitutes Glycin by Arginin at codon 388 is strongly correlated to increased aggressiveness of breast cancer *in vitro* and *in vivo*. Here, the overexpression of the FGFR4 Arg388 variant accelerated motility in MDA-MB-231 cells and altered gene expression towards a more aggressive phenotype (Bange et al., 2002; Stadler et al., 2006). Above that, breast cancer studies correlate the *FGFR4 Arg388* allele not only with accelerated disease progression but also with higher resistance to adjuvant systemic- or chemotherapies in primary breast cancer leading to a significantly shorter disease-free and overall survival (Bange et al., 2002; Thussbas et al., 2006). Unfortunately, due to the highly complex and heterogeneous genetic background of the patients, statistical analysis yielded at times marginal results and because of differences in patient stratification and statistical evaluation diverging results led to controversies (Jezequel et al., 2004; Spinola et al., 2005). Because of that and in spite of the strong association of the FGFR4 SNP with disease progression, this genetic configuration is not yet established as progression marker for clinical outcome or as basis for individual patient treatment decisions.

### **1.4.2 The TGF $\alpha$ -EGFR signalling cascade and its impact on human breast cancer**

The epidermal growth factor receptor (EGFR) plays an influential role in initiating the signaling that directs the behavior of epithelial cells and tumors of epithelial origin (Herbst, 2004). Its overexpression is present in the majority of solid tumors, including breast cancer, head and neck cancer, non-small-cell lung cancer and colon cancer (Herbst and Langer, 2002). For example in breast cancer the expression increases from 40.000 to  $2 \times 10^6$  EGFR molecules per cell (Carpenter and Cohen, 1979; Ennis et al., 1991; Kondapaka et al., 1997). Multiple ligands can bind the EGFR, but among these the epidermal growth factor (EGF) and the transforming growth factor- $\alpha$  (TGF $\alpha$ ) are the most important ligands among these (Salomon et al., 1995). Upon ligand binding, the EGFR either forms a homo- or heterodimer, which subsequently gets autophosphorylated at the intracytoplasmatic tyrosine phosphorylation domain. These phosphorylated tyrosine residues serve as binding sites for diverse docking proteins (Franklin et al., 2002). The Ras-Raf mitogen-activated protein kinase

## Introduction

pathway and the phosphatidylinositol 3' kinase and Akt pathway are the major signalling routes of the EGFR to regulate multiple processes including proliferation, or survival by target gene expression (Alroy and Yarden, 1997; Burgering and Coffey, 1995; Liu et al., 1999; Muthuswamy et al., 1999). In cancer, the EGFR additionally initiates the expression of target genes responsible for cell migration, adhesion and metastasis. In addition, angiogenesis, a process required for maintenance of tumor growth, can be regulated by the EGFR-signalling cascade by stimulation of the vascular endothelial growth factor (Figure 7) (Engebraaten et al., 1993; Goldman et al., 1993; Petit et al., 1997; Shibata et al., 1996).

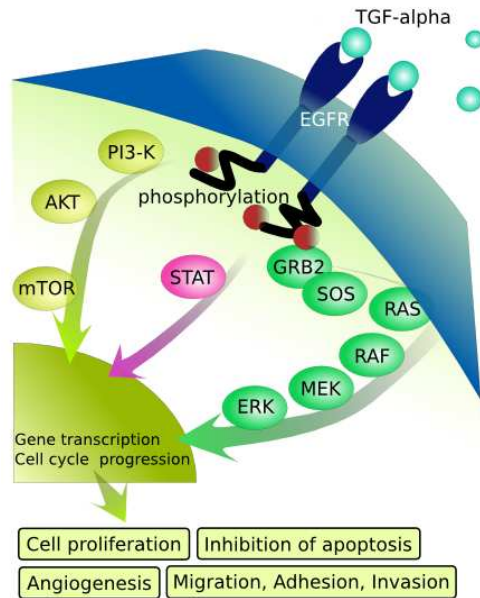


**Figure 7: The TGF $\alpha$ -EGFR signaling cascade; Upon TGF $\alpha$  stimulation, the EGFR gets activated by dimerization and followed by autotyrosine-phosphorylation. After binding of diverse docking proteins, the EGFR can activate either the Akt or the Erk-pathway, which results in the transcription of target genes that are implicated in proliferation, survival, angiogenesis, migration, adhesion or invasion; Deregulation of this pathway and following dysregulated intracellular signaling results in various diseases like cancer. [http://commons.wikimedia.org/wiki/Image:EGFR\\_signaling\\_pathway.png](http://commons.wikimedia.org/wiki/Image:EGFR_signaling_pathway.png)**

Valid models of carcinogenesis *in vivo* are an important and necessary tool to investigate cancer progression and the participating components to elucidate not only mechanisms of tumorigenesis but also to find and test appropriate ways of therapy. In recent years more than a few mouse models of every possible cancer was developed to study the initiation and progression of this disease in the background and with the impact of a whole organism and to overcome the heterogeneity of patient cohorts (Frese and Tuveson, 2007). For breast cancer numerous mouse models are available to study the impact of diverse influences in different oncogenetic backgrounds that trigger mammary tumor initiation (Hennighausen, 2000).

As the EGFR has a role in a variety of cellular processes and is often overexpressed in human breast cancer, modelling of breast cancer in mice via constitutive tissue-specific activation of the EGFR can be a very elegant and orthotopic model of mammary carcinogenesis.

### **1.4.3 The *WAP-TGF $\alpha$* mouse mammary carcinoma model**

The *WAP-TGF $\alpha$*  model is a routinely used mouse mammary tumor model (Pittius et al., 1988; Sandgren et al., 1995). In this model, TGF $\alpha$  overexpression is controlled by the whey acidic protein (WAP) promoter which specifically activates the transgene in mammary epithelial cells in mid-pregnancy. Thus, the process of mammary carcinogenesis is promoted by the constitutive overexpression of TGF $\alpha$ , a ligand of the epidermal growth factor receptor. Overexpression of TGF $\alpha$  in mammary epithelial cells results in accelerated alveolar development and impaired cell differentiation leading to failures in female lactation. Moreover, mammary involution is delayed and some alveolar structures fail to regress completely. As a consequence these hyperplastic alveolar nodules increase in number with successive pregnancies, and in some cases progress to tumors of variable histotype. These tumors have an onset of about 8 month and display well-differentiated carcinomas and adenocarcinomas (Sandgren et al., 1995). Whereas the C57BL/6 background requires continuous matings to get tumors established, mice transgenic for *WAP-TGF $\alpha$*  in the FVB background do not need be pregnant to establish mammary tumors.

### **1.4.4 The MMTV-PymT model**

Since the Polyoma Virus was discovered to be an oncogene *in vitro* some 50 years ago, mice transgenic for the Polyoma Middle T (PymT) became a fast and efficient *in vivo* model to study cancer of various tissue origins. Two of the principal signalling pathways that are stimulated by the middle T antigen are the mitogen-activated protein kinase (MAPK) and phosphatidylinositol-3-kinase (PI3K) with the following activation of the respective downstream molecules. These pathways contribute to either activation of proliferation, survival and transformation or inactivation of cell cycle arrest or apoptosis (Figure 8) (Dilworth, 2002). Under the transcriptional control of the mouse mammary tumor virus (MMTV) promoter, the PymT is exclusively expressed in the mammary gland. Here, the expression of Middle T results in synchronous appearance of multifocal tumors involving all mammary glands. This rapid conversion of the mammary epithelium appears in several transgenic strains after 3 weeks of age. Moreover, mice transgenic for PymT develop multiple pulmonary metastases after 3 month (Guy et al., 1992).

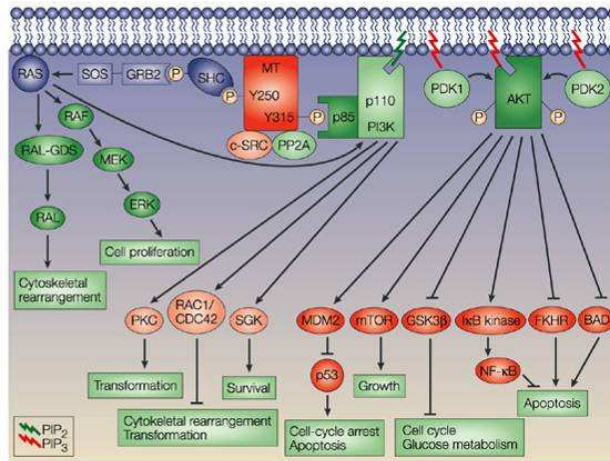


**Figure 8: Signalling pathways of the Polyoma Middle T Antigen; PyMT activates the mitogen-activated protein kinase (MAPK) and phosphatidylinositol-3-kinase (PI3K) whereas SRC is the main target of PyMT. The following downstream targets result in enhanced proliferation or survival leading to transformation of cells rapidly and very efficiently (Dilworth, 2002).**

### 1.5 Liver Metabolism and Cancer

The liver has a wide range of important functions including detoxification, protein synthesis, and production of biochemicals necessary for digestion. In addition, the liver plays a major role in metabolism and control processes like glycogen storage, decomposition of red blood cells and plasma protein synthesis (Maton, 1993).

#### 1.5.1 The impact of FGFR4 signalling on the hepatic bile acid synthesis, hyperlipidemia, insulin resistance and hypercholesterolemia

One major function of the liver is the production of bile acids. This cholesterol metabolite is then stored in the gall bladder and is released postprandially in the small intestine for the emulsification of lipids (Chiang, 2004; Russell, 2003). The regulation of bile acid synthesis is tightly regulated by a negative feedback loop to prevent the damage of the enterohepatic tissue. Here, the cholesterol 7 $\alpha$ -hydroxylase, the catalyzer of bile acid expression, is repressed by circulating bile acids itself (Jelinek et al., 1990). Responsible for this feedback loop is the regulation of the FGFR4/FGF15/FGF19 pathway by bile acids (Inagaki et al., 2005). Here, the nuclear bile acid receptor FXR, a key regulator of bile acid homeostasis, is activated by the binding of bile acid together with cholic acid and chenodeoxy-cholic acid (Kok et al., 2003; Sinal et al., 2000). After heterodimerization with the retinoid X receptor (RXRs) this transcription factor induces the expression of several target genes (Edwards et al., 2002). Amongst others FGF19/15 is expressed via FXR/RXR in the small intestine (Inagaki et al.,

Introduction

2005). FGF19/15 binds selectively to the FGFR4 that is the primarily expressed FGF receptor in the liver (Kan et al., 1999; Nicholes et al., 2002; Stark et al., 1991). The activation of the FGFR4 results in repression of CYP7A and following reduction of bile acid synthesis via the suppression of c-Jun N-terminal kinase (Holt et al., 2003; Xie et al., 1999). Mice lacking the FGFR4 have an increased bile acid pool size, a reduced JNK activity and enhanced expression of CYP7A (Yu et al., 2000). Along these lines, transgenic mice expressing a constitutively active form of the FGFR4 display increased activity of JNK and decreased expression of CYP7A (Yu et al., 2005). Hence the FGF19/15-FGFR4 pathway is involved in gut-liver signalling to maintain bile acid homeostasis (Figure 9).

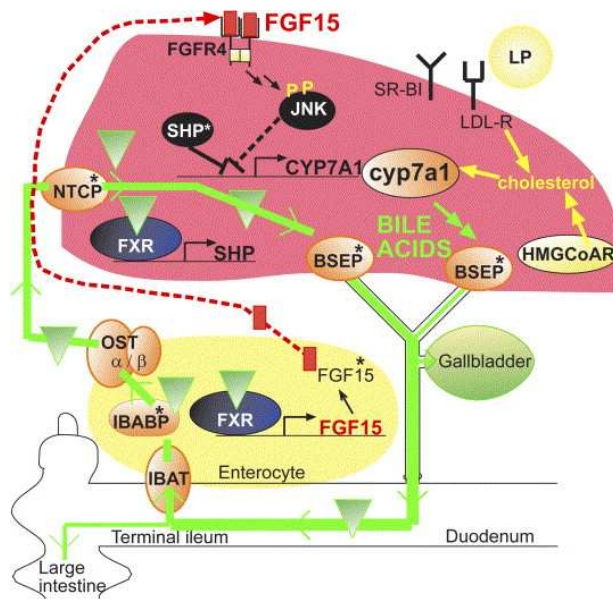


**Figure 9: Molecular action of the FGFR4 in gut-liver signalling; circulating bile acids in the intestine activate the expression of FGF15 via FXR/RXR signalling. FGF15 mediated activation of the FGFR4 in the liver results in JNK-dependent downregulation of CYP7A and following reduction in bile acid synthesis (Angelin, 2005).**

In maintaining homeostasis, FGFR4 and the FGF19 subfamily members additionally play an important role in systemic lipid and glucose homeostasis. Here, the hepatic activity of FGFR4 serves to prevent systemic hyperlipidemia and -cholesterolemia under normal conditions as shown in mice deficient for FGFR4 display increased white adipose tissue as well as triglyceride levels, free fatty acids and cholesterol levels (Figure 10). Furthermore, mice lacking FGFR4 displayed increased levels of blood glucose and a decreased glucose and insulin tolerance. Contrarily, hepatic FGFR4 induces fatty liver after high-fat diet and obesity in mice. In summary, the hepatic FGFR4 seems to be a potential target for intervention in

systemic cholesterol/bile acid and lipid and glucose metabolism (Huang et al., 2007; Ishikawa and Fidge, 1979; Yu et al., 2002; Yu et al., 2000).

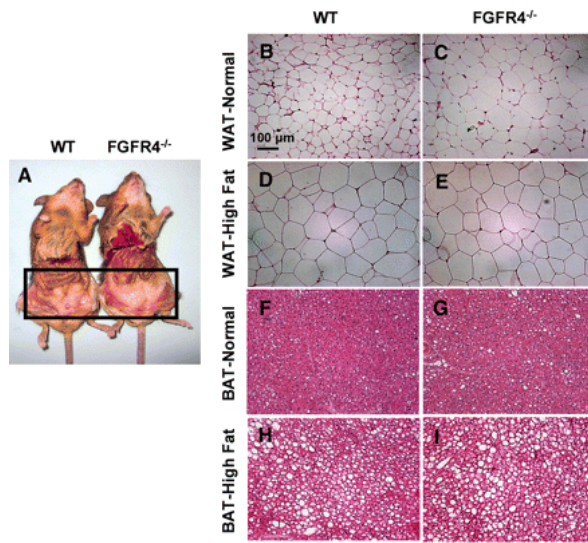


**Figure 10 : Mice lacking FGFR4 display an increase in white adipose tissue under normal conditions; the absence of the FGFR4 causes a 1.5-2-fold increase in reproductive white adipose tissue in males and females under normal conditions, whereas high fat diet fed mice display no difference in white adipose tissue regarding the phenotype (Huang et al., 2007).**

### 1.5.2 The impact of FGFR4 on hepatic carcinogenesis

Next to the metabolic function of FGFR4 in controlling bile acid synthesis, insulin resistance, hyperlipidemia and -cholesterolemia, this FGF receptor seems to be implicated in the progression of hepatocellular carcinoma. Mice deficient in FGFR4 display an accelerated DEN-induced carcinogenesis and the restoration of FGFR4 increases apoptosis in tumor cells suggesting a tumor suppressive function in HCC (Huang et al., 2008). In contrast, the FGFR4 was not suggested to regulate cellularity of normal or regenerating liver or cell proliferation during the response to liver injury (Hu et al., 1995; Yu et al., 2000). Interestingly, mice ectopically overexpressing FGF19 displayed hepatoma-like lesions and the inhibition of FGF19 by specific antibodies is reported to contribute to tumor reduction (Desnoyers et al., 2008; Nicholes et al., 2002). Additionally, after injection of xenobiotics, FGFR4 deficiency accelerates liver injury and liver fibrosis (Yu et al., 2002). Taken together, these data demonstrate that the FGFR4 critically contributes to hepatic carcinogenesis.

## 2 Specific Aims

Malignant transformation of cells is mostly based on specific alterations in the expression of oncogenes, tumor suppressors, tumor promotive and/or suppressive factors. The first aim of this study was to investigate the involvement of tumor suppressors and tumor promoting factors in oncogenesis in a human *in vitro* cell system. To this end, we intended to create a primary cell model in which the tumor suppressors p53 and Rb were downregulated. As the loss of p53 and Rb is a frequent and early event in carcinogenesis we hypothesized that the deletion of p53 and Rb would potentially initiate a process that mimics “natural” malignant transformation. Such a model system would offer the possibility to investigate the distinct and especially early steps of oncogenesis. This hypothesis is supported by Meuwissen et al. (2003) that could induce non-small cell lung cancer by the conditional loss of *p53* and *Rb* in mice.

Another approach towards the understanding of the influence of genetic factors in cancer progression focused on a single nucleotide polymorphism (SNP) in the human gene of the *fibroblast growth factor receptor 4 (FGFR4)* that substitutes a Glycin (Gly) with an Arginin (Arg) at codon 388 (*FGFR4 Arg388*). Since its discovery in 2002, the “abnormal” and frequent (50% of the human population) *FGFR4 Arg388* allele was correlated with the progression and poor clinical outcome of various human cancers. Due to the heterogeneity of patient cohorts, the correlation of the *FGFR4 Arg388* with cancer progression and poor clinical outcome sometimes led to controversial results. We therefore aimed to ultimately clarify the role of this SNP in breast cancer progression. Here, we hypothesized that a “knock in” (KI) *FGFR4 Arg385* (corresponding to human codon 388) inbred mouse could unequivocally demonstrate the involvement of the Arg388 allele in breast cancer progression by intercrossing these *FGFR4 Arg385* KI mice to mouse mammary tumor models. Furthermore we intended to use this mouse model to investigate the molecular mechanism that underlies the cancer progression accelerating effect of the *FGFR4 Arg388* isoform and to possibly identify novel interaction partners of the FGFR4 and especially the FGFR4 Arg385/388.

### 3 Materials and Methods

#### 3.1 Materials

##### 3.1.1 Laboratory Chemicals

Acrylamide	Serva, Heidelberg
Agar	Difco, USA
Agarose	BRL, Eggenstein
Ampicillin	Roche, Mannheim
Aprotinin	Sigma, Taufkirchen
APS (Ammonium peroxodisulfate)	Bio-Rad, München
ATP (Adenosine triphosphate)	Amersham Pharmacia, Freiburg
Basic FGF	Peptotec
Bisacrylamid	Roth, Karlsruhe
BSA (Bovine serum albumin)	Sigma, Taufkirchen
Chloroquine	Sigma, Taufkirchen
Coomassie G250	Serva, Heidelberg
Crystal Violet	Sigma, Taufkirchen
Deoxynucleotides (dG/A/T/CTP)	Roche, Mannheim
DTT (Dithiothreitol)	Sigma, Taufkirchen
EGF	Sigma, Taufkirchen
Ethidium bromide	Sigma, Taufkirchen
FGF19	Peptotech
Formaldehyde	PolySciences, Eppenstein
Geneticin (G418, GibCo)	Invitrogen, Eggenstein
Hemalaun	Fluka, Schweiz
Hemalaun-Eosin	Fluka, Schweiz
HEPES (N-(2-Hydroxyethyl)piperazine-N'-(2-ethanesulfonic acid))	Serva, Heidelberg
Hoechst33324 dye	Hoechst, Frankfurt am Main
Humaninsulin® Normal 40	Lilly, Giessen
Hydrogenperoxide	Aldrich, Steinheim
Kanamycin	Gibco, Eggenstein
L-Glutamine (GibCo)	Invitrogen, Eggenstein
Leupeptin	Sigma, Taufkirchen
Lipofectamine® (GibCo)	Invitrogen, Eggenstein
Lysozyme	Sigma, Taufkirchen
MTT (3-(4, 5-dimethyl-2-thiazolyl)-2, 5-diphenyl-2H-tetrazolium bromide)	Sigma, Taufkirchen
Oligofectamine®	Invitrogen, Eggenstein
Paraformaldehyde	Sigma, Taufkirchen
Penicillin/Streptomycin	Gibco, Eggenstein
Phenol	Roth, Karlsruhe
PMSF (Phenylmethanesulfonyl fluoride)	Sigma, Taufkirchen

## Materials and Methods

Polybren	Sigma, Taufkirchen
Ponceau S	Sigma, Taufkirchen
SDS (Sodium dodecyl sulfate)	Roth, Karlsruhe
Sodium azide	Serva, Heidelberg
Sodium orthovanadate	Sigma, Taufkirchen
TEMED (N,N,N',N'-Tetramethylethylenediamine)	Serva, Heidelberg
TPA (Tetradecanoyl-phorbol-13-acetate)	Sigma, Taufkirchen
Triton X-100	Serva, Heidelberg
Tween 20	Sigma, Taufkirchen
Xylol	Merck, Darmstadt

All other chemicals were purchased in analytical grade from Merck (Darmstadt).

### 3.1.2 Radiochemicals

[ $\gamma$ - <sup>32</sup> P]-dATP	PerkinElmer, France
[ $\alpha$ - <sup>33</sup> P]-dATP	PerkinElmer, France

### 3.1.3 Enzymes

Calf Intestine Alkaline Phosphatase	MBI Fermentas, St. Leon-Rot
DNase I, RNase free	Roche, Mannheim
LysC	Woka chemical, Hong Kong
Proteinase K	Sigma, Taufkirchen
Restriction Endonucleases	NEB, Frankfurt/ Main
	MBI Fermentas, St. Leon-Rot
	Boehringer, Mannheim
	Biolabs, New England
	Sigma, Taufkirchen
RNase A	Roche, Mannheim
T4-DNA Ligase	MBI Fermentas, St. Leon-Rot
Taq DNA Polymerase	Invitrogen, Eggenstein
Trypsin/EDTA	

### 3.1.4 “Kits“and Other Materials

BigDye <sup>®</sup> Terminator v1.1 Cycle Sequencing Kit	Applied Biosystems /Foster City
Cell culture materials	Greiner, Solingen
	Nunclon, Dänemark
	Falcon, UK
	Corning Incorporated, USA
Cellulose nitrate 0.45 $\mu$ m	Schleicher & Schüll, Dassel
DNA-Ladder	Eurogentec, Belgien
Enhanced Chemi Luminescent (ECL) Kit	PerkinElmer/NEN, Köln
Glutathion-Sepharose	Amersham Pharmacia, Freiburg
Hyperfilm MP	Amersham Pharmacia, Freiburg

## Materials and Methods

Matrigel	BD Biosciences, Pharmingen
Micro BCA Protein Assay Kit	Pierce, Sankt Augustin
Parafilm	Dynatech, Denkendorf
Poly Prep® Chromatography columns	Bio-Rad, München
Protein A-Sepharose	Amersham Pharmacia, Freiburg
Protein G-Sepharose	Amersham Pharmacia, Freiburg
QIAGEN Dneasy	Qiagen, Hilden
QIAquick Gel Extraction Kit (50)	Qiagen, Hilden
QIAquick PCR Purification Kit (50)	Qiagen, Hilden
QIAGEN Plasmid Mini Kit	Qiagen, Hilden
QIAGEN Plasmid Maxi Kit	Qiagen, Hilden
QIAGEN RNeasy Mini Kit	Qiagen, Hilden
Ready-to.go PCR beads	Amersham Pharmacia, Freiburg
slides and cover slips	Menzel
Sterile filter 0.22 µm, cellulose acetate	Nalge Company, USA
Sterile filter 0.45 µm, cellulose acetate	Nalge Company, USA
Vectastain Elite ABC Kit	Vector Laboratories (USA)
Whatman 3MM	Whatman, Rotenburg/Fulda

### 3.1.5 Growth factors and ligands

EGF (murine)	Toyoba, Japan
EGF(human)	Peprotech
TGFα	Peprotech
Basic FGF	Peprotech

## 3.2 Media

### 3.2.1 Bacterial media

LB or 2xYT media were used for cultivation of all Escherichia coli strains. If and as required 100µg/ml Ampicillin, 70µg/ml Kanamycin or 100µg/ml Chloramphenicol were added to the media after autoclavation. For the preparation of LB-plates 1.5% Agar was added.

LB-Medium	1.0% Trypton 0.5% Yeast Extract 1.0% NaCl pH 7.2
2x YT-Medium	1.6% Tryptone 1.0% Yeast Extract 1.0% NaCl pH 7.2

### 3.2.2 Cell culture media

Cell culture media and additives were obtained from Invitrogen (Eggenstein). Media were supplemented to the requirements of each cell line. Freeze medium contained 90% cell media and 10% DMSO.

**Dulbecco's Modified Eagle Medium (DMEM)** with 4,5 mg/ml Glucose, 10% FCS, 2 mM L-Glutamine, 1 mM sodiumpyruvate, 1% Penicillin/Streptomycin

**RPMI 1640**, 10% FCS, 2 mM L-Glutamine, 1% Penicillin/Streptomycin

The media for normal dermal fibroblasts (NHDF) were obtained from PromoCell (Heidelberg) and supplemented with 4% FCS, 1% Penicillin/Streptomycin, basicFibroblast Growth Factor 1ng/ml and human Insulin 5µg/ml

### 3.3 Stock solutions and commonly used buffers

Acrylamide solution (30/0.8%)	30.0% (w/v) Acrylamid 0.8% (w/v) Bisacrylamid
Citratbuffer	100mM Citronensäuremonohydrat, pH 6,0
HBS (2x)	46mM HEPES, pH 7,5 274mM NaCl 1,5mM Na <sub>2</sub> HPO <sub>4</sub> , pH 7,0
HNTG	20mM HEPES, pH 7.5 150mM NaCl 0.1% TritonX-100 10% Glycerol 10mM Na <sub>4</sub> P <sub>2</sub> O <sub>7</sub>
DNA loading buffer (6x)	0.05% Bromphenol blue 0.05% Xylencyanol 30% Glycerol 100mM EDTA pH 8.0
Laemmli buffer (2x)	65mM Tris/HCl pH 6.8 2% SDS 30% Glycerol 0.01% Bromphenol blue 5% β-Mercaptoethanol
Laemmli buffer (3x)	100mM Tris/HCl pH 6.8 3% SDS 45% Glycerol 0.01% Bromphenol blue 7.5% β-Mercaptoethanol

## Materials and Methods

MOPS (10x)	200mM Morpholinopropansulfonsäure 80mM Natriumacetat 10mM EDTA, pH 7,0
NET	50mM Tris/HCl pH 7.4 5mM EDTA 0.05% Triton X-100 150mM NaCl
PBS	137mM NaCl 27mM KCl 80mM Na <sub>2</sub> HPO <sub>4</sub> 1.5mM KH <sub>2</sub> PO <sub>4</sub> pH 7.4
RIPA Lysis Buffer	50mM Tris/HCl, pH8,0 150mM NaCl 1% Nonidet-P40 0.5% Desoxycholat 0.1% SDS
SD-Transblot	50mM Tris/HCl pH 7.5 40mM Glycine 20% Methanol 0.004% SDS
SSC (20x)	3,0M NaCl 0.3M Sodiumcitrate
“Strip” buffer	62.5mM Tris/HCl pH 6.8 2% SDS 100mM β-Mercaptoethanol
TAE	40mM Tris/Acetate pH 8.0 1mM EDTA
TE10/0.1	10mM Tris/HCl pH 8.0 0.1mM EDTA pH 8.0
Tris-Glycine-SDS	25mM Tris/HCl pH 7.5 200mM Glycine 0.1% SDS
Triton X-100 lysis buffer	50mM HEPES, pH 7.5 150mM NaCl 1mM EDTA 10% Glycerin

1% Triton X-100  
 10mM Na<sub>4</sub>P<sub>2</sub>O<sub>7</sub>  
 2mM VaO<sub>5</sub>  
 10mM NaF  
 1mM PMSF  
 100µg/l Aprotinin

### 3.4 Cells

#### 3.4.1 Eukaryotic cell lines

Cell Line	Description Origin	Reference
Cos-7	Kidney fibroblasts <i>Cercopithecus aethiops</i>	ATCC, USA
MCF10A	human mammary epithelial cells	ATCC, USA
HaCat	human lung keartinocytes	ATCC, USA
HEK293	human embryonic kidney fibroblasts	ATCC, USA
Phoenix A	HEK293, packaging cell line ampotrophic	ATCC, USA
Phoenix E	HEK293, packaging cell line ecotrophic	ATCC, USA
NHDF	normal human dermal fibroblasts	PromoCell, Germany
HMEC	human mammary epithelial cells	Lonza, Germany
Kg-1a	human acute myeloblastic leukemia	ATCC, USA
MDA-MB-231 (expressing empty pLXSN vector)	Human mammary carcinoma	ATCC, modified by Johannes Bange
MDA-MB-231 (expressing pLXSN vector-FGFR4 Gly388)	Human mammary carcinoma	ATCC, modified by Johannes Bange
MDA-MB-231 (expressing empty pLXSN vector FGFR4Arg388)	Human mammary carcinoma	ATCC, modified by Johannes Bange
MDA-MB435 S	human mammary carcinoma	ATCC, USA

All cell lines used in this study were grown as recommended by the supplier.

### 3.4.2 E. coli strains

<b>E. Coli strain</b>	<b>Genotype</b>	<b>Reference</b>
DH5 $\alpha$ F'	F' endA1 hsd17 (rk-mk+) supE44 recA1 gyrA (Nal) thi-1 $\Delta$ (lacZYA-argF196)	Genentech, USA
XL1-Blue	relA1 lac [F'proAB lacIqZ $\Delta$ M15 Tn10 (Tetr)] recA1 endA1 gyrA96 thi-1 hsdR17 supE44	Stratagene, NL
DH10bpir116	DH10 $\beta$ UmcC::pir116-Frt	Open Biosystems, USA

## 3.5 Antibodies

### 3.5.1 Primary Antibodies

<b>Antibody</b>	<b>Immunogen Origin</b>	<b>Reference</b>
Akt1/2	Rabbit, polyclonal; AA 345-480 of human Akt1	Santa Cruz, USA
p-Akt/PKB	Rabbit, polyclonal; phospho-Akt (Ser-473); recognizes p-Akt of human, rabbit and rat origin	NEB, Frankfurt/M.
$\beta$ -actin	Rabbit, polyclonal; directed against a C-terminal peptide	Sigma, Taufkirchen
CD34	Mouse, monoclonal, FITC labelled against human, CD34	Abcam, USA
CD44	Mouse monoclonal, FITC labelled against human CD44	Abcam, USA
Cyclin A	Rabbit, polyclonal; recognizes the full length human Cyclin A protein	Santa Cruz, USA
Cyclin B1	Mouse, monoclonal; peptide of murine Cyclin B1	Cell Signalling, MA
Cyclin D1	Mouse, monoclonal; protein fragment corresponding to AA 1-200 of human	Transduction Labs
EGFR (1005)	Rabbit, polyclonal against mouse, rat and human EGFR	Santa Cruz, USA
EGFR	Sheep, polyclonal; part of cytoplasmic domain of the human EGFR	UBI, Lake Placid

## Materials and Methods

EGFR (108.1)	Mouse, monoclonal/ ectodomain of the human EGFR	(Daub et al., 1997)
p-EGFR (Y-1173)	Rabbit, monoclonal; recognizes endogenous EGFR phosphorylated at Y1173	Cell Signalling, MA
ERK2 (C-14)	Rabbit, polyclonal; peptide at C-terminus of rat ERK2	Santa Cruz, USA
p-ERK	Rabbit, polyclonal; recognizes phospho-p44/p42	NEB, Frankfurt/M.
KI-67	Mouse, monoclonal; peptide between AA 1547-1742 of human KI-67	Transduction Labs
p-Rb	Rabbit, polyclonal; recognizes phospho-S780 of human Rb	Cell Signalling, MA
Tubulin	Mouse, monoclonal; ascites	Sigma, Taufkirchen
p-Tyr (4G10)	Mouse, monoclonal; recognizes phospho- (3)-tyrosine residues	UBI, Lake Placid
Rb	Mouse, monoclonal, against human residues 701-928 of human Rb	Cell Signalling, MA
p53 (FL-393)	Rabbit, polyclonal, against human full length p53 (1-393)	Santa Cruz, USA
actin	Rabbit, polyclonal, against N-terminus of actin	Sigma, Taufkirchen
Bcl-xl (clone 44)	Mouse, monoclonal, against human Bcl-xl as 18-233	Transduction Labs
Src (N-16)	Rabbit, polyclonal, against N-terminus of human src	Santa Cruz, USA
Bad	Rabbit, polyclonal, against human Bad phosphorylated on S-139	Stressgen, Canada
FGFR4 (C16)	Rabbit, polyclonal, against cytoplasmic domain of FGFR4 (25-145)	
FGFR4 (H-121)	Rabbit, polyclonal, against extracellular domain of FGFR4 (25-145)	Santa Cruz, USA
hTERT (H-231)	Rabbit, polyclonal, against as 900-1130 of human TERT	Santa Cruz, USA
Ras (259)	Mouse, monoclonal,	Santa Cruz, USA
Bcl-2 (clone 4D7)	Mouse, monoclonal, against human Bcl-2 as 61-76	Transduction Labs
FGFR4 GST(Ex)	Rabbit, polyclonal, FGFR4 (Ex)GST, expressed in HEK293	Homemade, Christiane Stadler
$\gamma$ H2AX (phospho	Rabbit, polyclonal, against human H2AX	Abcam, USA

S139) phosphorylated on S-139

### 3.5.2 Secondary Antibodies

For immunoblot analysis corresponding secondary antibodies conjugated with horseradish peroxidase (HRP) were used.

Antibody	Dilution	Origin
Goat anti-mouse-HRP	1:10000	Sigma, Taufkirchen
Goat anti-rabbit-HRP	1:25000	BioRad, München
Goat anti-sheep-HRP	1:10000	Jackson ImmunoResearch Labs, USA
Sheep anti-goat-HRP	1:10000	Jackson ImmunoResearch Labs, USA

## 3.6 Plasmids and oligonucleotides

### 3.6.1 Primary Vectors and Constructs

Vector	Origin	Reference
pcDNA3	Mammalian expression vector, Ampr, CMV promoter, BGH pA, high copy number plasmid	Invitrogen, USA
pSuper	Mammalian expression vector for short interfering RNA	OligoEngine, USA
pRETRO Super	Mammalian expression vector for short interfering RNA for retroviral infection	OligoEngine, USA
pSM2c	Mammalian expression vector for short hairpin RNA for retroviral infection	Open Biosystems, USA
pLXSN	Mammalian expression vector for retroviral infection	Clontech, USA

### 3.6.2 Oligonucleotides

#### RT-PCR Primers (mouse specific)

Gene	Primer Sequence
------	-----------------

GAPDH fwd	5'- CCAATATGATTCCACCCATGG -3'
GAPDH rev	5'- CCTTCTCCATGGTGGTGAAGA -3'
HPRT-LC fwd	5'- ATAAGCCAGACTTTGTTGGA-3'
HPRT-LC rev	5'- ATAAGCCAGACTTTGTTGGA-3'
FGFR4-LC fwd	5'- GCTTATGGATGACTCCTTACCCT -3'
FGFR4-LC rev	5'- AATGCCTCCAATACGATTCTC -3'
Cyclophilin fw	5'- GACGCCACTGTCGCTTTTCG -3'
Cyclophilin rev	5'- CTTGCCATCCAGCCATTCAGTC -3'
FGFR4 fwd	5'- CGTGGACAACAGCAACCCCTG -3'
FGFR4 rev	5'- GCTGGCGAGAGTAGTGGCCACG -3'
E-Cadherin fw	5'- GCTGGACCGAGAGAGTTA -3'
E-Cadherin rev	5'- TCGTTCTCCACTCTCACAT -3'
MMP13 fw	5'- TCCCTGGAATTGGCAACAAAG -3
MMP13 rev	5'- GGAATTTGTTGGCATGACTCTCAC -3'
MMP9 fw	5'- CCCTGGAACTCACACGACA -3'
MMP9 rev	5'- GGAAACTCACACGCCAGAAG -3'
CD44 fw	5'- TTGAATGTAACCTGCCGCTACGCA -3
CD44 rev	5'- TCGGATCCATGAGTCACAGTGCG -3'
flk-1 fw	5'- TCGTGCGTGACATCAAAGAG -3'
flk-1 rev	5'- TGGACAGTGAGGCCAGGATG -3'
Cox-2 fw	5'- CTGGTGCTGGTCTGATGATG -3'
Cox-2 rev	5'- GGCAATGCGGTTCTGATCTG -3'
CDK4 fw	5'- TGGCTGCCACTCGATATGAAC -3'
CDK4 rev	5'- CCTCAGGTCTGGTCTATATG -3'
p21 fw	5'- CGTTTTCGGCCCTGAGATGTT -3'
p21 rev	5'- ACCCGGGTCCTTCTTGTGTTTC-3'
cyclin D1 fw	5'- TCCCGCTGGCCATGAACTACC -3'
cyclin D1 rev	5'- GGCGCAGGCTTGACTCCAGAA -3'
CDK1 fw	5'- CCATGAACTGCCCAGGAG -3'
CDK1 rev	5'- CGGTGTGGTGTATAAGGGTAGA-3'
CDK2 fw	5'- CGATAACAAGCTCCGTCCAT -3'
CDK2 rev	5'- AGAAGTGGCTGCATCACAAG -3'
p53 fwd	5'- AACCGCCGACCTATCCTTACCATC -3'
p53 rev	5'- AGGCCCCACTTTCTTGACCATTGT -3'
N-Cadherin fw	5'- CCACAGACATGGAAGGCAATCC -3'
N-Cadherin rev	5'- CACTGATTCTGTATGCCG CATTC-3'
Rb fwd	5'- CATCTAATGGACTTCCAGAG -3'
Rb rev	5'- CATAACAGTCCTAACTGGAG -3'
MMP14 fw	5'- CGTTCGCTGCTGGACAAGG -3'
MMP14 rev	5'- GACTGAGAAGGGAGGCTGGAG -3'

LC: primer for RT-PCR analysis via Light Cycler©

#### RT-PCR Primers (human specific)

Gene	Primer Sequence
36B4 fwd	5'- CCCATTCTATCATCAACGGGTACAA -3'

36B4 rev	5'- CAGCAAGTGGGAAGGTGTAATCC-3'
Telo fw	5'- GGTTTT(TGAGGG) <sup>5</sup> T-3'
Telo rev	5'- TCCCGA(CTATCC) <sup>4</sup> CTACTA-3'
MMP9 fw	5'- GACGCAGACATCGTCATCCAGTTT -3'
MMP9 rev	5'- GCCGCGCCATCTGCGTTT -3'
MMP2 fw	5'- ATGGCAAGGAGTACAACAGC -3'
MMP2 rev	5'- GCTGGTGCAGCTCTCATATT -3'
MMP 14 fw	5'- CGCTACGCCATCCAGGGTCTCAA -3'
MMP 14 rev	5'- CGGTCATCATCGGGCAGCACAAAA -3'
AuroraKinaseA fw	5'- GAGAAAGCCGGAGTGGAGCATCAG -3'
AuroraKinaseA rev	5'- CATTCAGGGGGCAGGTAGTCCAG -3'
AuroraKinaseB fw	5'- GGCGGCCGGGAGAGTAGCA -3'
AuroraKinaseB rev	5'- ACCTTGAGCGCCACGATGAAATG -3'
Mad1 fw	5'- TGTGAGCGACTCTGACGA-3'
Mad1 rev	5'- GTGGGACACTGAAGTTACG-3'
Mad2 fw	5'- CTCTTCCTGTTCCCGTCCTT-3'
Mad2 rev	5'- CACCTTTAGCTGGCTGT-3'
GAPDH fwd	5'- CCAATATGATTCCACCCATGG-3'
GAPDH rev	5'- CCTTCTCCATGGTGGTGAAGA-3'
p16 fwd	5'- AGCATGGAGCCTTCGGCTGACT-3'
p16rev	5'- CTGTAGGACCTTCGGTGAAGTGA-3'
p21 fwd	5'- AGTGGACAGCGAGCAGCTGA-3'
p21rev	5'- TAGAAATCTGTCATGCTGGTCTG-3'
p27 fwd	5'- AAACGTGCGAGTGTCTAACGCGA -3'
p27rev	5'- CGCTTCCTTATTCCTGGGCATTG-3'
p53 fwd	5'- CCGCAGTCAGATCCTAGCG-3'
p53 rev	5'- AATCATCCATTGCTTGGGACG-3'
Rb fwd	5'- TGGCGTGCCTCTTGAGGTTGTAA-3'
Rb rev	5'- CTGGGTCTGGAAGGCTGAGGTTGC-3'
Rb -LC fwd	5'- GAATCATTCCGGACTTCTGAG-3'
Rb-LC rev	5'- TTCCTTGTGTTGAGGTATCCA-3'
p53-LC fwd	5'- TGCAGCTGTGGGTTGATTCC-3'
p53-LC rev	5'- AAACACGCACCTCAAAGCTGTTTC-3'

#### Genotyping Primers (*FGFR4* KI mice)

Gene	Primer Sequence
FGFR4_1	5'-CGTGGACAACAGCAACCCCTG-3'
FGFR4_2	5'-GCTGGCGAGAGTAGTGGCCACG-3'
neoR-1	5'-AGGATCTCCTGTCATCTCACCTTCCTCCTG-3'
neoR-2	5'-AGAACTCGTCAAGAAGGCGATAGAAGGCG-3'
PymT_3	5'-TCGCCGCTAAGACTGC-3'
PymT_3	5'- CCGCCCTGGGAATGATAG -3'
TGF $\alpha$ fw	5'-TGTCAGGCTCTGGAGAACAGC-3'
TGF $\alpha$ rv	5'-CACAGCGAACACCCACGTACC-3'
Cre-1	5'-AACATGCTTCATCGTCGG-3'

Cre-2	5'-TTAGGATCATCAGCTACACC-3'
-------	----------------------------

### **3.7 Methods of Molecular Cloning**

#### **3.7.1 Plasmid preparation**

Small amounts of plasmid DNA were prepared using the Qiagen Plasmid Mini Kit, larger amounts of DNA were obtained with the Qiagen Plasmid Maxi Kit following the manufacturer's recommendations.

#### **3.7.2 Enzymatic manipulation of DNA**

##### **3.7.2.1 Specific digestion of DNA samples by restriction endonucleases**

The ratio of Enzyme/DNA, the temperature, the buffer and the time of incubation were adjusted according to manufacturer's recommendations. Usually, incubations for 2 hours at 37°C with a calculated 5-fold overdigestion and the buffers as supplied by the manufacturer were chosen.

##### **3.7.2.2 Dephosphorylation of 5'-termini with calf intestine alkaline phosphatase (CIAP)**

For dephosphorylation, 1µg of cut vector DNA was incubated with 5 units CIAP in adequate reaction buffer (e.g. 50mM Tris/HCl pH 8, 0.1mM EDTA pH 8.5) at 37°C for 10 minutes. Either reactions were stopped by heat inactivation at 85°C for 10 minutes or DNA was directly purified using the QIAquick PCR Purification Kit.

##### **3.7.2.3 Ligation of vector and insert DNA**

Purified, digested and dephosphorylated vector DNA (40ng), the designated insert DNA, 1µl 10x T4 DNA Ligase buffer (0.66M Tris/HCl pH 7.5, 50mM MgCl<sub>2</sub>, 50mM DTT, 10mM ATP) and 1 unit T4 DNA Ligase were combined. A molar ratio between insert and vector of 3 to 1 was usually chosen. Reactions were either left on 16°C overnight or at 37°C for 2 hours and subsequently transformed into competent bacteria.

##### **3.7.2.4 Agarose gel electrophoresis**

Depending on the size of the fragments of interest 0.7-2% agarose gels were prepared in horizontal chambers. TAE buffer was used for the electrophoresis. Voltage was usually set to 4-10 V per cm width of the gel. After separation DNA fragments were stained by gently agitating gels in TAE containing 0.5µg/ml ethidium bromide and were subsequently viewed under UV light.

##### **3.7.2.5 Isolation of DNA fragments from agarose gels**

Following gel electrophoresis gel slices bearing DNA fragments of interest were cut out of the gel. Agarose was dissolved and DNA was purified using the QIAquick Gel Extraction Kit according to manufacturer's recommendations.

#### **3.7.3 Introduction of plasmid DNA into E.coli**

##### **3.7.3.1 Preparation of competent cells**

The preparation of competent cells was according to the procedure described by Chung and Miller (Chung and Miller, 1988). Competent cells were shock frozen in liquid nitrogen and

stored for up to one year at  $-70^{\circ}\text{C}$ . Transformation frequency ranged between  $10^5$  and  $10^7$  colonies/ $\mu\text{g}$  DNA.

### **3.7.3.2 Transformation of competent bacteria**

A 50 $\mu\text{l}$  aliquot of competent bacteria was added to a 50 $\mu\text{l}$  mixture of DNA usually ligation cocktails, 10 $\mu\text{l}$  5x KCM solution (500mM KCl, 150mM CaCl<sub>2</sub>, 250mM MgCl<sub>2</sub>) and water. After thoroughly mixing, samples were incubated on ice for 20 minutes, 10 minutes at room temperature and after addition of 300 $\mu\text{l}$  LB broth at 37 $^{\circ}\text{C}$  for 1 hour while constantly shaking. Bacteria were streaked out on appropriate agar plates containing ampicillin for the selection of the transformants.

### **3.7.4 Enzymatic amplification of DNA by polymerase chain reaction (PCR)**

Amplification of DNA was done via Ready-to-go beads (GE Healthcare). Following has to be added to the beads

1-5 $\mu\text{l}$  template cDNA or genomic DNA, 1-10ng

1 $\mu\text{l}$  "forward" oligonucleotide, 10pmol/ $\mu\text{l}$

1 $\mu\text{l}$  "reverse" oligonucleotide, 10pmol/ $\mu\text{l}$

Ad 25 $\mu\text{l}$  H<sub>2</sub>O

PCR reactions were carried out using an automated thermal cycler (Eppendorf).

The following standard protocol was adjusted to each specific application:

3 min 95 $^{\circ}\text{C}$  (initial denaturation)

30 cycles:

1 min 95 $^{\circ}\text{C}$  (denaturation)

1 min x $^{\circ}\text{C}$  (appropriate annealing temperature)

1-3 min 72 $^{\circ}\text{C}$  (extension)

5 min 72 $^{\circ}\text{C}$  (final extension)

4 $^{\circ}\text{C}$  hold

PCR products were either separated by agarose gel electrophoresis, excised and subsequently purified or directly purified with QIAquick Gel Extraction or PCR Purification Kit, respectively.

### **3.7.5 DNA sequencing**

Sequencing of DNA was performed following the "Big Dye Terminator Cycle Sequencing Protocol" (ABI). Pellets were dissolved in 20 $\mu\text{l}$  template suppression reagent, briefly boiled and analysed on a 310-Genetic Analyzer (ABI Prism).

## **3.8 Methods of mammalian cell culture**

### **3.8.1 Calcium-Phosphate transfection**

Cells were maintained in appropriate culture media at 7.5% CO<sub>2</sub> and 37 $^{\circ}\text{C}$ . Transfections were carried out using a modified calcium phosphate method. Briefly,  $2 \times 10^6$  cells were incubated overnight in 3ml of growth medium. 2 $\mu\text{g}$  of plasmid DNA was mixed with water and 0.25M CaCl<sub>2</sub> solution in a final volume of 500 $\mu\text{l}$ . The mixture was added to the same volume of 2x transfection buffer (HBS) and incubated for 15 minutes at room temperature

before it was added dropwise to the cells. After incubation for 12 hours at 37°C, the medium was replaced.

### **3.8.2 Transfection of plasmid DNA using lipofectamine®**

Target cells were transiently transfected using Lipofectamine® (Gibco-BRL) as described previously (Daub et al., 1997). Briefly, cells were seeded in 6cm plates. 350µl of serum-free medium containing 7µl of Lipofectamine and 2µg of total plasmid DNA per well were used. After 4 hours the transfection mixture was supplemented with an equal volume of medium containing 10% FCS. Then, cells were either stimulated or left untreated, lysed and subjected to Western Blot analysis.

### **3.8.3 Transfection of siRNAs using oligofectamine®**

SiRNAs were transiently transfected in cells using Oligofectamine® (Gibco-BRL) according to the manufacturer's recommendations. Briefly, 20pmol siRNA was mixed with the appropriate amount of OPTI-MEM medium, mixed with the oligofectamine reagent and incubated for 20 minutes at room temperature. The cells were washed once in OPTI-MEM containing 0% FCS. The mixture was put on the cells for 4 hours and thereafter the medium was changed to normal growth medium containing 10% FCS. Silencing efficiency was tested at different time-points after transfection by Western blot analysis.

### **3.8.4 Infection of cells**

In order to generate cell lines with a stable expression of a target gene cells were infected as previously described (Pear et al., 1993). Briefly,  $2 \times 10^6$  cells of the packaging cell line Phoenix E or A were seeded in 6-well dishes and transfected with Calcium-Transfection Method on the next day. Target cells were further seeded in 6-well dishes on the day of Calcium-Transfection. After 24 hours target cells were infected with the viral supernatant of the packaging cell lines

### **3.8.5 Stimulation of cells**

Cells were seeded in cell culture dishes of appropriate size and grown overnight to about 80% confluence. After serum-starvation for 24 to 48 hours cells were stimulated with appropriate growth factors, washed with cold PBS and then lysed for 10 minutes on ice.

## **3.9 Methods of Biochemistry and Cell Biology**

### **3.9.1 Lysis of cells with Triton X-100 lysis buffer**

Cells were washed with cold PBS and then lysed for 10 minutes on ice, tissue was directly lysed for 30 minutes on ice in buffer containing 50 mM HEPES, pH 7.5, 150mM NaCl, 1% Triton X-100, 1mM EDTA, 10% glycerol, 10mM sodium pyrophosphate, 2mM sodium orthovanadate, 10mM sodium fluoride, 1mM phenylmethylsulfonyl fluoride, and 10µg/mL aprotinin. Lysates were precleared by centrifugation at 13000 rpm for 10 minutes at 4°C.

### **3.9.2 Lysis of cells with RIPA lysis buffer**

Cells were washed with cold PBS and then lysed for 10 minutes on ice, tissue was directly lysed for 30 minutes on ice in buffer containing 50mM Tris/HCl, pH 8.0, 150mM NaCl 1%, Nonidet-P400 5%, Desoxycholat 0.1% SDS, 2mM sodium orthovanadate, 10mM sodium fluoride, 1mM phenylmethylsulfonyl fluoride, and 10µg/mL aprotinin. Lysates were precleared by centrifugation at 13000 rpm for 10 minutes at 4°C.

### 3.9.3 Determination of total protein concentration in lysates

The overall protein concentration was determined using the Micro BCA Protein Assay Kit (Pierce, Sankt Augustin) according to the supplied standard protocol.

### 3.9.4 Immunoprecipitation

An equal volume of HNTG buffer was added to the precleared cell lysates that had been adjusted for equal protein concentration. Proteins of interest were immunoprecipitated using the respective antibodies and 20-40 $\mu$ L of protein A- or G-Sepharose over night at 4°C.

Precipitates were washed three times with 0.5ml of HNTG buffer, suspended in 3x SDS sample buffer, boiled for 5 minutes, and subjected to Western Blot analysis.

### 3.9.5 SDS-polyacrylamide-gelelectrophoresis (SDS-PAGE)

SDS-PAGE was conducted as described previously (Maniatis, 1989). The following proteins were used as molecular weight standards:

Protein	MW (kD)
Myosin	205.0
$\beta$ -Galactosidase	116.25
Phosphorylase b	97.4
BSA	66.2
Ovalbumin	42.7
Carboanhydrase	29.0
Trypsin-Inhibitor	21.7
Lysozym	14.4

### 3.9.6 Transfer of proteins on nitrocellulose membranes

For immunoblot analysis proteins were transferred to nitrocellulose membranes (Gershoni and Palade, 1982) for 3 hours at 0.8mA/cm<sup>2</sup> using a "Semidry"-Blot device in the presence of Transblot-SD buffer. Following transfer proteins were stained with Ponceau S (2g/l in 2% TCA) in order to visualize and mark standard protein bands. The membrane was destained in water.

### 3.9.7 Immunoblot detection

After electroblotting the transferred proteins are bound to the surface of the nitrocellulose membrane, providing access for reaction with immunodetection reagents. Remaining binding sites were blocked by immersing the membrane in 1x NET, 0.25% gelatine or 5% milk, TBS-T for at least 4 hours. The membrane was then probed with the primary antibody overnight at 4°C. Antibodies were diluted 1:500 to 1:2000 in NET, 0.25% gelatine or 1% BSA, TBS-T. The membrane was washed 3x 20 minutes in 1x NET, 0.25% gelatine or TBS-T, incubated for 1 hour with secondary antibody and washed again as before.

Antibody-antigen complexes were identified using horseradish peroxidase coupled to the secondary anti-IgG antibody. Luminescent substrates were used to visualize peroxidase activity. Signals were detected with X-ray films. Membranes were stripped of bound antibody by shaking in strip-buffer for 1 hour at 50°C. Stripped membranes were blocked and reprobed.

### **3.9.8 RNA isolation and RT-PCR analysis**

Total RNA was isolated using the RNeasy Mini Kit (Qiagen, Hilden) and reverse transcribed using AMV Reverse Transcriptase (Roche, Mannheim). 2-10µg of RNA and 1µl of random primer in a volume of 10µl were incubated for 2 minutes at 68°C, followed by 10 minutes incubation at room temperature. After addition of 0.5µl RNase inhibitor, 4µl 5x AMV RT buffer, 4µl dNTPs (2.5 mM each) and 1µl AMV RT the volume was adjusted to 20µl. The reaction mix was incubated at 42°C for 1 hour and thereafter cDNA was purified using the Qiagen PCR purification kit (Qiagen, Hilden). For PCR amplification Light Cycler Technology© or PuReTaq Ready-To-Go PCR Beads (Amersham Biosciences, Piscataway, NJ) were used. Here 1µl RT-PCR products were used for PCR amplification according to the manufacturer's recommendations. PCR products were subjected to electrophoresis on 1.5-2% agarose gels and DNA was visualized by ethidium bromide staining.

### **3.9.9 Southern Blot analysis**

For analysis of the telomere length in p53/Rb double knockdown cells genomic DNA was subjected to standard protocol of southern blotting, after PCR amplification of the telomeres (Southern, 1974). Loading of DNA samples was verified by the single copy gene 36B4.

### **3.9.10 Proliferation assay**

5.000 or 15.000 cells were seeded in 6cm plates. The cells were grown in the presence of medium containing 10% FCS or. The cell number was counted (Coulter counter, Beckton Dickinson) at the indicated time points and the population doubling rate was calculated. Furthermore, cell proliferation in response to the inhibitors Gefitinib and Cetuximab was measured by MTT assay. Briefly, 5.000 cells were seeded in 48 well plates. The cells were allowed to grow for 72 hours and at that time point, MTT (3-[4,5-dimethylthiazol-2-yl]-2,5-diphenyltetrazolimbromide; thiazolyl blue, Sigma, Taufkirchen) was added to each well at a final concentration of 1mg/ml. The plates were incubated for 2 hours. The yellow MTT dye is reduced by mitochondrial dehydrogenase activity to a purple formazan, which was then solubilized (SDS, 2-Butanol and HCl) and absorbance was measured at 570nm on a micro-plate reader. All data are shown as mean ± SDM.

### **3.9.11 Migration assay**

15.000-20.000 cells seeded on to a membrane with 8µM pores of a modified Boyden chamber (Schubert and Weiss) containing 400µl serum-free or 0.1% FCS medium with or without inhibitors. The lower chamber was filled with 600µl medium containing 4-10% fetal calf serum. The cells were allowed to migrate for 16-24 hours through the pores and were then stained by crystal violet. Stained cells were washed in PBS and pictures were taken on a Zeiss Axiovert 300 microscope (Carl Zeiss, Jena). For spectrophotometric measurement of stained cells the membranes were incubated for 1 hour in 5% Acetic acid to dissolve the crystal violet and thereafter measured in an ELISA reader (BioRad) at 570 nm.

### **3.9.12 Anchorage independent growth**

50.000 cells were seeded in uncoated culture dishes to prevent adherens of the cells. After 72hours cells were analysed under the microscope for occurrence of cell-clusters that indicate anchorage independent growth of the cells. Furthermore, anchorage independent growth was calculated by Soft Agar Assays. Here, cells ( $1 \times 10^5$ ) were added to 3 ml of DMEM supplemented with 10% FBS and 0.3% agar and layered onto 6ml of 0.5% agar beds in 60mm dishes. After 24-96hours anchorage independent growth of cells was calculated and quantified microscopically.

### **3.9.13 Focus formation assay**

The Focus Formation Assay was performed by infection of mouse embryonic fibroblast (MEFs) with pLXSN (Clontech, Palo Alto, USA) based retroviruses containing the oncogenes v-scr (positive control) HER2, EGFR or v-Kit. 24hours after infection cells were starved in medium containing 4% FCS and maintained for 21 days. Afterwards cells were stained with crystal violet and foci were counted macroscopically.

### **3.9.14 Karyotyping**

5.000-15.000 cells were seeded on cover slips in 24-well plates. On the next day, cells were treated with 10nM Nocodazol to arrest cells in mitoses. After 24hours cells were washed with prewarmed PBS and swollen with 0.075M KCl for 30minutes on 37°C. After the treatment with 0.075 M KCl cells burst and the released chromosomes were fixed with acetate/methanol (1:3) 3x5minutes. Afterwards cover slips were dried over night and then stained with mounting media containing DAPI. Mitotic spreads were analysed for karyotypical abnormalities microscopically.

### **3.9.15 Cell branching assay**

For cell branching assays 96-well plates were coated for at least 3 hours with 50µl Matrigel (contains laminin, collagen type IV, heparan sulfate proteoglycan and entactin; BD Biosciences) diluted in according cell medium. Then 10.000 cells were seeded in triplicates on to the Matrigel in medium containing 0-10% FCS with or without inhibitors. The cells were allowed to invade the matrix for one week. The medium was changed every second day during the assay. Bright field pictures were taken on a Zeiss Axiovert 300 microscope (Carl Zeiss, Jena).

### **3.9.16 Apoptosis assay and cell cycle analysis by propidium Iodide staining**

5.000-15.000 cells were seeded into 12-well plates (Nunc). 24 hours later apoptosis was induced by adding chemotherapeutic drugs or inhibitors in DMSO to the medium. After 48 hours the supernatant of each reaction was collected and the cells were trypsinized. After centrifugation the cells were incubated for 2 hours in a Propidium-Iodide buffer (0.1% Na-Citrate, 0.1% Triton X-100, 20µM Propidium-Iodide) and thereafter subjected to flow cytometric analysis (Beckton-Dickinson Biosciences) as described previously (Nicoletti et al., 1991). Cell cycle profiles and apoptosis were determined using the Cell Quest Pro software (Beckton Dickinson Biosciences).

### **3.9.17 Senescence assay**

Senescence assays (Cell Signalling, USA) were performed on  $1 \times 10^5$  cells seeded in 6cm dishes. After 24hours cells were stained for  $\beta$ -galactosidase expression according to manufactures recommendation and analysed under a light microscope (Visitron Systems, Zeiss).

### **3.9.18 Indirect flow cytometry**

Cells in the logarithmic growth phase were collected using 10mM EDTA and dissolved in 1ml 3% FCS in PBS. The cell number was adjusted to 250.000 cells per reaction and cells were incubated for 30 minutes with 10µg/ml of each FITC-labeled primary antibody at 4°C. The cells were washed 3 times and resuspended in 3% FCS/PBS and fluorescence intensity was measured in a flow cytometer (Beckton Dickinson Biosciences) and analyzed using the Cell Quest Pro software.

### 3.9.19 Stable isotope labelling by amino acids *in vivo* and *in vitro* (SILAC) and mass spectrometry

Livers from all *FGFR4* genotypes, *FGFR4* knockout (kindly provided by Wallace L. McKeenan, PhD, Center for Cancer and Stem Cell Biology, Institute of Biosciences and Technology, Texas, Houston, USA) or SILAC mice were prepared and washed in 0.9% NaCl to get rid of the excess blood. Then every liver was snap frozen in liquid nitrogen and stored at -80°C until use. Here, the liver was grinded in liquid nitrogen and lysed for 30 minutes in Triton-X 100 Lysis buffer containing proteinase and phosphatase inhibitors. The lysate was centrifuged for 10min 3000rpm and the supernatant was filtered using a sterile 45µm filter to preclear the lysate. MDA-MB-231 cells expressing empty pLXSN, pLXSNG388 or R388 were subcultured in RPMI media containing 10% dialyzed FCS, 1% L-Glutamine and 1% Penicillin/Streptomycin. To incorporate appropriate isotope labeled amino acids cells were grown in the corresponding media for at least six cell doublings. MDA-MB-231 cells expressing empty pLXSN vector were grown in RPMI containing [<sup>13</sup>C<sub>6</sub>] arginine and [4,4,5,5-D<sub>4</sub>]lysine (=Arg<sup>6</sup>/Lys<sup>4</sup>). MDA-MB-231 cells expressing pLXSN G388 or R388 were either in native amino acids (=Arg<sup>0</sup>/Lys<sup>0</sup>) or [<sup>13</sup>C<sub>6</sub>, <sup>15</sup>N<sub>4</sub>] arginine and [<sup>13</sup>C<sub>6</sub>, <sup>15</sup>N<sub>2</sub>] lysine (=Arg<sup>10</sup>/Lys<sup>8</sup>) to perform a “label switch”. Labeled arginine and lysine was added in 62.8µg/µl and 105.3µg/µl, respectively. Cells were washed with pre-chilled PBS and lysed in Triton-X 100 Lysis buffer containing proteinase and phosphatase inhibitors. The lysate was then centrifuged for 10min 3000rpm.

Next, FGFR4 from liver or cell lysates was immunoprecipitated (80-100mg) using a homemade α-FGFR4 antibody. Next to the *FGFR4 KO* livers, specific blocking peptides were used as a further control to identify proteins that bind unspecifically to the beads or the antibody. The samples were pooled and prepared for mass spectrometry as described previously (Selbach and Mann, 2006). The samples were analyzed by online liquid chromatography–tandem mass spectrometry (LC-MS/MS) on a LTQ-Orbitrap mass spectrometer (Thermo Electron). The identified peptides were assigned to proteins using Mascot (Matrix Science) and quantified with MSQuant.

### 3.10 Methods of mouse genetics

#### 3.10.1 Mice and gene targeting

The animals used in this study were kept in a barrier facility at the Max Planck Institutes in Martinsried, Germany. The *FGFR4 Arg385 KI* mice were generated using standard ES cell homologous recombination and blastocyst injection techniques as described previously (Seitzer et al., 2009).

#### 3.10.2 Genotyping and intercrosses to oncomice

Genotyping was done by PCR of genomic tail-DNA isolated using the Qiagen Blood & Tissue DNeasy Kit according to manufacture’s recommendation. The removal of the selection cassette was detected using neoR-specific primers. Removal of the Cre transgene was determined by Cre-specific primers. Primer for detecting the genotype of the *FGFR4* allele were specific for amplifying a 168bp band spanning the *FGFR4-SNP* with subsequent restriction of the amplification product via *MvaI* restriction enzyme to distinguish the different *FGFR4* alleles. The presence of the *TGFα* and *PymT* transgene was confirmed by performing PCR analysis with TGFα Primers as mentioned above.

### **3.10.3 Isolation of mouse embryonic fibroblasts (MEFs)**

Mouse embryonic fibroblasts were isolated from E13.5 embryos as described previously (Conner, 2001). The cells were cultured in DMEM high glucose containing 10% fetal calf serum, 1% L-Glutamine and 1% Penicillin/Streptomycin (Todaro and Green, 1963).

### **3.10.4 Tumor analysis**

To analyse the occurring tumors, mice were sacrificed by cervical dislocation and opened ventrally. All mammary glands were excised for tumor-measurement. Tumor size and mass were analysed by metrical measurement and weighing of the tumor tissue and the mammary gland tissue independently. Raw-data were normalised to bodyweight. All data are shown as mean  $\pm$  SDM. All p-values were calculated using the students T-Test and values  $< 0.03$  were considered statistically significant.

### **3.10.5 Analysis of lung metastases**

For pathological analysis and quantitation of metastases, prepared lungs were sectioned and analysed at 800 to 1000 $\mu$ m intervals. Sections were stained with hematoxilin and eosin (H&E, Fluka, Switzerland) to identify lung metastases under the light microscope. Metastatic burden was calculated based on number and size of metastatic lesions.

### **3.10.6 Immunohistochemistry on murine organs and tumor sections**

Tumor samples and tissues were fixed in 70 % Ethanol at 4°C overnight. On the next day samples were embedded in paraffin and sections of 4-8 $\mu$ M were cut on a microtome (HM355S, microm). The sections were subjected to deparaffinisation in xylene and rehydrated in a graded series of ethanol. Antigen retrieval was achieved by cooking in citrate buffer (pH 6) in a microwave. Immunohistochemical staining was done with the Vectastain Staining Kit (Vector Laboratories, Burlingame) following the manufacture's protocol. After blocking with 10% horse serum in PBS buffer containing 3% Triton-X for one hour, the sections were incubated with the primary antibody ( $\alpha$ FGFR4 Hs121, Santa Cruz) at 4°C overnight. The secondary antibody ( $\alpha$ -rabbit, VectorLabs, USA) was incubated for one hour in PBS buffer containing 3% Triton-X. Mayer's Hematoxylin (Fluka, Switzerland) was used as counterstain.

### **3.10.7 Injection of nude mice**

For injection 6-8 week old female Balb/C Nu/Nu mice were used. Here  $7 \times 10^6$  NHDF cells (p53/Rb double knockdown or mock transfected) or  $2 \times 10^6$  MDA-MB-435S (as a positive control) cells were injected subcutaneously in the flank of the mice. The state of health of the injected mice was controlled repeatedly per week. If there was a visible tumor growth mice were sacrificed by cervical dislocation and the tumor growth was monitored.

## 4 Results

### 4.1 Establishment of an *in vitro* transformation system

#### 4.1.1 Knockdown strategy of p53 and Rb; physiological output on proliferation and G2 Arrest upon p53 and Rb reduction in non-cancerous human primary cells

In order to establish an *in vitro* transformation system, two strategies were tested to efficiently knockdown the tumor suppressors p53 and Rb. On the one hand, several siRNAs against p53 and Rb were tested for their knockdown capacity. The most efficient ones were then cloned in the pRETRO Super vector and transfected in HEK293 cells to obtain stable knockdown cells. Unfortunately, these constructs had a low or no knockdown efficacy due to a possibly ineffective structure of the siRNAs.

On the other hand plasmids containing shRNAs against p53 and Rb that were available at the core facility of the MPI of Biochemistry in Martinsried were tested. As shown in Figure 11 both constructs displayed a sufficient knockdown after transfection into HEK293 cells. Hence, these constructs were further used to generate a stable knockdown of p53 and Rb in non-cancerous immortalized cell lines HEK293, HaCaT and MCF10A. As a negative control HEK293, HaCaT and MCF10A cells were stably transfected with a construct expressing a non-silencing shRNA.

## Results

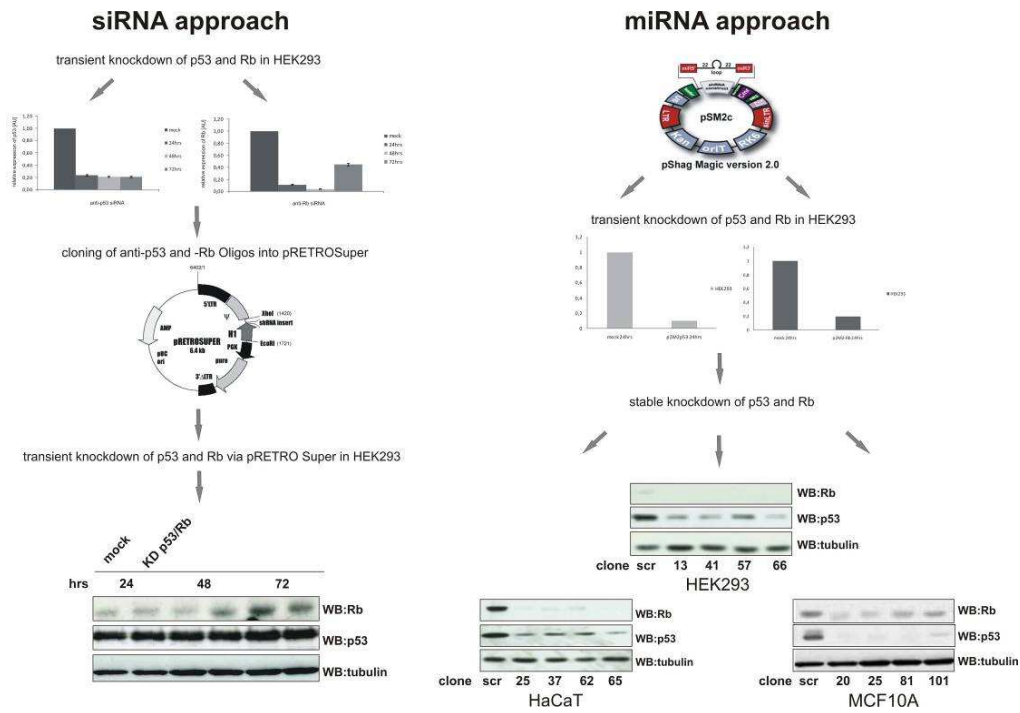


**Figure 11: Knockdown strategy of the tumor suppressors p53 and Rb; The knockdown strategy on the left hand displays the use of the siRNA approach; after analyzing the knockdown efficacy of several siRNAs the most efficient siRNAs were cloned into pRETROSuper for stable transfection. Transient transfection of the constructs displayed an insufficient knockdown of the target genes; on the right hand p53 and Rb were downregulated by a miRNA approach in HEK293, HaCaT and MCF10A cells; transient knockdown displayed sufficient efficacy, so that stable double-knockdown clones were established.**

As p53 and Rb are key regulators of the cell cycle and the main guardians of the integrity of the genome (Classon and Harlow, 2002; Vogelstein et al., 2000), the impact of a stable knockdown of these two tumor suppressors was assayed by a proliferation and cell cycle arrest assay via FACS analysis. As seen in Figure 12 A the knockdown of p53 and Rb resulted in an accelerated proliferation of all tested cell lines. Accordingly, the cell lines displayed a decreased growth arrest after treatment with doxorubicin for 24 hours, a chemotherapeutic drug that causes DNA damage which guides cells into growth arrest or apoptosis (Figure 12 B). Hence the knockdown of p53 and Rb in HEK293, HaCaT and MCF10A cell lines displayed the expected cell biological output to manipulate cells into uncontrolled cell growth by loss of cell cycle control even in the presence of a DNA-damaging agent.

Results

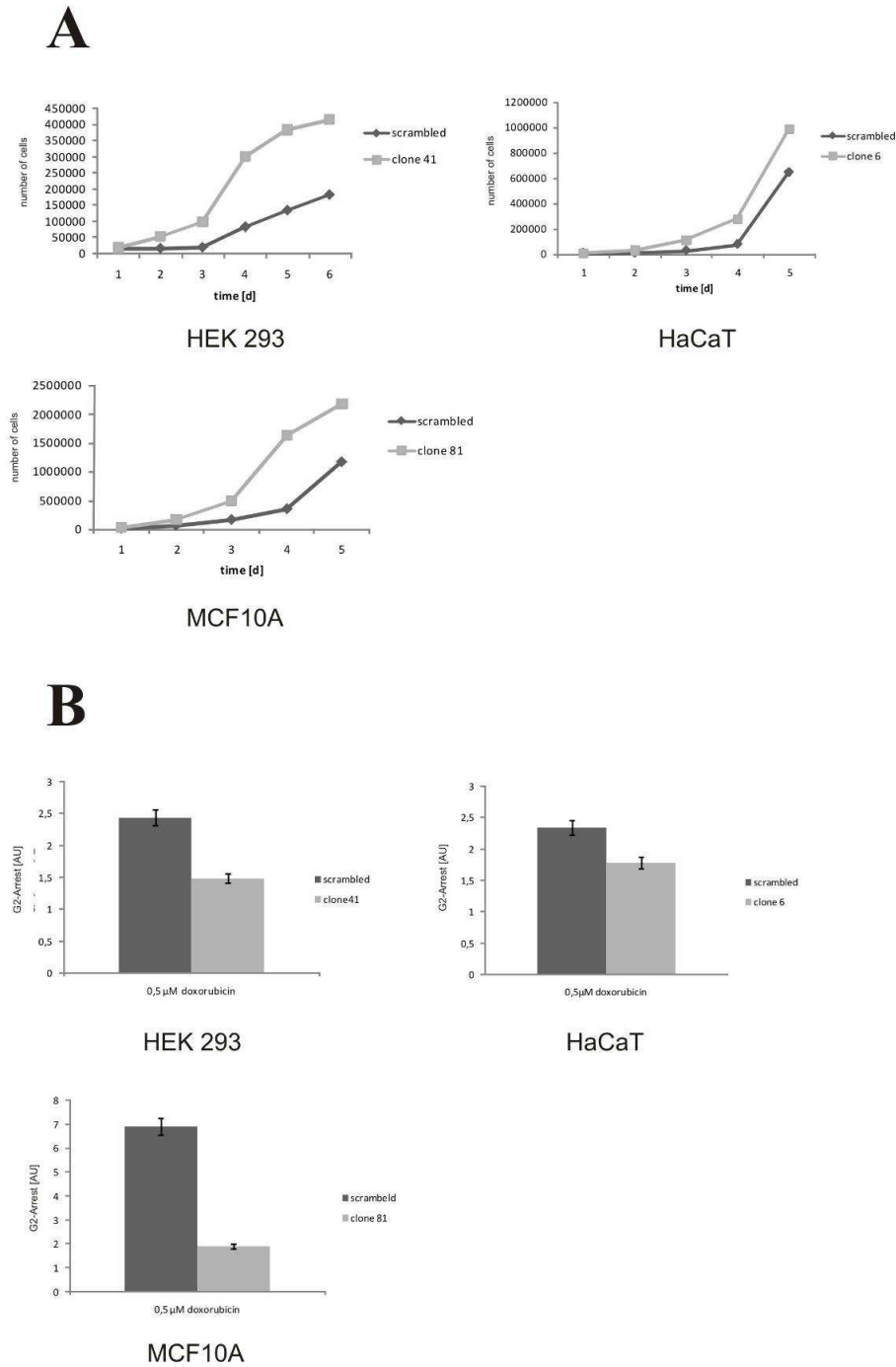


**Figure 12: Increased cell proliferation and decreased G2-Arrest in p53/Rb knockdown cell lines** A) The knockdown of p53 and Rb facilitates proliferation in HEK293, HaCaT and MCF10 A cells (n=3); B) The knockdown of p53 and Rb decreases the number of cells arresting in G2 after 24 hours of doxorubicin-treatment (0.5 μM) in HEK293, HaCaT and MCF10 A cells (n=3);

#### 4.1.2 Reduction of p53 and Rb in primary normal human dermal fibroblasts (NHDF)

Routinely used non-cancerous cell lines are artificially immortalized and thereby released from senescence and primed for the establishment of a neoplastic phenotype. Furthermore, the perpetual subculturing of these cells enables the accumulation of mutations. For that reason, typical non-cancerous cell lines do not reflect the status of real primary cells. Therefore, the stable knockdown of the tumor suppressors p53 and Rb was established in normal human dermal fibroblasts as seen in Figure 13 (further referred as NHDFdk). As a negative control NHDF cells were stably transfected with a construct expressing a non-silencing shRNA (further referred NHDFscr).

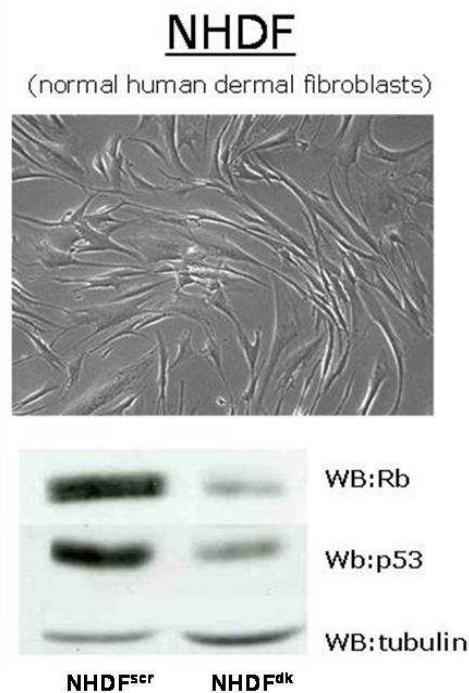


**Figure 13: Stable knockdown of p53 and Rb in normal human dermal fibroblasts (NHDF); NHDFscr cells were stably transfected with a non-silencing shRNA construct; knockdown verification via Western Blot Analysis; tubulin served as a loading control**

##### 4.1.2.1 Increased proliferation, morphological changes and decreased senescence in NHDF cells deficient for p53 and Rb

As a proliferative advantage should be also observed in NHDF deficient for p53 and Rb the population doubling rate (PDR) was monitored in comparison to mock transfected NHDFscr. Moreover, the calculation of population doubling rates displays a possible prolonged life span

and immortalisation of the manipulated cells. These processes are necessary to take place and are one of the first anti-cancer barriers to be overcome in the process of oncogenesis (Ha et al., 2008; Prieur and Peeper, 2008). As shown in Figure 14A NHDFdk cells display an increased PDR compared to mock transfected cells indicating a loss of cell cycle control induced by the knockdown of p53 and Rb. Furthermore, after 15 population doublings (PDs) NHDFs normally enter replicative senescence, a process activated by diverse intrinsic and extrinsic stresses e.g. telomere shortening (Prieur and Peeper, 2008). In contrast NHDFdk overcome this permanent growth arrest and display a normal growth rate even after 30 calculated population doublings. Therefore, NHDFdk seem to be immortalized as the doubling of a normal growth rate is expected to occur only in immortalized cell lines (Gray-Schopfer et al., 2006).

Under the microscope, NHDFdk cells display a more vital phenotype than NHDFscr cells and show a smaller cell volume. This phenotype is similar to transformed NIH 3T3. As the knockdown cells exhibited accelerated proliferation, the expression of typical cell cycle progressors, like Cyclin A or D were analyzed in NHDFdk cells (Figure 14B). Whereas NHDFscr show downregulation of Cyclin A and D and thereby decelerate their proliferation over time, at least Cyclin D gets upregulated in NHDFdk indicating increased proliferation. Furthermore, the mRNA expression level of the two cell cycle promoting kinases Aurora Kinase A and B were analyzed as shown in Figure 14C. Similar to Cyclin A and D, NHDFscr cells display a decrease in Aurora Kinase A and B over time indicating a deceleration of the cell cycle. In contrast, NHDFdk cells exhibit an increase of both Aurora Kinase A and B over time. Along these lines, the overexpression of these two cell cycle kinases is a common event in transformed cells (Keen and Taylor, 2004).

Results

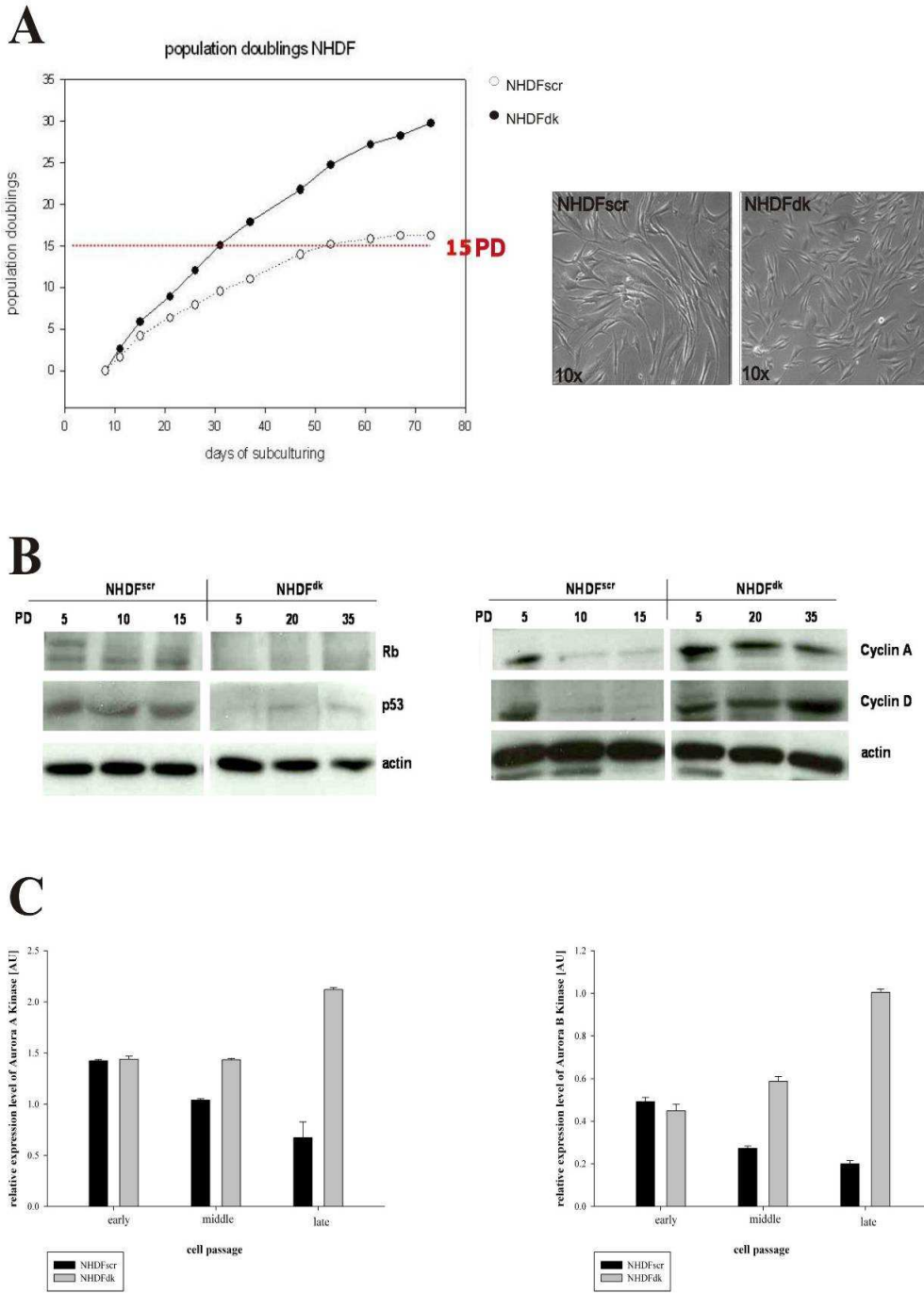
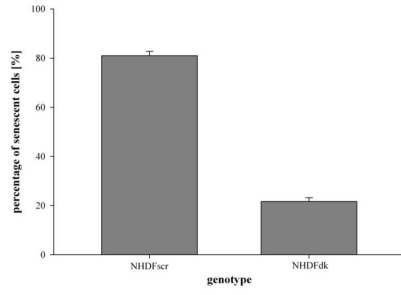
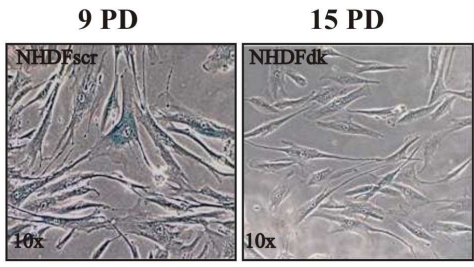


**Figure 14: Increased proliferation and morphological changes in NHDFdk cells** A) NHDF deficient for p53 and Rb display an increased proliferation, prolonged life span and seem to be immortalized. Further NHDFdk display a smaller and more viable phenotype (n=2); B) NHDFdk cells maintain the expression of the cell cycle promotor Cyclin A and increase the expression of Cyclin D indicating a progressed cell cycle; (n=2); C) NHDFdk cells overexpress Aurora Kinase A and B indicating an increased proliferation (n=2); PD=population doubling

Next to the analysis of cell cycle progression in NHDFdk cells, the occurrence of senescence was analyzed via staining of  $\beta$ -galactosidase, an enzyme which is predominantly expressed in senescent cells (Bandyopadhyay et al., 2005). As seen in Figure 15A senescence in NHDFscr cells occurs after 9 PDs whereas NHDFdk cells display no senescence even after 15 PDs. The occurrence of senescence was further quantified. Hence, the NHDFdk display increased proliferation with a decreased onset of senescent cells, a prolonged life span and seem to overcome senescence and enter an immortalized phenotype. To further analyze the occurrence of permanent growth arrest the expression pattern of NHDFdk regarding the senescence inducing and thereby tumor suppressive proteins p27, p21 and p16 were monitored (Figure 15B). On mRNA level all investigated tumor suppressors displayed a clear downregulation or no upregulation in high population doubling rates compared to NHDFscr cells. Here the expression of tumor suppressors is accelerated indicating the induction of senescence visualized by the  $\beta$ -galactosidase staining (Herbig et al., 2004).

Results

**A**



**B**

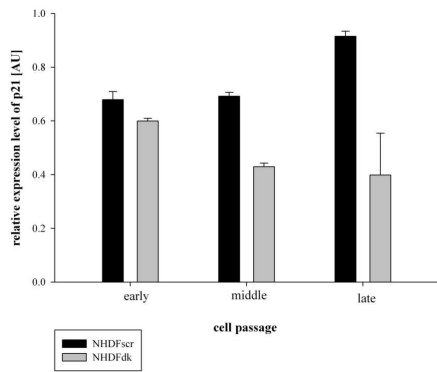
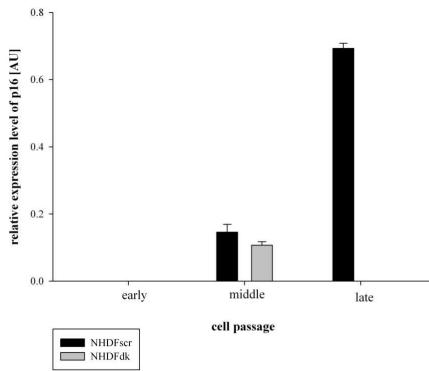
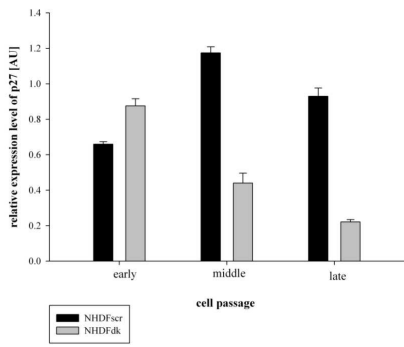
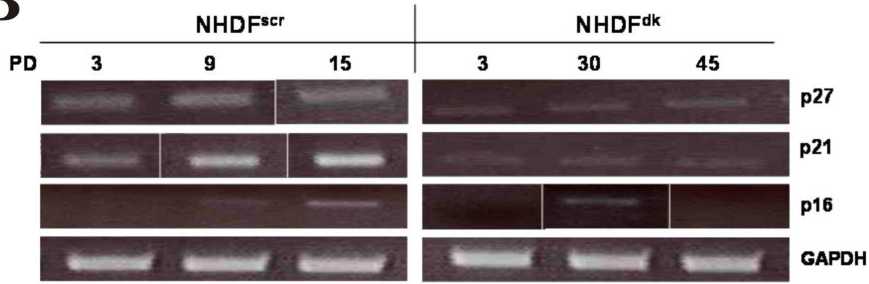
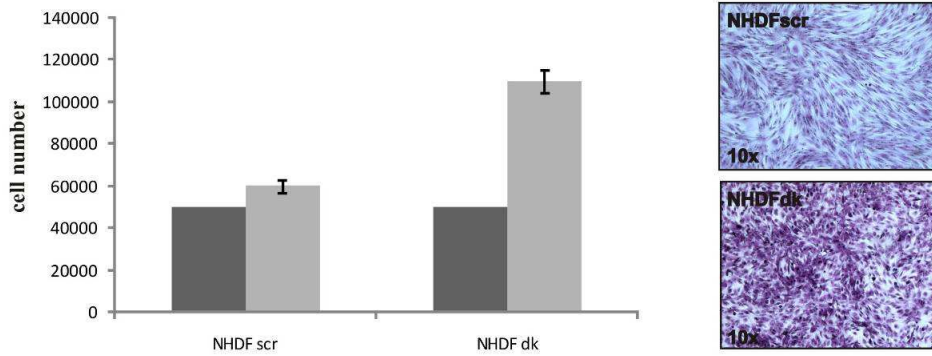


**Figure 15: Decreased senescent phenotype in NHDFdk cells and downregulation of tumor suppressors** A)  $\beta$ -galactosidase staining of senescent cells; Senescence in NHDFscr occurs after 9PDs, NHDFkd cells display only a slight positive  $\beta$ -galactosidase staining even after 15 PDs; the percentage of positively stained cells was quantified (n=3); B) tumor suppressors p27, p16 and p21 are downregulated in NHDFdk cells compared to NHDFscr cells indicating the absence of senescence (n=2); expression were quantified on GAPDH expression level; PD= population doubling

#### 4.1.2.2 Reduction of contact inhibition, anchorage independence and invasion in NHDF deficient for p53 and Rb

Transformed cells acquire or loose specific characteristics associated with a malignant phenotype of cancer cells. An important property of cells of the multicellular organism is their ability to stop proliferating when the space allotted to them has been filled. Also *in vitro*, normal cells fill the surface of the culture dish but stop in the G1/G0 phase of the cell cycle, when a dense monolayer has been formed. For tumor formation *in vivo* or focus formation *in vitro* it is essential for a single cell to overcome such a contact inhibition (Herrlich et al., 2000). For that reason, NHDFdk cells and NHDFscr cells were seeded on subconfluency and grown for 72 hours. As seen in Figure 16A, NHDFdk cells clearly continue proliferating in a confluent culture compared to NHDFscr controls indicating the reduction of contact inhibition. If this confluent cell culture was stained with crystal violet, NHDFdk cells display a disordered cell layer compared to the typical fibroblastic layer of NHDFscr cells. A further characteristic of a malignant cell is the ability to grow anchorage independently. By acquisition of anchorage independence, cancer cells are able to disseminate from the primary tumor and enter the lymphatic or blood stream for the invasion of distant organs. For that purpose, NHDFdk and scr cells were seeded in non-coated culture dishes to prevent adherence of the cells. The prevention of adherence should induce anoikis in the NHDFscr cells, a form of apoptosis induced by the loss of cell-cell or cell-matrix interactions. As seen in Figure 16B NHDFdk cells are able to build cell clusters by proliferating over 72 hours. In contrast, NHDFscr cells display a reduced number of cells after 72 hours indicating apoptosis by anoikis. Hence, NHDFdk cells acquired the ability to grow without adherence (Chiarugi and Giannoni, 2008; Simpson et al., 2008). To further characterize the malignant phenotype of the NHDFdk cells the expression of known oncogenes was analyzed. As seen Figure 16C the oncogene H-RAS is not expressed in NHDFdk cells. In contrast, the oncogenic kinase SRC is overexpressed in NHDFdk over time. That overexpression possibly contributes to the pre-malignant phenotype of NHDFdk cells namely the loss of contact inhibition and the ability to grow anchorage independently.

**A**



**B**

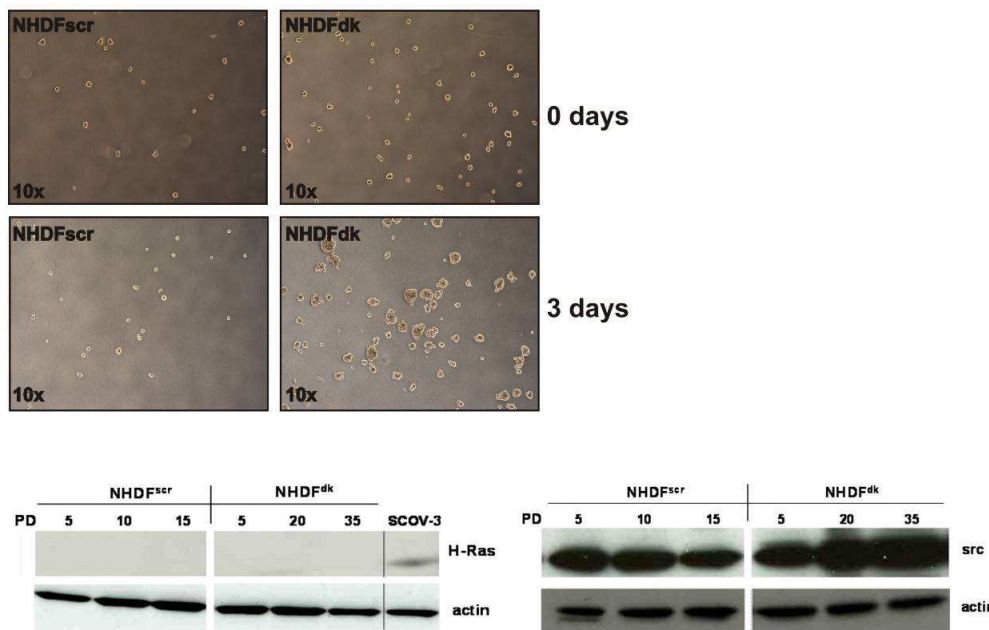


**Figure 16: NHDFdk display loss of contact inhibition and increased anchorage independent growth; A) NHDFdk cells display cell proliferation in confluent subculture indicating the loss of contact inhibition; NHDFdk cells stained with crystal violet display a disordered cell layer compared to NHDFscr (n=3); B) NHDFdk display anchorage independent growth in non-coated cell culture dishes and form typical cell clusters compared to NHDFscr cells (n=3); expression analysis of known oncogenes shows an overexpression of SRC in NHDFdk cells over time; H-RAS is not expressed (n=2); PD= population doubling**

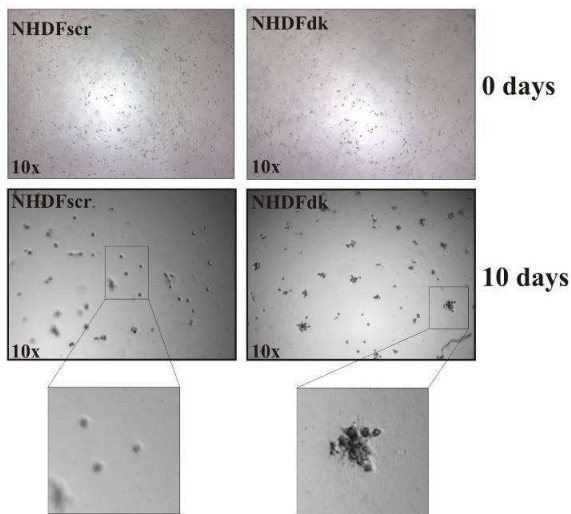
A further indication for a cancerous and invasive potential is the branching in Matrigel by deconstructing the pseudo-extracellular matrix by upregulation of Matrix-Metalloproteinases (Staheta et al., 2008). As seen in Figure 17A NHDFdk cells display cell clusters when grown for 10 days on Matrigel. In contrast, NHDFscr cells were not able to grow under these

## Results

conditions. This proliferation is the first hint for an invasive potential of cells. Furthermore, as seen in the magnification of Figure 17A NHDFdk cells display a slight branching ability compared to mock transfected cells. Hence, the NHDFdk cells seem to be able to degrade the Matrigel. To further analyze the invasive potential the m-RNA expression of the Matrix-Metalloproteases (MMP) 14, 9 and 2 was analyzed as the activation of MMPs is essential for the decomposition of Matrigel. As seen in Figure 17B MMP 14 is not upregulated in NHDFdk cells. In contrast, MMP9 and 2 are clearly upregulated in NHDFdk cells when compared to NHDFscr cells. Thus, MMP9- and 2-overexpression in NHDFdk cells may explain the observed slight invasive phenotype.

Taken together, these results indicate that the knockdown of p53 and Rb in NHDF enables the acquisition of typical properties of cancer cells and display distinct hallmarks of progressing oncogenesis in NHDFdk cells.

**A**



**B**

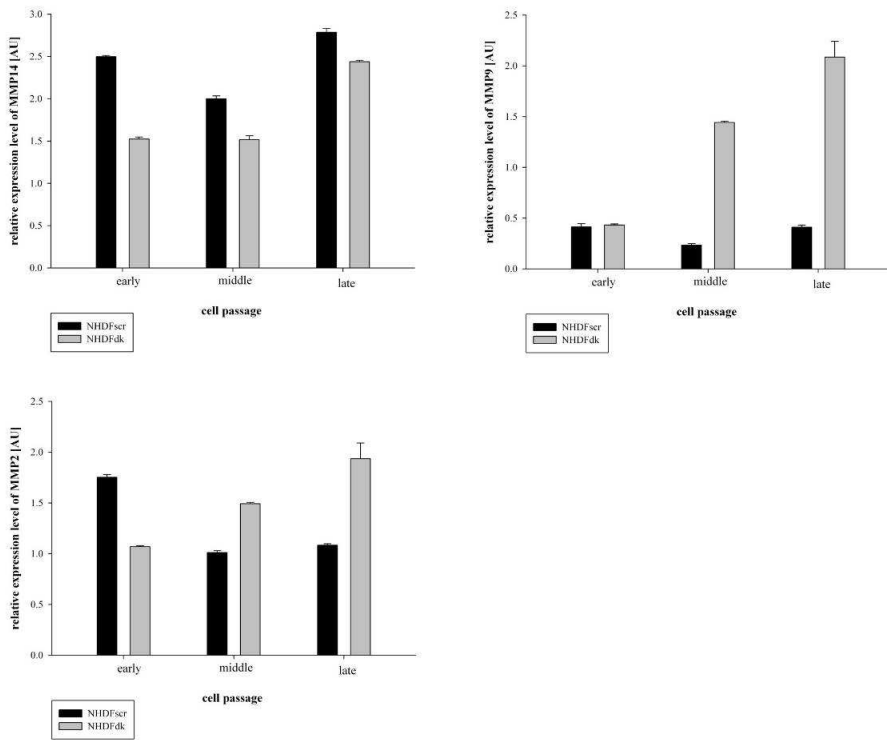


**Figure 17: Invasion in NHDFdk cells and expression of MMPs; A) NHDFdk display focus formation in Matrigel with a slight branching activity, indicating a certain invasiveness when compared to NHDFscr**

(n=3); B) NHDFdk cells overexpress MMP2 and 9 over time; MMP14 is not overexpressed when compared to NHDFscr cells (n=2)

#### **4.1.2.3 NHDFdk cells display karyotypic abnormalities and tolerate extended telomere shortening**

The acquisition of typical properties of cancer cells depends on aberrations of the destabilized genome. Uncontrolled cell division cycles can result in chromosomal aberrations and progressing genomic instability. Once the genome is altered through aberrant fusions, translocations or deletions, malignant cells can change their gene expression pattern and their physiological behaviour. Hence, genomic instability and DNA-damage are one of the most prominent processes in cellular transformation (Cheung and Deng, 2008; Hanahan and Weinberg, 2000; Jeggo, 2005; Li and Li, 2006; Lingle et al., 2005).

To analyze NHDFdk cells for the occurrence of genomic instability, the expression of several markers for DNA-damage and uncontrolled cell division were monitored over time. As seen in Figure 18A NHDFdk cells upregulate the active form of H2AX, the so called  $\gamma$ H2AX, which gets activated by damaged DNA, thereby initiating a signalling cascade that results in either growth arrest and DNA-repair or apoptosis (Fillingham et al., 2006; Halicka et al., 2005). The upregulation of this Histone in its active form occurs at high population doubling rates, indicating that the DNA damage takes place as a result of the prolonged life span and uncontrolled cell proliferation induced by the loss of p53 and Rb. Furthermore, the m-RNA expression of Mad (mitotic- arrest-deficient-like) 1 and Mad 2 were analyzed. These two cell cycle checkpoint proteins prevent cells of entering in anaphase if the chromosomes are not properly organized for cell division. Several studies showed that the loss of Mad1 and 2 in cancer cells results in chromosomal instability. The overexpression of Mad1 and 2 results in suppression of proliferation or the malignant phenotype of cancer cells (Chen et al., 1995; Vastrik et al., 1995; Zou et al., 2006). As seen in Figure 18A the expression of Mad2 is comparable between NHDFdk and NHDFscr cells. In contrast, Mad1 is lost in NHDFdk cells over time and gets clearly upregulated in NHDFscr cells. These data indicate an elevated cell cycle rate in NHDFdk cells and possible chromosomal instability as a result of a defective checkpoint control.

Because of these results, the number of chromosomes in NHDFscr and NHDFdk was analyzed over time to investigate if there are accelerated chromosomal alterations with increasing population doublings. Accordingly, the number of chromosomes in NHDFscr cells was kept stable till senescence occurs. In comparison, NHDFdk cells lost their integrity of the genome after about 25 PDs with an increasing number of aneuploid cells displaying more or

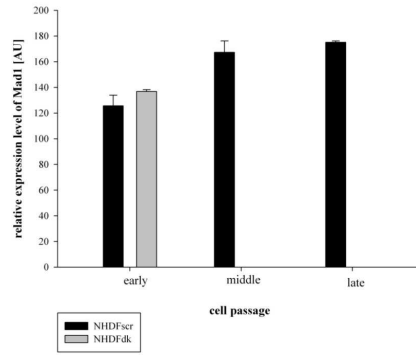
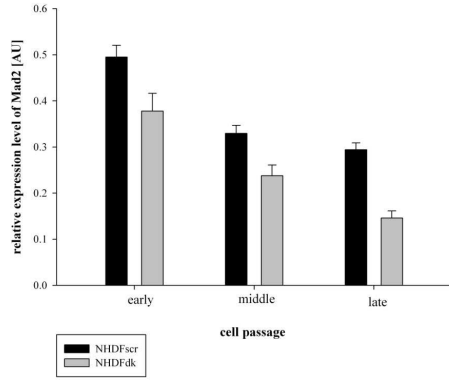
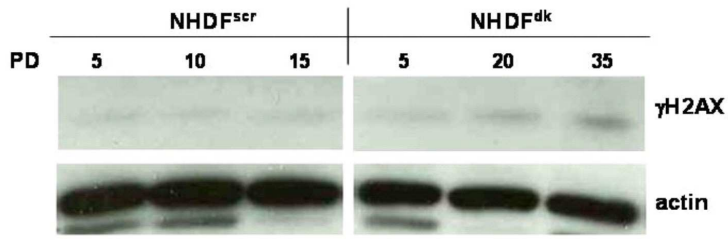
## Results

less than 46 chromosomes. These results indicate that one of the most prominent hallmarks of cancer, the genomic instability and the accumulation of chromosomal aberrations, takes place after the loss of p53 and Rb in normal human dermal fibroblasts.

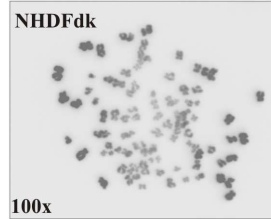
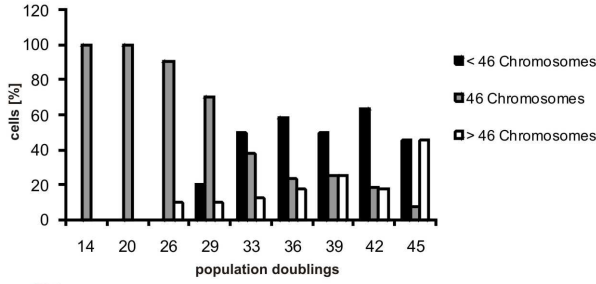
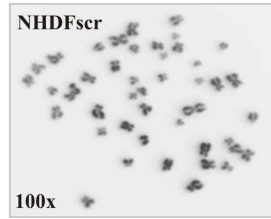
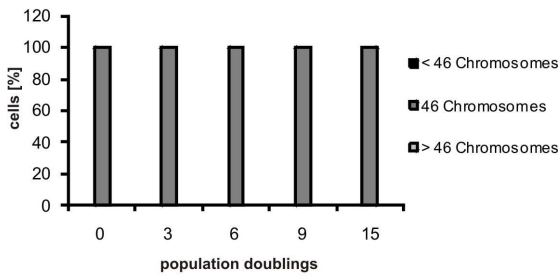
As telomere shortening is a barrier of tumorigenesis by initiating permanent growth arrest, reactivation of telomerase is a common event in cancer progression. As seen in Figure 18C NHDFdk cells do not reactivate telomerase expression as analyzed by Western Blotting. These data indicate the possibility of another mechanism of telomere-stabilizing, so called ATL (alternative telomere lengthening) that should prevent cells from entering a mitotic crisis (Cesare and Reddel, 2008; Shay and Wright, 2005). As NHDFdk cells do not reexpress telomerase it was important to analyze the length of telomeres in these cells as another mark of chromosomal aberration. For that purpose, a telomeric PCR was performed as seen in Figure 18C. The single copy gene 36B4 served as loading control. Here, NHDFdk cells display an augmented telomere shortening compared to NHDFscr cells. Human embryonic lung cells (HEL), Melanocytes and mammary epithelial Ac745 cells served as a control regarding the telomere length of primary cells. MDA-MB435S and MDA-MB-231 cells served as a positive control regarding telomere lengthening via telomerase reactivation. This result indicates that the loss of p53 and Rb enables the cell to tolerate an extended telomere shortening that may result in the aforementioned instability of the genome.

Results

**A**



**B**



**C**

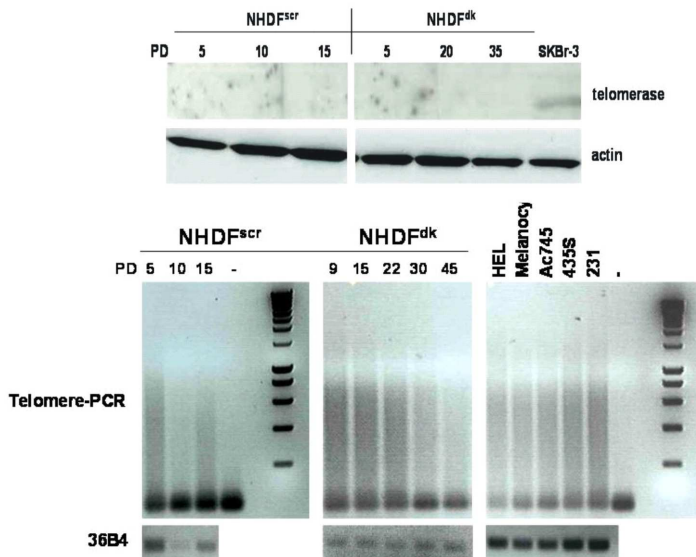


Figure 18: NHDFdk cells show accelerated DNA damage and chromosomal aberrations and tolerate an extended telomere shortening; A)  $\gamma$ H2AX gets upregulated in NHDFdk cells as an indicator of DNA damage; whereas the expression of Mad2 display no difference the expression of Mad1 is lost in NHDF dk cells over time compared to NHDFscr cells (n=2); B) karyotypal analysis of NHDFscr cells display a normal genome whereas NHDFdk cells accumulate aneuploid cells over time; C) NHDFdk cells display no reactivation of telomerase expression; NHDFdk cells tolerate extended telomere shortening compared to NHDFscr cells (n=10); PD= population doubling

#### 4.1.2.4 NHDFdk cells do not establish a stem cell-like cancer cell subpopulation

In recent years, more and more attention has been drawn to stem cells and their implication in tumor progression. Cancer-stem cells seem to be involved in tumor initiation and progression and seem to be responsible for resistance certain therapies (Bjerkvig et al., 2005; Dean et al., 2005; O'Brien et al., 2007). Further, recent publications show, that a lot of routinely used cancer cell lines and tumors contain a subpopulation of cancer stem cells that display a highly aggressive malignant phenotype when isolated from their original culture (Ho et al., 2007; Huang et al., 2008; Sung et al., 2008). For this reason, two experiments were performed to analyze, if NHDFdk cells developed a cancer stem cell subpopulation. As stem cells upregulate the ABCG2 transporter, a Hoechst 33324 dye assay was performed (Scharenberg et al., 2002). If the ABCG2 transporter is upregulated the dye should be transported out of the cell. As seen in Figure 19A there is no difference between NHDFscr or NHDFdk cells demonstrating that this stem cell marker is not present to accelerate the efflux of Hoechst 33324. Furthermore, there was no stem cell-like subpopulation detectable microscopically, as stem cells display a roundish, barely attached phenotype.

Next, a surface expression assay of stem cell markers was performed via FACS analysis. Here, the expression of CD34 and CD44 were analyzed. Cos7 cells and KG1a cells served as negative and positive control, respectively. As shown in Figure 19B CD34 is not expressed in NHDFdk cells. In contrast, CD44 is upregulated in NHDFdk cells. However, this elevated surface expression of CD44 seems to be rather a result of the loss of p53 than an indication for the presence of a stem cell subpopulation (Godar et al., 2008).

In summary, NHDFdk cells neither overexpress ABCG2 nor express typical stem cell surface markers. Hence, NHDFdk cells seem not to develop a cancer stem cell subpopulation as a result of p53 and Rb deficiency.

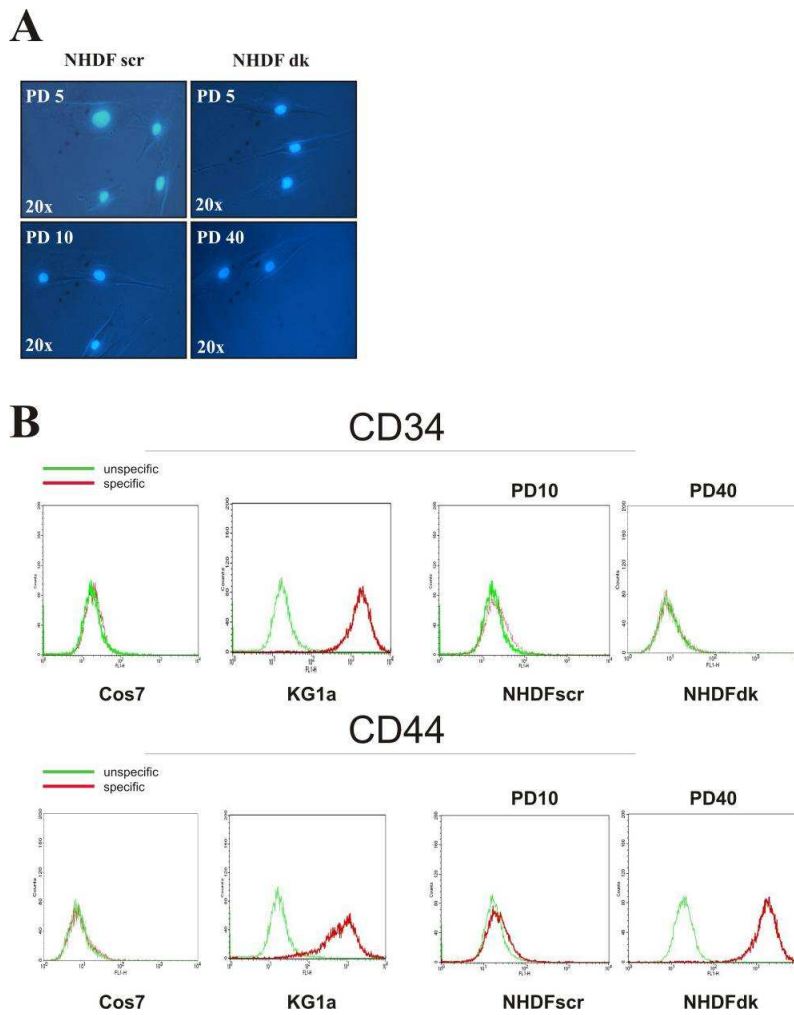


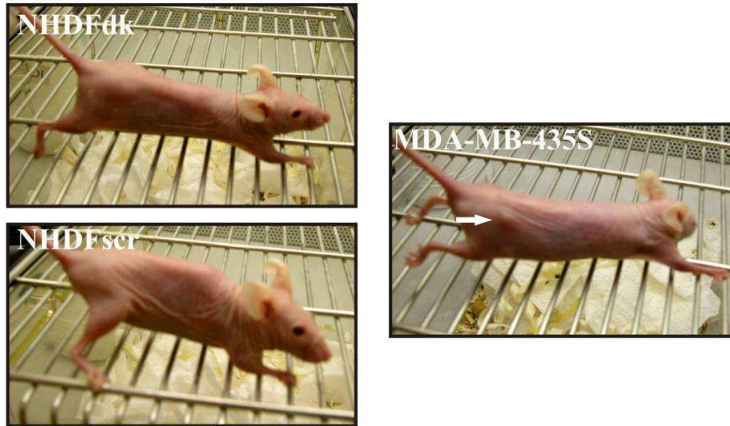
**Figure 19: NHDFdk cells do not develop a stem-cell like cancer cell subpopulation; A) NHDFdk do not express the Hoechst 33324 efflux pump and stem cell marker ABCG2 (n=3); B) NHDFdk cells do not express the stem cell surface marker CD34, but do express CD44 (n=3); PD= population doubling**

**4.1.2.5 The malignancy of NHDF cells deficient for p53 and Rb is not potent enough to induce tumor growth in nude mice**

All aforementioned experiments display a distinct hint for the successful malignant transformation of NHDF cells deficient for p53 and Rb. Nevertheless, it is essential to investigate the malignancy of cells in a so called “animal culture” that examines subcutaneous tumor growth in nude mice. For that purpose, NHDFdk and NHDFscr cells were injected subdermally in the flanks of female Balb/C Nu/Nu mice to monitor tumor growth *in vivo*. The injection of the highly aggressive MDA-MB-435S cells served as a positive control for tumor growth. As seen in Figure 20A only the MDA-MB-435S cells display visible tumor growth

after 3 month. In contrast, even after 9 month, no visible tumors could be detected in mice injected with NHDFdk cells (Figure 20 A/B). As expected, mice injected with the negative control NHDFscr cells displayed no tumor growth after 9 month. These data suggest that the knockdown of p53 and Rb just partially transforms NHDF cells, but this level of malignancy is not potent enough to promote tumor growth *in vivo*. Furthermore, the used Balb/C nude mice just partially lack their immunessystem, which may explain the relatively poor tumor growth. The use of other nude mice strains possibly could overcome this limitation and may result in tumor growth of the NHDFdk cells.

**A**



**B**

cell line	tumors/inj.mice	time [month]
NHDFdk	0/5	9
NHDFscr	0/3	9
MDA-MB-435S	2/2	3

Figure 20: NHDF cells deficient for p53 and Rb display no tumor growth *in vivo* (NHDFdk); A) injected NHDFdk cells display no tumor growth *in vivo*; NHDFscr cells served as negative control, MDA-MB-435S cells served as positive control and display obvious tumor growth indicated by the white arrow; B) nine month after cell injection wether NHDFdk (0/5) nor NDHDscr (0/3) cells display visible tumor growth; MDA-MB-435S cells display visible tumor growth after 3 month (2/2)

## 4.2 The impact of the FGFR4 and its variant Arg385 on tumor progression

Since an impact of the human *FGFR4* Arg388 allele on tumor progression was only shown in correlative studies on patient populations with an otherwise heterogeneous genetic background, there was an urgent need to ultimately prove the influence of this single nucleotide polymorphism (SNP) on tumor progression *in vivo*. Here, the defined genetic background of a mouse model overcomes the problem of genetic heterogeneity of patient cohorts and thus the cause of diverging conclusions. We generated a *FGFR4* Arg385 (corresponding to human codon 388) knock-in (KI) model in the genetic background of SV/129 mice, which represents the first directly targeted KI mouse model to investigate the impact of a single nucleotide polymorphism on the progression of cancer. In order to generate the *FGFR4* Arg385 allele, the Glycine in exon 8 was changed to an Arginine by site-directed mutagenesis. A neomycin selection cassette flanked by loxP sites was cloned between exons 10 and 11 (Figure 21A). After gene targeting, neomycin-resistant ES-cell clones were analyzed by southern blotting and PCR-RFLP of the genomic DNA (Figure 21B 1-2) (Southern, 1974).

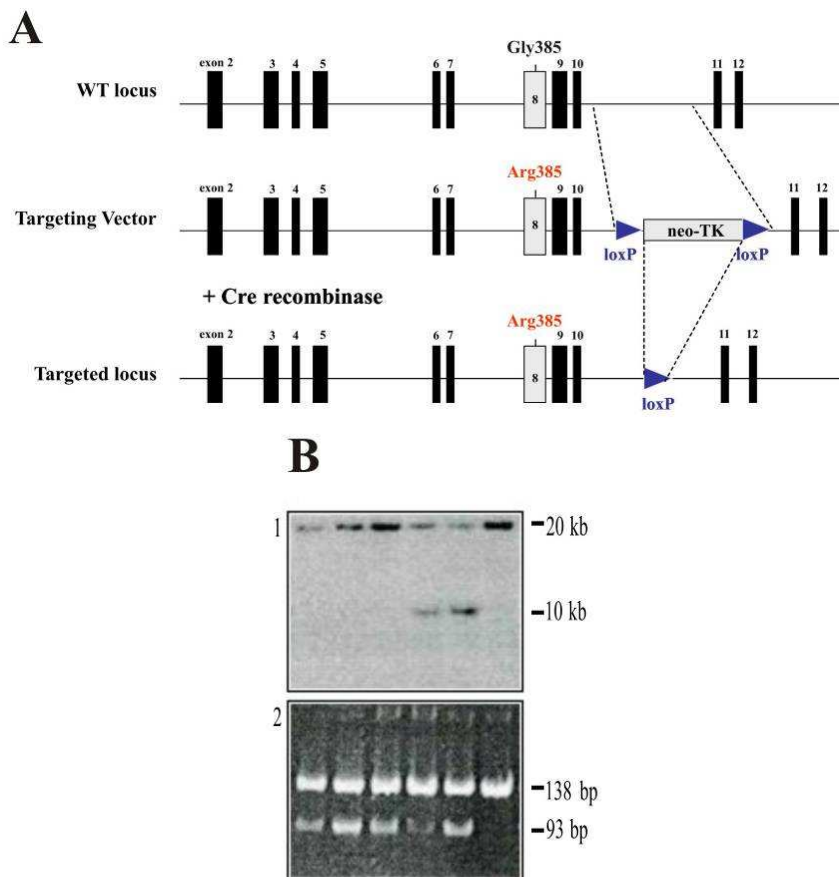


**Figure 21:** A) *FGFR4* Arg385 KI gene-targeting construct: *FGFR4* wt locus spanning exons 2 to 12 of the murine *FGFR4* genomic sequence; targeted locus: exon 8 contains the SNP established via specific mutagenesis, selection-cassette flanked by loxP-sites for Cre-deletion is introduced between exon 10 and 11;

B) 1) Southern Blot analysis of ES-cell clones after gene targeting: positive clones display an additional 10kb fragment detected by a 5'external probe 2) genotyping of ES-cell clones via PCR-restriction fragment length polymorphism (RFLP): positive clones contain an additional fragment of 93 bp after *Mva I* restriction enzyme (S. Streit, 2004)

Gly385: Glycin at codon 385; Arg385: Arginin at codon 385; Neo: Neomycin-resistance; TK: thymidin-kinase-cassette

Next, positive clones were injected into blastocysts of pseudo-pregnant mice to generate chimeras. These mice were then backcrossed to C57BL/6 mice to raise the first generation of *FGFR4* Arg385 KI mice. In order to delete the neomycin selection cassette, the *FGFR4* Arg385 mice were crossed to mice transgenic for the *Cre-recombinase* (Deleter-Cre).

*FGFR4* Arg385 KI Cre-deleted mice were analyzed by segregation analysis of a statistically significant number of mice for Mendelian inheritance of the *FGFR4* allele (Table 8). In backcrosses to *FGFR4* Gly/Gly385 mice, the offspring displayed the expected distribution of 1:1 from *FGFR4* Gly/Gly385 to *FGFR4* Gly/Arg385. Heterozygote intercrosses displayed the

expected distribution of 1:2:1 from *FGFR4 Gly/Gly385* to *Gly/Arg385* to *Arg/Arg385*. Hence, the *FGFR4 Arg385* allele is inherited in the correct Mendelian ratio.

**Backcross: *FGFR4 Gly/Gly385* x *FGFR4 Gly/Arg385***

	Gly/Gly	Gly/Arg	Arg/Arg	total
mice	65	55	0	120
[%]	54	46	0	100
exp [%]	50	50	0	

**Intercross: *FGFR4 Gly/Arg385* x *FGFR4 Gly/Arg385***

	Gly/Gly	Gly/Arg	Arg/Arg	total
mice	25	57	25	107
[%]	23	54	23	100
exp [%]	25	50	25	

**Table 8: Segregation analysis of *FGFR4 Arg385* KI mice: The *FGFR4 Arg385* allele is inherited in the correct Mendelian ratio; progeny of backcrosses (*FGFR4 Gly/Gly385* x *FGFR4 Gly/Arg385*) is distributed 1:1, progeny of intercrosses (*FGFR4 Gly/Arg385* x *FGFR4 Gly/Arg385*) is distributed 1:2:1.**

#### 4.2.1 Characterisation of the *FGFR4 Arg385* KI mouse

In humans, the *FGFR4 Arg388* allele is expressed in various tissues without any differences compared to the *FGFR4 Gly388* and has yet no known impact on the healthy organism itself (Bange et al., 2002). Similarly, the *FGFR4 Arg385* KI mouse model displays no obvious phenotype that distinguishes it from *FGFR4 Gly385* carrying mice (data not shown). To analyze if the generated *FGFR4 Arg385* KI mice display a pathological phenotype matching human patients with the same SNP genotype and show similar characteristics of FGFR4 expression, localization and distribution, we first analyzed FGFR4 mRNA- and protein- levels and analyzed the localization and distribution in various tissues of 3 month old female mice with different FGFR4 genotypes.

As shown in Figure 22A and B FGFR4 is expressed in various tissues including mammary gland, lung, brain or liver. The investigated *FGFR4 Gly/Gly385*, *FGFR4 Gly/Arg385* and *FGFR4 Arg/Arg385* mice displayed no altered expression of the FGFR4 neither on mRNA nor on the protein level in the presence of the *FGFR4 Arg385* allele. Next, we analyzed the expression and localization of the FGFR4 in different tissues immunohistochemically. Figure 22C displays the FGFR4 expression and localization in the lung and the mammary gland of *FGFR4 Gly/Gly385* and *FGFR4 Arg/Arg385* mice. Here, the lung tissue, displays a clear FGFR4 staining in smooth muscles, blood vessels and bronchial epithelial cells. In the mammary gland tissue, blood vessels and ductal epithelial cells show distinct FGFR4

## Results

expression. The magnification shown further indicates a membranous and cytoplasmic localization of the FGFR4. Figure 22D summarizes the immunohistochemical analysis of FGFR4 expression and quantifies the levels of FGFR4 staining in the different compartments of the investigated tissue. Similar to the observations on mRNA-level and protein-level neither localization, distribution nor the level of expression changes in the presence of the *FGFR4 Arg385* allele. Here, FGFR4 is detectable in various tissues and, as with mRNA or protein expression levels; there is no difference between the different *FGFR4* allele carriers. These results indicate that the *FGFR4 Arg385* allele has not altered expression, localization or distribution *in vivo*. These conclusions match previously published data on human samples (Partanen et al., 1991).

Hence the *FGFR4 Arg385* KI mice display the same characteristics as their human counterparts in mRNA and protein expression levels, -localisation and -distribution.

Results

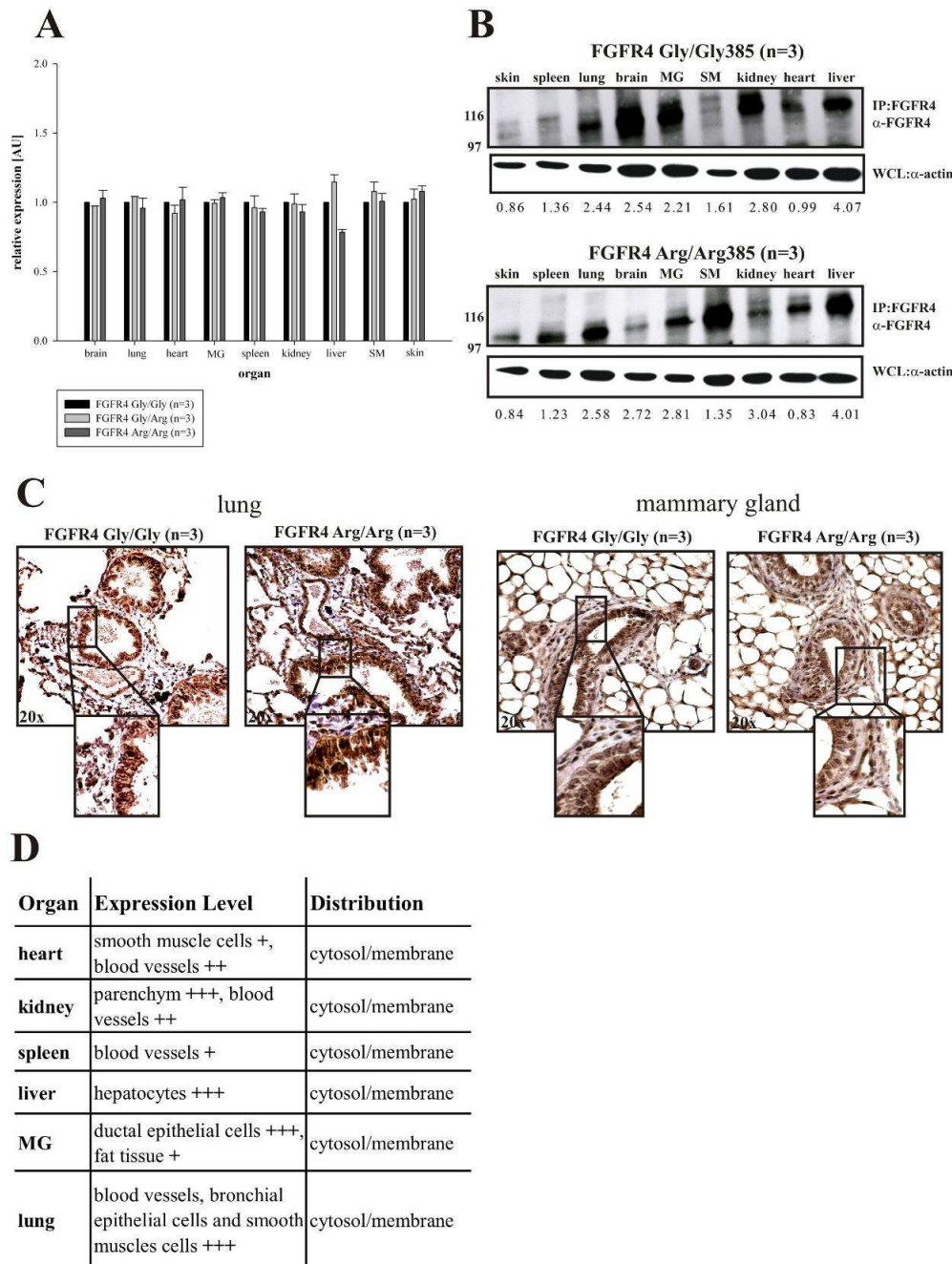


**Figure 22: Characterisation of the *FGFR4 Arg385* KI mice; A) mRNA expression levels in different tissues of 3 month old female mice carrying the *FGFR4 Gly/Gly385* (n=3), *Gly/Arg385* (n=3) or *Arg/Arg385* (n=3) locus quantified by LightCycler® analysis: Expression levels are normalized to HPRT gene expression and blotted relatively to the expression in *FGFR4 Gly/Gly385* mice which was set to 1; *FGFR4* is equally expressed in various tissues regarding the *FGFR4* isotype; all data are shown as mean ± SDM. B) Protein-expression levels in different tissues of 3 month old female mice carrying the *FGFR4 Gly/Gly385* (n=3), *Gly/Arg385* (n=3) or *Arg/Arg385* (n=3) locus analysed by immunoprecipitation and Western Blotting of *FGFR4*: Actin served as a loading control and as normalization value of *FGFR4* expression levels; *FGFR4* is equally expressed in various tissues regarding the *FGFR4* isotype; all data are shown as mean**

C) Lung and mammary gland tissue of 3 month old female mice carrying the *FGFR4 Gly/Gly385* (n=3) or *Arg/Arg385* (n=3) locus: FGFR4 expression was analyzed immunohistochemically and evaluated microscopically (20x); the higher magnification of the lung and mammary gland shows membranous and cytosolic localization of the FGFR4 as well as FGFR4 negative cells as a staining control; FGFR4 is equally expressed regarding the FGFR4 isotype.

D) Table of FGFR4 expression pattern in different tissues of 3 month old female mice carrying the *FGFR4 Gly/Gly385* (n=3) or *Arg/Arg385* (n=3) locus: FGFR4 was analyzed immunohistochemically and quantified for expression level and localization of the FGFR4 protein; FGFR4 is expressed in various tissues with a cytosolic and membranous localization; FGFR4 is equally expressed in various tissues regarding the FGFR4 isotype; cell types with negative FGFR4 staining are not listed.

MG: mammary gland; SM=skeletal muscle

## 4.2.2 The impact of the FGFR4 and its variant Arg385 *in vitro*

### 4.2.2.1 The impact of the FGFR4 Arg385 on fibroblast transformation

Mouse embryonic fibroblasts (MEFs) display an easily available *in vitro* system to investigate the impact of genetically altered loci in mice. Therefore, we analyzed the impact of the *FGFR4 Arg385* allele on biological mechanisms *in vitro* using isolated E13.5 mouse embryonic fibroblasts. Previous reports of clinical studies do not implicate the *FGFR4 Arg388* allele in tumor initiation, but rather associate it with enhanced disease progression once cancer has been initiated (Bange et al., 2002; Streit et al., 2004). Thus, we firstly investigated the impact of this SNP on the transformation of MEFs by focus formation assays. Here some primary cells loose contact inhibition as a consequence of overexpression of proto-oncogenes and grow in local multilayers that result in the formation of cell foci. In order to study the impact of the *FGFR4 Arg385* allele on focus formation we initiated neoplastic transformation of *FGFR4 Gly/Gly385*, *FGFR4 Gly/Arg385* and *FGFR4 Arg/Arg385* MEFs via infection with viruses carrying overexpression modules for several oncogenes. We used the human proto-oncogenes HER2, EGFR and the feline viral oncogene v-kit to determine if either one of the *FGFR4* alleles would influence the transformation capacity and the progression of MEFs in cooperation with different receptor tyrosine kinases acting as the initiating oncogenes. Infection of MEFs with viruses containing expression modules of the oncogene v-src served as a positive control as v-src triggers cell transformation at very early time points. Infection of MEFs with viruses containing expression modules of the empty pLXSN-vector served as a negative control to calculate the spontaneous transformation rate of the infected MEFs. In Figure 23A the number of foci in *FGFR4 Gly/Gly385*, *FGFR4 Gly/Arg385* and *FGFR4 Arg/Arg385* MEFs is plotted against the investigated oncogenes after 21 days of focus formation. MEFs heterozygous for the *FGFR4 Arg385* display a significantly increased focus formation in cooperation with the initiating oncogenes HER2 (p=0.00033) and EGFR (p=0.017). MEFs homozygous for the *FGFR4 Arg385* show a significantly enhanced focus formation with all three investigated oncogenes (HER2-p=0.00016, EGFR-

Results

p=0.0000095, v-kit-p=0.00012). These results suggest that the *FGFR4 Arg385* allele significantly promotes cell transformation in cooperation with classical oncogenes. Remarkably, cell transformation by the EGFR or v-kit, which are commonly regarded as weak oncogenes, led to an unusually high number of foci. These results indicate yet unknown crosstalk between FGFR4 Arg385 and other receptor tyrosine kinases similar to the known crosstalk between FGFR4 and HER2 (Koziczak and Hynes, 2004).

Further, we wanted to monitor the progression of transformation in *FGFR4 Gly/Gly385* and *FGFR4 Arg/Arg385* MEFs over time. Therefore, we performed the focus formation by terminating the assay at different time points (7 days, 14 days and 21 days). As it is clearly shown in Figure 23B, *FGFR4 Arg/Arg385* carrying MEFs not only transform considerably faster, but also generate an increased number of foci. These results indicate that the FGFR4 Arg385 is clearly involved in the progression of transformed cells initiated by different oncogenes. Furthermore, the *FGFR4 Arg385* allele seems to facilitate the transformation of MEFs resulting in a higher number of foci that form at earlier time points.

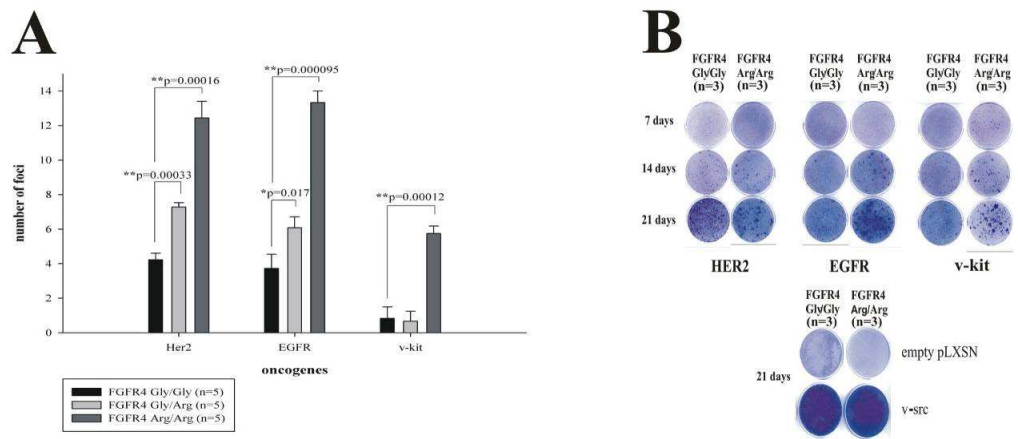


**Figure 23: The *FGFR4 Arg385* allele promotes cell transformation in MEFs** A) Focus Formation Assay in *FGFR4 Gly/Gly385* (n=5), *FGFR4 Gly/Arg385* (n=5) and *FGFR4 Arg/Arg385* (n=5) carrying MEFs: MEFs transformed by the overexpression of HER2, EGFR or v-kit display a statistically significant increase in the formation of foci in the presence of the *FGFR4 Arg385* allele after 21 days (HER2: Gly/Arg-p=0.00033, Arg/Arg-p=0.00016; EGFR: Gly/Arg-p=0.017, Arg/Arg-p=0.000095; v-kit: Arg/Arg-p=0.00012); overexpression of the empty vector served as negative control; transformation by v-src served as positive control; all data are shown as mean ± SDM; all p-values were calculated using the students T-test and values ≤ 0.03 were considered statistically significant.

B) Focus Formation Assay in *FGFR4 Gly/Gly385* (n=3) and *FGFR4 Arg/Arg385* (n=3) carrying MEFs monitored over time: Foci growth was determined after 7, 14 and 21 days; *FGFR4 Arg/Arg385* MEFs show an earlier onset of transformation and a higher progression of foci growth over time; overexpression of the empty vector served as negative control; transformation by v-src served as positive control.

#### 4.2.2.2 Impact of FGFR4 Arg385 on proliferation, life span, migration and apoptosis of MEFs

To support these observations by molecular analytical methods, we determined, whether the molecular action of the FGFR4 Arg385 itself is responsible for the accelerated transformation rate in *FGFR4 Arg385* carrying MEFs. Therefore we analyzed the expression and the activation status of the FGFR4 in *FGFR4 Gly/Gly385*, *FGFR4 Gly/Arg385* and *FGFR4 Arg/Arg385* MEFs. The Western Blot Analysis in Figure 24A displays neither an overexpression nor a hyperactivation of the FGFR4 Arg385 in MEFs.

Next, we wanted to investigate the involvement of the FGFR4 Arg385 on several physiological processes that could be responsible for the facilitated and accelerated transformation rate in *FGFR4 Arg385* carrying MEFs. To exclude the dependence of an enhanced transformation rate from a higher proliferative potential or a prolonged life span of *FGFR4 Arg385* carrying MEFs, we compared the population doubling rate of *FGFR4 Gly/Gly385*, *FGFR4 Gly/Arg385* and *FGFR4 Arg/Arg385* MEFs. Here, *FGFR4 Arg385* carrying MEFs display no increased proliferative capacity compared to *FGFR4 Gly/Gly385* carrying MEFs as seen in Figure 24B. Further, we investigated the impact of the *FGFR4 Arg385* allele on senescence to determine if the FGFR4 Arg385 extends the life span of the cell and thereby facilitates neoplastic transformation (Collado et al., 2007). To do that, we stained MEFs, subcultured for 30 days, for the expression of  $\beta$ -galactosidase to visualize senescent cells. As shown in Figure 24C *FGFR4 Arg385* carrying MEFs do not display a prolonged life span or an obvious difference in the initiation of senescence neither by microscopic analysis nor by the quantification of the percentage of senescent cells between the *FGFR4 Gly385* and *FGFR4 Arg385* alleles (Figure 24C).

Migration of cancer cells contributes to accelerated tumor progression. As a motility enhancing effect of the FGFR4 Arg388 had already been shown by Bange and colleagues with the MDA-MB-231 human mammary carcinoma cell line model (Bange et al., 2002) we further investigated the influence of the *FGFR4 Arg385* allele on the migratory capacity of normal MEFs. Therefore, we analyzed the migration in Boyden Chamber assays microscopically and quantified these results via ELISA analysis. In contrast to the results by Bange et al., no difference was observed when *FGFR4 Gly/Gly385* were compared to *FGFR4 Arg/Arg385* MEFs in their migratory behaviour (Figure 24D).

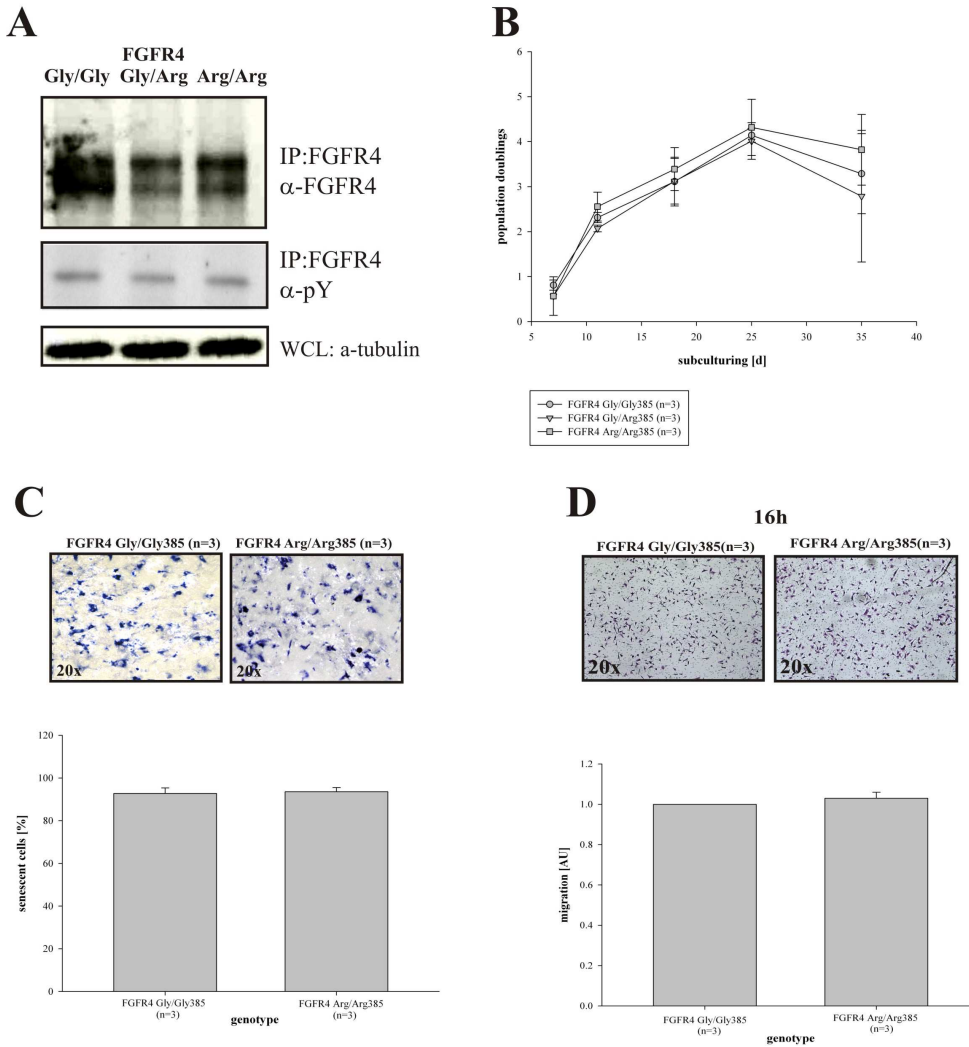


**Figure 24: The *FGFR4 Arg385* allele does not promote a prolonged life span or migration in MEFs; A) Expression analysis of the *FGFR4* in *FGFR4 Gly/Gly385* (n=3), *FGFR4 Gly/Arg385* (n=3) and *FGFR4 Arg/Arg385* (n=3) MEFs: expression and activation of the immunoprecipitated *FGFR4* was detected via western blotting; MEFs carrying the *FGFR4 Arg385* allele show no altered expression or activity of the *FGFR4*.**

**B) Proliferation and life span in *FGFR4 Gly/Gly385* (n=3), *FGFR4 Gly/Arg385* (n=3) and *FGFR4 Arg/Arg385* (n=3) MEFs: cell number of seeded MEFs was monitored over time to calculate the population doubling rate; MEFs display no altered proliferation or a prolonged life span in the presence of the *FGFR4 Arg385* allele;**

**C) Senescence Assay in *FGFR4 Gly/Gly385* (n=3) and *FGFR4 Arg/Arg385* (n=3) MEFs: apparently senescent MEFs were stained for  $\beta$ -galactosidase expression and the amount of senescent cells were calculated and quantified microscopically (20x); MEFs display no altered occurrence of senescence in the presence of the *FGFR4 Arg385* allele;**

**D) Migration Assay in *FGFR4 Gly/Gly385* (n=3) and *FGFR4 Arg/Arg385* (n=3) MEFs; migratory capacity of MEFs to 4% FCS was analyzed in Boyden Chamber assays after 16 hours microscopically (20x) and quantified via ELISA analysis; MEFs display no altered migratory capacity in the presence of the *FGFR4 Arg385* allele;**

All data are shown as mean  $\pm$  SDM.

The neoplastic transformation of cells can further be induced via mutations that accumulate within an unstable genome. Generally, primary cells undergo apoptosis due to mitotic crisis that is induced by genomic instability. If the cells overcome this mitotic crisis the acquired mutations can contribute to cancerous transformation (Hanahan and Weinberg, 2000; Jeggo, 2005). Therefore, we analyzed the response of *FGFR4 Gly/Gly385*, *FGFR4 Gly/Arg385* and *FGFR4 Arg/Arg385* MEFs to treatment with chemotherapeutic drugs that intercalate with DNA. In response to doxorubicin MEFs display a significantly reduced extent of apoptosis over 48 hours when they express the *FGFR4 Arg385* allele as homo- or heterozygotes (*Gly/Arg*- $p=0.000008$ , *Arg/Arg*- $p=0.000000001$ ) (Figure 25A). These data suggest that the *FGFR4 Arg385* protects the cell from through DNA-damage-induced apoptosis. Furthermore, we aimed to investigate the underlying mechanism of this effect. It is known, that oncogenic receptor tyrosine kinases can overcome apoptosis by more efficient DNA-repair (Skorski, 2002). This accelerated repair results in a delay of the cell cycle phase G2 in response to DNA-damaging drugs. Therefore, we analyzed the cell cycle distribution of *FGFR4 Gly/Gly385*, *FGFR4 Gly/Arg385* and *FGFR4 Arg/Arg385* MEFs upon treatment with doxorubicin for 24 hours. As shown in Figure 25B, MEFs homozygous for the *FGFR4 Arg385* allele display a significant increase in the percentage of cells in G2 after 24 hours of doxorubicin treatment compared to MEFs homozygous for the *FGFR4 Gly385* allele ( $p=0.019$ ). These data suggest that an accelerated DNA-repair mechanism keeps the cells in G2 to repair the occurred DNA-damage resulting in a lower percentage of apoptotic cells after 48 hours. To analyze the effect of G2 delay and anti-apoptosis on the molecular level we determined the expression of several target genes involved in DNA-damage, apoptosis and survival after doxorubicin treatment over time in *FGFR4 Gly/Gly385* and *FGFR4 Arg/Arg385* MEFs. As seen in Figure 25C,  $\gamma$ H2AX, an indicator of DNA-damage and apoptosis is highly upregulated in *FGFR4 Gly385* MEFs, indicating more intense downstream signalling towards apoptosis as a result of extended DNA-damage (Tanaka et al., 2006). Caspase-3 cleavage and the phosphorylation of the pro-apoptotic protein Bad do not differ between the *FGFR4* isotypes. The tumor suppressor Rb is upregulated in *FGFR4 Gly385* expressing MEFs whereas the tumor suppressor p53 is downregulated. This may lead to a higher DNA repair response and to the observed G2 delay in *FGFR4 Arg385* expressing MEFs. As the pro-apoptotic proteins Caspase3 and Bad do not differ between the *FGFR4* genotypes we analyzed typical pro-survival genes that may switch the balance towards survival in *FGFR4 Arg385* MEFs. The protein p-Akt that is known as a potent pro-survival signal is clearly upregulated in *FGFR4 Arg385* expressing MEFs after doxorubicin treatment compared to

FGFR4 Gly385 expressing MEFs (Wang et al., 2008). In contrast, p-Erk is equally expressed between the isotypes. Further, the expression of the pro-survival genes BCL2 and BCLX are clearly upregulated in *FGFR4 Arg385* MEFs, a further hint for increased cell survival, as these proteins are linked to the inhibition of anticancer-drug induced apoptosis via Akt (Lin et al., 2008; Woo et al., 2005).

Similarly, the apoptotic response of *FGFR4 Arg/Arg385* MEFs towards cisplatin, that also induces DNA-damage, is significantly reduced compared to *FGFR4 Gly/Gly385* MEFs ( $p=0.0002$ ). In contrast, after 48 hours of treatment with taxol, which interferes with the organization of the mitotic spindle, MEFs do not alter their apoptotic response in the presence of the *Arg385 allele* (Figure 25D).

In conclusion, the *FGFR4 Arg385* allele seems to promote cell survival in response to DNA-damage via two mechanisms. Firstly, FGFR4 Arg385 seems to support accelerated DNA-repair and secondly contributes to the upregulation of typical pro-survival genes as a counterbalance of apoptotic downstream signaling (Skorski, 2002).

Results

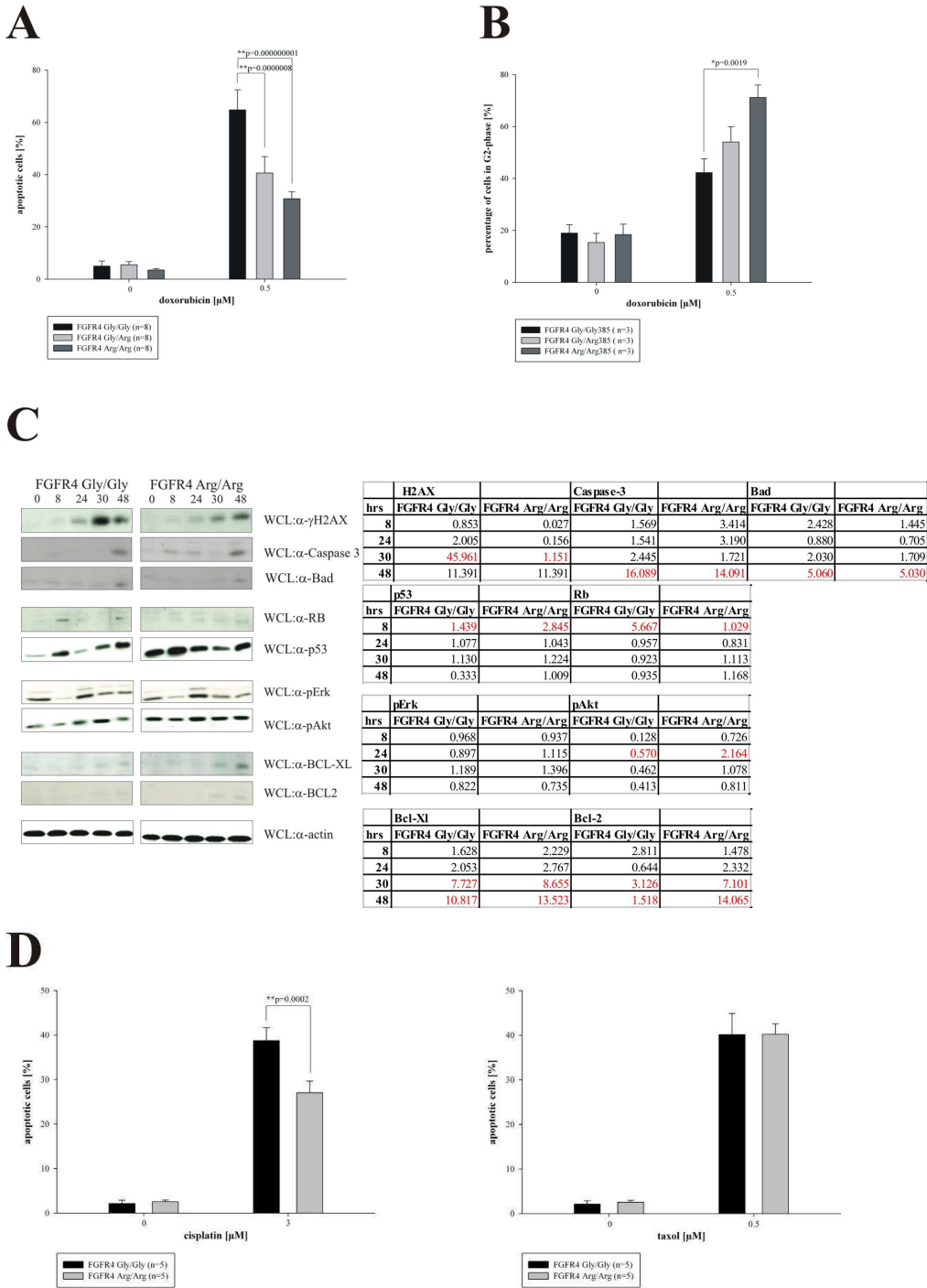


**Figure 25: The *FGFR4 Arg385* allele promotes cellular survival in MEFs; A) Cellular survival in *FGFR4 Gly/Gly385* (n=8), *FGFR4 Gly/Arg385* (n=8) and *FGFR4 Arg/Arg385* (n=8) carrying MEFs: MEFs were treated with 0.5 μM doxorubicin for 48 hours to induce cellular stress by DNA-damage; apoptosis was measured via FACS Analysis; MEFs display a significantly reduced number of apoptotic cells in the presence of the *FGFR4 Arg385* allele in response to the treatment with doxorubicin (Gly/Arg-p=0.0000008, Arg/Arg-p=0.00000001);**

B) Cell cycle distribution in *FGFR4 Gly/Gly385* (n=3), *FGFR4 Gly/Arg385* (n=3) and *FGFR4 Arg/Arg385* (n=3) carrying MEFs: MEFs were treated with 0.5  $\mu$ M doxorubicin for 24 hours to induce cellular stress by DNA-damage; cell cycle distribution was measured via FACS Analysis; MEFs homozygous for the *FGFR4 Arg385* display a significantly increased number of cells in G2-phase in response to the treatment with doxorubicin; (Arg/Arg-p=0.019);

C) Molecular mechanisms of the *FGFR4 Gly/Gly385* (n=3) and *FGFR4 Arg/Arg385* (n=3) carrying MEFs in response to doxorubicin treatment monitored over time: Expression of analyzed proteins was detected by Western Blotting. Actin served as a loading control and normalization value. MEFs homozygous for the *FGFR4 Arg385* allele display an increased upregulation of pro-survival genes like p-Akt, BCL-XL and BCL-2

D) Cellular survival in *FGFR4 Gly/Gly385* (n=5) and *FGFR4 Arg/Arg385* (n=5) carrying MEFs: MEFs were treated with 3  $\mu$ M cisplatin and 0.5  $\mu$ M taxol for 48 hours to induce cellular stress by DNA-damage; apoptosis was measured via FACS Analysis; MEFs display a significantly reduced number of apoptotic cells in the presence of the *FGFR4 Arg385* allele in response to cisplatin treatment but not towards taxol; (Arg/Arg-p=0.0002);

All data are shown as mean  $\pm$  SDM; all p-values were calculated using the students T-test and values  $\leq$  0.03 were considered statistically significant

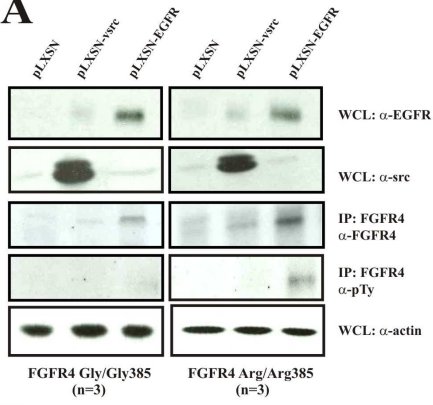
#### 4.2.2.3 Impact of *FGFR4 Arg385* on proliferation, migration, invasion and apoptosis in transformed MEFs

As the transformation of *FGFR4 Arg385* MEFs with EGFR displays a unusually high efficiency in the focus formation assay compared to *FGFR4 Gly/Gly385* MEFs we wanted to investigate the involvement of the *FGFR4 Arg385* allele on several physiological processes after stable transformation with EGFR. As the migratory capacity of MEFs does not alter in the presence of the *FGFR4 Arg385* allele in non-transformed MEFs, we further wanted to analyze if these processes are possibly influenced by the *FGFR4 Arg385* allele in transformed cells. Therefore, we stably transformed *FGFR4 Gly/Gly385* and *FGFR4 Arg/Arg385* MEFs by the overexpression of EGFR. As a positive control we stably transformed MEFs through the overexpression of the oncogene v-src. As a negative control we stably expressed the pLXSN vector to calculate spontaneous transformation of MEFs. After selection with G418, EGFR and v-src were analyzed via western blotting and quantification to ensure equal expression in the infected MEFs. As shown in Figure 26A, EGFR and v-src are equally expressed. Additionally, FGFR4 expression was analyzed in transformed cells to investigate if the overexpression of EGFR or v-src has any impact on FGFR4 expression. Interestingly, FGFR4 is upregulated in EGFR transformed cells and in *FGFR4 Arg/Arg385* MEFs. Above that, the phosphorylation status of the *FGFR4 Arg385* MEFs is enhanced in MEFs transformed with EGFR indicating a higher activity of *FGFR4 Arg385* compared to the *Gly385* isotype. This finding could be an explanation for the unusually strong transformation rate in the focus formation assay of *FGFR4 Arg/Arg385* MEFs infected with EGFR. Moreover, the upregulation of the FGFR4 is a further indication of a so far unknown crosstalk between these two receptors. We further investigated if this upregulation of the *FGFR4 Arg/Arg385* compared to *FGFR4 Gly/Gly385* in MEFs transformed with EGFR influences

cellular processes including proliferation, migration, invasion or survival. Furthermore, we aimed to show if these processes are possibly not influenced by the *FGFR4 Arg/Arg385* in v-src transformed cells as there was no upregulation of the FGFR4 expression detectable in the Western Blot compared to MEFs transformed with EGFR. First, we analyzed the influence on proliferation by monitoring the cell number over time and calculating the population doubling rate of MEFs. As shown in Figure 26B MEFs transformed with EGFR display no proliferative advantage in the presence of the *FGFR4 Arg385* allele. Likewise, MEFs transformed with v-src are not altered in their proliferation rate depending on their FGFR4 genotype. Similarly, the non-transformed MEFs stably expressing the empty pLXSN also do not display changes in proliferation behaviour. As primary MEFs display an anti-apoptotic effect in response to the DNA-damaging agents doxorubicin and cisplatin in the presence of the *FGFR4 Arg385* allele, we wanted to reproduce these results in MEFs transformed by EGFR or v-src. Figure 26C displays the percentage of apoptotic cells determined by FACS analysis after treatment with 0.5 $\mu$ M doxorubicin, 3 $\mu$ M cisplatin and 0.5 $\mu$ M taxol after 48 hours. MEFs transformed with EGFR display a significant decrease in apoptosis in the presence of the *FGFR4 Arg385* allele in response to the DNA-damaging agents doxorubicin and cisplatin (cisplatin-p=0.021; doxorubicin-p=0.0000046). No difference was apparent for the response to taxol. In MEFs transformed with v-src neither the chemotherapeutic drugs nor the *FGFR4* isotypes result in an alteration of the anti-apoptotic response. The non-transformed MEFs expressing the empty pLXSN displayed the same significant results as the primary MEFs in their response to doxorubicin, cisplatin and taxol after 48 hours (cisplatin-p=0.0000039; doxorubicin-p=0.016).

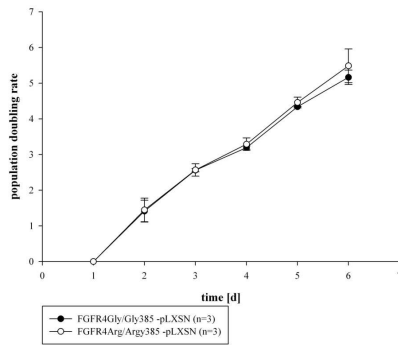
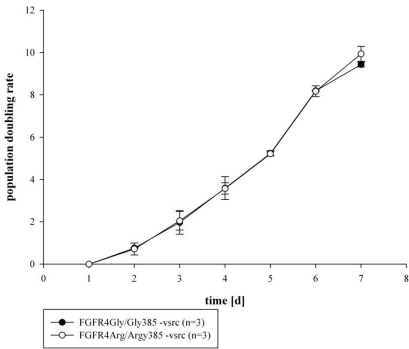
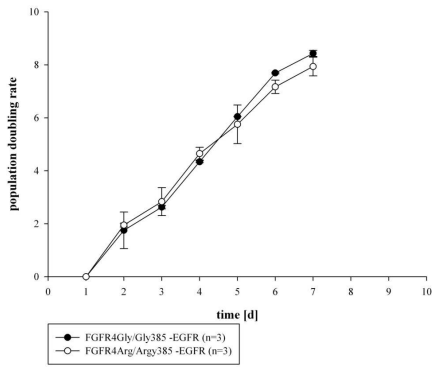
Results

**A**



	FGFR4 Gly/Gly385	FGFR4 Arg/Arg385	
EGFR-expression	pLXSN-vsrc	241.92	330.22
	pLXSN-EGFR	2345.88	2029.98
vsrc-expression	pLXSN-vsrc	1324.89	1916.89
	pLXSN-EGFR	86.38	109.12
FGFR4-expression	pLXSN-vsrc	121.26	756.24
	pLXSN-EGFR	967.27	1666.70
pTyFGFR4-expression	pLXSN-vsrc	121.04	158.62
	pLXSN-EGFR	152.06	9841.63

**B**





**All data are shown as mean  $\pm$  SDM; all p-values were calculated using the students T-test and values  $\leq$  0.03 were considered statistically significant**

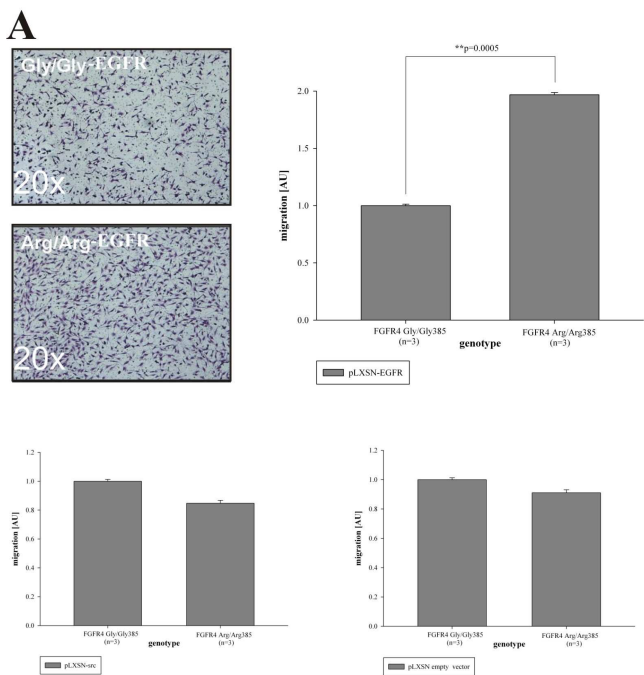
Next we analyzed the differences in cell motility in dependence of *FGFR4* genotype. Therefore we analyzed the migration of *FGFR4 Gly/Gly385* and *FGFR4 Arg/Arg385* MEFs transformed with EGFR and v-src or stably expressing the empty pLXSN vector in a Boyden chamber assay to 4% FCS for 16 hours. Migration was analyzed microscopically after crystal violet staining and quantified via ELISA analysis. In contrast to non-transformed MEFs, *FGFR4 Arg/Arg385* (n=3) MEFs transformed with EGFR display a significantly (p=0.005) increased migratory capacity compared to *FGFR4 Gly/Gly385* MEFs (Figure 27A). This significant difference was not apparent in MEFs transformed with v-src or non-transformed MEFs stably expressing the pLXSN vector. These data indicate, that *FGFR4 Arg/Arg385* influences migration only in transformed cells and that the involvement of the FGFR4 seems to be dependent on the oncogenetic background. This increased motility of *FGFR4 Arg/Arg385* expressing MEFs transformed with EGFR seems to be one of the contributing factors of accelerated focus formation. Next to migration and the loss of contact inhibition that contributes to tumor progression, cancer cells acquire the ability to survive without anchorage. This anchorage independent ability to grow in combination with enhanced motility and invasivity allows cancer cells to metastasize thereby making tumors more aggressive. To analyze if MEFs transformed with EGFR or v-src display a more aggressive phenotype in the presence of the *FGFR4 Arg385* allele we performed a soft agar assay to investigate the impact of the *FGFR4 Arg385* on anchorage independent growth in *FGFR4 Gly/Gly385* and *FGFR4 Arg/Arg385* MEFs transformed with EGFR or v-src. Soft Agar colony formation was analyzed and quantified by counting formed colonies. As shown in Figure 27B MEFs transformed with EGFR display a significantly enhanced anchorage independent growth after 24 and 96 hours if they express the *FGFR4 Arg/Arg385* (24h-p:0.00004; 48h-p:0.00003). In contrast, no alterations were apparent between *FGFR4 Gly/Gly385* and *FGFR4 Arg/Arg385* MEFs after 96 hours transformed by v-src. The negative control of non-transformed MEFs expressing the empty pLXSN vector was not able to grow anchorage independently. These data demonstrate that the *FGFR4 Arg/Arg385* is implicated in the process of anchorage independent growth and likewise with migration dependent on the oncogenic background.

For successful metastasis, cancer cells acquire the ability to degrade the extracellular matrix surrounding them to spread and invade the surrounding tissue. To determine this activity and the influence of *FGFR4* isotypes on oncogene-primed MEFs we performed a Matrigel assay to analyze invasivity and branching of *FGFR4 Gly/Gly385* and *FGFR4 Arg/Arg385* MEFs transformed by EGFR or v-src. As shown in Figure 27C MEFs transformed with EGFR

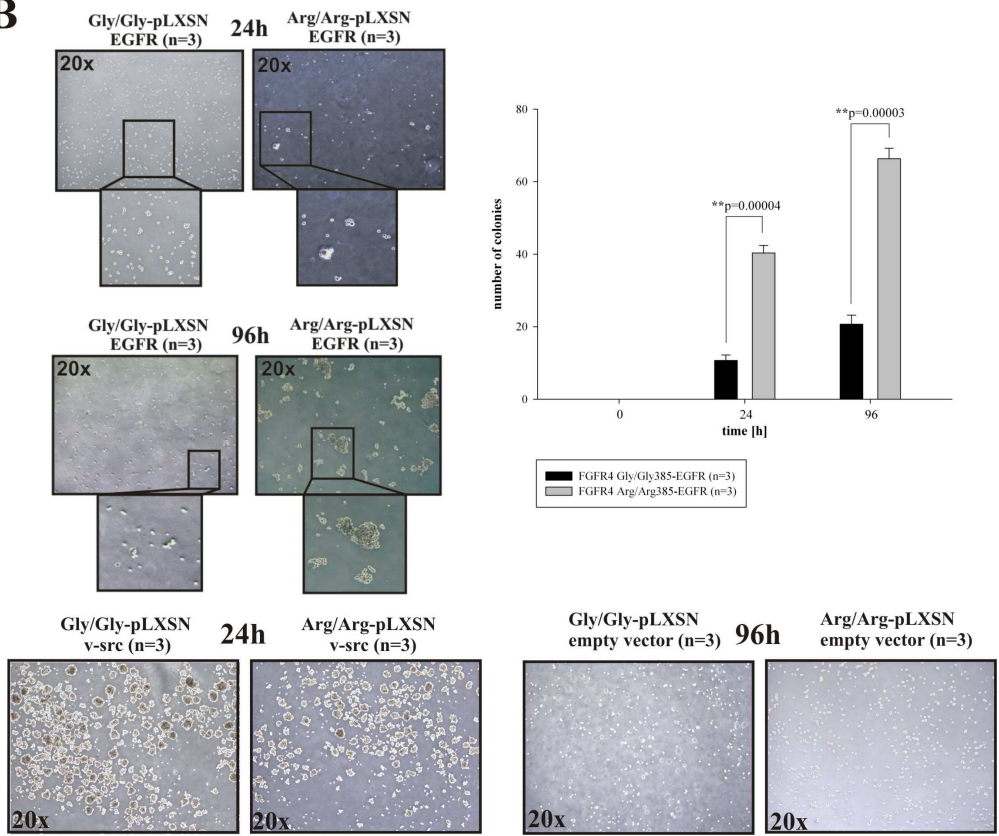
Results

display significantly enhanced branching in Matrigel after 24 and 96 hours if they express the *FGFR4 Arg/Arg385* isotype (96h-p:0.0009). In contrast, no alterations were apparent between *FGFR4 Gly/Gly385* and *FGFR4 Arg/Arg385* MEFs after 96 hours transformed by v-src. The negative control of non-transformed MEFs expressing the empty pLXSN vector was not able to branch in Matrigel. These data demonstrate that the *FGFR4 Arg/Arg385* is clearly implicated in the invasive process of branching in Matrigel and likewise in cell motility and soft agar colony formation dependent on the oncogenic background.

These results demonstrate that in MEFs, *FGFR4 Arg385* significantly influences physiological processes including motility, invasivity and survival that all contribute to tumor progression. These processes are distinct from those affected by *FGFR4 Gly385* and, furthermore, the impact of the *FGFR4 Arg385* is in dependence on the genetic background that confers cell transformation *in vitro*.



**B**



C

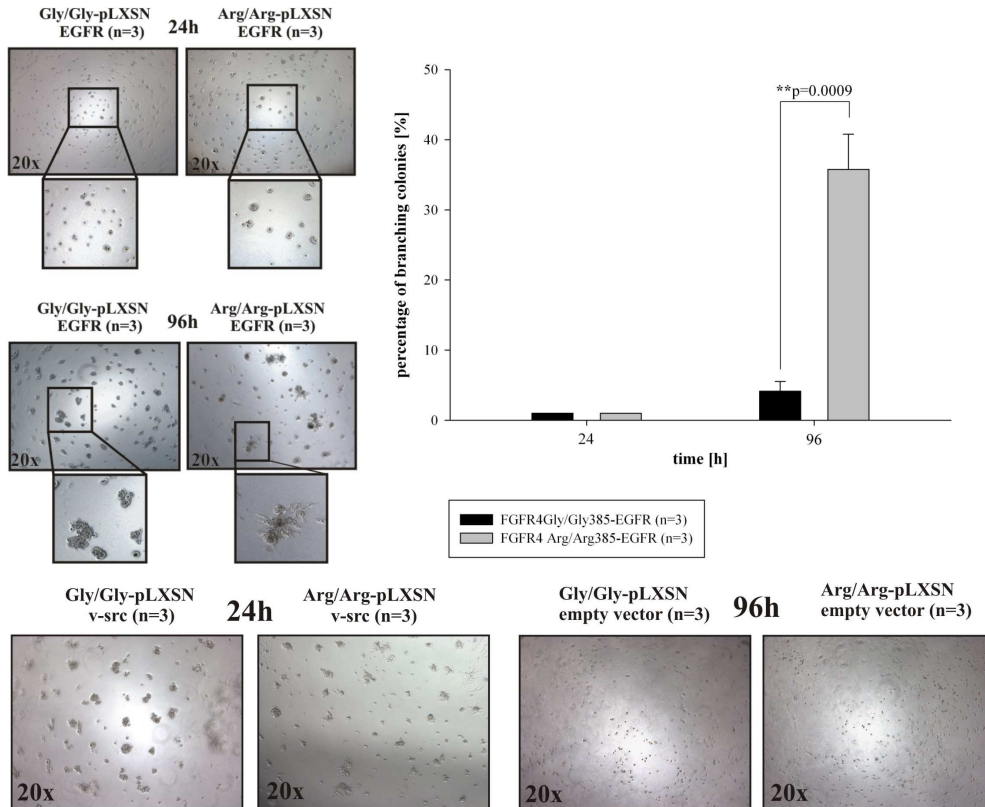


Figure 27: The *FGFR4 Arg385* allele promotes migration, soft agar colony formation and invasion in EGFR-transformed MEFs; A) Migration assay of stably transformed *FGFR4 Gly/Gly385* (n=3), and *FGFR4 Arg/Arg385* (n=3) MEFs: Migratory capacity was analyzed microscopically after crystal violet staining (20x) and quantified via ELISA analysis. MEFs transformed with EGFR and homozygous for the *FGFR4 Arg385* allele display a significantly ( $p=0.0005$ ) increased migratory capacity to 4% FCS in a boyden chamber assay after 16h compared to MEFs homozygous for the *FGFR4 Gly385* allele; MEFs transformed with v-src displayed no difference in their migratory capacity regarding their *FGFR4* allele. MEFs stably expressing the empty pLXSN-vector served as a negative control.

B) Soft Agar Assay of stably transformed *FGFR4 Gly/Gly385* (n=3), and *FGFR4 Arg/Arg385* (n=3) MEFs: Anchorage independent growth was analyzed and quantified microscopically (20x) after the indicated time points. MEFs transformed with EGFR and homozygous for the *FGFR4 Arg385* allele display a significantly increased capacity of anchorage independent growth in Soft Agar after 24-96h compared to MEFs homozygous for the *FGFR4 Gly385* allele (24h- $p=0.00004$ ; 96h- $p=0.00003$ ); MEFs stably expressing the empty pLXSN-vector served as a negative control. MEFs transformed with v-src displayed no difference in their capacity to proliferate anchorage independent regarding their *FGFR4* allele.

C) Invasion Assay in Matrigel of stably transformed *FGFR4 Gly/Gly385* (n=3) and *FGFR4 Arg/Arg385* (n=3) MEFs: branching in Matrigel was analyzed and quantified microscopically (20x) after the indicated time points; MEFs transformed with EGFR and homozygous for the *FGFR4 Arg385* display a significantly increased invasion in Matrigel after 96h compared to MEFs homozygous for the *FGFR4 Gly385* allele ( $p=0.00009$ ); MEFs stably expressing the empty pLXSN-vector served as a negative control. MEFs transformed with v-src displayed no difference in their capacity to branch in Matrigel regarding their *FGFR4* allele.

All data are shown as mean  $\pm$  SDM; all p-values were calculated using the students T-test and values  $\leq 0.03$  were considered statistically significant

To further analyze the underlying mechanism of accelerated MEF migration, soft agar colony formation and invasion, the expression of several genes associated with tumor progression, aggressiveness and invasiveness of transformed cells was investigated. For that purpose, the mRNA levels of these proteins were measured in MEFs transformed with EGFR carrying the *FGFR4 Gly385* or *Arg385* allele. As seen in Figure 28 the cluster of tumor suppressors displays no detectable difference in regard of the *FGFR4* isotypes. Regarding cell cycle and proliferation markers, the expression of the cell cycle dependent kinases (CDK) 1, 2 and 4 were measured. As the *FGFR4* is known to have weak mitogenic activity, no difference between *FGFR4 Gly/Gly385* and *FGFR4 Arg/Arg385* expressing MEFs was expected. In contrast, there was a significantly higher expression of CDK1 in *FGFR4 Arg/Arg385* expressing MEFs transformed with EGFR ( $p=0.0091$ ). As CDK1 is strongly associated with migration, this significant overexpression seems to promote the increased migration of the transformed MEFs resulting in a more aggressive phenotype of *FGFR4 Arg/Arg385* carrying MEFs transformed with EGFR (Manes et al., 2003). In the cluster of proteins that are associated with invasion, MMP13 as well as MMP14 were found to be overexpressed in *FGFR4 Arg/Arg385* carrying MEFs transformed with EGFR, likely contributing to a higher metastatic potential (MMP13- $p=0.002$ ; MMP14- $p=0.004$ ) (Ellsworth et al., 2008; Jiang et al., 2006; Rizki et al., 2008). Next to MMPs, N-cadherin was highly overexpressed in MEFs carrying the *FGFR4 Arg385* isotype indicating a higher potential of migration and invasion (Lafleur et al., 2005; Nagi et al., 2005; Su et al., 2008). This data reflect the results derived from the physiological experiments presented in Figure 27 and suggests a more aggressive and invasive phenotype of MEFs carrying the *FGFR4 Arg385* allele when transformed with the EGFR oncogene.

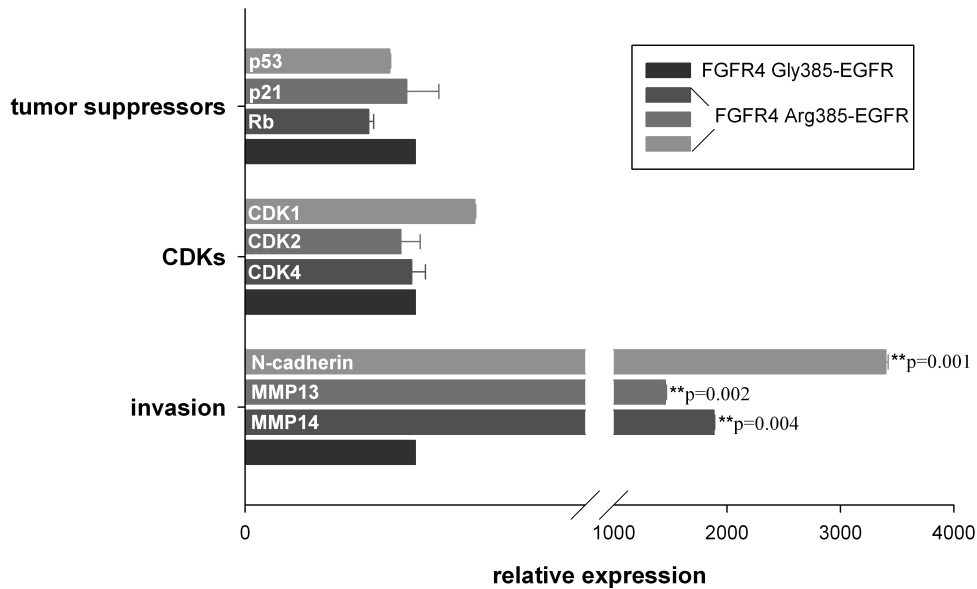


Figure 28: Expression Analysis of MEFs carrying the *FGFR4 Gly385* (n=3) or *Arg385* (n=3) allele transformed with EGFR: target gene expression was analyzed via semiquantitative RT-PCR; GAPDH served as housekeeping gene for normalization; expression values of *FGFR4 Arg/Arg385* MEFs are blotted relatively to the expression values of *FGFR4 Gly/Gly385* MEFs and grouped regarding their physiological function; N-cadherin (p=0.001), MMP13 (p=0.002) and MMP14 (p=0.004) are significantly upregulated in the presence of the *FGFR4 Arg/Arg385* allele suggesting a more aggressive phenotype; all data are shown as mean  $\pm$  SDM; all p-values were calculated using the students T-test and values  $\leq 0.03$  were considered statistically significant

### 4.2.3 The impact of the *FGFR4* and its variant *Arg385* on tumor progression *in vivo*

#### 4.2.3.1 The *FGFR4 Arg385* allele promotes tumor mass and size of *WAP-TGF $\alpha$* but not *MMTV -PymT* derived tumors

The *in vitro* experiments with primary and transformed MEFs demonstrate the impact of the *FGFR4 Arg385* on cell biological properties that are relevant to tumor progression namely survival, motility, anchorage independence and invasivity in Matrigel. Furthermore, the impact of the *FGFR4 Arg385* allele seems to be dependent on the oncogenic background. To ultimately clarify the influence of the *FGFR4 Arg385* on accelerated tumor progression and aggressiveness we investigated the impact of the *Arg385* isotype on tumor progression in a mouse breast cancer model *in vivo*. As the *FGFR4* is known to be upregulated in breast cancer and furthermore the *FGFR4 Arg385* allele is known to promote progression of mammary

## Results

carcinoma in humans we wanted to investigate the impact of this allele on mammary cancer progression in a clean background-free cancer model system. Similar to the experiments *in vitro* we wanted to analyze the involvement of the *FGFR4 Arg385* on tumor progression in combination with the well established *WAP-TGF $\alpha$*  and the *MMTV-PyMT* transgenes. In the *WAP-TGF $\alpha$*  mouse tumor model, mammary carcinoma is induced by the overexpression of TGF $\alpha$  resulting in the hyperactivation of the EGFR (Sandgren et al., 1995). In the *MMTV-PyMT* mouse mammary carcinoma model, neoplastic transformation of the mammary gland is initiated by the overexpression of the Polyoma Middle T resulting in hyperactive, oncogenic src (Guy et al., 1992).

Therefore, we crossed the *FGFR4 Arg385 KI* mice to oncomice either transgenic for *WAP-TGF $\alpha$*  or *MMTV-PymT* in the C57BL/6 background. To ensure normal lactation of female mice, the transgene was only inherited by males. To distinguish the different *FGFR4* alleles, the genotyping was done by PCR-RFLP by the aforementioned restriction site (Figure 29A). To confirm the presence of the transgenes in the progeny we performed genotyping with specific primers for *TGF $\alpha$*  or *PymT* (Figure 29B).

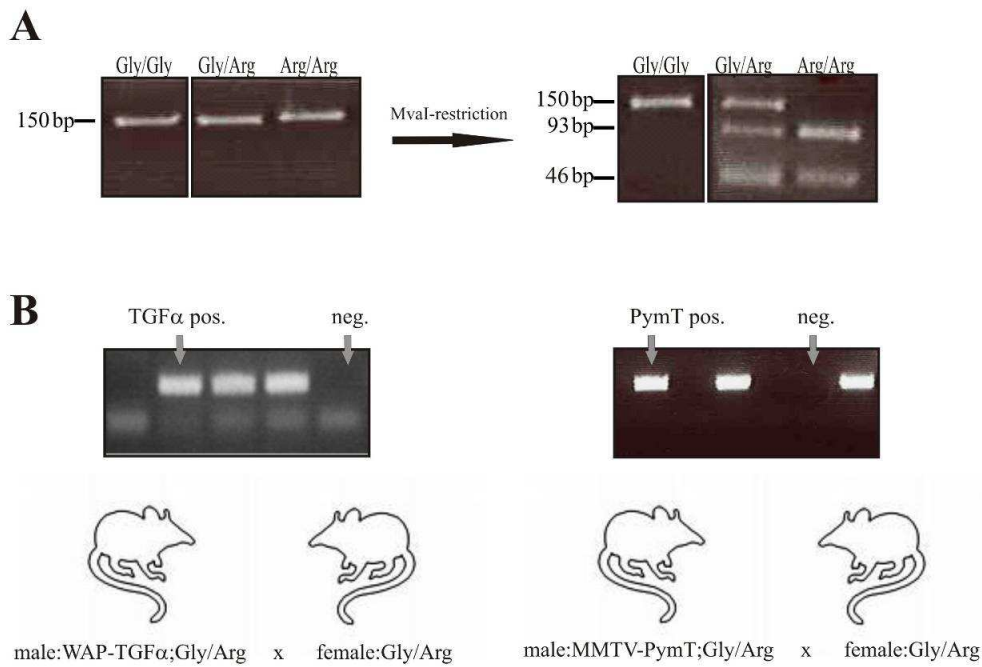


**Figure 29:** A) Genotyping of *FGFR4 Arg385* KI mice: amplification product was cut by *MvaI* to obtain specific banding to distinguish the *FGFR4* alleles

**B) Conformation of the *WAP-TGF $\alpha$*  and MMTV-PyMT transgen and crossing scheme of *FGFR4 Arg385* KI mice and oncomice transgenic for *WAP-TGF $\alpha$*  or *MMTV-PyMT*: the *WAP-TGF $\alpha$*  and the *MMTV-PyMT* transgen were only inherited by males to ensure normal lactation of the females.**

To investigate the impact of the *FGFR4 Arg385* on tumor progression in the *WAP-TGF $\alpha$*  model we analyzed the tumors of 6 month old female *FGFR4 Gly/Gly385*, *FGFR4 Gly/Arg385* and *FGFR4 Arg/Arg385* mice. The analyzed criteria for tumor progression are the mass, area and the percentage of mass and area of the analyzed tumors. As shown in Figure 30A the tumor mass is significantly increased in mice homozygous for the *FGFR4 Arg385* allele and transgenic for *WAP-TGF $\alpha$*  when compared to *FGFR4 Gly385* controls (Arg/Arg-p=0.01). Figure 30B shows the percentage of tumor mass that is significantly increased in *FGFR4 Arg385* carrying mice transgenic for *WAP-TGF $\alpha$*  (Gly/Arg-p=0.004; Arg/Arg-p=0.0004). Furthermore, the tumor area is significantly increased in *WAP-TGF $\alpha$*  transgenic mice in the presence of the *FGFR4 Arg385* allele when compared to *FGFR4 Gly385* control mice (Figure 30C)(Gly/Arg-p=0.006; Arg/Arg-p=0.0005). Just as the percentage of tumor mass, the percentage of tumor area is significantly increased in *FGFR4 Arg385* carrying mice transgenic for *WAP-TGF $\alpha$*  (Gly/Arg-p=0.000000006; Arg/Arg-p=0.000000001) (Figure 30D). These results indicate that the *FGFR4 Arg385* allele is a potent enhancer of *WAP-TGF $\alpha$* -induced mammary tumors in mass and area. Furthermore, the higher significance in the percentages of tumors and the area of tumors suggest that the *FGFR4 Arg385* is not an enhancer of cancer cell proliferation, but seems to accelerate processes like migration resulting in the increase of the invaded area in the mammary gland. Moreover, the more significant increase in tumor area may result from a facilitated neoplastic transformation rate in *FGFR4 Arg385* carrying mice transgenic for *WAP-TGF $\alpha$* . These results are in line with the *in vitro* experiments with transformed MEFs.

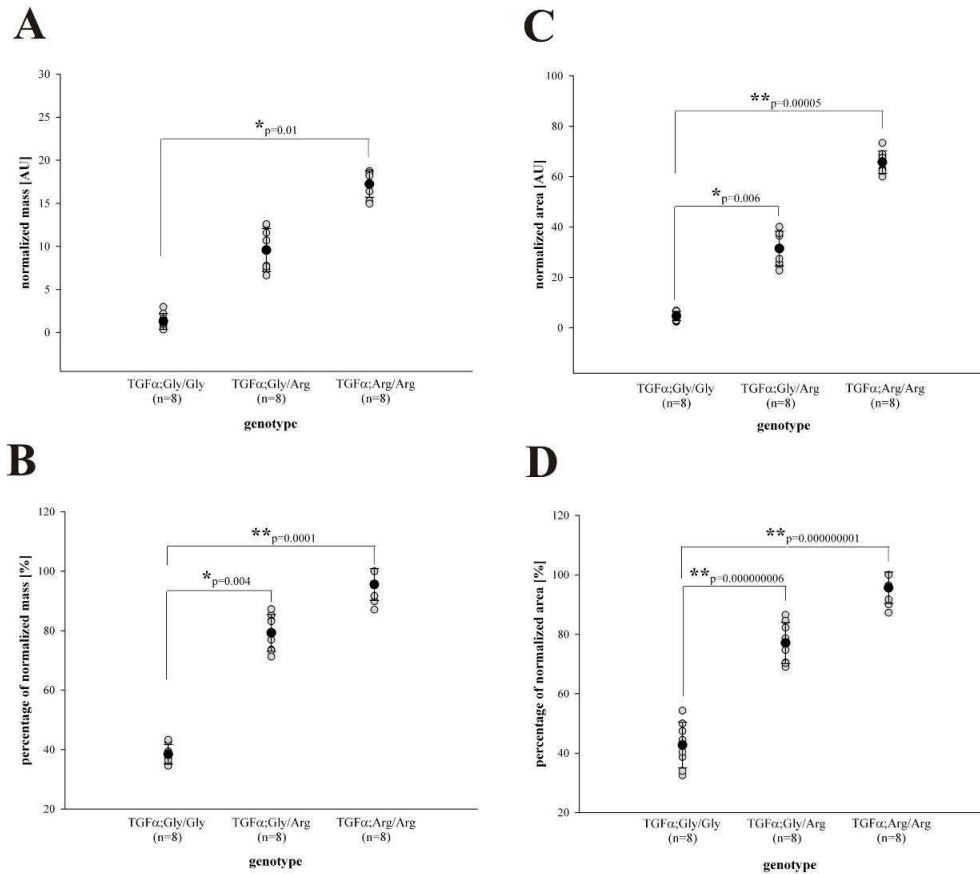


**Figure 30: The *FGFR4* Arg385 allele significantly progresses *WAP-TGFα* induced tumors; In Figure 3 (A-D) every data point represents the values of one female mouse transgenic for *WAP-TGFα* carrying the *FGFR4* Gly/Gly385 (n=8) *FGFR4* Gly/Arg385 (n=8) or *FGFR4* Arg/Arg385 (n=8) allele: Mice were sacrificed after 6 month of tumor progression. The values of the investigated tumors were normalized on body weight and plotted against the different investigated *FGFR4* genotypes; all data are shown as mean ± SDM; all p-values were calculated using the students T-test and values ≤ 0.03 were considered statistically significant.**

(A) Analysis of the normalized tumor mass of the sacrificed mice transgenic for *WAP-TGFα* regarding their *FGFR4* genotype: Mice homozygous for the *FGFR4* Arg385 allele display a significantly increased tumor mass after 6 month of tumor progression compared to mice homozygous for the *FGFR4* Gly385 allele (Arg/Arg-p=0.01).

(B) Analysis of the percentage of tumor mass proportional to mammary gland tissue of the sacrificed mice transgenic for *WAP-TGFα* regarding their *FGFR4* genotype: Mice display a significantly increased percentage of tumor mass after 6 month of tumor progression in the presence of the *FGFR4* Arg385 allele compared to mice homozygous for the *FGFR4* Gly385 allele (Gly/Arg-p=0.004; Arg/Arg-p=0.0001)

(C) Analysis of the normalized tumor area of the sacrificed mice transgenic for *WAP-TGFα* regarding their *FGFR4* genotype: Mice display a significantly increased tumor mass after 6 month of tumor progression in the presence of the *FGFR4* Arg385 allele compared to mice homozygous for the *FGFR4* Gly385 allele (Gly/Arg-p=0.006, Arg/Arg-p=0.00005).

(D) Analysis of the percentage of tumor area proportional to mammary gland tissue of the sacrificed mice transgenic for *WAP-TGFα* regarding their *FGFR4* genotype: Mice display a significantly increased percentage of tumor mass after 6 month of tumor progression in the presence of the *FGFR4* Arg385 allele compared to mice homozygous for the *FGFR4* Gly385 allele (Gly/Arg-p=0.000000006, Arg/Arg-p=0.000000001).

Furthermore, the potent tumor enhancing impact of the *FGFR4 Arg385* allele is apparent when comparing an *FGFR4 Arg/Arg385* carrying mouse to a *Gly/Gly385* control transgenic for *WAP-TGF $\alpha$*  sacrificed after 8 month of tumor progression (Figure 31). Mice transgenic for *WAP-TGF $\alpha$*  display more as well as larger tumors in the presence of the *FGFR4 Arg385* allele as indicated by the white arrows.

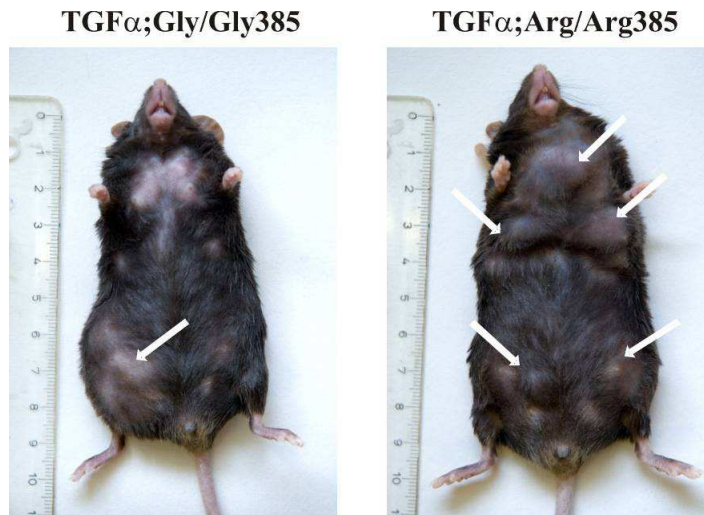


**Figure 31: Tumor progression in mice transgenic for *WAP-TGF $\alpha$*  sacrificed after 8 month: As indicated by the white arrows, mice homozygous for the *FGFR4 Arg385* allele display a visibly increased tumor progression after 8 month compared to mice homozygous for the *FGFR4 Gly385* allele**

In addition to the *WAP-TGF $\alpha$*  mouse model, we also investigated the tumor promoting impact of the *FGFR4 Arg385* allele in the *MMTV-PymT* mouse mammary carcinoma model. Because of the *in vitro* results in MEFs transformed with *v-src* we investigated whether in this model the tumor promoting action of the *FGFR4 Arg385* allele is just like *in vitro* not apparent *in vivo*, to further confirm that the tumor enhancing effect of the *FGFR4 Arg385* is dependent on the oncogene background.

We analyzed the tumors of 3 month old female *FGFR4 Gly/Gly385*, *FGFR4 Gly/Arg385* and *FGFR4 Arg/Arg385* mice. The measured criteria for tumor progression are the mass and area of the analyzed tumors. As seen in Figure 32A and B there is neither a significant difference in tumor mass nor in tumor size between *FGFR4 Gly/ Gly385*, *FGFR4 Gly/Arg385* and *FGFR4 Arg/Arg385* mice transgenic for *MMTV-PymT*. Thus, the tumor promoting effect of the *FGFR4 Arg385* allele is dependent on the genetic background, which triggers oncogenesis.

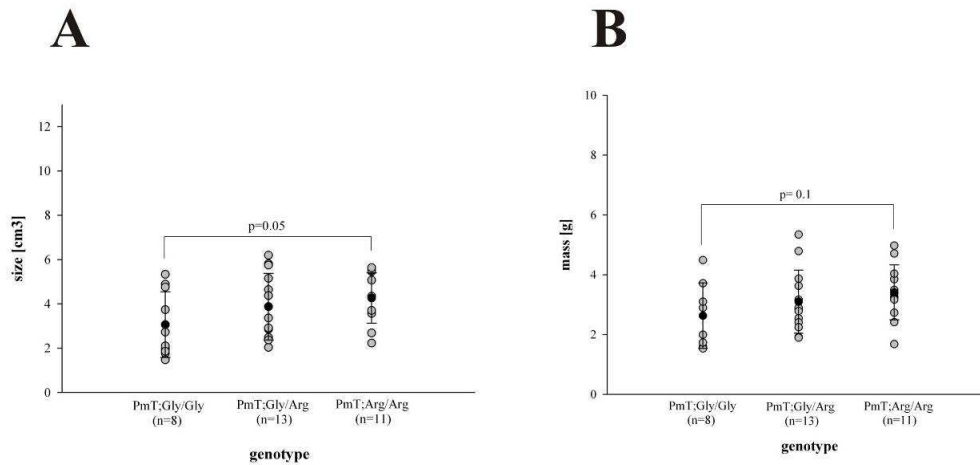


**Figure 32: The *FGFR4 Arg385* allele does not promote *MMTV-PyMT* induced mammary tumors: (A) Analysis of tumor size in 3 month old *FGFR4 Gly/Gly385* (n=8), *FGFR4 Gly/Arg385* (n=13) and *FGFR4 Arg/Arg385* (n=11) mice transgenic for *MMTV-PyMT*: Mice carrying the *FGFR4 Arg385* allele display no difference in the size of tumors compared to mice homozygous for the *FGFR4 Gly385* allele; (B) Analysis of tumor mass in 3 month old *FGFR4 Gly/Gly385* (n=8), *FGFR4 Gly/Arg385* (n=13) and *FGFR4 Arg/Arg385* (n=11) mice transgenic for *MMTV-PyMT*: Mice carrying the *FGFR4 Arg385* allele display no difference in the mass of tumors compared to mice homozygous for the *FGFR4 Gly385* allele; all data are shown as mean  $\pm$  SDM; all p-values were calculated using the students T-test and values  $\leq$  0.03 were considered statistically significant.**

The analyzed control mammary glands of *FGFR4 Gly/Gly385*, *FGFR4 Gly/Arg385* and *FGFR4 Arg/Arg385* mice without an oncogenic background do not alter in their mass, size or pathology as seen in Figure 33A and B. These data demonstrate that the *FGFR4 Arg385 KI* has no influence on the pathohistology of a non-malignant mammary gland.

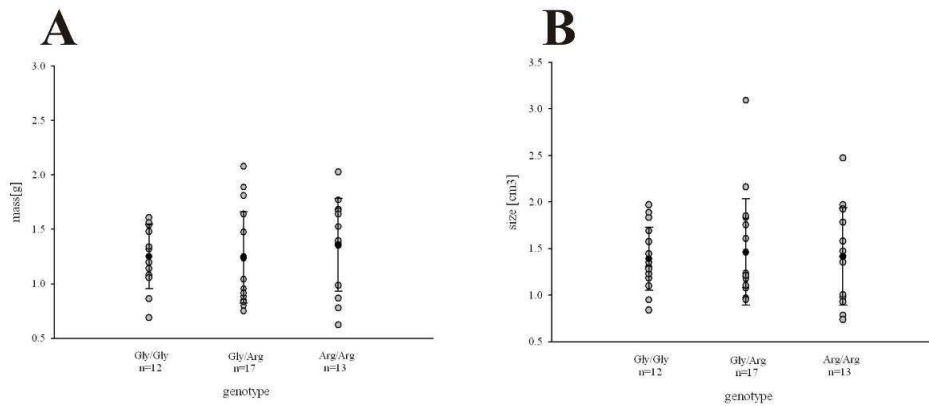


**Figure 33: The *FGFR4 Arg385* allele has no influence on non-malignant mammary glands; (A) Analysis of mammary gland mass in *FGFR4 Gly/Gly385* (n=12), *FGFR4 Gly/Arg385* (n=17) and *FGFR4 Arg/Arg385* (n=13) mice. Mice carrying the *FGFR4 Arg385* allele display no difference in the mass of mammary glands compared to mice homozygous for the *FGFR4 Gly385* allele. (B) Analysis of mammary gland size in *FGFR4 Gly/Gly385* (n=12), *FGFR4 Gly/Arg385* (n=16) and *FGFR4 Arg/Arg385* (n=12). Mice carrying the *FGFR4 Arg385* allele display no difference in the mass of mammary glands compared to mice homozygous for the *FGFR4 Gly385* allele; all data are shown as mean  $\pm$  SDM.**

#### 4.2.3.2 The impact of FGFR4 Arg385 on tumor mass and size of WAP-TGF $\alpha$ derived tumors over time

To further analyze the tumor promoting effect of FGFR4 Arg385 in the WAP-TGF $\alpha$  model we followed tumor progression of WAP-TGF $\alpha$  induced mammary carcinoma over time by sacrificing the female mice at defined periods during tumor progression.

We first checked the visible time point of tumor incidence to investigate if the FGFR4 Arg385 allele facilitates the onset of neoplastic transformation and thereby decreases the time point of tumor incidence. Therefore, we monitored and analyzed the visible time point of tumor incidence in *FGFR4 Gly/Gly385*, *FGFR4 Gly/Arg385* and *FGFR4 Arg/Arg385* mice transgenic for WAP-TGF $\alpha$ . As shown in Figure 34A the visible time point of tumor incidence is significantly decreased in mice carrying the *FGFR4 Arg385* allele ( $p=0.001$ ). To ensure that these data are independent of the genetic background, we backcrossed the WAP-TGF $\alpha$  oncomice and the *FGFR4 Arg385 KI* mice at least five times to the FVB background. Here, we also analyzed the visible tumor incidence in *FGFR4 Gly/Gly385*, *FGFR4 Gly/Arg385* and *FGFR4 Arg/Arg385* mice transgenic for WAP-TGF $\alpha$ . Like in the C57BL/6 background, the visible tumor incidence is significantly decreased in mice carrying the *FGFR4 Arg385* allele ( $p=0.002$ ) (Figure 34B).

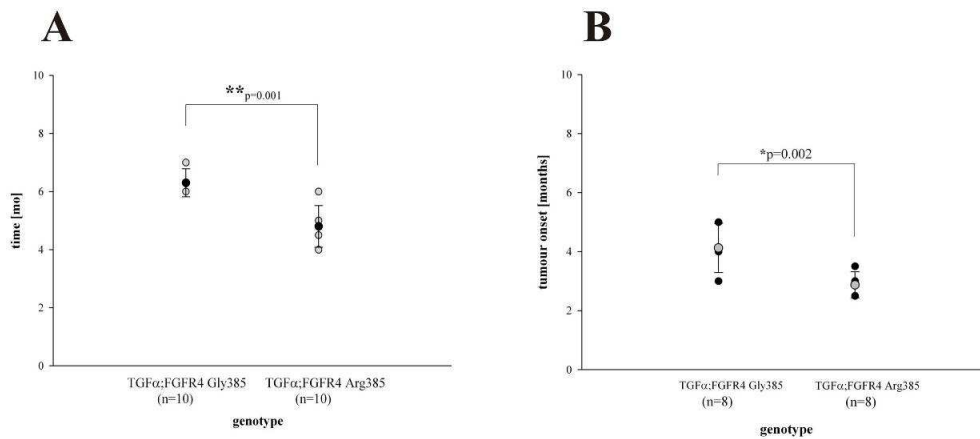


**Figure 34: FGFR4 Arg385 decreases visible time point of tumor onset: (A) Time point of visible tumor incidence in *FGFR4 Gly385* (n=10) and *FGFR4 Arg385* (n=10) mice transgenic for WAP-TGF $\alpha$  in the C57BL/6 background tumors occur significantly earlier in the presence of the *FGFR4 Arg385* allele ( $p=0.001$ ).**

**B) Time point of visible tumor incidence in *FGFR4 Gly385* (n=8) and *FGFR4 Arg385* (n=8) mice transgenic for WAP-TGF $\alpha$  in the FVB background: tumors occur significantly earlier in the presence of the *FGFR4 Arg385* allele ( $p=0.002$ ).**

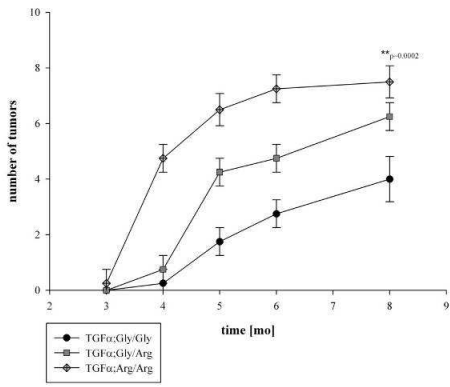
All data are shown as mean  $\pm$  SDM; all p-values were calculated using the students T-test and values  $\leq 0.03$  were considered statistically significant.

In the C57BL/6 background we further investigated the tumor progression over time. Therefore, we analyzed the tumors at the indicated time points in *FGFR4 Gly/Gly385*, *FGFR4 Gly/Arg385* and *FGFR4 Arg/Arg385* mice transgenic for *WAP-TGF $\alpha$* . The analyzed criteria for tumor progression were the number of tumors, the mass, area and the percentage of mass and area of the dissected tumors. Figure 35A displays the increasing amount of tumors induced by *WAP-TGF $\alpha$* . Here, mice homozygous for the *FGFR4 Arg385* allele just partly establish a significant larger amount of tumors at very late points of tumor progression (8 month Arg/Arg-p=0.0002). However, *FGFR4 Arg385* carrying mice seem to induce a larger amount of tumors simultaneously, but importantly, increase their number of tumors over time faster than *FGFR4 Gly/Gly385* mice transgenic for *WAP-TGF $\alpha$* . In Figure 35B the progression of tumor mass is shown. Here, mice homozygous for the *FGFR4 Arg385* allele just partly establish a significant higher tumor mass at very early time points (4 month Arg/Arg-p=0.00002). Nevertheless, the *FGFR4 Arg385* allele seems to clearly progress tumor mass over time. In contrast, the percentage of tumor mass is significantly increased in *FGFR4 Arg/Arg385* mice (4 month Arg/Arg-p=0.0008; 5 month Arg/Arg-p=0.005; 6 month Arg/Arg-p=0.003) (Figure 35C). Contrarily to the tumor mass, the tumor area, as shown in Figure 35D, is mostly significantly increased in *FGFR4 Arg/Arg385* mice (4 month Arg/Arg-p=0.000005; 5 month Arg/Arg-p=0.009; 6 month Arg/Arg-p=0.007). The most significant difference between *FGFR4 Arg385* and *FGFR4 Gly385* carrying mice is shown in the percentage of tumor area (Figure 35E). Here, mice heterozygous for the *FGFR4 Arg385* allele partly display a significant increase (5month Gly/Arg-p=0.0004) and mice homozygous for the *FGFR4 Arg385* display a significant increase in the percentage of tumor mass at all analyzed time points (4 month Arg/Arg-p=0.00008; 5 month Arg/Arg-p=0.003; 6 month Arg/Arg-p=0.0000003; 8 month Arg/Arg-p=0.0003)

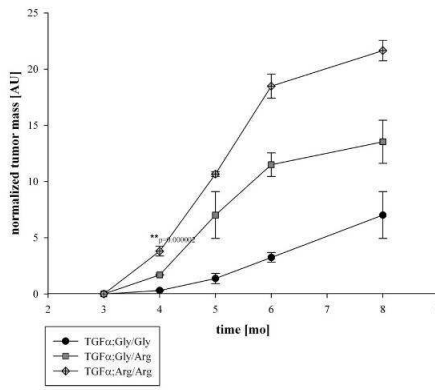
These data further indicate the earlier onset of neoplastic transformation by the *FGFR4 Arg385* allele. The highly significant differences in tumor area and the percentage of tumor area further suggest once again, that the impact of the *FGFR4 Arg385* is not on proliferation but rather the motility of cancer cells and their invasion of the surrounding tissue. In summary, the *FGFR4 Arg385* allele promotes breast tumor progression over time in number, mass and size of the occurring tumors and seems to facilitate the initiation of oncogenesis and thereby advances the time point of tumor onset.

Results

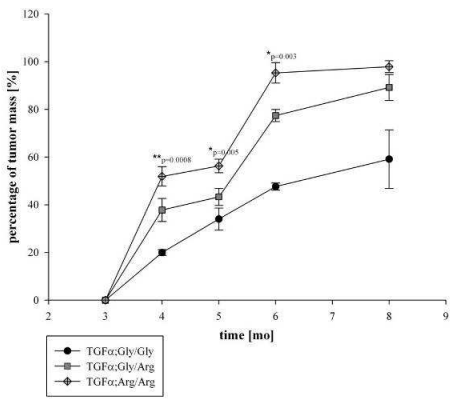
**A**



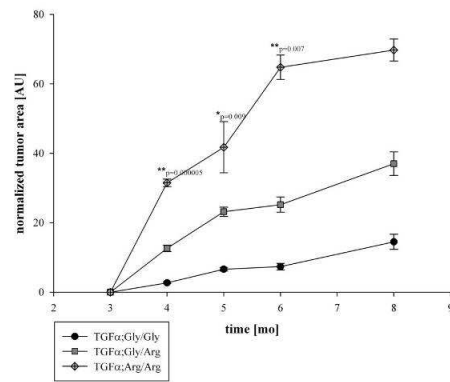
**B**



**C**



**D**



**E**

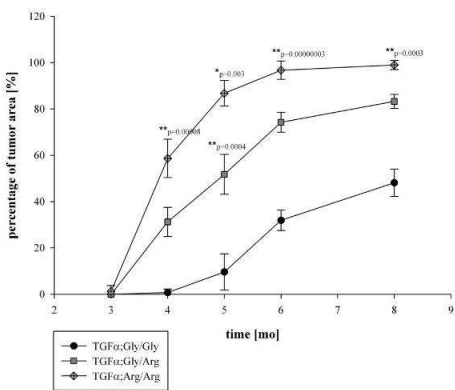


**Figure 35: The *FGFR4* Arg385 allele promotes *WAP-TGF $\alpha$*  induced mammary tumors over time; A) Progression of tumor number in *FGFR4* Gly/Gly385 (n $\geq$ 3), *FGFR4* Gly/Arg385 (n $\geq$ 3) and *FGFR4* Arg/Arg385 (n $\geq$ 3) mice transgenic for *WAP-TGF $\alpha$* : Mice homozygous for *FGFR4* Arg385 partly establish a significantly higher number of tumors over time (8month Arg/Arg-p=0.0002). B) Progression of tumor mass in *FGFR4* Gly/Gly385 (n $\geq$ 3), *FGFR4* Gly/Arg385 (n $\geq$ 3) and *FGFR4* Arg/Arg385 (n $\geq$ 3) mice transgenic for *WAP-TGF $\alpha$* : mice homozygous for *FGFR4* Arg385 partly display a significant increase of tumor mass over time (4month Arg/Arg-p=0.00002). C) Progression of percentage of tumor mass in *FGFR4* Gly/Gly385 (n $\geq$ 3), *FGFR4* Gly/Arg385 (n $\geq$ 3) and *FGFR4* Arg/Arg385 (n $\geq$ 3) mice transgenic for *WAP-TGF $\alpha$*  proportional to mammary gland tissue: mice homozygous for *FGFR4* Arg385 partly display a significant increase in the percentage of tumor mass over time (4month Arg/Arg-p=0.0008, 5month Arg/Arg-p=0.005, 6month Arg/Arg-p=0.003). D) Progression of tumor area in *FGFR4* Gly/Gly385 (n $\geq$ 3), *FGFR4* Gly/Arg385 (n $\geq$ 3) and *FGFR4* Arg/Arg385 (n $\geq$ 3) mice transgenic for *WAP-TGF $\alpha$*  mice homozygous for *FGFR4* Arg385 partly display a significantly increase in the tumor area over time (4month Arg/Arg-p=0.000005, 5month Arg/Arg-p=0.009, 6month Arg/Arg-p=0.007). E) Progression of percentage of tumor area in *FGFR4* Gly/Gly385 (n $\geq$ 3), *FGFR4* Gly/Arg385 (n $\geq$ 3) and *FGFR4* Arg/Arg385 (n $\geq$ 3) mice transgenic for *WAP-TGF $\alpha$*  proportional to mammary gland tissue: mice homozygous and heterozygous for *FGFR4* Arg385 partly display a significant increase in the percentage of tumor area over time (5month Gly/Arg-p=0.0004, 4month Arg/Arg-p=0.00008, 5month Arg/Arg-p=0.003, 6month Arg/Arg-p=0.0000003, 8month Arg/Arg-p=0.0003). All data are shown as mean  $\pm$  SDM; all p-values were calculated using the students T-test and values  $\leq$  0.03 were considered statistically significant.**

#### 4.2.3.3 Molecular characterisation of *WAP-TGF $\alpha$* derived tumors with different *FGFR4* genotypes

To further investigate the underlying mechanism of the tumor promoting effect of the *FGFR4* Arg385 allele, we studied molecular differences of the *FGFR4* alleles. In many human cancers overexpression of the FGFR4 is a commonly observed feature of tumors (Ezzat et al., 2002; Gowardhan et al., 2005; Jaakkola et al., 1993; Jeffers et al., 2002). Therefore, we examined FGFR4 expression in *WAP-TGF $\alpha$* -derived 6 month old tumors from *FGFR4* Gly/Gly385, *FGFR4* Gly/Arg385 and *FGFR4* Arg/Arg385 mice by immunoprecipitation and quantified the expression. Here, the FGFR4 protein is clearly overexpressed in tumors compared to mammary gland without an oncogenic background; however, there was no detectable difference in FGFR4Arg385 expressing tissue (Figure 36A).

Furthermore, we analyzed the constitutive phosphorylation status of *WAP-TGF $\alpha$* -derived tumors from 6 month old *FGFR4* Gly/Gly385, *FGFR4* Gly/Arg385 and *FGFR4* Arg/Arg385 mice by immunoprecipitation. As shown in Figure 36B, FGFR4 Arg/Arg385 displays a significantly enhanced phosphorylation and thereby a higher activation state than FGFR4 Gly/Gly385 or FGFR4 Gly/Arg385 (p=0.012). This result indicates a possible hint for the tumor promoting potential of the *FGFR4* Arg385 allele to influence the kinase activity and thereby leading to a tumor promoting effect. Because of the higher phosphorylation of the FGFR4 Arg/Arg385, we determined the expression and activation of p-Erk and p-Akt to analyze if the higher phosphorylation of the FGFR4 Arg/Arg385 results in a higher activation

of typical downstream molecules. However, the quantification of p-Erk and p-Akt of WAP-TGF $\alpha$ -derived 6 month old tumors from *FGFR4 Gly/Gly385*, *FGFR4 Gly/Arg385* and *FGFR4 Arg/Arg385* mice does not display significant differences with respect to different *FGFR4* genotypes (Figure 36B). We further checked the expression levels of the FGFR4 of WAP-TGF $\alpha$ -derived 3 month old hyperplastic mammary glands and 6 month old adenocarcinomas from *FGFR4 Gly/Gly385* and *FGFR4 Arg/Arg385* mice immunohistochemically. Interestingly, the expression of the FGFR4 in *Arg/Arg385* hyperplasias is clearly increased compared to hyperplasias in *Gly/Gly385* mice transgenic for WAP-TGF $\alpha$  (Figure 36C). Similar to the Western Blot analysis the expression of the FGFR4 in adenocarcinomas does not alter in the presence of the *FGFR4 Arg385* (Figure 36D). This result indicates that the expression of the FGFR4 Arg/Arg385 in mammary oncogenesis is accelerated with an earlier onset that could result in enhanced tumor progression.

Next to the analysis of the FGFR4 expression in primary tumors, we wanted to investigate the expression of genes associated with aggressive breast cancer. We primarily analyzed genes that are involved in migration, invasion and angiogenesis in 6 month old tumors from *FGFR4 Gly/Gly385* and *FGFR4 Arg/Arg385* mice transgenic for WAP-TGF $\alpha$ . As seen in Figure 36 E genes related to tumor suppression, cell cycle, angiogenesis and Matrix-Metalloproteases (MMPs) were investigated. Here, the expression in *FGFR4 Gly/Gly385* expressing WAP-TGF $\alpha$ -induced tumors was set on 100% and the expression in *FGFR4 Arg/Arg385* expressing WAP-TGF $\alpha$ -induced tumors was determined relative to this expression.

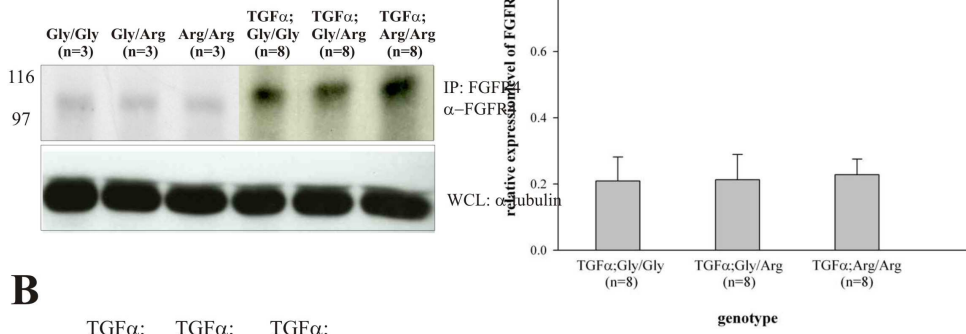
First, we analyzed the expression of the FGFR4 and EGFR to exclude that the tumor progressive impact is a result of the overexpression of the FGFR4 Arg385 or the EGFR and to ensure, that these two proteins are equally expressed among the investigated mice. As seen in Figure 36E both, the FGFR4 and the EGFR display no overexpression in the presence of the *FGFR4 Arg385* allele on the mRNA level. In the set of analyzed tumor suppressors, the only significant alteration was measured for p21, which is significantly downregulated in *FGFR4 Arg/Arg385* expressing WAP-TGF $\alpha$ -induced tumors ( $p=0.03$ ). This tumor suppressor is known to predict the poorest prognosis if its downregulated together with high EGFR expression (Somlo et al., 2008). Regarding cell cycle and proliferation markers, the expression of the cell cycle dependent kinases (CDK) 1, 2 and 4 and Cyclin B was measured. As FGFR4 is known to have a weak mitogenic activity, no difference between *FGFR4 Gly/Gly385* or *FGFR4 Arg/Arg385* expressing tumours was expected. In contrast, there was a significantly higher expression of CDK1 in *FGFR4 Arg/Arg385* expressing tumours

( $p=0.0091$ ). As CDK1 is strongly associated with migration, this significant overexpression seems to not promote higher proliferation but an increase in migratory action of the tumor cells resulting in a more aggressive phenotype of *FGFR4 Arg/Arg385* carrying tumours (Manes et al., 2003). In the group of invasion, the expression of proteins associated with metastasis and angiogenesis were analyzed. Here, CD44 and flk-1 are significantly overexpressed in *FGFR4 Arg/Arg385* tumors (CD44- $p=0.02$ ; flk-1- $p=0.02$ ). The impact of CD44 on invasion is still controversial, however, its metastasis-promoting impact is widely accepted (Godar et al., 2008; Mylona et al., 2008; Sheridan et al., 2006). Next to CD44 also flk-1 is significantly overexpressed in *FGFR4 Arg/Arg385* expressing tumors. This indicates a more aggressive potential of *FGFR4 Arg/Arg385* tumours as flk-1 promotes angiogenesis leading to a more aggressive behaviour of the tumor and its metastatic capacity (Liang and Hyder, 2005). In the cluster of MMPs, MMP13 as well as MMP14 are overexpressed in *FGFR4 Arg/Arg385* contributing to a higher metastatic potential (MMP13- $p=0.021$ ; MMP14- $p=0.02$ ) (Ellsworth et al., 2008; Jiang et al., 2006; Rizki et al., 2008).

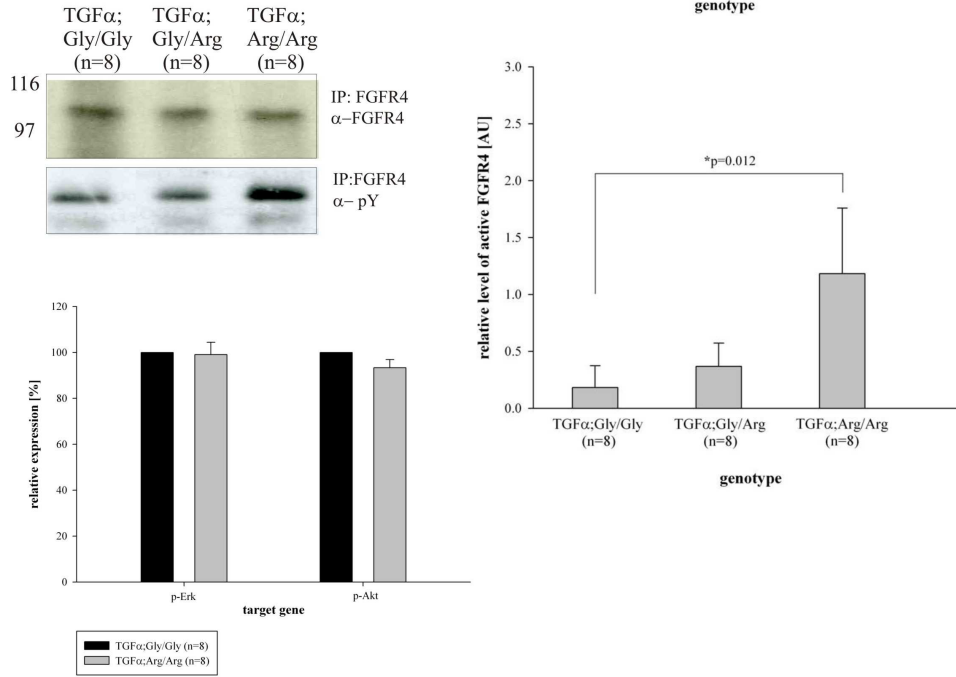
These data are in line with the data obtained from expression analysis in EGFR-transformed MEFs and strongly suggest a more aggressive behaviour of *WAP-TGF $\alpha$*  induced tumors expressing the *FGFR4 Arg/Arg385* resulting in increased tumor progression.

Results

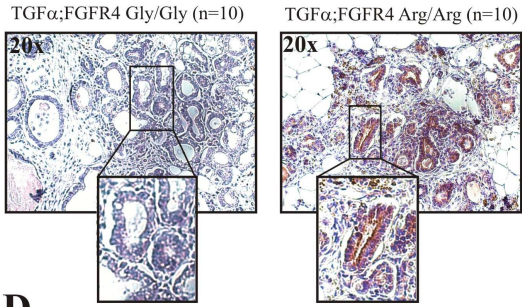
**A**



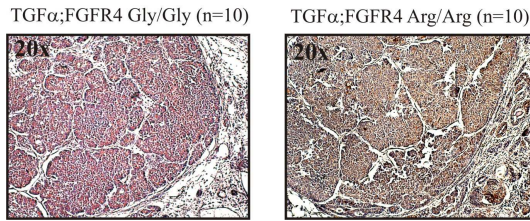
**B**



**C**



**D**



**E**

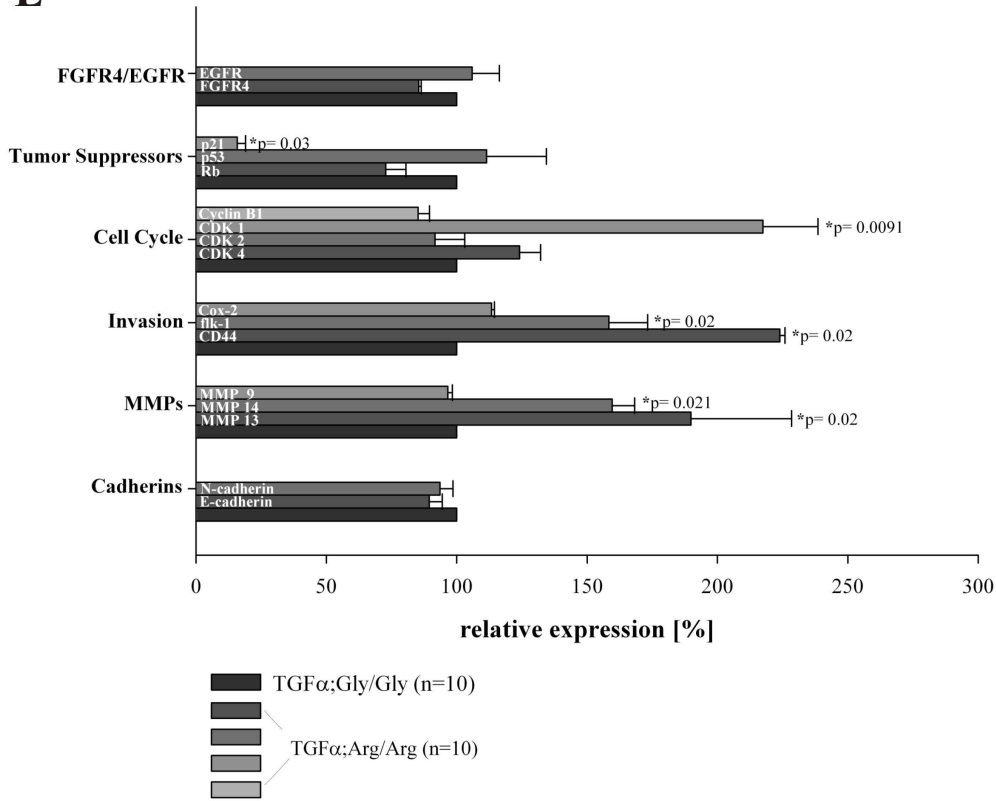


**Figure 36: Molecular characterisation of WAP-TGFα derived tumors regarding the *FGFR4* isotypes A)** Analysis of *FGFR4* expression in *FGFR4 Gly/Gly385* (n=3), *FGFR4 Gly/Arg385* (n=3) or *FGFR4*

*Arg/Arg385* (n=3) mammary glands compared to mammary tumors of *FGFR4 Gly/Gly385* (n=8), *FGFR4 Gly/Arg385* (n=8) or *FGFR4 Arg/Arg385* (n=8) mice transgenic for *WAP-TGF $\alpha$*  after 6 month of tumor progression: FGFR4 expression was analyzed via immunoprecipitation and Western Blotting. Tubulin served as a loading control and normalization value for the quantification of the FGFR4 expression; FGFR4 is overexpressed in *WAP-TGF $\alpha$*  derived tumors compared to normal mammary gland; there is no difference detectable in mice carrying the *FGFR4 Arg385* allele compared to mice homozygous for the *FGFR4 Gly385* allele;

B) Analysis of the activation status of the FGFR4 in mammary tumors of *FGFR4 Gly/Gly385* (n=8), *FGFR4 Gly/Arg385* (n=8) or *FGFR4 Arg/Arg385* (n=8) mice transgenic for *WAP-TGF $\alpha$*  after 6 month of tumor progression: Mice homozygous for the *FGFR4 Arg/Arg385* allele display a significantly increased phosphorylation of the FGFR4 compared to mice homozygous for the *FGFR4 Gly/Gly385* allele in *WAP-TGF $\alpha$*  derived tumors; FGFR4 expression served as a loading control and for the quantification of the phosphorylation levels (Arg/Arg-p=0.012); phosphorylation of downstream signaling molecules p-Erk and p-Akt display no difference regarding the *FGFR4* genotype;

C) FGFR4 expression in hyperplasic mammary glands of *FGFR4 Gly/Gly385* (n=10) or *FGFR4 Arg/Arg385* (n=10) mice transgenic for *WAP-TGF $\alpha$* ; FGFR4 expression was detected immunohistochemically and analyzed microscopically (20x) after 3 month of tumor progression: The higher magnification displays a clear overexpression of the FGFR4 Arg/Arg385 compared to the FGFR4 Gly/Gly385 in hyperplasic mammary glands derived from mice transgenic for *WAP-TGF $\alpha$* ; hyperplasic mammary glands derived from mice transgenic for *WAP-TGF $\alpha$*  display no pathohistological differences regarding their FGFR4 alleles.

D) FGFR4 expression in mammary adenocarcinoma of *FGFR4 Gly/Gly385* (n=10) or *FGFR4 Arg/Arg385* (n=10) mice transgenic for *WAP-TGF $\alpha$*  after 8 month of tumor progression: FGFR4 expression was detected immunohistochemically and analyzed microscopically (20x); FGFR4 is overexpressed in *WAP-TGF $\alpha$*  derived mammary adenocarcinomas but no difference is detectable in the expression level of the FGFR4 Arg/Arg385 compared to the FGFR4 Gly/Gly385; mammary adenocarcinoma derived from mice transgenic for *WAP-TGF $\alpha$*  display no pathohistological differences regarding their FGFR4 alleles.

E) Expression analysis of tumors derived from *FGFR4 Gly/Gly385* (n=10) or *FGFR4 Arg/Arg385* (n=10) mice transgenic for *WAP-TGF $\alpha$*  after 6 month of tumor progression: target gene expression was analyzed via semi-quantitative RT-PCR; GAPDH served as housekeeping gene for normalization; expression values of *FGFR4 Arg/Arg385* tumors are blotted relatively to the expression values of *FGFR4 Gly/Gly385* tumors and grouped regarding their physiological function; mRNA expression level of FGFR4 or EGFR does not differ between the different genotypes; Tumors significantly overexpress genes involved in migration, invasion, vascularization in the presence of the *FGFR4 Arg/Arg385* allele; p21 is significantly downregulated in the presence of the *FGFR4 Arg/Arg385* allele (MMP14-p=0.02, MMP13-p=0.021, MMP9-p=0.019, flk-1-p=0.02, CD44-p=0.02, CDK1-p=0.0091, p21-p=0.03);

All data are shown as mean  $\pm$  SDM; all p-values were calculated using the students T-test and values  $\leq$  0.03 were considered statistically significant.

#### 4.2.3.4 The impact of the *FGFR4 Arg385* allele on lung metastasis of *WAP-TGF $\alpha$* derived tumors

Cancer cells can acquire the ability to circulate in the blood or lymphatic stream in the organism to establish distant metastases. As clinical outcome of cancer is strongly dependent on the invasive stage of the primary tumor it is essential to investigate the impact of the *FGFR4 Arg385* allele on aggressiveness and invasiveness of *WAP-TGF $\alpha$* -derived tumors. Importantly, the expression of genes involved in cell invasivity and metastasis are significantly upregulated in *WAP-TGF $\alpha$*  derived tumors homozygous for the *FGFR4 Arg385*, suggesting that these tumors may develop a more aggressive and invasive phenotype.

Therefore, we investigated distant metastases in the lungs of *FGFR4 Gly/Gly385*, *FGFR4 Gly/Arg385* and *FGFR4 Arg/Arg385* mice transgenic for *WAP-TGF $\alpha$* . First we calculated the

incidence of lung metastases in *FGFR4 Gly385* and *FGFR4 Arg385* mice transgenic for *WAP-TGF $\alpha$* . Strikingly, *FGFR4 Arg385* display a significant earlier incidence of lung metastases when compared to *Gly385* mice (Figure 37A)( $p=0.007$ ). Yet again, this result indicates a faster progression of tumors expressing the *FGFR4 Arg385* as their ability to invade distant organs is acquired earlier. However, as seen in Figure 37B, mice display no patho-histological alterations of lung metastases in the presence of the *FGFR4 Arg385* allele when compared with *FGFR4 Gly/Gly385* mice transgenic for *WAP-TGF $\alpha$* . Furthermore, we investigated the number and size of metastases in the invaded lungs of *FGFR4 Gly/Gly385*, *FGFR4 Gly/Arg385* and *FGFR4 Arg/Arg385* mice transgenic for *WAP-TGF $\alpha$*  after 8 month of tumor progression. As shown in Figure 37C mice expressing the *FGFR4 Arg385* allele partly display a significant increase in the number of metastases in the investigated lungs. Mice heterozygous for the *FGFR4 Arg385* allele show significantly more metastases, that are bigger than  $320\mu\text{M}$  ( $320\mu\text{M Gly/Arg-p}=0.007$ ). Mice homozygous for the *FGFR4 Arg385* allele show significantly more metastases that are smaller than  $80\mu\text{M}$  or bigger than  $320\mu\text{M}$  ( $80\mu\text{M Arg/Arg-p}=0.004$ ;  $320\mu\text{M Arg/Arg-p}=0.009$ ). The significant increase in metastases bigger than  $320\mu\text{m}$  indicates that tumor cells expressing the *FGFR4 Arg/Arg385* are able to invade the lung at an earlier time point. The significant increase in metastases smaller than  $80\mu\text{m}$  indicates, that more tumor cells acquire the ability to invade distant organs in the presence of the *FGFR4 Arg/Arg385* allele resulting in a higher number of metastases. These data go in line with the significant upregulation of genes involved in metastasis in the expression analysis in *WAP-TGF $\alpha$* -derived tumors homozygous for the *FGFR4 Arg385*. Furthermore, these results suggest that the *FGFR4 Arg385* allele contributes to accelerated tumor cell invasion as well as an earlier incidence and faster growth of metastases.

Results

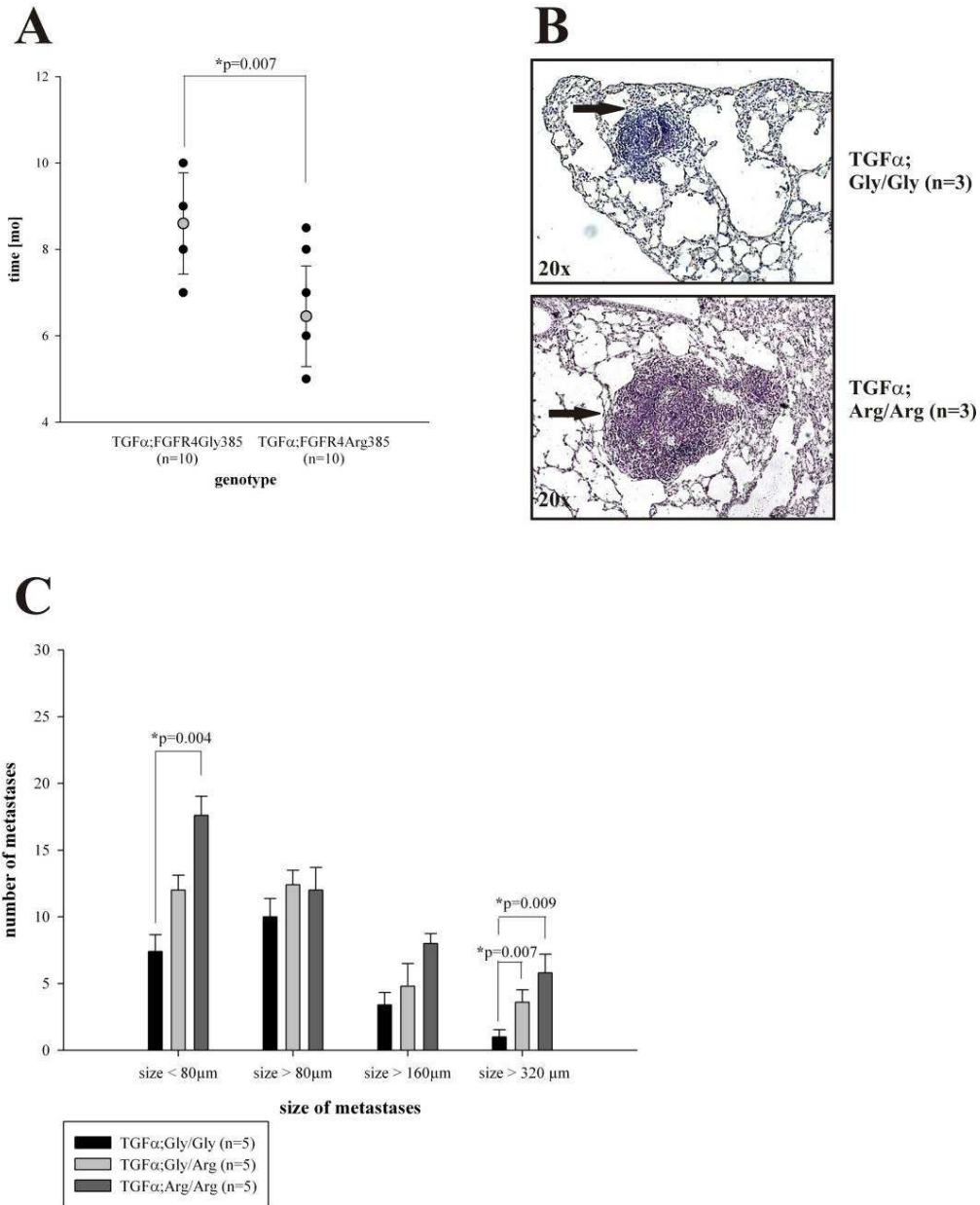


**Figure 37: The *FGFR4 Arg385* promotes lung metastasis in *WAP-TGFα* induced mammary carcinoma:** (A) Incidence of cancer cell metastasis in the lung of *FGFR4 Gly/Gly385* (n=10) and *FGFR4 Arg/Arg385* (n=10) mice transgenic for *WAP-TGFα*: mice transgenic for *WAP-TGFα* display a significantly decreased incidence of metastasis to the lung in the presence of the *FGFR4 Arg385* allele (p=0.007). (B) HE-staining of lung metastases in 6 month old *FGFR4 Gly/Gly385* (n=3), and *FGFR4 Arg/Arg385* (n=3) mice transgenic for *WAP-TGFα*: black arrows indicate metastases; no obvious pathohistological changes were found to be induced by the different *FGFR4* genotypes. (C) Analysis of occurred metastases of 8 month old *FGFR4 Gly/Gly385* (n=5), *FGFR4 Gly/Arg385* (n=5) and *FGFR4 Arg/Arg385* (n=5) mice transgenic for *WAP-TGFα*: size of metastases is plotted against number of metastases; mice hetero- or homozygous for *FGFR4 Arg385* partly display a significantly

accelerated number of metastases (>320 $\mu$ M Gly/Arg-p=0.007, <80 $\mu$ M Arg/Arg-p=0.004, >320 $\mu$ M Arg/Arg-p=0.009). All data are shown as mean  $\pm$  SDM; all p-values were calculated using the students T-test and values  $\leq$  0.03 were considered statistically significant.

### 4.3 Investigation of new *FGFR4* interaction partners

The most prominent influence of *FGFR4* and its Arg388 variant is its implication in cancer correlating with a poor clinical outcome. Furthermore, *FGFR4* is involved in the maintainance of liver homeostasis. However, the distinct mechanisms by which the *FGFR4* supports oncogenesis or liver metabolism have yet to be elucidated. For that purpose, we performed a proteomic analysis of *FGFR4* interaction partners by SILAC-based mass spectrometry *in vitro* and *in vivo*.

#### 4.3.1 Investigation of new *FGFR4* binding partners in MDA-MB-231 cells

As the *FGFR4* is expressed at rather low levels compared to e.g. HER-family receptors and the scientific tools like antibodies represent a limitation in the investigation of this receptor, we chose MDA-MB-231 breast tumor-derived cells modified by Bange et al. (2002) as model system. Here, *FGFR4* is overexpressed either in its Gly388 or Arg388 variant and exerts its cancer progression accelerating effects (Bange et al. 2002). *FGFR4* overexpression, extensively simplifies the detection of the *FGFR4* protein via mass spectrometry and the differences between the *FGFR4* alleles can be analyzed in the same model system.

To perform quantitative mass spectrometry analysis of *FGFR4* interaction partners we used the SILAC Technology do achieve differerential metabolic labelling of the cells (Ong and Mann, 2006). To verify the obtained interaction partners we performed a so called “label switch”. Quantitative mass spectrometry was performed on MDA-MB-231 cells overexpressing either the Gly388 or Arg388 variant by Arg<sup>0</sup>/Lys<sup>0</sup> as well as Arg<sup>10</sup>/Lys<sup>8</sup> labels. Parental MDA-MB-231 cells expressing the empty pLXSN vector served as a negative control and were labeled Arg<sup>4</sup>/Lys<sup>6</sup>. Labelling of cells and sample preparation was done as previously described (Andersen et al., 2005; Shevchenko et al., 1996) (Figure 38 ).

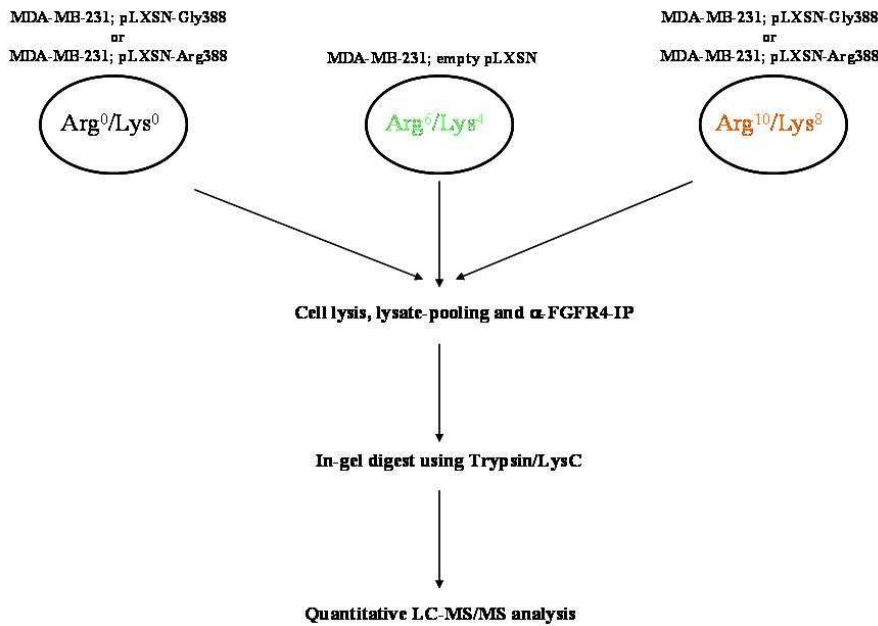


**Figure 38:** Simplified scheme of the experimental setup to analyze FGFR4 interaction partners in MDA-MB-231 cells expressing either empty pLXSN vector, pLXSN-FGFR4 Gly388 or pLXSN-FGFR Arg388; cell lines were subcultured in media containing modified amino acids for SILAC labelling; between MDA-MB-231 cells expressing FGFR4 Gly388 and Arg388 a label switch was performed to verify the results. After cell lysis, lysates were pooled 1:1; FGFR4 and its interactors were immunoprecipitated and subjected for in-gel digest with Trypsin and LysC followed by quantitative LC-MS/MS analysis.

Table 9 displays all proteins that are potential interaction partners of the FGFR4. Identified proteins were normalized to their detection value in MDA-MB-231 cells expressing the empty pLXSN. Therefrom, all proteins with a 5-fold upregulation compared to the negative control are putative interaction partners of the FGFR4. Table 9 further displays the intensity of interaction indicated by the upregulation compared to the negative control and the differences between the FGFR4 Gly388 and Arg388 variant at which the value 1 means no difference in interaction.

The FGFR4 Gly388 and Arg388 themselves were found to be highly upregulated as a result of the overexpression in MDA-MB-231 cells. These results indicate that the experimental setup as well as the overexpression system worked properly. Further, the protein tyrosine phosphatase, receptor type F (PTPRF, LAR), the neurogenic locus notch homolog protein 2 (NOTCH2), the Ephrin type-A receptor 2 (EPHA2) and most interestingly the Epidermal Growth Factor (EGFR) were found to be highly upregulated. LAR is a transmembrane phosphatase and is known to regulate the function of various receptor tyrosine kinases. Its activity is known to be negatively regulated by the EGFR (Ruhe et al., 2006). Loss of LAR is associated with increased hepatocyte cell proliferation by c-MET, insulin resistance and increased tumor cell metastasis (Machide et al., 2006; Mander et al., 2005; McArdle et al.,

2005). Overexpression of LAR induces apoptosis in mammalian cells (Weng et al., 1998). Above that, LAR is implicated in the regulation of FGF-induced signalling by interacting with FRS2 (Wang et al., 2000). EPHA2 is a transmembrane receptor tyrosine kinase that is upregulated on many human aggressive cancer cells. Unlike other receptors, it displays kinase activity without ligand binding (EphrinA1) that causes tumor progression. In breast cancer cells, including MDA-MB-231, EPHA2 negatively regulates malignant cancer cell behavior upon ligand or antibody binding that induces cell adherence (Carles-Kinch et al., 2002; Noblitt et al., 2004).

EGFR overexpression in MDA-MB-231 cells is associated with several key features of cancer development and progression and represents a valid target in various cancers. In MDA-MB-231 cells, the stimulation of the EGFR via multiple mechanisms results in an increase of their malignant behavior (Wang et al., 2009; Zheng et al., 2009). These data indicate that MDA-MB-231 cells overexpressing the FGFR4 Gly388 or Arg388 variant present a useful model to study potential interaction partners of the FGFR4 in breast cancer cells. Furthermore, FGFR4 seems to interact with a variety of receptor tyrosine kinases. However, all potential interaction partners displayed no difference between the different *FGFR4* isotypes.

Protein Names	Gene Names	RP <sub>1</sub>	RP <sub>2</sub>	PEP
Fibroblast growth factor receptor 4	FGFR4	39	38	0
Protein tyrosine phosphatase, receptor type, F	LAR	3	3	4.0149E-27
Epidermal growth factor receptor	EGFR	2	3	3.9283E-37
Ephrin type-A receptor 2	EPHA2	5	5	1.1434E-22

Protein Names	Gene Names	ratio FGFR4Gly388 (n=2)	stdv	ratio FGFR4Arg388 (n=2)	stdv	ratio FGFR4Arg388Gly388 (n=2)	stdv
Fibroblast growth factor receptor 4	FGFR4	26.42	7.97	36.19	17.71	1.26	0.04
Protein tyrosine phosphatase, receptor type, F	LAR	16.59	7.87	14.32	6.31	1.06	0.24
Epidermal growth factor receptor	EGFR	6.50	1.85	7.60	1.95	1.14	0.16
Ephrin type-A receptor 2	EPHA2	7.97	0.09	8.74	1.70	1.05	0.06

**Table 9: Summary of possible new interaction partners of the FGFR4 in MDA-MB-231 cells; potential interaction partners were verified by the “label switch”; evaluation criteria of identified proteins were upregulation  $\geq 5$ -fold, Razor Peptides (=RPs)  $> 2$ , PEP  $< 0.03$ ; The table further displays fold of upregulation and fold difference between the *FGFR4* isotypes; value 1 implies equal interaction between the *FGFR4* isotypes**

#### 4.3.2 Validation of the EGFR/FGFR4 interaction

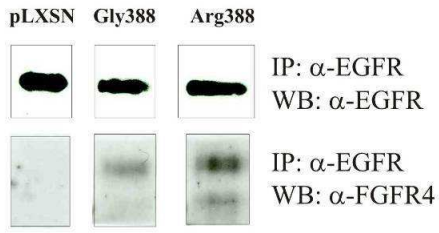
Interestingly, the data obtained from the mass spectrometry analysis in MDA-MB-231 cells, displayed the EGFR amongst others as an interaction partner of the FGFR4. The EGFR is a key regulator of various processes in cancers, approved therapeutic target and the main component of tumor progression in the *WAP-TGF $\alpha$*  mouse mammary carcinoma model used

in our experiments. Therefore, the validation of the potential interaction between the EGFR and the FGFR4 preceded the validation of the other analyzed interaction partners.

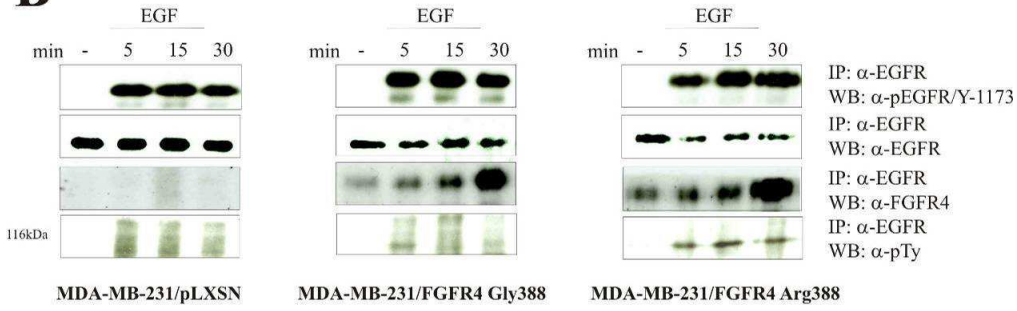
First we aimed to show, that the FGFR4 gets co-immunoprecipitated with the EGFR in MDA-MB-231 cells overexpressing either the empty pLXSN, pLXSN-Gly388 or -Arg388 (Figure 39A). These data indicate a first hint for the interaction of these two receptors. In contrast to the mass spectrometry analysis, the Western Blot Analysis displayed an increased content of co-immunoprecipitated FGFR4 Arg388 compared to FGFR4 Gly388. As expected, the negative control displayed no co-immunoprecipitated FGFR4 as FGFR4 is barely expressed in MDA-MB-231 cells. Nevertheless, as proteins are mostly localized in clusters on the membrane, co-immunoprecipitation is no final evidence for an interaction of two receptors. Therefore, we investigated the EGFR-FGFR4 interaction upon EGF stimulation. As shown in Figure 39B, the EGFR displays increased phosphorylation in the presence of the overexpressed FGFR4. Furthermore, the EGFR in MDA-MB-231 cells overexpressing the FGFR4 Arg388 is even more activated than in the presence of the FGFR4 Gly388. Interestingly, the co-immunoprecipitated FGFR4-Arg388 is more active than the FGFR4-Gly388. Above that, phosphorylation of the FGFR4 increases over time upon EGF stimulation. These data are confirmed by the quantification of the Western Blot Analysis (Figure 39C) Furthermore, the activation of the downstream signalling protein Akt is increased in MDA-MB-231 cells overexpressing the FGFR4 Arg388 upon EGF stimulation. The activation of Erk did not differ between the different FGFR4 isoforms (data not shown). This result indicates a physiological interaction of the FGFR4 and EGFR upon EGF stimulation. Similarly, the EGFR-FGFR4 interaction is hardly seen in unstimulated cells. In summary, the FGFR4 and the EGFR are direct interaction partners. Here, FGFR4 seems to support EGFR induced signalling by receptor phosphorylation upon EGF stimulation, whereas the FGFR4 Arg388 enhances the signal.

Results

**A** MDA-MB-231



**B**



**C**

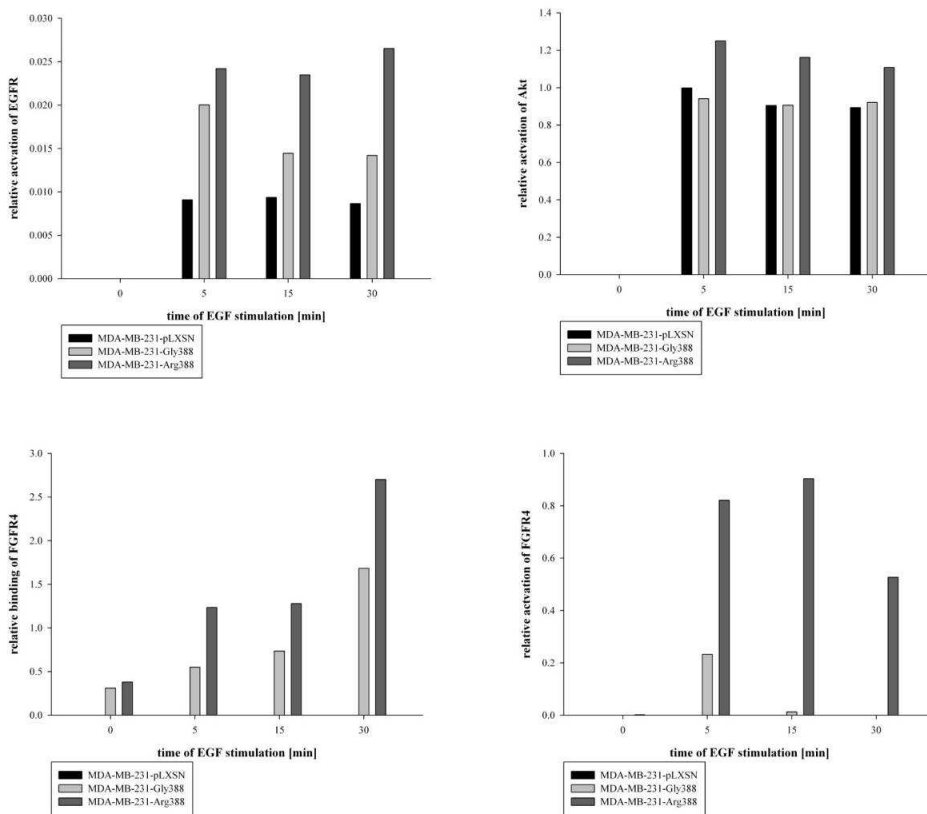
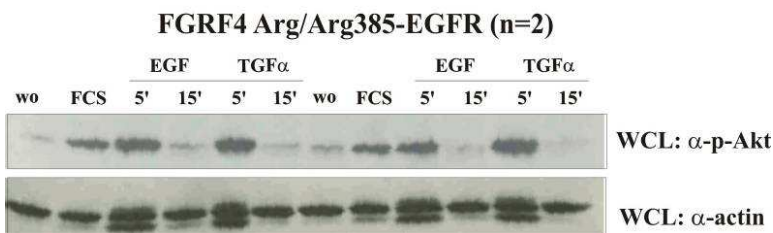
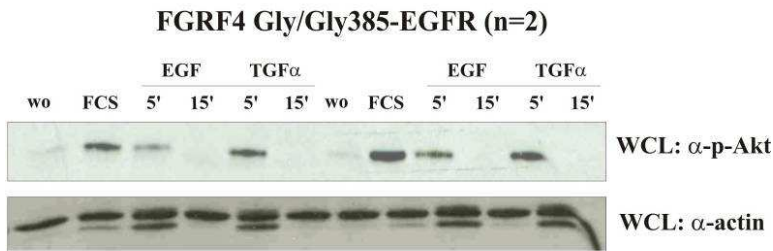


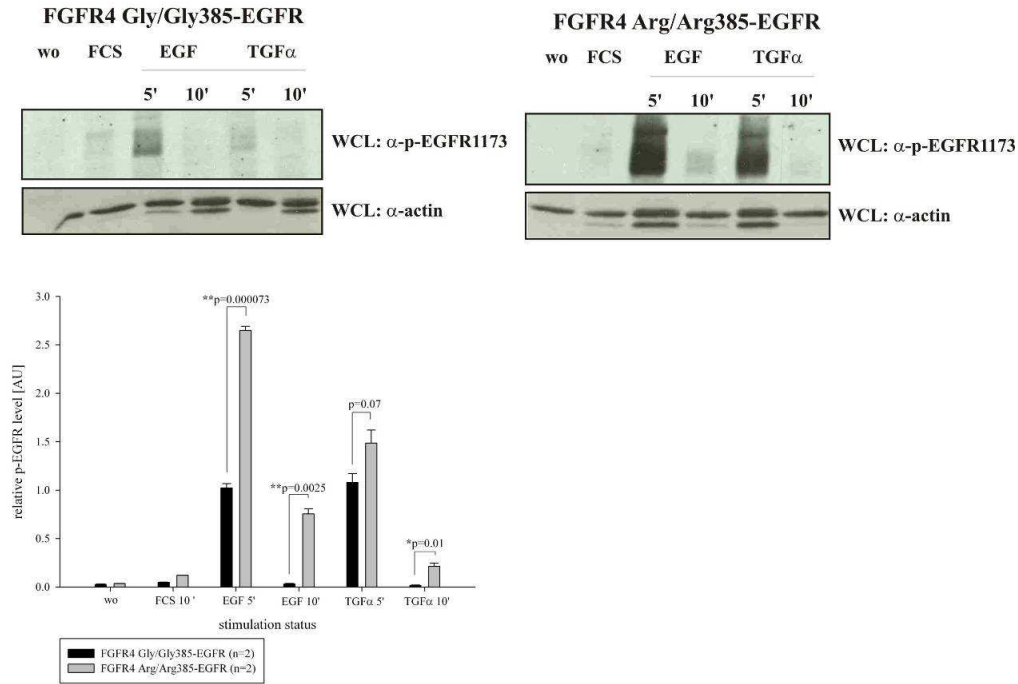
**Figure 39: Validation of the EGFR/FGFR4 interaction; A) Co-Immunoprecipitation of EGFR and FGFR4 in MDA-MB-231 cells overexpressing the empty pLXSN, pLXSN-Gly388 and -Arg388: Interaction of EGFR and FGFR4 Arg388 seems to be stronger than EGFR and FGFR4 Gly388; B) EGFR-FGFR4 interaction upon EGF-stimulation: increased phosphorylation of the EGFR and accelerated FGFR4 interaction and activation in MDA-MB-231 cells expressing the FGFR4 Arg388; C) Quantification of Western Blot Analysis of EGF stimulated MDA-MB-231 cells: MDA-MB-231 cells expressing the FGFR4 Arg388 display an accelerated EGFR and Akt activation, total EGFR and tubulin served as normalization value for quantification, respectively; the co-immunoprecipitated FGFR4 Arg388 displays a accelerated binding to the EGFR and increased activation compared to the co-immunoprecipitated FGFR4 Gly388**

To further confirm the data obtained in MDA-MB-231 cells we investigated the signalling upon EGF and TGF $\alpha$  stimulation in MEFs derived from the *FGFR4 Arg385 KI* mice transformed with EGFR. MEFs transformed with EGFR displayed an accelerated and prolonged activation of Akt in the presence of the *FGFR4 Arg385* allele upon EGF and TGF $\alpha$  stimulation (Figure 40A). The activation of Erk shows no difference between the different *FGFR4* isotypes (data not shown). Similar to the MDA-MB-231 cells overexpressing the FGFR4 Arg388, MEFs transformed with EGFR and expressing the FGFR4 Arg385 display a significant increase in pEGFR levels compared to FGFR4 Gly385 MEFs (EGF5' -p=0.000073, EGF10' -p=0.0025, TGF $\alpha$ 5' -p=0.07, TGF $\alpha$ 10' -p=0.01) (Figure 40B). Above that, MEFs transformed with EGFR display an activation of the FGFR4 upon EGF and TGF $\alpha$  stimulation (Figure 40C). Similar to MDA-MB-231 cells, MEFs expressing the *FGFR4 Arg385* allele display an increased activation of the FGFR4. These data confirm the results obtained in MDA-MB-231 cells. The FGFR4 Arg385 clearly supports the activation and following downstream signaling of the EGFR.

**A**



**B**



**C**

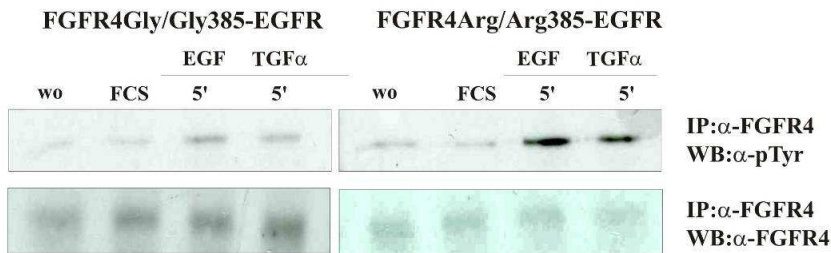


**Figure 40: Western Blot analysis of MEFs derived from *FGFR4* Gly385 or Arg385 homozygous mice transformed with EGFR upon EGF and TGF $\alpha$  stimulation; A) MEFs transformed with EGFR display an increased and prolonged activation of Akt upon EGF and TGF $\alpha$  stimulation when expressing the *FGFR4* Arg385 allele; B) MEFs transformed with EGFR display a significantly increased activation of the EGFR upon EGF and TGF $\alpha$  stimulation when expressing the *FGFR4* Arg385 allele (EGF5'-p=0.000073, EGF10'-p=0.0025, TGF $\alpha$ 5'-p=0.07, TGF $\alpha$ 10'-p=0.01); actin served as a normalization value for quantification C) In MEFs, transformed with EGFR, FGFR4 gets activated upon EGF and TGF $\alpha$  stimulation whereas the FGFR4 Arg385 displays an increased phosphorylation compared to the FGFR4 Gly385; All data are shown as mean  $\pm$  SDM; all p-values were calculated using the students T-test and values  $\leq$  0.03 were considered statistically significant.**

### **4.3.3 The FGFR4 Arg385 influences the migratory behavior and the sensitivity towards Gefitinib in MDA-MB-231 cells**

To further investigate the interaction between the EGFR and the FGFR4, we analyzed the influence of the FGFR4 Arg385 on the biological properties of MDA-MB-231 cells. We firstly analyzed the proliferation of MDA-MB-231 cells overexpressing the empty pLXSN, pLXSN-Gly385 and -Arg385. As shown in Figure 41A the overexpressed FGFR4 had no influence on the proliferation of MDA-MB-231 cells under normal conditions. As shown in Figure 41B overexpression of the FGFR4 results in a tremendous increase in migration indicating the immense capacity of the FGFR4 to promote the migratory behavior of cells (Gly388-p=0.001, Arg388-p=0.001). Above that, MDA-MB-231 cells overexpressing the FGFR4 Arg388 display accelerated migratory behavior compared to MDA-MB-231 cells overexpressing the FGFR4 Gly388. In contrast to the data of Bange et al., FGFR4 Gly388 did not suppress the migration of MDA-MB-231 cells. This may be due to the scratch assay of Bange et al. (2002) that possibly resulted in a different response compared to a Boyden Chamber Assay that monitors changes in chemotactic migration rather than cell-cell contact.

Results

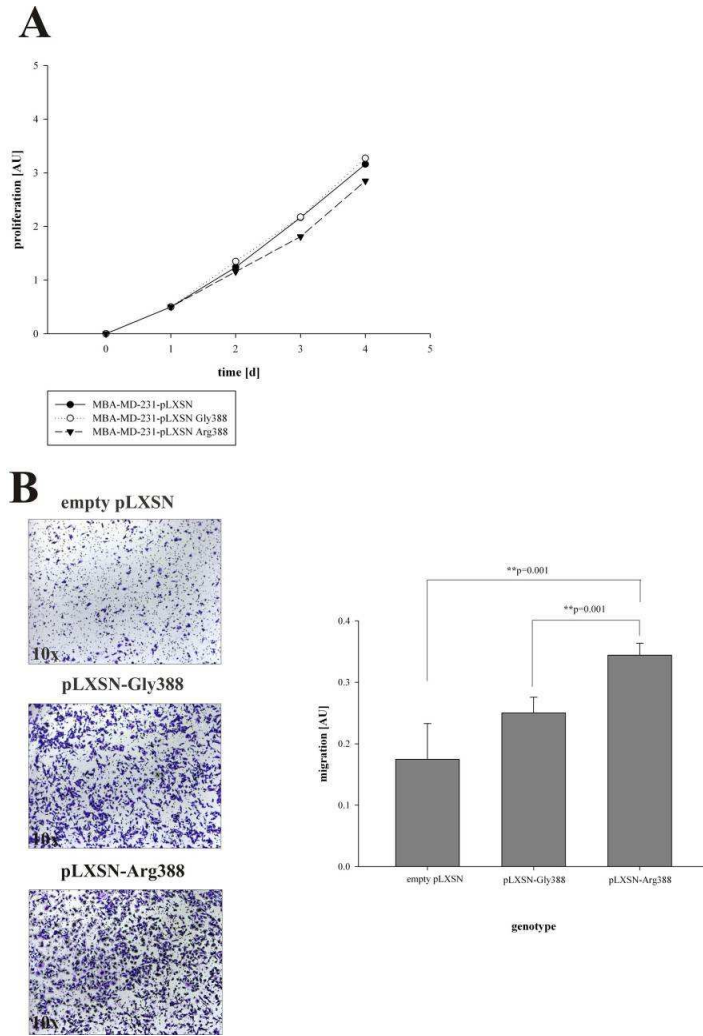


**Figure 41: Biological properties of MDA-MB-231 cells expressing empty pLXSN, pLXSN-Gly388 or pLXSN-Arg388; A) MDA-MB-231 cells do not alter their proliferative capacity by overexpressing the FGFR4; B) MDA-MB-231 cells display a partly significantly increased migratory capacity by overexpressing the FGFR4 (FGFR4 Arg388-p=0.001); MDA-MB-231 cells overexpressing the *FGFR4* Arg388 allele display a significantly accelerated migration compared to MDA-MB-231 cells expressing the *FGFR4* Gly388 allele (FGFR4 Arg388-p=0.001); All data are shown as mean  $\pm$  SDM; all p-values were calculated using the students T-test and values  $\leq 0.03$  were considered statistically significant.**

To further analyze the physiological connection between the EGFR and the FGFR4 we investigated the differences between the different FGFR4 alleles in MDA-MB-231 overexpressing cells upon exposure to Gefitinib. This small molecule tyrosine kinase inhibitor blocks EGFR phosphorylation by competing with ATP and thereby inhibits EGFR-mediated downstream signalling (Herbst et al., 2004). Therefore, physiological processes that require the dimerization of the EGFR and the FGFR4 should lead to different results in the presence

of Gefitinib compared to those obtained without an EGFR inhibitor. We first determined the response of MDA-MB-231 cells either overexpressing the empty pLXSN vector or FGFR4 Gly388 or FGFR4 Arg388 towards increasing concentrations of Gefitinib (0.025-20 $\mu$ M) in a MTT-proliferation assay (Figure 42A). Interestingly, FGFR4 Arg388 expressing cells display a typical dose response curve whereas FGFR4 Gly388 and empty pLXSN vector expressing cells display no response up to 20 $\mu$ M of Gefitinib. The analyzed  $IC_{50}$  was estimated to be 18.72  $\mu$ M for both, MDA-MB-231 cells expressing the empty pLXSN or FGFR4 Gly388. In contrast, the calculated  $IC_{50}$  for MDA-MB-231 cells overexpressing the *FGFR4 Arg388* allele was 9.53 $\mu$ M. These results indicate a higher sensitivity of MDA-MB-231-FGFR4Arg388 cells towards Gefitinib and suggest a higher EGFR-dependence of these cells. Further, we wanted to determine if the decreased proliferation results from a proliferative stop or apoptosis induced by Gefitinib. Therefore, we investigated the impact of FGFR4 Arg388 overexpression on apoptosis in response to Gefitinib treatment in MDA-MB-231 cells. As shown in Figure 42B FGFR4 Arg388 expressing MDA-MB-231 cells display a significantly increased apoptotic response towards Gefitinib after 96 hours compared to MDA-MB-231 cells expressing the FGFR4 Gly388 (20 $\mu$ M-p=0.012; 10 $\mu$ M-p=0.0022). These data indicate that MDA-MB-231 cells expressing the *FGFR4 Arg388 allele* display an increased sensitivity towards Gefitinib regarding cellular survival. As MDA-MB-231 cells acquired a significantly accelerated migratory capacity by overexpressing the *FGFR4 Arg388* allele we determined the migratory behavior of MDA-MB-231 cells in the presence of Gefitinib (2.5 $\mu$ M) (Figure 42C). After 15 hours of migration in Boyden Chamber Assays, MDA-MB-231 cells expressing the *FGFR4 Arg388* allele display 22.28% inhibition of migration compared to the DMSO treated control cells. In contrast, MDA-MB-231 cells overexpressing the *FGFR4 Gly388* allele displayed only 6.28% of inhibition. This result indicates that the migratory capacity of MDA-MB-231 cells overexpressing the FGFR4 Arg388 is dependent on the molecular action of the EGFR and furthermore displays an increased response towards Gefitinib treatment.

In conclusion, the treatment of MDA-MB-231 cells with Gefitinib suggests a strong physiological connection between FGFR4 and EGFR regarding cellular survival and migration. Above that, the dependence of the molecular interaction between FGFR4 and EGFR is increased in the presence of the *FGFR4 Arg388* allele.

Results

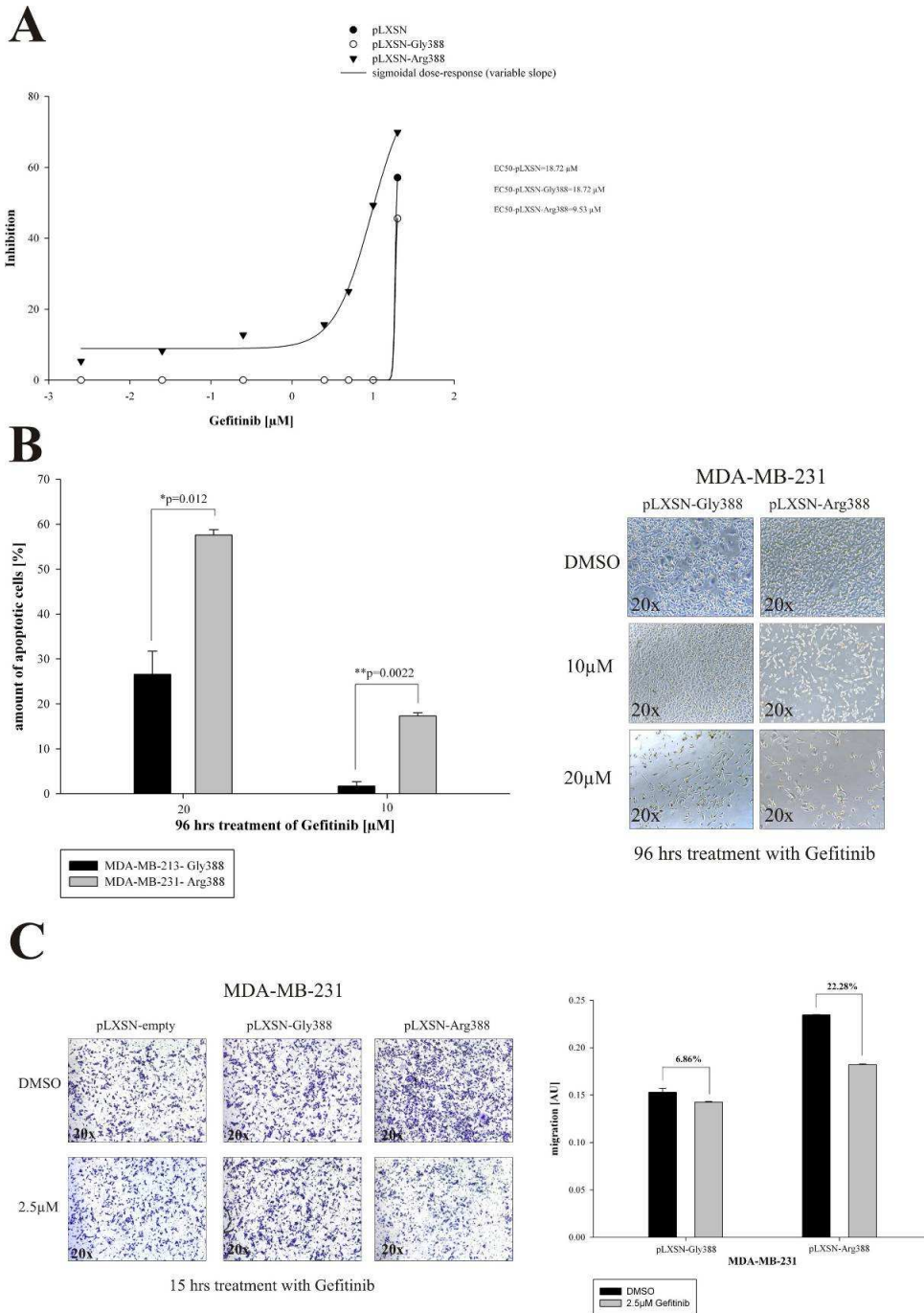


**Figure 42: Impact of Gefitinib in MDA-MB-231 cells expressing empty pLXSN, pLXSN-Gly388 or pLXSN-Arg388 on proliferation, apoptosis and migration; A) MDA-MB-231 cells overexpressing the *FGFR4 Arg388* allele display a increased sensitivity ( $IC_{50}=9.53$ ) towards Gefitinib compared to *FGFR4 Gly388* or control cells ( $IC_{50}=18.72$ ); B) MDA-MB-231 cells display a significant increase in apoptosis in the presence of the *FGFR4 Arg388* allele compared to the *FGFR4 Gly388* towards Gefitinib (20 μM- $p=0.012$ ; 10 μM- $p=0.0022$ ); C) MDA-MB-231 cells display a decrease in migration in the presence of the *FGFR4 Arg388* allele compared to the *FGFR4 Gly388* in response to Gefitinib; All data are shown as mean**

± SDM; all p-values were calculated using the students T-test and values ≤ 0.03 were considered statistically significant.

#### 4.3.4 Investigation of new interaction partners of the hepatic FGFR4 *in vivo*

Stable isotope labelling in cell culture (SILAC) has become a versatile tool for quantitative, mass spectrometry (MS)-based proteomics. In order to investigate global interactions and connections tissue-specifically and with the impact of an whole organism Kruger et al. established an *in vivo* SILAC by feeding mice with a diet containing either the natural or the  $^{13}\text{C}_6$ -substituted version of lysine (Figure 43).

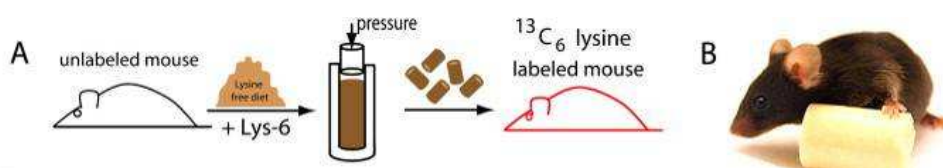


**Figure 43: In Vivo labelling of C57BL/6 mice:** mice were fed with a diet containing either the natural or  $^{13}\text{C}_6$ -substituted version of lysine; The efficiency of labeling is dependent on the cell proliferation rate of the specific tissue; the F2 generation is labeled completely (Kruger et al., 2008)

The FGFR4 is involved in various metabolic processes in the liver including lipid-, glucose- and bile acid metabolism as well as in liver carcinogenesis (Huang et al., 2008; Huang et al., 2007). Also recent publications provide some evidence for the molecular action of the FGFR4 and its Arg388 variant the distinct mechanism including interaction partners is still unknown (Stadler et al., 2006; Wang et al., 2006; Wang et al., 2008).

#### 4.3.5 Quantitative analysis of hepatic FGFR4 binding partners and their differences regarding the *FGFR4* isotypes

In order to investigate novel interaction partners of the hepatic FGFR4, a mass spectrometry analysis was performed to identify all proteins co-immunoprecipitated with the FGFR4. To allow a quantifiable analysis of the interaction partners the labelled SILAC-mouse was used as an internal standard (Kruger et al., 2008). To exclude unspecific binding partners the first experimental step was to establish FGFR4 blocking peptides to selectively block the antibody-FGFR4 interaction to identify all unselective binders. As seen in Figure 44A a FGFR4 overexpressing construct that was used to generate the homemade  $\alpha$ -FGFR4ex

antibody (C. Stadler, 2005) was transfected in HEK293 cells. The recombinant FGFR4 protein was purified and digested with either Trypsin or LysC. The obtained blocking peptides were tested in a FGFR4 immunoprecipitation for their blocking efficacy. As shown in Figure 44A especially the tryptic digest of the FGFR4 blocking peptides clearly diminished the antibody-FGFR4 interaction. Therefore, the synthesized blocking peptides were applicable for the following mass spectrometry analysis of novel FGFR4 interaction partners in the liver.

Figure 44B displays the experimental setup regarding the investigation of novel FGFR4 interaction partners via *in vivo* SILAC. The SILAC mouse was used as an internal standard to achieve quantifiable results. The hepatic FGFR4 of the unlabelled mouse was immunoprecipitated in the presence of the blocking peptides to detect unspecific binding partners. In the quantitative LC-MS/MS analysis FGFR4 and its specific interaction partners should be highly upregulated in the labelled fraction. Unspecific interaction partners should display a 1:1 ratio compared to the unlabelled fraction incubated with the blocking peptides. Although the blocking peptides displayed a high efficacy in the Western Blot analysis, mass spectrometry analysis detected ~ 300 proteins as specific binding partners of the FGFR4 (data not shown). Such a high number of binding partners can not be a result of physiologically relevant interactions. Therefore, quantitative mass spectrometry analysis of hepatic FGFR4 interaction partners can not be performed with the blocking peptides employed in these experiments. In order to improve the specificity of the blocking reaction, we sequenced the obtained blocking peptide mixture to synthesize specific blocking peptides (Figure 44C). In contrast to the blocking peptide mix obtained from the tryptic digest, all of the synthesized blocking peptides were inactive in the Western Blot analysis (data not shown). For that reason, the investigation of hepatic FGFR4 interaction partners was done with the liver of *FGFR4 KO* mice (Yu et al., 2000) that were kindly provided by Wallace L. McKeehan, PhD, Center for Cancer and Stem Cell Biology, Institute of Biosciences and Technology, Texas, Houston, USA. Figure 44 D and E shows the experimental setup to identify interaction partners of the hepatic FGFR4 and their differences between the FGFR4 isoforms.

Results

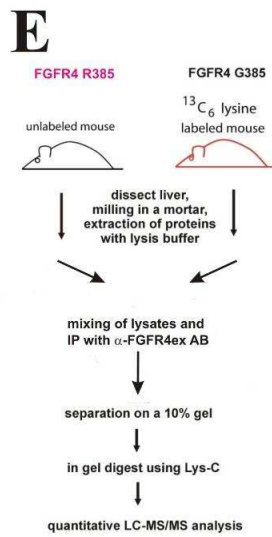
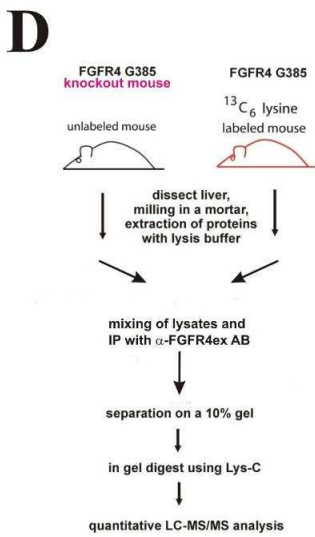
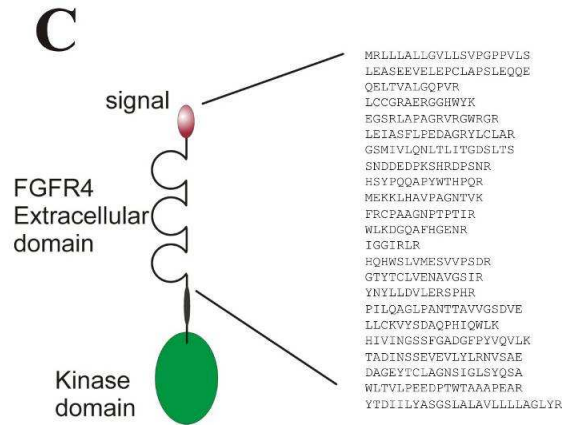
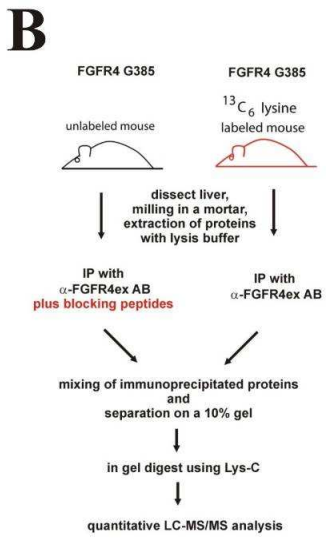
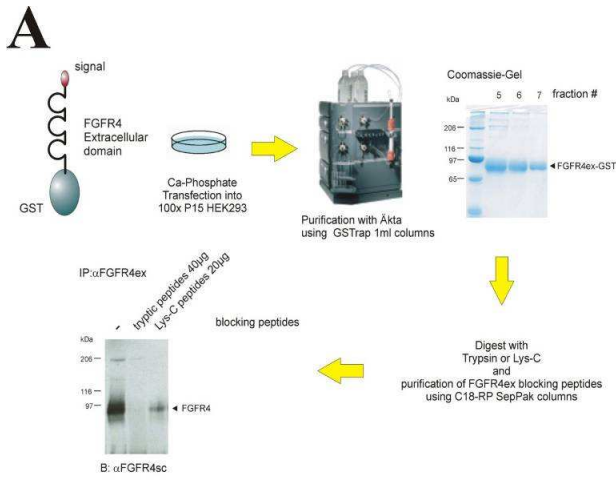


**Figure 44: Investigation of hepatic interaction partners of the FGFR4 via *in vivo* SILAC:** A) Synthesis of blocking peptides; HEK293 were used to transiently transfect a vector containing the extracellular domain of the FGFR4 tagged with GST. Via specific signal peptides, the recombinant protein can be delivered to the cell media; after digestion with either Trypsin or Lysin the efficiency of the blocking peptides were tested in an immunoprecipitation experiment with FGFR4.

B) Experimental scheme to analyze interaction partners of hepatic FGFR4 via blocking peptides; to enable a quantifiable analysis, the labelled SILAC mouse was used as an internal standard; livers of labelled and unlabelled mice were dissected and lysed; with unlabelled liver-lysates FGFR4 was immunoprecipitated in the presence of the blocking peptides preventing the binding of FGFR4 with the antibody for the detection of unspecific binding partners; in labelled liver-lysates, FGFR4 was immunoprecipitated without blocking peptides to analyze FGFR4 binding partners.

C) Sequence analysis for the generation of specific blocking peptides.

D) Experimental scheme to analyze interaction partners of hepatic FGFR4 via *FGFR4 KO* mice; to enable a quantifiable analysis, the labelled SILAC mouse was used as an internal standard; livers of labelled and unlabelled mice were dissected, lysed and mixed together for FGFR4 immunoprecipitation.

E) Experimental scheme to analyze interaction partners of hepatic FGFR4 Arg385; to enable a quantifiable analysis, the labelled SILAC mouse was used as an internal standard; livers of labelled and unlabelled mice were dissected, lysed and mixed together for FGFR4 immunoprecipitation.

Table 10 displays all identified FGFR4 isotype interaction partners. Here, significance ( $PEP < 0.03$ ), amount of razor peptides (RPs,  $> 1$ ) and an upregulation of at least 3 fold in *FGFR4 KO* experiments identified potential FGFR4 interaction partner. FGFR4 is highly upregulated in SILAC mice compared to *FGFR4 KO* mice. Therefore, the experimental workflow displays proper settings for the investigation of hepatic interaction partners of the FGFR4. Furthermore, the FGFR4 is not differentially expressed between the *FGFR4* isotypes, a fact that was already shown by the characterization of the *FGFR4 Arg385 KI* mice.  $\beta$ Klotho is a known high affinity interaction partner of the FGFR4. This single-transmembrane protein is the essential co-receptor for the activation of downstream signaling events upon FGF19/15 stimulation of the FGFR4 (Kurosu and Kuro, 2009; Wu et al., 2007). Therefore, the identification of  $\beta$ Klotho as a strong interaction partner was the “positive control” in the MS-analysis. As seen in Table 10  $\beta$ Klotho is highly upregulated in SILAC mice compared to *FGFR4 KO* mice indicating yet again proper experimental settings. Besides that, the *in vivo* SILAC analysis of our mice yielded so far unknown interaction partners that could contribute to the elucidation of the molecular action of the FGFR4 and its Arg385/388 variant. Hydroxyacid-oxidase 1 (Hao1) is a mainly peroxisomal protein that oxidizes glycolate and glyoxycolate with a subsequent production of H<sub>2</sub>O<sub>2</sub> and is primarily expressed in the liver and pancreas. Downregulation of Hao1 in rats results amongst others in the upregulation of proteins associated with oxidative stress (Recalcati et al., 2003). Propanoyl-CoA C-acetyltransferase (Scp2) plays an important role in the intracellular movement of cholesterol and possibly other lipids. Its deficiency results in multiple phenotypes in humans (Ferdinandusse et al., 2006). In mice loss of Scp2 induces alterations in the biliary lipid

## Results

secretion and hepatic cholesterol metabolism (Fuchs et al., 2001). Formimidoyl-transferase-cyclodeaminase (Ftcd) is suggested to control folic acid liver metabolism (Bashour and Bloom, 1998). Furthermore, Ftcd is recognized as a liver specific antigen that is detected in sera of patients with autoimmune hepatitis (Lapierre et al., 1999). Above that, Ftcd is overexpressed in hepatocellular carcinoma (HCC) and is therefore suggested to contribute to the diagnosis of early stage HCC (Fuchs et al., 2001). Hydroxymethylglutaryl-CoA-synthase (Hmgcs2) is a key regulator of keton body production and is highly expressed in liver and colon. It is known that Hmgcs2 is transcriptionally regulated by c-myc and FKHRL1, a member of the forkhead in rhabdomyosarcoma family that represses the transcription of Hmgcs2 in HepG2 cells upon insulin stimulation. Furthermore, Hmgcs2 is implicated in colon cancer via its downregulation (Camarero et al., 2006; Nadal et al., 2002). Among these potential interactors Hao1 and Scp2 display stronger interaction with the FGFR4 Arg385 variant indicated by a higher ratio compared to the FGFR4 Gly385. All afore mentioned potential interaction partners are not yet implicated in tyrosine kinase signalling or known to interact with RTKs. Therefore, fundamental follow-up experiments are necessary to first put these proteins into the context of the molecular action of receptor tyrosine kinases. Next to these potential new interactors the most interesting target is the epidermal growth factor receptor (EGFR). The EGFR was found to significantly interact with the FGFR4 and furthermore has a higher affinity to the FGFR4 Arg385 isotype. Besides others, the EGFR-RAS-MAPKK axis is one of the most important pathways for cell proliferation in liver (Llovet and Bruix, 2008). These data show various new interaction partners of hepatic FGFR4. The direct interaction with the FGFR4 and their involvement in FGFR4-mediated signalling should be the subject of further investigations.

RP <sub>s</sub> KO _1	RP <sub>s</sub> KO _2	RP <sub>s</sub> Gly385 _1	RP <sub>s</sub> Arg385 _1	RP <sub>s</sub> Arg385 _2	Protein Names	Gene Names	Protein IDs	PEP
3	4	7	6	5	Beta-klotho	Betakl	IP100118044;IP100473391	5.68E-158
3	3	5	4	3	Hydroxyacid oxidase 1	Hao1	IP100123750	1.29E-73
4	4	5	6	4	Fibroblast growth factor receptor 4	Fgfr4	IP100742377;IP100761669;IP100129219;IP100473948;IP100473231	1.89E-138
12	13	8	5	6	Propanoyl-CoA C-acyltransferase	Scp2	IP100134131;IP100648476;IP100648007	2.61E-180
2	2	3	5	3	Epidermal growth factor receptor	Egfr	IP100121190;IP100411099;IP100357770;IP100122341;IP100229006;IP100626433	4.76E-29
7	3	4	6	2	Formimidoyltransferase-cyclodeaminase	Ftcd	IP100129011	2.41E-75
9	6	4	3	7	Hydroxymethylglutaryl-CoA synthase	Hmgcs2	IP100420718	3.27E-274

## Results

Gene Names	Protein Names	ratio FGFR4 KO (n=2)	stdv FGFR4 KO (n=2)	ratio FGFR4 Gly385 (n=1)	ratio FGFR4 Arg385 (n=2)	stdv FGFR4 Arg385 (n=2)	ratio FGFR4 Arg385/Gly385
Betakl	Beta-klotho	28.2	2.88	3.2	2.4	0.96	0.7
Hao1	Hydroxyacid oxidase 1	19.7	4.02	0.1	1.6	1.48	27.8
Fgfr4	Fibroblast growth factor receptor 4	12.9	9.33	1.5	1.3	0.22	0.8
Scp2	Propanoyl-CoA C-acyltransferase	7.8	1.20	0.2	3.6	2.89	18.6
Egfr	Epidermal growth factor receptor	5.8	1.23	0.3	1.3	0.31	3.8
Ftd	Formimidoyltransferase-cyclodeaminase	3.5	0.22	0.4	1.0	0.52	2.7
Hmgcs2	Hydroxymethylglutaryl-CoA synthase	3.3	0.29	1.8	1.8	0.43	1.0

**Table 10: Listing of identified interaction partners of hepatic FGFR4 and their differences between the *FGFR4* isotypes; List displays razor peptides of identified protein (RPs), protein and gene names, protein IDs and their significance (PEP < 0.03); furthermore, the list displays the intensity of the interaction partners and their differences between the *FGFR4* alleles**

## 5 Discussion

### 5.1 Loss of p53 and Rb in human primary cells as a model of oncogenesis *in vitro*

*In vitro* systems are necessary tools to investigate and understand the distinct steps of the processes that govern cells into a malignant phenotype. The advantages of *in vitro* models are lower costs as well as a simplification and acceleration of experimental approaches. The disadvantage of *in vitro* models is the absent influence of a whole organism that has a distinct impact on physiological processes via metabolism, release of hormones or the immunessystem (van Staveren et al., 2009).

Therefore, manipulated cell culture models should mimic the *in vivo* situation as close as possible. So far, transformation models manipulate the cell via oncogenes, viral proteins or re-expression of telomerase. These manipulations occur barely and take place as late events in human carcinogenesis. Above that, except the re-expression of telomerase, most models directly transform primary cells without any further necessary cellular alteration. Because of that, these *in vitro* transformation systems disable the investigation of early steps of tumorigenesis as well as the analysis of necessary alterations towards a neoplastic phenotype (Hahn et al., 1999; Kyo et al., 2003; MacKenzie et al., 2002; Mondello et al., 2003; Zongaro et al., 2005).

Therefore, there is a big need in investigating natural *in vitro* transformation models to establish a proper alternative to *in vivo* models. In this study, a model was established in primary human cells by the stable reduction of p53 and Rb. Both, p53 and Rb are lost or mutated in many human cancers and, together with other tumor suppressors, the inactivation of p53 and Rb takes place as one of the earliest events in tumorigenesis (Diehl, 2002; Hollstein et al., 1999; Malumbres and Barbacid, 2001; Palmero and Peters, 1996; Sherr, 2000; Sherr and McCormick, 2002). Furthermore, the successful transformation after a double loss of these two tumor suppressors was already shown as a very elegant model of non-small-cell-lung-cancer *in vivo* (Meuwissen et al., 2003). Thus, the reduction of p53-and Rb expression would possibly enable the transformation of primary cells and, furthermore, provide an insight into the multiple steps towards malignant transformation of human cells.

As a highly efficient knockdown displays the basis of a proper oncogenesis model, the first step was the establishment of a competent knockdown approach. Here, the knockdown via siRNA-constructs was analyzed compared to miRNA-constructs (P2Magic)(Paddison et al., 2004). The miRNA-constructs displayed a more efficient knockdown than the pRETROSuper

constructs of both p53 and Rb. The siRNA-sequence seemed to be improper for the stable expression after cloning into the pRETROSuper vector. But the main reason is possibly the fact, that the P2Magic constructs express the shRNA as a mir-30 transcript. This expression strategy displays following advantages regarding the knockdown efficacy. First, adding the miR30 loop and 125nt of miR30 flanking sequence on either side of the hairpin is known to result in >10-fold increase in Drosha and Dicer processing of the expressed hairpins when compared to older designs. Increased Drosha and Dicer processing translates into greater siRNA production and greater potency for expressed hairpins. Second, by using the miR30 the 5' end of antisense strand gets unstabilized which results in strand specific incorporation of miRNAs into RISC (Miyagishi and Taira, 2002; Paddison et al., 2004).

After the establishment of an appropriate knockdown-approach, Rb and p53 were stably knocked down by the specific shRNAs in the non-cancerous cell lines HEK293, HaCat and MCF10A. As p53 and Rb are key regulators of the cell cycle and genomic integrity, the loss of these two tumor suppressors should result in an accelerated cell cycle and a decrease in apoptosis (Bennett et al., 1998). Therefore, the proliferation of double knockdown cells was monitored and the cell cycle distribution upon a weak doxorubicin treatment was investigated with the expected results. Because of that, this knockdown seems to be not only sufficient for a distinct reduction of the protein level, but also to achieve expected physiological outputs, which makes this knockdown strategy a proper approach to establish an *in vitro* transformation model (Naidu et al., 2007).

Routinely used non-cancerous cell lines are artificially immortalized and thereby released from senescence and primed for the establishment of a neoplastic phenotype. Further, the perpetual subculturing of these cells enables the accumulation of mutations that maybe alter the physiology of these cells. Therefore, typical non-cancerous cell lines do not reflect the status of real primary cells. For that reason, the double knockdown of p53 and Rb was efficiently established in normal human dermal fibroblasts (NHDF, further referred as NHDFdk). As a negative control, NHDF cells were stably infected with a non-silencing shRNA construct (further referred as NHDFscr). Similar to the knockdown in non-cancerous cell lines, the reduction of p53 and Rb should result in several physiological outputs. The first advantage that most pre-cancerous cells achieve is the increased ability to proliferate. According to that, NHDFdk cells display increased proliferation doubling rates (PDR) indicating the loss of an accurate cell cycle control by the reduction of p53 and Rb. This phenotype is confirmed molecularly in the upregulation of the cell cycle promoter Cyclin D.

The step of uncontrolled cell growth is necessary for the primary cell to acquire further necessary properties.

Morphological changes are also typical for pre-cancerous cells. In the case of fibroblasts the typical morphology gets replaced by the irregular size of pre-malignant cells. This was also seen in NHDFdk cells that became smaller, rounder and even seemed to be barely attached.

The first stage of cellular transformation is represented by the achievement of an unlimited proliferation capacity, called immortalization. Primary cells are characterized by a permanent growth arrest after a defined number of population doublings induced by several mechanisms like telomere shortening. The cellular senescence is suggested to be a protective mechanism to circumvent instability of the genome and possible neoplastic transformation (Ha et al., 2008; Prieur and Peeper, 2008). In contrast, pre-cancerous cells avoid cellular senescence. A prolonged life span contributes in turn to an immortalized phenotype. As NHDFdk cells doubled the stated proliferation rate of NDHF (15 PDRs), the cells can be described as immortal (Gray-Schopfer et al., 2006). This could also be verified by a  $\beta$ -galactosidase assay that marks senescent cells, which were absent in NHDFdk even after 15 PDs. To confirm these data on the molecular level, the mRNA level of the tumor suppressors p16, p21 and p27 were analyzed over time. Especially p16 and p21 are potent promoters of cellular senescence (Dulic et al., 2000). Whereas NHDFdk cells suppress the expression of these tumor suppressors or maintain their expression, NHDFscr cells clearly upregulate the expression of p16, p21 and p27 that results in permanent growth arrest.

For complete malignant transformation it is essential for the cell to expand its relevant biological properties. These abilities include the loss of contact inhibition that allows tumor formation. Here, the cells overcome the proliferative stop when the space allotted to them is filled and a dense monolayer is formed (Herrlich et al., 2000). As NHDFdk did not stop proliferating in subconfluent culture and their cell-layer displayed a disordered appearance, these cells seemed to achieve the ability to partly overcome this proliferative stop by contact to other cells.

The loss of cell-cell or cell-matrix contacts in primary cells usually activates "anoikis". Anoikis is a form of apoptosis that occurs in cells that are detached from their surrounding tissue. By this mechanism the organism is able to get cells out of a cell layer if its position there is incorrect (Chiarugi and Giannoni, 2008; Simpson et al., 2008). Cancer cells are able to survive without cell-cell contacts. The anchorage independence enables the invasion of the organism by entering the blood or lymphatic stream. In contrast to NHDFscr cells, NHDFdk cells were able to grow in suspension in non-coated culture dishes indicating the acquisition

of anchorage independent growth. Next to anchorage independence, NHDFdk cells were able to form foci in Matrigel and displayed a slight branching. Malignant cells are often capable in degrading the extracellular matrix (ECM) for the invasion of surrounding and distant tissues. Hence, the slight branching of NHDFdk cells in Matrigel indicates a slight invasive behaviour of these cells. To confirm the loss of contact inhibition, anchorage independence and the slight branching in Matrigel on the molecular level, the expression of oncogenes were monitored over time. In NHDFdk cells SRC gets clearly upregulated over time. In all probability, the overexpression of SRC causes the malignant phenotype as SRC is one of the most potent oncogenes and is involved in a broad variety of cellular processes including proliferation, migration or cell-cell adhesion (Frame, 2002; Irby and Yeatman, 2000; Sakamoto et al., 2001; Warmuth et al., 2003). Its overexpression is frequent in many cancers as its activation can be achieved via diverse mechanisms and src signalling can thereby lead to even more cellular phenomena (Martin, 2001). In contrast H-Ras is not upregulated. Although H-Ras is also considered a strong oncogene and its upregulation is frequent in various cancers and transformed cells, its tumorigenicity seems to be dependent on a distinct cellular context and cooperative events (Bahk et al., 2008) that may be not present in the p53/Rb knockdown model. Further studies show, that its overexpression is also involved in oncogene-induced senescence resulting in permanent growth inhibition of normal cells caused by DNA-damage (Di Micco et al., 2006).

Further, the expression of Matrix-Metallo-Proteases (MMPs) was monitored over time. MMPs are essential for degrading the ECM for invasion and are often overexpressed in cancer cells (Stahtea et al., 2008). Compared to NHDFscr cells that were not capable to form foci or branch in Matrigel, NHDFdk cells clearly overexpress MMP9 and slightly MMP 2 that might be the molecular explanation for the observed growth and slight branching in matrigel. In summary, NHDFdk cells seem to develop a transformed phenotype over time that is indicated by the acquisition of typical properties that cancer cells exhibit. Furthermore, these properties could be explained by the overexpression or suppression of genes that are associated with the observed phenotypes. To analyze the expression pattern of NHDFdk cells in more detail a micro array analysis or a proteomic analysis should be done in further experiments. Results obtained from these expression analyses potentially help in the understanding of distinct expression pattern or their alterations in oncogenesis. In addition, further target genes of the p53 or Rb pathway could be identified.

Genomic instability is critical in the accumulation of mutations that in turn cause the development of a neoplastic phenotype. Therefore, genomic instability is one of the most

important events in tumorigenesis. To get a first insight of a potential DNA-damage in NHDFdk cells, the expression of  $\gamma$ H2AX was analyzed. Upon DNA-damage, H2AX gets phosphorylated and amongst others activates the DNA-damage signaling by p53 or Rb (Fillingham et al., 2006; Halicka et al., 2005). The obtained accelerated activation of  $\gamma$ H2AX in NHDFdk cells indicates an increase in DNA damage over time. The activation of H2AX is associated with early precursor lesions (but not normal tissues) of the bladder, breast, lung, and colon (Bartkova et al., 2005). In advanced breast and lung carcinomas, the DNA damage response is constitutively activated (Lukas et al., 2003). Furthermore,  $\gamma$ H2AX is suggested to be a prognostic marker in melanoma (Wasco et al., 2008). Next to active H2AX, the expression of Mad (mitotic-arrest-deficient-like) 1 was abolished in NHDFdk cells over time. The cell cycle checkpoint protein Mad 1 prevents the entry of the cells in anaphase if the chromosomes are not properly organized for cell division. Several studies display that the loss of Mad1 in cancer cells results in chromosomal instability. The overexpression of Mad1 results in suppression of proliferation or the malignant phenotype of cancer cells (Chen et al., 1995; Vastrik et al., 1995; Zou et al., 2006). Hence, the activation of H2AX and the loss of expression of Mad1 indicate genomic instability and DNA-damage caused by an uncontrolled cell division in NHDFdk cells. According to this, the karyotype analysis of mock transfected and double knockdown-cells displayed an accelerated aneuploidy in form of loss or gain of chromosomes in NHDFdk cells that increases over time. Although this form of aneuploidy is often thought to be rather a consequence than a cause of oncogenesis this genomic instability seems to contribute to the oncogenic progress in these cells. These data highlight, that NHDFdk cells display an excellent *in vitro* model to investigate the contribution of genomic instability to oncogenesis. Therefore a karyotypic analysis should be done by spectral karyotyping analysis (SKY) to determine the loss or gain of specific chromosomes over time in detail or the occurrence of chromosomal abnormalities by translocation, deletions or fusions of chromosomes (Padilla-Nash et al., 2007). Furthermore, the sequencing of specific genes could give insight in the genetic alterations of these cells. Hence, NHDFdk cells could contribute to the creation of a possible “mutational timetable” of oncogenesis that could give a deep insight in the development and behaviour of cancerous cells.

A further subject of the genomic constitution of NHDFdk cells was the analysis of telomere length. Telomere shortening not only induces cellular senescence, but short telomeres often lead to genomic instability that governs cells into a mitotic crisis and apoptosis as a tumor-protective mechanism (Kim et al., 1994; Shay and Bacchetti, 1997; Wright and Shay, 2001).

If cells overcome this mitotic crisis by the reactivation of telomerase or alternative telomere lengthening (ALT), the cells usually get cancerous (Cesare and Reddel, 2008; Shay and Wright, 2005). As NHDFdk cells did not reactivate the expression of telomerase and these cells neither enter a permanent growth arrest nor apoptosis, the extended telomere shortening seems to be tolerated by the cells. Furthermore, the telomeres should be stabilized via alternative telomere lengthening (ALT). Otherwise, telomere dysfunction would result in permanent growth arrest or cell death (Campisi, 2005; d'Adda di Fagagna et al., 2003). Interestingly, so called ALT-cells or ALT-tumors often do not exhibit p53 expression and often display a profound genomic instability according to the established model (Chen et al., 2006; Scheel et al., 2001).

In recent years it has become accepted, that genomic alterations and changes in expression patterns can support the cells in "reacquiring" a so called "stemness". Several publications report of the existence of a subpopulation of cancer cells in routinely used cancer cell lines that display a more aggressive phenotype after selection from the parental cell line (Ho et al., 2007; Huang et al., 2008; Sung et al., 2008). Therefore, the NHDFdk cells were investigated for a stem cell like subpopulation to analyze if the p53/Rb doubleknockdown could serve as *in vitro* model for the establishment of a stem cell like cancer cell subpopulation. However, NHDFdk cells did not display any stem cell like subpopulation analyzed by several stem cell markers.

The ultimate evidence of the successful transformation of NHDF cells deficient for p53 and Rb is the tumor formation *in vivo*. Fully transformed cells overcome even the cancer-preventive influences of a mammalian organism. Therefore, NHDFdk cells were injected into BalbC; Nu/Nu mice to monitor tumor growth. Even after 9 month NHDFdk cells were not able to form a visible tumor. These data suggest that the knockdown of p53 and Rb just partially transforms NHDF cells with the lack of the necessary lack of malignancy to promote tumor growth *in vivo*. Furthermore, the used Balb/C nude mice just partially lack an immunessystem that potentially turns these mice into an unusable system to monitor tumor growth of less aggressive cell lines. The use of other nude mice strains possibly could result in tumor growth of the NHDFdk cells.

In summary, the loss of p53 and Rb promotes several physiological mechanisms towards a neoplastic phenotype of cells. NHDF cells with reduced levels of p53 and Rb overcome permanent growth arrest and lost contact inhibition as well as anchorage dependence. These processes seem to be promoted by the occurred genomic instability. Nevertheless, the transformation by the loss of p53 and Rb is not potent enough to induce tumor growth *in vivo*.

Therefore, this *in vitro* model develops just partially transformed cells. For all that, the modelling of oncogenesis in fibroblasts can not stand for the tumorigenesis of all tissues. Fibroblasts are basically easier transformable than any other cell type. To prove if this approach is really appropriate for studying cancer development, it is essential to establish the double knockdown of p53 and Rb in other primary cells, for example epithelial cells. However, the loss of p53 and Rb displays a natural model of partial *in vitro* oncogenesis and provides the possibility of investigating the distinct steps of tumorigenesis with a special focus on the loss of genomic integrity.

## ***5.2 FGFR4 Arg385 promotes MEF transformation in vitro and accelerates tumor growth and metastasis in the WAP-TGF $\alpha$ mouse mammary tumor model***

Breast Cancer is the most frequently diagnosed cancer in women in the United States and Europe and the fifth leading cause of cancer death. Breast cancers have a huge histopathological and genetic diversity that all results in a variety of clinical outcomes. This diversity is confronted by just a few prognostic markers that turn breast cancer into a complex and difficult disease to be cured. Therefore, the investigation of new prognostic markers and their impact on tumor progression and clinical outcome is of highest priority.

Receptor tyrosine kinases (RTKs) are often implicated in the progression of breast cancer via a dysregulated signaling leading to uncontrolled cell growth. The family of Fibroblast Growth Factor Receptors (FGFR) are implicated either by overexpression like in pancreatic- or prostate carcinoma (Eswarakumar et al., 2005; Gowardhan et al., 2005; Morrison et al., 1994) or by activating mutations leading to abnormal fusion proteins or nucleotide substitutions (Cappellen et al., 1999; Fioretos et al., 2001; Jang et al., 2001; Macdonald et al., 1995). The fourth family member of the FGFRs, the FGFR4, was often associated with tumor progression (Ho et al., 2009). Furthermore, its inactivation or the inhibition of its ligand FGF19 results in impaired tumor growth (Desnoyers et al., 2008; Ho et al., 2009). A single nucleotide polymorphism in the FGFR4 that substitutes a Glycine (Gly) to an Arginine (Arg) is correlated with accelerated tumor progression of various cancers and is suggested to be involved in resistances to certain therapies in breast cancer (Bange et al., 2002; Desnoyers et al., 2008; Ho et al., 2009; Jaakkola et al., 1993; Jezequel et al., 2004; Morimoto et al., 2003; Morrison et al., 1994; Shah et al., 2002; Spinola et al., 2005; Spinola et al., 2005; Streit et al., 2004; Streit et al., 2006; Thussbas et al., 2006; Wang et al., 2004). However, the correlative

studies on clinical data also resulted in controversial results due to the genetic heterogeneity of patient cohorts (Jezequel et al., 2004). In this study the impact of the change of a single nucleotide in the mouse genome, in the gene encoding the receptor tyrosine kinase FGFR4, was investigated for the first time on the initiation and progression of breast cancer *in vivo*. First, the mouse model was characterized to ensure an accurate modelling of the human situation. As the *FGFR4 Arg385* KI is inherited in a Mendelian ratio, the KI does not seem to interfere with embryonic development of *Arg385*-carrying mice. Like humans, who carry the *Arg388* allele mice carrying the *FGFR4 Arg385* display no obvious phenotype that distinguishes them from *Gly388*-carriers (Bange et al., 2002). In FGFR4 expression, localization and distribution, the KI model also matches its human counterpart. The expression of the *FGFR4 Arg388/385* allele does not differ from the *Gly 388/385* allele in humans as well as in the *FGFR4 Arg385 KI* mice (Bange et al., 2002).

To investigate the impact of the FGFR4 Arg385 on physiological processes we first analyzed the differences of the *FGFR4* alleles in mouse embryonic fibroblasts (MEFs). MEFs display a typical and easy available *in vitro* system to investigate an altered physiology of genetically modified mice. As the most prominent impact of the *FGFR4 Arg385* allele is the disease progression once the cancer has been initiated, we aimed to investigate the impact of the FGFR4 Arg385 on the transformation rate of MEFs (Bange et al., 2002; Morimoto et al., 2003; Spinola et al., 2005; Streit et al., 2004; Streit et al., 2006). Accordingly, MEFs carrying the *Arg385* allele showed a significant higher transformation rate than control fibroblasts when infected with different oncogenes in a Focus Formation Assay. Furthermore, *FGFR4 Arg385* MEFs not only display a higher number of foci but remarkably transform with an earlier onset and an accelerated growth once the foci are established.

In search of the molecular mechanism underlying this effect, we interestingly could show that *FGFR4 Arg385* MEFs display a significant increased survival in response to DNA-damaging agents. Upon doxorubicin treatment, the FGFR4 Arg385 seems to support a more efficient DNA-repair that is shown by a significantly delayed G2-Arrest and the upregulation of p53 at early time points of response. Moreover, the FGFR4 Arg385 seems to significantly decrease apoptosis by the distinct upregulation of genes that are involved in pro-survival signalling like p-Akt, BCL-2 and BCL-XL (Masumoto et al., 1999; Pietras et al., 1994). The support of DNA-repair as well as pro-survival signalling is a common feature by receptor tyrosine kinases (Lin et al., 2008; Wang et al., 2008; Woo et al., 2005). Furthermore, the upregulated target genes are known to be integrators of damage signals and get upregulated by the downstream signalling of several receptor tyrosine kinases like EGFR, HER2 or kit (Blume-

Jensen et al., 1998; Carson et al., 1994; Kumar et al., 1996; Wang et al., 1999). The accelerated upregulation of anti-apoptotic genes is possibly caused by an accelerated crosstalk of the FGFR4 Arg385 to other proteins. Contrarily, apoptotic markers like Caspase 3 cleavage or phosphorylation of Bad did not differ between the genotypes. These data indicate that FGFR4 Arg385 does not inhibit apoptotic signalling but rather upregulates pro-survival genes as counterbalance to the apoptotic downstream signalling. These two mechanisms seem to enable the cell to manage DNA-damage without entering apoptosis. In turn, this advantage potentially contributes to an extended tolerance towards genomic instability that in turn displays the prerequisite of a malignant cellular transformation (Jeggo, 2005; Skorski, 2002). Interestingly, taxol that does not initiate DNA damage did not cause the anti-apoptotic response of the FGFR4 Arg385, indicating, that the FGFR4 Arg385 just contributes to survival towards DNA-damaging agents.

As the focus formation via the overexpression of EGFR resulted in an unusual high number of foci we wanted to investigate if the *FGFR4 Arg385* allele contributes to EGFR driven transformation. Therefore, we stably transformed the MEFs with EGFR. Interestingly, FGFR4 was upregulated in EGFR transformed MEFs and the FGFR4 Arg385 was detected to be hyperactive in MEFs transformed with EGFR compared to FGFR4 Gly385. These results indicate a possible crosstalk between these two receptors as it is already known between the Her2 and FGFR4 (Koziczak and Hynes, 2004). Furthermore, the anti-apoptotic response to DNA-damage of FGFR4 Arg385 could be reproduced in MEFs transformed with EGFR. Moreover, the FGFR4 Arg385 isotype was strongly associated with significantly increased migration, a significantly higher potential in soft agar colony formation and accelerated branching in Matrigel. These data indicate that the FGFR4 Arg385 progresses the aggressive phenotype of cells via processes connected to migration and invasion (Bange et al., 2002). Furthermore, as a migratory effect is not detectable in non-transformed MEFs, these data clearly indicate that the FGFR4 Arg385 is not an oncogene per se, but rather supports oncogenes by the promotion of several physiological processes. Contrarily, FGFR4 Arg385 had no impact on the proliferation of EGFR transformed MEFs.

Interestingly, no impact of the FGFR4 Arg385 could be detected when MEFs were transformed with v-src neither in anti-apoptosis nor in soft agar colony formation or branching in Matrigel. These results suggest that the impact of FGFR4 Arg385 is clearly dependent on the oncogenic background that triggers the neoplastic transformation and indicates once more a rather supportive than independent action of the FGFR4 Arg385.

To further characterize these physiological outputs the expression of various genes related to migration, invasion and proliferation were analyzed. The equal expression of cell cycle dependent kinases (CDK) thereby reflects the equal proliferative behaviour of *Gly385*- and *Arg385*-carrying MEFs. Especially MMPs and N-cadherin, powerful indicators of highly invasive cells, are strongly overexpressed in *Arg385*-carrying MEFs (Lafleur et al., 2005; Nagi et al., 2005; Su et al., 2008). These data confirm the impact of the *FGFR4 Arg385* allele on processes like migration and invasion.

After this clear implication of the *FGFR4* and its variant *Arg385* in defined physiological processes that are involved in tumor progression and aggressiveness we aimed to show for the first time the influence of the *FGFR4 Arg385* on tumor progression and accelerated aggressiveness. Above all, the impact of the *FGFR4 Arg385* allele yielded at times marginal results due to the highly complex and heterogeneous genetic background of the patients leading to controversial results (Jezequel et al., 2004; Spinola et al., 2005). Because of that the *FGFR4* SNP is not yet established as a progression marker for clinical outcome or as basis for individual patient treatment decisions. The *FGFR4 Arg385* KI mouse overcomes the problem of heterogenetic patient cohorts to clarify the possible impact of the *FGFR4 Arg385* in tumor progression.

The *FGFR4* is known to be upregulated in diverse cancers including breast cancer (Ezzat et al., 2002; Gowardhan et al., 2005; Jaakkola et al., 1993; Jeffers et al., 2002). Furthermore, the *FGFR4 Arg385* allele is known to promote mammary carcinoma in humans. Therefore, we investigated the impact of this SNP on mammary cancer progression (Bange et al., 2002). Similar, to the experiments *in vitro* we wanted to analyze the involvement of the *FGFR4 Arg385* on tumor progression in combination with the well established *WAP-TGF $\alpha$*  and the *MMTV-PyMT* transgenes (Pittius et al., 1988; Sandgren et al., 1995). The *WAP-TGF $\alpha$*  model induces mammary carcinoma by the overexpression of TGF $\alpha$  that results in hyperactive EGFR. The *MMTV-PyMT* model elicit mammary tumors by the constitutive activation of src by PymT (Pittius et al., 1988; Sandgren et al., 1995). The *WAP-TGF $\alpha$*  induced oncogenesis closely models human mammary carcinogenesis. First, the onset of tumors is moderate indicating that just a few cells overcome the anti-cancer barriers to form neoplasias. Second, working in the C57BL/6 background requires pregnancy of the mice, which is consistent with the human situation, where pregnancy can contribute to mammary hyperplasias as the human breast epithelial cells starts proliferation in pregnancy to ensure nursing. Last, the hyperactivated EGFR in the *WAP-TGF $\alpha$*  model display an oncogenic force that is more common in human breast cancer in comparison to models that trigger mammary oncogenesis

via viral oncoproteins as in the *MMTV-PymT* model. In addition, expression studies displayed, that the *FGFR4* was upregulated in the *MMTV-PymT* and *WAP-TGF $\alpha$*  mouse mammary carcinoma model (S. Streit, 2004). These facts qualified these models for the investigation of the *FGFR4 Arg385* allele on tumor progression. For that reason, the *FGFR4 Arg385 KI* mice were crossed to mice transgenic for *WAP-TGF $\alpha$*  and mice transgenic for *MMTV-PymT*.

We show that the *FGFR4 Arg385* allele directly promotes TGF $\alpha$ -induced mammary tumors in mass and area significantly. In addition, these tumors display a faster progression with a partly significant increase over time depending on the different *FGFR4* genotypes. Furthermore, *FGFR4 Arg385* decreases the visible time point of tumor incidence. Therefore, the involvement of the *FGFR4 Arg385* allele is no longer limited on tumor progression but also includes the facilitation of tumor initiation. A correlation between the tumor initiating ability of the *FGFR4 Arg388* allele is already shown on clinical prostate cancer data (Wang et al., 2004). Moreover, the analysis of the criteria of tumor progression displayed a more significant difference in the area and the percentage of tumor area. These data indicate, that the impact of the *FGFR4 Arg385* is rather migratory than proliferative. This goes in line with the results of MEFs transformed with EGFR that were promoted in migration and invasion via the *FGFR4 Arg385* allele. As transgenic mouse models so far do not completely mimic the situation in human breast cancers several disadvantages of the *WAP-TGF $\alpha$*  model must be considered. As the *WAP*-promoter is regulated by hormones, the expression of TGF $\alpha$  is also active in the developing virgin mammary gland and potentially in the embryonic mammary bud influencing the mammary gland in very early development. Second, although the *WAP*-promotor is mammary gland specific, this promoter is active at very low levels in variety of tissues including the brain. Next, the expression of a ligand does not exclude the influence of other systemic processes on tumor progression, or the fact, that the *FGFR4 Arg385* allele influences tumor progression not directly in the mammary epithelial cells. These effects could be excluded via mammary gland transplantation.

Furthermore, we analyzed the molecular action of the *FGFR4 Arg385* in tumors to investigate the underlying mechanism of the accelerated tumor progression. Although *FGFR4 Arg385* is not overexpressed in primary tumors compared to *FGFR4 Gly385* its activity is significantly upregulated. The amino acid substitution in the *FGFR4* results in the change to a hydrophilic amino acid. Therefrom, the structure of the *FGFR4 Arg385* possibly disables an accurate binding of negative regulators to the kinase domain or vice versa enables an accelerated binding of activators. In turn, the varying regulation of the receptor possibly leads to a differing downstream signalling and target gene expression. So far, two studies display an

altered target gene expression in the presence of the FGFR4 Arg385. Here, the *FGFR4 Arg385* expression results in the upregulation of the metastasis-associated gene Ehm2 in prostate cancer and the pro-migratory gene EDG-2 in MDA-MB-231 cells overexpressing the *Arg388* allele that is suppressed by the overexpression of the FGFR4 Gly385 (Stadler et al., 2006; Wang et al., 2006). Furthermore, Wang and colleagues showed an increased stability of the FGFR4 Arg385 receptor in prostate cancer cell lines (Wang et al., 2008). The delayed internalization of the *FGFR4 Arg385* allele potentially results from an altered structure leading to a relatively higher phosphorylation status of the FGFR4 Arg385. However, the distinct differences of the molecular mechanism of the FGFR4 Arg385 compared to the FGFR4 Gly385 have to be elucidated. As Stadler et al. and Wang et al. could show different expression of target genes in the presence of the FGFR4 Arg385, micro array analysis of WAP-TGF $\alpha$  derived tumors possibly helps to investigate differences between the FGFR4 allele regarding their target gene expression. Further, a mass spectrometry analysis of co-immunoprecipitated interaction partners of the FGFR4 Gly385 and FGFR4 Arg385 in tumors could show, if the interaction partners or the binding of the interaction partners differ between the FGFR4 isotypes. Furthermore, a phosphoproteomic analysis could define differences in the activated FGFR4 phosphosites or a difference of downstream signalling between the FGFR4 alleles. Differences in the structure of the FGFR4 Arg385 and its position in the cellular membrane induced by the change to a hydrophilic amino acid could be elucidated by crystallography or electron microscopy.

Furthermore, we analyzed several target genes involved in tumor progression, invasion and vascularization of WAP-TGF $\alpha$  derived tumors to further specify the impact of the FGFR4 Arg385 on tumor aggressiveness. Here, the expression analysis clearly displays a more aggressive phenotype of WAP-TGF $\alpha$  derived tumors expressing the FGFR4 Arg385. The significant downregulation of the tumor suppressor p21 is known to predict the poorest prognosis together with high EGFR expression (Somlo et al., 2008). The significant upregulation of the cell cycle dependent kinase (CDK) 1 once more involves the FGFR4 Arg385 in an accelerated migratory capacity of cancer cells (Manes et al., 2003). Contrarily, all of the other analyzed cell cycle proteins do not differ regarding the FGFR4 isotypes. This result confirms molecularly the exclusion of the FGFR4 Arg385 from a proliferative impact. Moreover, genes associated with invasion were significantly upregulated in FGFR4 Arg385 expressing tumors. CD44 that is significantly overexpressed, promotes metastases (Godar et al., 2008; Mylona et al., 2008; Sheridan et al., 2006), likewise flk-1, by promoting angiogenesis leading to a more aggressive behaviour of the tumor (Liang and Hyder, 2005).

Accordingly, MMP13 as well as MMP14 are significantly overexpressed in *FGFR4 Arg/Arg385* carrying tumors contributing to a higher metastatic potential (Ellsworth et al., 2008; Jiang et al., 2006; Rizki et al., 2008).

Due to the differences in the expression pattern of *FGFR4 Arg385* carrying tumors towards a more aggressive phenotype, it was essential to investigate the impact of the *FGFR4 Arg385* on metastasis. Above that, the clinical outcome of cancer is dependent on the invasive stage of the primary tumor. If the *FGFR4 Arg385* is involved in the onset of metastasis, the allele all the more could serve as a prognostic marker in breast cancer patients. Next to invading the bone or the liver, breast cancer cells mostly establish pulmonary metastases (Lee, 1983). Therefore, the lungs of the different *FGFR4* genotypes transgenic for *WAP-TGF $\alpha$*  were analyzed. Remarkably, the *FGFR4 Arg385* allele not only promotes aggressiveness but also supports invasion of the lung. Metastasis formation sets in earlier and the lungs of *FGFR4 Arg385* carrying mice are more intensely invaded. Therefore, the significantly altered expression in genes involved in invasion is reflected by the fact that cancer cells expressing the *FGFR4 Arg385* allele display a significantly accelerated potential in invading the lung to form distant metastases *in vivo*. These data strongly associate the *FGFR4 Arg385* allele with poor prognosis and thereby highlight the receptor as a marker of breast cancer progression.

In contrast, *FGFR4 Arg385* was not able to promote mammary cancer progression in mice transgenic for *MMTV-PyMT* neither in tumor mass or area. However, the negative results in the *MMTV-PyMT*-model display an indirect evidence of a cancer cell specific action of the *FGFR4*. If the cancer promoting effect would be caused apart the cancer cell, the *FGFR4 Arg385* should promote mammary tumor progression induced by *MMTV-PyMT*. This goes in line with the results derived from MEFs stably transformed with v-src. Here, *FGFR4 Arg385* could not promote any of the analyzed physiological mechanism including migration or invasion. These findings underline the dependency of the *FGFR4 Arg385* allele on the oncogenic background of neoplastic transformation. Above that, *TGF $\alpha$*  induced tumors include a hyperactive EGFR; the *PyMT* activates src leading to tumor formation. As a receptor tyrosine kinase, EGFR possibly crosstalk to *FGFR4* and this crosstalk differs in cancer cells expressing the *FGFR4 Arg385* allele. Contrarily, src is a downstream molecule. Here, the *FGFR4* and its *FGFR4 Arg385* allele are possibly unable to significantly influence the activity of src that is strongly activated by *PyMT*. This fact further confirms the supportive role of the *FGFR4* and its *Arg385* allele on tumor progression. Besides that, the malignant transformation of src takes place so rapidly and intensively that possible impacts of the *FGFR4 Arg385* may not be detectable.

Our data demonstrate that the *FGFR4 Arg385* allele is a potent enhancer of breast tumor development, progression and metastasis formation *in vivo*. The development of an antibody blocking the FGFR4 or its ligands could possibly be used in combination with classical cancer therapies like chemotherapeutic drugs as already shown in several studies (Ho et al., 2009; Pai et al., 2008). The strong impact of the FGFR4 on disease outcome is further underlined by Roidl and colleagues who could show that breast cancer cell lines with a acquired chemoresistance upregulate the FGFR4 (Roidl et al., 2009). Further, the FGFR4 predicts failure in tamoxifen treatment of breast cancer patients (Meijer et al., 2008). Above that, the FGFR4 could not only be targeted, but the allelic identity of this receptor may conceivably be included as a diagnostic parameter in the individual determination of therapy decisions. This notion is strongly supported by our previous findings, that the time of mammary cancer relapse after different drug-treatments is associated with different *FGFR4* alleles (Thusbas et al., 2006). These data suggest the further use of the *FGFR4 Arg385* KI model also for the investigation of cancer treatment and mechanism of resistance with respect to the *FGFR4* alleles.

As recent publications correlate the *FGFR4 Arg388* allele with various types of cancer our KI model could indicate the impact of the SNP on their progression and outcome. In particular, diseases related to the liver should be investigated as several recent publications implicate the FGFR4 in liver function and homeostasis (Desnoyers et al., 2008; Huang et al., 2007). Moreover, our data clearly postulate the generation of similar KI models to causally determine the impact of SNPs, which could be connected to various diseases and physiological processes.

In summary, our KI model clearly demonstrates an important role of the FGFR4 and especially the *Arg388* allele in mammary tumor progression. Our findings strongly support a role of the *FGFR4 Arg388* allele as a marker for poor clinical outcome in breast cancer progression and metastasis. On this account, these data further validate the FGFR4 and its isoforms as a target for the development of prototypical drugs. Above all, our findings highlight the impact of germline alterations including SNPs in receptor tyrosine kinase genes for the clinical progression of cancer and generally pinpoint the importance of individualized therapy regimens for cancer patients and emphasize the individual nature of this disease.

### **5.3 Investigation of new *FGFR4* binding partners *in vitro* and *in vivo***

The FGFR4 is implicated in the development and progression of various cancers and the clinical outcome of patients. The FGFR4 further mediates chemoresistance and was shown to

be a potential target in cancer therapy (Ho et al., 2009; Roidl et al., 2009; Streit et al., 2004). Furthermore, its *Arg388* variant is associated with enhanced tumor progression and above that with a poor clinical outcome of cancer patients (Bange et al., 2002; Streit et al., 2006). However, the distinct mechanisms that trigger FGFR4 driven oncogenesis and, importantly, the accelerated progression by the FGFR4 *Arg388* are still uncertain.

The FGFR4 is a receptor tyrosine kinase that mediates cellular signaling upon ligand stimulation, dimerization with other receptors and binding of downstream effectors (Eswarakumar et al., 2005). Therefore, we emphasized the investigation of new FGFR4 interaction partners. Furthermore, the FGFR4 *Arg388* variant substitutes a Glycine to an Arginine in the juxtamembrane domain indicating that the hydrophilic Arginine possibly alters the structure of the receptor resulting in an altered binding behavior compared to the FGFR4 *Gly388*.

For that purpose, we performed a proteomic analysis of FGFR4 interaction partners by SILAC based mass spectrometry. SILAC based proteomics displays a powerful tool to investigate global interactions on a quantifiable level. To analyze interaction partners of the FGFR4 *in vitro*, we decided to use MDA-MB-231 breast cancer cells, modified by Bange et al. (2002), as a model system. Here, FGFR4 is overexpressed either in its *Gly388* or *Arg388* variant enabling the analysis of the different FGFR4 isoforms in the same model system. Above that, the overexpression-system in MDA-MB-231 cells enables extensively simplified protein detection via mass spectrometry and the analysis of potential interaction partners of the FGFR4.

The identified proteins displayed the FGFR4 as the mostly upregulated protein indicating a proper experimental setup that reflects the overexpression system in MDA-MB-231 cells. Furthermore, FGFR4 *Arg388* is not upregulated compared to *Gly388* demonstrating an equal overexpression among the variants. Mass spectrometry analysis of FGFR4 co-immunoprecipitated proteins detected several interesting potential interaction partners. To verify these identified proteins, we performed a label switch and excluded proteins that were upregulated in just one setup. To further strengthen the specificity of interaction partners we listed only proteins that were upregulated at least 5-fold.

The identified potential interaction partners were LAR, EPHA2 and the EGFR. LAR is a transmembranous phosphatase and is known to be negatively regulated by the EGFR (Ruhe et al., 2006). Depletion of LAR accelerates hepatocyte cell proliferation by c-MET, insulin resistance and increased metastasis (Machide et al., 2006; Mander et al., 2005; McArdle et al., 2005). Furthermore, LAR is implicated in the regulation of FGF-induced signalling by

interacting with FRS2 (Wang et al., 2000). Therefore, an interaction of LAR and FGFR4 is conceivably possible. Since LAR is a tyrosine phosphatase the interaction with FGFR4 potentially display a novel negative regulation of the FGFR4. Here, LAR co-immunoprecipitation and FGFR4 dephosphorylation upon ligand stimulation would give a deeper insight in the interaction and the regulatory function of LAR regarding FGFR4 signalling. EPHA2 and EGFR are known transmembraneous receptors that are linked to the promotion of malignant phenotypes in MDA-MB-231 cells as well as various cancer types (Carles-Kinch et al., 2002; Noblitt et al., 2004; O'Neill et al., 2007; Wang et al., 2009; Zheng et al., 2009). However, the interaction with FGFR family members or the contribution to FGF-mediated signalling is not described so far. Therefore, the distinct mechanism and the impact of the interaction of these proteins with the FGFR4 should be the subject of further investigations. The results obtained from the mass spectrometry analysis indicate that MDA-MB-231 cells overexpressing the FGFR4 Gly388 or Arg388 variant present a useful model to study potential interaction partners of the FGFR4 in breast cancer cells and the differences regarding the FGFR4 isotypes. Here, FGFR4 seems to interact with different receptor tyrosine kinases. However, one should keep in mind that overexpression systems do not reflect the situation of proteins that are expressed endogenously. The interaction of the FGFR4 with the detected proteins has to be investigated precisely as overexpression systems can lead to results that are irrelevant for the endogenous or *in vivo* situation. Therefore, the interaction partners must be followed up in systems with endogenous FGFR4 expression with a special focus on *in vivo* studies, and the impact of the interaction should be determined by the depletion or blocking of the novel interactor. Furthermore, expression studies on clinical samples could help to elucidate a potential co-expression and its prognostic value on the outcome of cancer patients.

Nevertheless, the MDA-MB-231 cells display a powerful system to get a first insight on the FGFR4 signalling complex. However, all potential interaction partners displayed no differences between the different *FGFR4* isotypes. Besides that, interactors that specifically bind the FGFR4 Gly388 or Arg388 variant could not be detected. To detect potential differences in the binding of the interactors a mass spectrometry analyses upon ligand stimulation possible enables a deeper insight in the interaction profiles regarding the *FGFR4* alleles.

The most interesting interaction partner that was identified is the EGFR. The EGFR is associated with several key features of cancer development and growth. Next to non-small cell lung cancer the EGFR displays a promising target in various cancers. In MDA-MB-231

cells, the stimulation of the EGFR via multiple mechanisms results in an increase of their malignant behavior (Wang et al., 2009; Zheng et al., 2009). Furthermore, the *in vivo* studies that determined the promoting impact of the FGFR4 Arg385 on breast cancer were done on the basis of an EGFR-dependent mammary carcinoma model. Therefore, we decided to have a closer look on the interaction of the EGFR and the FGFR4. Here, we could show that the FGFR4 in MDA-MB-231 cells gets co-immunoprecipitated with the EGFR and gets phosphorylated upon EGF stimulation in a time dependent manner. Above that, the interaction and activation with the FGFR4 Arg388 variant was accelerated compared to the FGFR4 Gly388. Furthermore, downstream Akt gets more phosphorylated upon EGF stimulation in the presence of the *FGFR4 Arg388* allele. These data verify the interaction of the EGFR and FGFR4 and furthermore display a physiological connection upon ligand stimulation. The accelerated phosphorylation of the EGFR and downstream Akt upon EGF and TGF $\alpha$  stimulation is also present in EGFR-transformed MEFs expressing the FGFR4 Arg385. Additionally, immunoprecipitated FGFR4 Arg385 displays an accelerated phosphorylation upon EGF and TGF $\alpha$  stimulation than the FGFR4 Gly385. These data confirm the interaction of the EGFR and FGFR4 also in an *ex vivo* system. Above all, the interaction of these two receptors and the accelerated activation in the presence of the FGFR4 Arg385 is consequently suggested to be the molecular explanation for the accelerated tumor progression in the *WAP-TGF $\alpha$*  mouse mammary carcinoma model. Here, clinical data from human patient samples could potentially confirm this interaction by co-expression of these two receptors. Furthermore, the human patient samples could possibly then correlate the worse clinical outcome of *FGFR4 Arg388* carriers together with high EGFR expression. In this case, the FGFR4 Arg388 and EGFR would achieve a high impact in their prognostic value of the outcome of cancer patients.

Moreover, we could show the MDA-MB-231 cells expressing the FGFR4 Arg388 display an increased sensitivity towards Gefitinib treatment in proliferation, apoptosis and migration. The accelerated response towards Gefitinib treatment potentially results from the elevated interaction and downstream signaling of the EGFR and FGFR4 Arg388. These data conclude that several physiological mechanisms are dependent on the EGFR-FGFR4 interaction and further indicate that the FGFR4 and especially the Arg388 variant induces certain EGFR dependence, as MDA-MB-231 cells are usually referred as rather insensitive towards Gefitinib treatment. To ultimately verify these results, specific inhibition of the EGFR by a blocking antibody would finally determine this effect as the level of Gefitinib response is dependent on the expression of several other proteins (Ferrer-Soler et al., 2007). Here, for

example Akt, that is hyperactivated in MDA-MB-231 cells expressing the FGFR4 Arg388, predicts sensitivity to gefitinib. Therefore, the obtained reduction in cellular survival and migration could also result from decreased Akt activity. Furthermore, these data should be confirmed in cancer cell lines from various tissue origins and above that, with an endogenous expression of the FGFR4 and its *FGFR4 Arg388* allele. Further, the treatment of our *FGFR4 Arg385 KI* mice crossed to *WAP-TGF $\alpha$*  mice with EGFR-inhibitors could evidence the *in vivo* significance of the accelerated sensitivity of EGFR-driven breast cancer in the presence of the *FGFR4 Arg388* allele. Besides that, clinical data from human tumor samples treated with Gefitinib could clarify if the response gets significantly increased by the presence of the *FGFR4 Arg388* allele in human conditions. This would expand the prognostic value of the *FGFR4 Arg388* allele on response to cancer therapy as it is already known in response to tamoxifen (Thussbas et al., 2006). Taken together, the interaction between the EGFR and FGFR4 in MDA-MB-231 cells is the first reported direct interaction between the HER and FGFR family. Above that, this interaction opens up the possibility of new prognostic and therapeutic interventions and gives a deeper insight in the mechanism of breast cancer progression driven by EGFR and FGFR4.

In 2008, Kruger et al. presented the first study based on *in vivo* SILAC by feeding mice with a diet containing heavy lysine (Kruger et al., 2008). Therefore, the limitations posed by *in vitro* studies are now circumvented by SILAC-based *in vivo* proteomics that provides the actual “global view” on the proteome of a certain tissue. Here, organs derived from SILAC mice serve as an internal standard for a large number of subsequent experiments. Furthermore, investigation of cell types that are difficult to study *ex vivo*, are effortlessly approachable. Besides that, *in vivo* SILAC is independent from a biological scale ranging from the analysis of whole organs down to interacellular compartments or single proteins (Kruger et al., 2008). In this study, we investigated the interactom of the FGFR4 in murine liver to get a deeper insight in the molecular action of the FGFR4 in the regulation of liver homeostasis and hepatocellular carcinogenesis. Moreover, we aimed to analyze the interaction differences between the FGFR4 Gly385 and FGFR4 Arg385 by the use of our generated *FGFR4 Arg385 KI* mouse.

One major function of the liver is the production of bile acids (Chiang, 2004; Russell, 2003). The regulation of bile acid synthesis is tightly regulated by a negative feedback loop to prevent the damage of the enterohepatic tissue. Here, the cholesterol 7 $\alpha$ -hydroxylase, the catalyzer of bile acid expression, is repressed by circulating bile acids itself (Jelinek et al., 1990). Responsible for this feedback loop is the regulation of the FGFR4/FGF15 pathway by

bile acids (Inagaki et al., 2005). In maintaining homeostasis, FGFR4 and the FGF19 subfamily members additionally play an important role in systemic lipid and glucose homeostasis. Here, the hepatic activity of the FGFR4 serves to prevent systemic hyperlipidemia and-cholesterolemia. In summary, the hepatic FGFR4 seems to be a potential target for intervention in systemic cholesterol/bile acid, lipid and glucose metabolism (Huang et al., 2007; Ishikawa and Fidge, 1979; Yu et al., 2002; Yu et al., 2000). Besides that, the FGFR4 seems to be implicated in the progression of hepatocellular carcinoma. Surprisingly, previous data implicate the FGFR4 as a tumor suppressor as well as a tumor promoting factor (Desnoyers et al., 2008; Hu et al., 1995; Huang et al., 2008; Nicholes et al., 2002). To further analyze the underlying mechanism by which the FGFR4 regulates bile acid homeostasis and liver carcinogenesis we aimed to investigate the interaction partners of the murine FGFR4 in liver. In order to address this question we first investigated the optimal conditions to study the liver interactome of the FGFR4. In the course of that, we specifically focused on the minimization of unspecific binders. As liver tissue exhibits high protein content, a so called “beads-only control” was not sufficient to exclude all false positive results. For that reason, we generated blocking peptides derived from tryptic digestion of the expressed FGFR4Ex-GST construct in HEK293 cells. Although the Western Blot analysis displayed a high efficacy of blocking the antibody-FGFR4 interaction, subsequent mass spectrometry analysis exhibited an unphysiological high number of interactors. That may be due to the fact that an insufficient purification of the homemade FGFR4Ex-GST antibody resulted in remaining anti-GST antibody that was additionally established by the immunized rabbit (C. Stadler, 2005). This remaining GST-antibody in turn gets also blocked by the peptides as we used a mixture derived from tryptic digest. Compared to the internal SILAC standard these proteins subsequently appear to be upregulated although they are not interacting with the FGFR4. To circumvent that problem we sequenced the obtained blocking peptides and synthesized over 20 blocking peptides to specifically block the antibody-FGFR4 interactions. However, successive Western Blot Analysis only displayed a low or no blocking efficacy of the synthesized peptides. As these tools were not powerful enough to maximize the exclusion of unspecific binders we decided to use *FGFR4 KO* livers as a negative control to finally determine the murine hepatic FGFR4 interactome (kindly provided by Wallace L. McKeehan, PhD, Center for Cancer and Stem Cell Biology, Institute of Biosciences and Technology, Texas, Houston, USA). By the use of the *FGFR4 KO* liver lysates we tremendously decreased the amount of regulated potential FGFR4 interaction partners. Here, the enormous upregulation of the FGFR4 and its co-receptor  $\beta$ Klotho demonstrated a proper experimental

setup. Further, we identified a variety of so far unknown potential interaction partners. Unfortunately, except the EGFR none of these interaction partners was connected to tyrosine kinase signaling or interaction with receptor tyrosine kinases so far. Interestingly, all these potential interaction partners are involved in liver homeostasis in the cholesterol- and lipid metabolism. Hao1 oxidizes glycolate and glyoxycolate (Recalcati et al., 2003). Scp2 plays an important role in the intracellular movement of cholesterol. In mice loss of Scp2 induces alterations in the biliary lipid secretion and hepatic cholesterol metabolism (Fuchs et al., 2001). Ftcd is suggested to control folic acid liver metabolism (Bashour and Bloom, 1998). Above that, Ftcd is overexpressed in hepatocellular carcinoma (HCC) and is therefore suggested to contribute to the diagnosis of early stage HCC (Fuchs et al., 2001). Hmgcs2 is a key regulator of keton body production in the liver. It is known that Hmgcs2 is transcriptionally regulated by c-myc and FKHL1 (Camarero et al., 2006; Nadal et al., 2002). Among these potential interactors Hao1 and Scp2 display a stronger interaction to the FGFR4 Arg385 variant indicated by a higher ratio compared to the FGFR4 Gly385. As the FGFR4 is known to be a critical modulator of these processes, the intracellular interaction of these identified proteins with the FGFR4 is theoretically imaginable. Nevertheless, fundamental follow-up experiments are necessary to firstly put these proteins in context to the molecular action of receptor tyrosine kinases. Further, the interaction of these proteins with the FGFR4 and their involvement in FGFR4-mediated signalling has to be precisely elucidated. Co-immunoprecipitation studies would provide first insights in the interaction with the FGFR4. Furthermore, interaction upon various stimuli including FGFR4 ligands and metabolic stimuli would offer the possibility to investigate the physiology of these potential interaction partners with the FGFR4. These experiments could be repeated by the use of *FGFR4* KO mice to investigate the same physiological interactions in an *in vivo* context.

Next to these potential new interactors the most interesting and promising target is the epidermal growth factor receptor itself. The EGFR was found to significantly interact with the hepatic FGFR4 and furthermore displays a higher interaction to the FGFR4 Arg385. Furthermore, several publications show that the EGFR as well as the FGFR4 are highly implicated in liver physiology. Regarding liver cell proliferation, published data present only conflictive data so far. Here, the EGFR-RAS-MAPKK axis is one of the most important pathways for cell proliferation in liver (Llovet and Bruix, 2008). Furthermore, although liver specific *EGFR* KO induces no further phenotypes, mice lacking the hepatic EGFR display an increased mortality after partial hepatectomy indicating that the EGFR is indispensable for proper liver regeneration (Natarajan et al., 2007). In contrast, the FGFR4 was not suggested to

regulate cellularity of normal or regenerating liver or cell proliferation during response to liver injury (Hu et al., 1995; Yu et al., 2000). That is maybe due to the fact that the FGFR4 plays a rather supportive role by interacting with the EGFR. Contrarily, after injection of Carbon-tetrachloride, *FGFR4*-deficiency accelerates liver injury and liver fibrosis suggesting that the FGFR4 may have a role in liver injury-induced regeneration (Yu et al., 2002). Interestingly, liver injury induced by Carbon-Tetrachloride can be reduced by the systemic administration of EGF (Berlanga et al., 1998). These data implicate both the EGFR as well as the FGFR4 in the protection of liver injury. A double knockout of both *EGFR* and *FGFR4* could give first insights in their interplay regarding liver cell proliferation after a partial hepatectomy or liver injury. In regulating liver metabolism the conditional loss of *EGFR* in prenatal murine livers is known to result in decreased body weight. Interestingly, mice lacking *FGFR4* displayed decreased glucose and insulin tolerance (Huang et al., 2007; Ishikawa and Fidge, 1979; Yu et al., 2002; Yu et al., 2000). In hepatocellular carcinoma (HCC), EGFR signalling is highly implicated in the progression of HCC and the subject of many ongoing clinical trials that specifically target EGFR signalling (Llovet and Bruix, 2008). Interestingly, mice ectopically overexpressing *FGF19*, display hepatoma-like lesions and the inhibition of FGF19 by specific antibodies is reported to contribute to tumor reduction (Desnoyers et al., 2008; Nicholes et al., 2002). In contrast, mice deficient for *FGFR4* display an accelerated DEN-induced carcinogenesis and the restoration of FGFR4 increases apoptosis in tumor cells suggesting a tumor suppressive function in HCC (Huang et al., 2008). Therefore, the impact of EGFR-FGFR4 interaction on liver physiology, liver injury, regeneration and cancer has to be further elucidated.

In conclusion, the SILAC based MS-screen shows various new interaction partners of the hepatic FGFR4. Besides that, these results indicate that *in vivo* SILAC is a powerful tool to get first insights into the interactome of a certain protein; however, the data obtained with *in vivo* SILAC based mass-spectrometry has to be critically optimized with a special focus on false positive interaction partners and has to be further critically confirmed by decisive follow-up experiments.

In the pool of identified potential interaction partners, the EGFR displays the most interesting and promising target in the elucidation of the molecular action of the FGFR4 and furthermore its Arg385/388 variant. This potential interaction should be the subject of further investigation in both liver homeostasis and cancer as previous publications present antithetic data. Furthermore, one should keep in mind that all aforementioned studies had no focus on the *FGFR4* Arg385 allele, that possibly lead to another physiological output compared to the

*FGFR4* Gly385 variant. Therefore, *in vivo* studies with our *FGFR4* Arg385 KI mice together with *EGFR* knockout (Sibilia and Wagner, 1995) or the *mig-6* knockout mice (Ferby et al., 2006), that lead to hyperactivated EGFR, could finally determine the impact of the *FGFR4* Arg385 allele on the interplay with the EGFR and their combined impact on liver physiology.

## 6 Summary

In the first project, an *in vitro* transformation model should be established by the stable reduction of p53 and Rb. So far, human *in vitro* transformation systems include the expression of oncogenes, viral proteins or telomerase. These manipulations display mostly inartificial ways of oncogenesis. The stable knockdown of p53 and Rb mimics the frequent and early loss of these proteins in human cancer and should therefore be a natural model of carcinogenesis. In primary human fibroblasts the loss of these tumor suppressors induces characteristic changes in their expression pattern based on the genomic instability that occurs. These changes result in an accelerated cell cycle, unlimited life span, loss of contact inhibition and adherence independence. However, the neoplastic transformation of NHDF was not malignant enough to induce tumor growth in nude mice. Nevertheless, this study suggests that the loss of p53 and Rb in normal human primary cells can serve as an accurate model of oncogenesis with a special focus on genomic instability.

In the second project, the impact of the *FGFR4 Arg388* allele on tumor progression *in vivo* was investigated. The *FGFR4 Arg388* occurs frequently in the human population and has been implicated in the progression of various cancers. In this study, generated *FGFR4 Arg385 KI* (corresponding to human codon 388) mice were crossed to *WAP-TGF $\alpha$*  transgenics. The development and progression of mammary tumors and pulmonary metastases were significantly increased in *WAP-TGF $\alpha$*  mice carrying the *FGFR4 Arg385* allele. These data were supported by accelerated cell survival and increased *in vitro* transformation of *FGFR4 Arg385* carrying MEFs. In transformed MEFs, the *FGFR4 Arg385* promotes cancer cell survival, migration and invasion. These results demonstrate that the *FGFR4 Arg388* allele qualifies as a prognostic marker for breast cancer patients and represents a prototypical drug target for individualized cancer therapy development.

In the last project, we aimed to investigate the interactome of the *FGFR4 in vitro* and *in vivo* and the differences regarding the *FGFR4* isoforms. Therefore, we performed SILAC based mass spectrometry analysis on the MDA-MB-231 breast cancer cell line model established by Bange et al. and on murine liver of our *FGFR4 Arg385 KI* mice. *In vitro* and *in vivo* we could interestingly show that the EGFR is a strong interaction partner of the *FGFR4* with a higher affinity towards the *FGFR4 Arg385/388* allele and subsequent increased downstream signalling. Furthermore, MDA-MB-231 cells expressing the *FGFR4 Arg388* allele are more sensitive to the EGFR inhibitor Gefitinib. Our data suggest that the *FGFR4 Arg385/388*-EGFR signaling complex might account for the observed accelerated tumor progression in

## Summary

*WAP-TGF $\alpha$*  transgenic mice and highlights the prognostic value of these two receptor tyrosine kinases in breast cancer.

## 7 Zusammenfassung

Im ersten Teil dieser Arbeit war es das Ziel ein zelluläres System zu etablieren in dem die Karzinogenese primärer Zellen verfolgt werden kann. Hierbei sollte ein Model entwickelt werden, dass sich so nah wie möglich der *in vivo* Situation angleicht. Da bis heute keine derartigen Modelle zur Verfügung stehen, sollte die Transformation primärer humaner Fibroblasten durch den stabilen *Knockdown* der beiden Tumor Suppressoren p53 und Rb erreicht werden. Die maligne Veränderung der manipulierten Fibroblasten wurde über die Zeit mit Hilfe verschiedenster Experimente überprüft. Diese Fibroblasten zeigten genomische Instabilität, die zu einer Veränderung in ihrem Genexpressionsmuster führte. Dies wiederum führte zu zellulären Eigenschaften, die charakteristisch für Krebszellen sind. Dazu zählt der Verlust der Kontaktinhibition wie auch die Fähigkeit ohne Adhärenz zu wachsen. Obwohl kein Tumorwachstum dieser Fibroblasten in Nacktmäusen beobachtet werden konnte, zeigt dieses Model, dass es möglich ist, primäre Zellen durch den Verlust von p53 und Rb teilweise zu transformieren. Daher kann die Veränderung einer Primärzelle zur Krebszelle in einem derartigen Modell vor allem bezüglich genomischer Instabilität untersucht werden.

Im zweiten Projekt sollte der Einfluss des *FGFR4 Arg388* Alleles auf die Progression von Brustkrebs *in vivo* untersucht werden. Dieser *single nucleotide polymorphism* (SNP) ist häufig im menschlichen Genom zu finden wurde bereits zahlreich mit der Progression und einer schlechten Prognose korreliert. In diesem Projekt wurden *FGFR4 Arg385* KI Mäuse (entsprechend codon 388 im menschlichen Genom) in das *WAP-TGF $\alpha$*  Brustkrebsmodell eingekreuzt. Sowohl die Progression des Primärtumors als auch die Metastasierung in die Lunge waren signifikant erhöht wenn die Mäuse das *FGFR4 Arg385* Allele trugen. Diese Ergebnisse konnten durch *in vitro* Experimente unterstützt werden. In MEFs erhöht der *FGFR4 Arg/Arg385* die Transformationsrate und das Überleben der Zellen nach chemotherapeutischer Behandlung. Stabil transformierte *FGFR4 Arg/Arg385* MEFs zeigen außerdem eine erhöhte Migration und Invasion. Diese Daten zeigen, dass das *FGFR4 Arg385* Allel zum einen ein geeigneter Marker für die Prognose von Brustkrebspatienten ist und zum anderen auch ein Zielprotein für die Entwicklung spezifischer Therapien darstellt.

Im letzten Teil der Arbeit sollte das Interaktom des FGFR4 mittels SILAC basierender Massenspektrometrie *in vitro* und *in vivo* untersucht werden. *In vitro* wurde das von Bange et al. etablierte MDA-MB-231 Brustkrebsmodell verwendet, *in vivo* die Lebern der generierten *FGFR4 Arg385* KI Mäuse. In beiden Fällen konnte unter anderem der EGFR als Interaktionspartner identifiziert werden. In MDA-MB-231 Zellen konnte weiterhin gezeigt

werden, dass der EGFR eine höhere Affinität zum FGFR4 Arg388 aufweist und dadurch die EGFR vermittelte Signaltransduktion erhöht wird. Außerdem zeigen MDA-MB-231 Zellen, die FGFR4 Arg388 exprimieren, eine höhere Sensitivität gegenüber Gefitinib. Unsere Daten deuten darauf hin, dass der FGFR4 Arg385-EGFR Signalkomplex die molekulare Erklärung der erhöhten Tumorprogression in *WAP-TGF $\alpha$*  transgenen Mäuse zu sein scheint.

## 8 Appendix

### 8.1 Abbreviations

°C	degree celsius
A	Ampère
ALT	alternative mechanism of telomere lengthening
Amp	Ampicillin
APS	Ammoniumperoxodisulfat
APS	amonium peroxodisulfat
Arg	Arginine
ATCC	American type culture collection
ATM	for ataxia telangiectasia mutated
ATP	adenosin triphosphat
ATR	ataxia telangiectasia related
bp	base pair
BSA	bovine serum albumin
CDK	cyclin-dependent kinase
cDNA	complementary DNA
Chk2	checkpoint kinase 2
c-jun	Cellular homologue to v-jun (avian sarcoma virus)
CYP7A	Cholesterol-7alpha-hydroxylase
Da	Dalton
DEN	Diethyl-nitrosamine
DMEM	Dulbecco's Modified Eagle Medium
DMSO	Dimethylsulfoxid
DNA	desoxyribonucleic acid
dNTP	Desoxyribonukleosidtriphosphat
DTT	Dithiorethiol
E	embryos on day
E.coli	Escherichia coli
e.g.	for example
E2F	elongation factor 2
ECL	Enhanced Chemical Luminescence
EDTA	Ethylendiamin-N, N, N', N'-tetraacetat
EGF	epidermal growth factor
EGFR	epidermal growth factor receptor
ELISA	Enzyme linked Immunosorben Assay
Erk	extracellular signal-regulated kinase
ES-cells	embryonic stem cells
et al.	et alterum
FACS	fluorescence associated cell sorting
FBS	foetal bovine serum
FGF	fibroblast growth factor
FGFR	fibroblast growth factor receptor
FITC	fluorescein isothiocyanate
FRS2	FGF receptor substrate 2
FXR	farnesoid x receptor
G	Glycine
g	gramm

Gab1	Grb2-associated binder-1
GFP	green fluorescence protein
Gly	Glycine
Grb2	Growth factor receptor binding protein 2
GSH	Glutathion
GST	Glutathion-S-Transferase
h	hour
H2AX	H2A histone family member X
HCC	human hepatocellular carcinoma
HE	Hemalaun-Eosin
HEPES	N-(2-Hydroxyethyl)-piperazin-N'-2-ethansulfonsäure
HER	humane EGFR
HPV	human papilloma virus
HRP	horese radish peroxidase
hTERT	active subdomain of telomerase
ICH	immunohistochemistry
Ig	Immunoglobulin
IP	immunoprecipitation
JAK	janus kinase
JNK	c-jun N-terminal kinase
kb	Kilobasen
kd	double-knockout
kDa	Kilodalton
KI	knock in
KO	knockout
LB	„Luria Bertani“ media
LC-MS/MS	liquid chromatography based mass spectrometry
M	Molar
mAb	monoclonal antibody
MAP	mitogen activated protein
MAPK	mitogen activated protein kinase
MDM2	mouse double minute 2
MEFs	mouse embryonic fibroblasts
min	minute
miRNA	microRNA
MMP	Matrix-Metalloproteinase
MMTV	mouse mammary tumor virus
mRNA	messenger RNA (Boten-RNA)
MW	molecular weight
n	nano
neo	neomycin
NHDF	normal human dermal fibroblasts
ON	over night
p	pico
p53	Tumor protein 53
PAGE	Polyacrylamid-gelelectrophoresis
PBS	phosphate-buffered saline
PCR	polymerase chain reaction
PD	population doubling
PDGF	platelet-derived growth factor
pH	negative decade logarithm of H <sup>+</sup> concentration

PH-Domäne	Pleckstrin homology domain
PI	propidium iodid
PI 3-Kinase	Phosphatidylinositol 3-Kinase
PLC $\gamma$	Phospholipase C- $\gamma$
PMSF	Phenylmethylsulfonyl-Fluorid
PTB	phosphotyrosine binding
PTP(n)	Proteintyrosinphosphatases
PY	Phosphotyrosin
PymT	Polyoma middle T
R	Arginine
Raf	Homologue to v-raf (murine sarcoma viral)
Ras	Homologue to v-ras (rat sarcoma viral oncogene)
Rb	retinoblastoma gene product
RFLP	restriction length polymorphism
RNA	ribonucleic acid
RNase	Ribonuklease
rpm	rounds per minute
RT	Raumtemperatur
RTK(n)	receptor tyrosine kinases
RXR	retinoid X receptor
scr	scrambled/mock transfected cells
SDS	sodium dodecyl sulfate
SDS-PAGE	SDS Polyacrylamid Gelelektrophorese
sec	second
SH2	3-Domain Src Homology 2, 3 Domain
SHC	SH2-domain containing
SHP-2	SH2-Domäne containing Phosphatase 2
shRNA	shot hairpin RNA
SILAC	stable isotope labelling by amino acids in cells
siRNA	small interfering RNA
SNP	single nucleotide polymorphism
Sos	son of sevenless
src	Homologue to v-src (sarcoma viral oncogene)
ss	single stranded
Stat	Signal transducer and activator of transcription
SV40 LT	papilloma simian virus 40 large T antigen
TA	annealing temperature
TAE	Tris-Acetate-EDTA
Taq	Thermus aquaticus
TEMED	N, N, N', N'-Tetramethylethylenediamin
TGF $\alpha$	transforming growth factor alpha
TM	melting temperature
Tris	Tris(hydroxymethyl)aminomethan
Triton X-100	4-(2', 2', 4', 4'-Tetramethylbutyl)-phenyldecaethylenglycoether
Tween 20	Polyoxyethylensorbitanmonolaureat
U	Units
UV	Ultraviolet
V	Volt
VEGFR	vascular endothelial growth factor receptor
w/v	weight/volume
WAP	whey acidic protein

Appendix

WB	Western-Blot
WT	Wildtype
$\alpha$	anti
$\mu$	micro

## **8.2 Acknowledgements**

I especially want to thank my supervisor Prof. Axel Ullrich, who initiated my interesting projects and always supported me with ideas and motivation. Prof Axel Ullrich always made it possible to realize ideas, taught me to focus straight forward and to think out of the box. Next to his support in my research I also want to thank Prof. Axel Ullrich for his generous parties, the Ringberg Symposium, the Spetses Summer School 2007 and to keep an outstanding team spirit between his department-members.

Further I would like to thank Prof. Domdey at the Ludwigs-Maximilians-University of Munich to agree in supervising me.

I want to thank all the members of the Ullrich department and especially Thomas Mayr for introducing me into mousework, Philipp Mertins for his help in the MS-liver project, Renate Gautsch for special instructions with the cell culture, Pjotr Knyazev and Tatjana Knyazeva, who never stopped helping me out especially with the Southern Blotting, Michaela Bairlein for a lot of fruitful discussions and being a perfect flat-mate and Isabella and Verena for her general support.

I want to thank all my office mates for keeping me in a good mood in the office. Thanks to Buschi, Martin, Matze, Sepp, HaJü, Felix, Robert and Susan for making fun out of an ordinary working day.

My special thanks go to the people of the animal facility, who took care of my mice. Especially I want to thank Heinz Brandstetter and Corinna Moerth for a lot of discussion and instructions.

I want to thank my family for their love and motivation.

Finally I want to thank my husband Markus for all his love and support.

## 9 References

- Alroy, I., and Yarden, Y. (1997). The ErbB signaling network in embryogenesis and oncogenesis: signal diversification through combinatorial ligand-receptor interactions. *FEBS Lett* *410*, 83-86.
- Ameyaw, M. M., Tayeb, M., Thornton, N., Folayan, G., Tariq, M., Mobarek, A., Evans, D. A., Ofori-Adjei, D., and McLead, H. L. (2002). Ethnic variation in the HER-2 codon 655 genetic polymorphism previously associated with breast cancer. *J Hum Genet* *47*, 172-175.
- Andersen, J. S., Lam, Y. W., Leung, A. K., Ong, S. E., Lyon, C. E., Lamond, A. I., and Mann, M. (2005). Nucleolar proteome dynamics. *Nature* *433*, 77-83.
- Angelin, B. (2005). Telling the liver (not) to make bile acids: a new voice from the gut? *Cell Metab* *2*, 209-210.
- Bahk, Y. Y., Cho, I. H., and Kim, T. S. (2008). A cross-talk between oncogenic Ras and tumor suppressor PTEN through FAK Tyr861 phosphorylation in NIH/3T3 mouse embryonic fibroblasts. *Biochem Biophys Res Commun* *377*, 1199-1204.
- Bandyopadhyay, D., Gatza, C., Donehower, L. A., and Medrano, E. E. (2005). Analysis of cellular senescence in culture in vivo: the senescence-associated beta-galactosidase assay. *Curr Protoc Cell Biol Chapter 18*, Unit 18 19.
- Bange, J., Precthl, D., Cheburkin, Y., Specht, K., Harbeck, N., Schmitt, M., Knyazeva, T., Muller, S., Gartner, S., Sures, I., *et al.* (2002). Cancer progression and tumor cell motility are associated with the FGFR4 Arg(388) allele. *Cancer Res* *62*, 840-847.
- Bartkova, J., Horejsi, Z., Koed, K., Kramer, A., Tort, F., Zieger, K., Guldberg, P., Sehested, M., Nesland, J. M., Lukas, C., *et al.* (2005). DNA damage response as a candidate anti-cancer barrier in early human tumorigenesis. *Nature* *434*, 864-870.
- Bartkova, J., Rezaei, N., Liontos, M., Karakaidos, P., Kletsas, D., Issaeva, N., Vassiliou, L. V., Kolettas, E., Niforou, K., Zoumpourlis, V. C., *et al.* (2006). Oncogene-induced senescence is part of the tumorigenesis barrier imposed by DNA damage checkpoints. *Nature* *444*, 633-637.
- Bashour, A. M., and Bloom, G. S. (1998). 58K, a microtubule-binding Golgi protein, is a formiminotransferase cyclodeaminase. *J Biol Chem* *273*, 19612-19617.
- Baylin, S., and Bestor, T. H. (2002). Altered methylation patterns in cancer cell genomes: cause or consequence? *Cancer Cell* *1*, 299-305.
- Bellus, G. A., Bamshad, M. J., Przylepa, K. A., Dorst, J., Lee, R. R., Hurko, O., Jabs, E. W., Curry, C. J., Wilcox, W. R., Lachman, R. S., *et al.* (1999). Severe achondroplasia with developmental delay and acanthosis nigricans (SADDAN): phenotypic analysis of a new skeletal dysplasia caused by a Lys650Met mutation in fibroblast growth factor receptor 3. *Am J Med Genet* *85*, 53-65.
- Bennett, M. R., Macdonald, K., Chan, S. W., Boyle, J. J., and Weissberg, P. L. (1998). Cooperative interactions between RB and p53 regulate cell proliferation, cell senescence, and apoptosis in human vascular smooth muscle cells from atherosclerotic plaques. *Circ Res* *82*, 704-712.
- Berlanga, J., Caballero, M. E., Ramirez, D., Torres, A., Valenzuela, C., Lodos, J., and Playford, R. J. (1998). Epidermal growth factor protects against carbon tetrachloride-induced hepatic injury. *Clin Sci (Lond)* *94*, 219-223.
- Berube, N. G., Smith, J. R., and Pereira-Smith, O. M. (1998). The genetics of cellular senescence. *Am J Hum Genet* *62*, 1015-1019.
- Bjerkvig, R., Tysnes, B. B., Aboody, K. S., Najbauer, J., and Terzis, A. J. (2005). Opinion: the origin of the cancer stem cell: current controversies and new insights. *Nat Rev Cancer* *5*, 899-904.

## References

- Blais, A., and Dynlacht, B. D. (2004). Hitting their targets: an emerging picture of E2F and cell cycle control. *Curr Opin Genet Dev* 14, 527-532.
- Blais, A., and Dynlacht, B. D. (2007). E2F-associated chromatin modifiers and cell cycle control. *Curr Opin Cell Biol* 19, 658-662.
- Blume-Jensen, P., and Hunter, T. (2001). Oncogenic kinase signalling. *Nature* 411, 355-365.
- Blume-Jensen, P., Janknecht, R., and Hunter, T. (1998). The kit receptor promotes cell survival via activation of PI 3-kinase and subsequent Akt-mediated phosphorylation of Bad on Ser136. *Curr Biol* 8, 779-782.
- Bond, J. A., Haughton, M. F., Rowson, J. M., Smith, P. J., Gire, V., Wynford-Thomas, D., and Wyllie, F. S. (1999). Control of replicative life span in human cells: barriers to clonal expansion intermediate between M1 senescence and M2 crisis. *Mol Cell Biol* 19, 3103-3114.
- Bringold, F., and Serrano, M. (2000). Tumor suppressors and oncogenes in cellular senescence. *Exp Gerontol* 35, 317-329.
- Brookes, S., Rowe, J., Ruas, M., Llanos, S., Clark, P. A., Lomax, M., James, M. C., Vatcheva, R., Bates, S., Vousden, K. H., *et al.* (2002). INK4a-deficient human diploid fibroblasts are resistant to RAS-induced senescence. *Embo J* 21, 2936-2945.
- Burgering, B. M., and Coffey, P. J. (1995). Protein kinase B (c-Akt) in phosphatidylinositol-3-OH kinase signal transduction. *Nature* 376, 599-602.
- Burke, D., Wilkes, D., Blundell, T. L., and Malcolm, S. (1998). Fibroblast growth factor receptors: lessons from the genes. *Trends Biochem Sci* 23, 59-62.
- Burkhardt, D. L., and Sage, J. (2008). Cellular mechanisms of tumour suppression by the retinoblastoma gene. *Nat Rev Cancer* 8, 671-682.
- Camarero, N., Mascaró, C., Mayordomo, C., Vilardell, F., Haro, D., and Marrero, P. F. (2006). Ketogenic HMGCS2 is a c-Myc target gene expressed in differentiated cells of human colonic epithelium and down-regulated in colon cancer. *Mol Cancer Res* 4, 645-653.
- Campisi, J. (2005). Senescent cells, tumor suppression, and organismal aging: good citizens, bad neighbors. *Cell* 120, 513-522.
- Campisi, J., and d'Adda di Fagnana, F. (2007). Cellular senescence: when bad things happen to good cells. *Nat Rev Mol Cell Biol* 8, 729-740.
- Cappellen, D., De Oliveira, C., Ricol, D., de Medina, S., Bourdin, J., Sastre-Garau, X., Chopin, D., Thiery, J. P., and Radvanyi, F. (1999). Frequent activating mutations of FGFR3 in human bladder and cervix carcinomas. *Nat Genet* 23, 18-20.
- Carles-Kinch, K., Kilpatrick, K. E., Stewart, J. C., and Kinch, M. S. (2002). Antibody targeting of the EphA2 tyrosine kinase inhibits malignant cell behavior. *Cancer Res* 62, 2840-2847.
- Carpenter, G., and Cohen, S. (1979). Epidermal growth factor. *Annu Rev Biochem* 48, 193-216.
- Carr, A. M. (2000). Cell cycle. Piecing together the p53 puzzle. *Science* 287, 1765-1766.
- Carson, W. E., Haldar, S., Baiocchi, R. A., Croce, C. M., and Caligiuri, M. A. (1994). The c-kit ligand suppresses apoptosis of human natural killer cells through the upregulation of bcl-2. *Proc Natl Acad Sci U S A* 91, 7553-7557.
- Cavenee, W. K., Dryja, T. P., Phillips, R. A., Benedict, W. F., Godbout, R., Gallie, B. L., Murphree, A. L., Strong, L. C., and White, R. L. (1983). Expression of recessive alleles by chromosomal mechanisms in retinoblastoma. *Nature* 305, 779-784.

## References

- Cesare, A. J., and Reddel, R. R. (2008). Telomere uncapping and alternative lengthening of telomeres. *Mech Ageing Dev* 129, 99-108.
- Chen, J., Willingham, T., Margraf, L. R., Schreiber-Agus, N., DePinho, R. A., and Nisen, P. D. (1995). Effects of the MYC oncogene antagonist, MAD, on proliferation, cell cycling and the malignant phenotype of human brain tumour cells. *Nat Med* 1, 638-643.
- Chen, Y. J., Hakin-Smith, V., Teo, M., Xinarianos, G. E., Jellinek, D. A., Carroll, T., McDowell, D., MacFarlane, M. R., Boet, R., Baguley, B. C., *et al.* (2006). Association of mutant TP53 with alternative lengthening of telomeres and favorable prognosis in glioma. *Cancer Res* 66, 6473-6476.
- Cheung, A. L., and Deng, W. (2008). Telomere dysfunction, genome instability and cancer. *Front Biosci* 13, 2075-2090.
- Chiang, J. Y. (2004). Regulation of bile acid synthesis: pathways, nuclear receptors, and mechanisms. *J Hepatol* 40, 539-551.
- Chiarugi, P., and Giannoni, E. (2008). Anoikis: a necessary death program for anchorage-dependent cells. *Biochem Pharmacol* 76, 1352-1364.
- Chin, L., Artandi, S. E., Shen, Q., Tam, A., Lee, S. L., Gottlieb, G. J., Greider, C. W., and DePinho, R. A. (1999). p53 deficiency rescues the adverse effects of telomere loss and cooperates with telomere dysfunction to accelerate carcinogenesis. *Cell* 97, 527-538.
- Chung, C. T., and Miller, R. H. (1988). A rapid and convenient method for the preparation and storage of competent bacterial cells. *Nucleic Acids Res* 16, 3580.
- Classon, M., and Harlow, E. (2002). The retinoblastoma tumour suppressor in development and cancer. *Nat Rev Cancer* 2, 910-917.
- Cobrinik, D. (2005). Pocket proteins and cell cycle control. *Oncogene* 24, 2796-2809.
- Cohen, M. M., Jr., and Krieborg, S. (1995). Cutaneous manifestations of Apert syndrome. *Am J Med Genet* 58, 94-96.
- Collado, M., Blasco, M. A., and Serrano, M. (2007). Cellular senescence in cancer and aging. *Cell* 130, 223-233.
- Conner, D. A. (2001). Mouse embryo fibroblast (MEF) feeder cell preparation. *Curr Protoc Mol Biol Chapter* 23, Unit 23 22.
- Counter, C. M., Avilion, A. A., LeFeuvre, C. E., Stewart, N. G., Greider, C. W., Harley, C. B., and Bacchetti, S. (1992). Telomere shortening associated with chromosome instability is arrested in immortal cells which express telomerase activity. *Embo J* 11, 1921-1929.
- Coussens, L., Yang-Feng, T. L., Liao, Y. C., Chen, E., Gray, A., McGrath, J., Seeburg, P. H., Libermann, T. A., Schlessinger, J., Francke, U., and *et al.* (1985). Tyrosine kinase receptor with extensive homology to EGF receptor shares chromosomal location with neu oncogene. *Science* 230, 1132-1139.
- d'Adda di Fagagna, F., Reaper, P. M., Clay-Farrace, L., Fiegler, H., Carr, P., Von Zglinicki, T., Saretzki, G., Carter, N. P., and Jackson, S. P. (2003). A DNA damage checkpoint response in telomere-initiated senescence. *Nature* 426, 194-198.
- Dannenberg, J. H., and te Riele, H. P. (2006). The retinoblastoma gene family in cell cycle regulation and suppression of tumorigenesis. *Results Probl Cell Differ* 42, 183-225.
- Daub, H., Wallasch, C., Lanke, A., Herrlich, A., and Ullrich, A. (1997). Signal characteristics of G protein-transactivated EGF receptor. *Embo J* 16, 7032-7044.
- Dean, M., Fojo, T., and Bates, S. (2005). Tumour stem cells and drug resistance. *Nat Rev Cancer* 5, 275-284.

## References

- Desnoyers, L. R., Pai, R., Ferrando, R. E., Hotzel, K., Le, T., Ross, J., Carano, R., D'Souza, A., Qing, J., Mohtashemi, I., *et al.* (2008). Targeting FGF19 inhibits tumor growth in colon cancer xenograft and FGF19 transgenic hepatocellular carcinoma models. *Oncogene* *27*, 85-97.
- Dhalluin, C., Yan, K. S., Plotnikova, O., Lee, K. W., Zeng, L., Kuti, M., Mujtaba, S., Goldfarb, M. P., and Zhou, M. M. (2000). Structural basis of SNT PTB domain interactions with distinct neurotrophic receptors. *Mol Cell* *6*, 921-929.
- Di Micco, R., Fumagalli, M., Cicalese, A., Piccinin, S., Gasparini, P., Luise, C., Schurra, C., Garre, M., Nuciforo, P. G., Bensimon, A., *et al.* (2006). Oncogene-induced senescence is a DNA damage response triggered by DNA hyper-replication. *Nature* *444*, 638-642.
- Diehl, J. A. (2002). Cycling to cancer with cyclin D1. *Cancer Biol Ther* *1*, 226-231.
- Dilworth, S. M. (2002). Polyoma virus middle T antigen and its role in identifying cancer-related molecules. *Nat Rev Cancer* *2*, 951-956.
- Dimri, G. P., Lee, X., Basile, G., Acosta, M., Scott, G., Roskelley, C., Medrano, E. E., Linskens, M., Rubelj, I., Pereira-Smith, O., and *et al.* (1995). A biomarker that identifies senescent human cells in culture and in aging skin in vivo. *Proc Natl Acad Sci U S A* *92*, 9363-9367.
- Dulic, V., Beney, G. E., Frebourg, G., Drullinger, L. F., and Stein, G. H. (2000). Uncoupling between phenotypic senescence and cell cycle arrest in aging p21-deficient fibroblasts. *Mol Cell Biol* *20*, 6741-6754.
- Dyson, N., Howley, P. M., Munger, K., and Harlow, E. (1989). The human papilloma virus-16 E7 oncoprotein is able to bind to the retinoblastoma gene product. *Science* *243*, 934-937.
- Edwards, P. A., Kast, H. R., and Anisfeld, A. M. (2002). BAREing it all: the adoption of LXR and FXR and their roles in lipid homeostasis. *J Lipid Res* *43*, 2-12.
- Elenbaas, B., Spirio, L., Koerner, F., Fleming, M. D., Zimonjic, D. B., Donaher, J. L., Popescu, N. C., Hahn, W. C., and Weinberg, R. A. (2001). Human breast cancer cells generated by oncogenic transformation of primary mammary epithelial cells. *Genes Dev* *15*, 50-65.
- Ellsworth, R. E., Seebach, J., Field, L. A., Heckman, C., Kane, J., Hooke, J. A., Love, B., and Shriver, C. D. (2008). A gene expression signature that defines breast cancer metastases. *Clin Exp Metastasis*.
- Engelbraaten, O., Bjerkvig, R., Pedersen, P. H., and Laerum, O. D. (1993). Effects of EGF, bFGF, NGF and PDGF(bb) on cell proliferative, migratory and invasive capacities of human brain-tumour biopsies in vitro. *Int J Cancer* *53*, 209-214.
- Ennis, B. W., Lippman, M. E., and Dickson, R. B. (1991). The EGF receptor system as a target for antitumor therapy. *Cancer Invest* *9*, 553-562.
- Eswarakumar, V. P., Lax, I., and Schlessinger, J. (2005). Cellular signaling by fibroblast growth factor receptors. *Cytokine Growth Factor Rev* *16*, 139-149.
- Ezzat, S., Huang, P., Dackiw, A., and Asa, S. L. (2005). Dual inhibition of RET and FGFR4 restrains medullary thyroid cancer cell growth. *Clin Cancer Res* *11*, 1336-1341.
- Ezzat, S., Zheng, L., Winer, D., and Asa, S. L. (2006). Targeting N-cadherin through fibroblast growth factor receptor-4: distinct pathogenetic and therapeutic implications. *Mol Endocrinol* *20*, 2965-2975.
- Ezzat, S., Zheng, L., Zhu, X. F., Wu, G. E., and Asa, S. L. (2002). Targeted expression of a human pituitary tumor-derived isoform of FGF receptor-4 recapitulates pituitary tumorigenesis. *J Clin Invest* *109*, 69-78.
- Ferby, I., Reschke, M., Kudlacek, O., Knyazev, P., Pante, G., Amann, K., Sommergruber, W., Kraut, N., Ullrich, A., Fassler, R., and Klein, R. (2006). Mig6 is a negative regulator of EGF receptor-mediated skin morphogenesis and tumor formation. *Nat Med* *12*, 568-573.

## References

- Ferdinandusse, S., Kostopoulos, P., Denis, S., Rusch, H., Overmars, H., Dillmann, U., Reith, W., Haas, D., Wanders, R. J., Duran, M., and Marziniak, M. (2006). Mutations in the gene encoding peroxisomal sterol carrier protein X (SCPx) cause leukoencephalopathy with dystonia and motor neuropathy. *Am J Hum Genet* 78, 1046-1052.
- Ferrer-Soler, L., Vazquez-Martin, A., Brunet, J., Menendez, J. A., De Llorens, R., and Colomer, R. (2007). An update of the mechanisms of resistance to EGFR-tyrosine kinase inhibitors in breast cancer: Gefitinib (Iressa) - induced changes in the expression and nucleo-cytoplasmic trafficking of HER-ligands (Review). *Int J Mol Med* 20, 3-10.
- Fillingham, J., Keogh, M. C., and Krogan, N. J. (2006). GammaH2AX and its role in DNA double-strand break repair. *Biochem Cell Biol* 84, 568-577.
- Fioretos, T., Panagopoulos, I., Lassen, C., Swedin, A., Billstrom, R., Isaksson, M., Strombeck, B., Olofsson, T., Mitelman, F., and Johansson, B. (2001). Fusion of the BCR and the fibroblast growth factor receptor-1 (FGFR1) genes as a result of t(8;22)(p11;q11) in a myeloproliferative disorder: the first fusion gene involving BCR but not ABL. *Genes Chromosomes Cancer* 32, 302-310.
- Fischer, O. M., Streit, S., Hart, S., and Ullrich, A. (2003). Beyond Herceptin and Gleevec. *Curr Opin Chem Biol* 7, 490-495.
- Frame, M. C. (2002). Src in cancer: deregulation and consequences for cell behaviour. *Biochim Biophys Acta* 1602, 114-130.
- Franklin, W. A., Veve, R., Hirsch, F. R., Helfrich, B. A., and Bunn, P. A., Jr. (2002). Epidermal growth factor receptor family in lung cancer and premalignancy. *Semin Oncol* 29, 3-14.
- Frese, K. K., and Tuveson, D. A. (2007). Maximizing mouse cancer models. *Nat Rev Cancer* 7, 645-658.
- Friend, S. H., Bernards, R., Rogelji, S., Weinberg, R. A., Rapaport, J. M., Albert, D. M., and Dryja, T. P. (1986). A human DNA segment with properties of the gene that predisposes to retinoblastoma and osteosarcoma. *Nature* 323, 643-646.
- Fuchs, M., Hafer, A., Munch, C., Kannenberg, F., Teichmann, S., Scheibner, J., Stange, E. F., and Seedorf, U. (2001). Disruption of the sterol carrier protein 2 gene in mice impairs biliary lipid and hepatic cholesterol metabolism. *J Biol Chem* 276, 48058-48065.
- Gershoni, J. M., and Palade, G. E. (1982). Electrophoretic transfer of proteins from sodium dodecyl sulfate-polyacrylamide gels to a positively charged membrane filter. *Anal Biochem* 124, 396-405.
- Godar, S., Ince, T. A., Bell, G. W., Feldser, D., Donaher, J. L., Bergh, J., Liu, A., Miu, K., Watnick, R. S., Reinhardt, F., et al. (2008). Growth-inhibitory and tumor-suppressive functions of p53 depend on its repression of CD44 expression. *Cell* 134, 62-73.
- Goldman, C. K., Kim, J., Wong, W. L., King, V., Brock, T., and Gillespie, G. Y. (1993). Epidermal growth factor stimulates vascular endothelial growth factor production by human malignant glioma cells: a model of glioblastoma multiforme pathophysiology. *Mol Biol Cell* 4, 121-133.
- Golub, T. R., Slonim, D. K., Tamayo, P., Huard, C., Gaasenbeek, M., Mesirov, J. P., Coller, H., Loh, M. L., Downing, J. R., Caligiuri, M. A., et al. (1999). Molecular classification of cancer: class discovery and class prediction by gene expression monitoring. *Science* 286, 531-537.
- Gowardhan, B., Douglas, D. A., Mathers, M. E., McKie, A. B., McCracken, S. R., Robson, C. N., and Leung, H. Y. (2005). Evaluation of the fibroblast growth factor system as a potential target for therapy in human prostate cancer. *Br J Cancer* 92, 320-327.
- Gray-Schopfer, V. C., Cheong, S. C., Chong, H., Chow, J., Moss, T., Abdel-Malek, Z. A., Marais, R., Wynford-Thomas, D., and Bennett, D. C. (2006). Cellular senescence in naevi and immortalisation in melanoma: a role for p16? *Br J Cancer* 95, 496-505.

Formatiert: Deutsch (Deutschland)

## References

- Guy, C. T., Cardiff, R. D., and Muller, W. J. (1992). Induction of mammary tumors by expression of polyomavirus middle T oncogene: a transgenic mouse model for metastatic disease. *Mol Cell Biol* 12, 954-961.
- Ha, L., Merlino, G., and Sviderskaya, E. V. (2008). Melanomagenesis: overcoming the barrier of melanocyte senescence. *Cell Cycle* 7, 1944-1948.
- Hackel, P. O., Gishizky, M., and Ullrich, A. (2001). Mig-6 is a negative regulator of the epidermal growth factor receptor signal. *Biol Chem* 382, 1649-1662.
- Hahn, W. C., Counter, C. M., Lundberg, A. S., Beijersbergen, R. L., Brooks, M. W., and Weinberg, R. A. (1999). Creation of human tumour cells with defined genetic elements. *Nature* 400, 464-468.
- Hahn, W. C., Dessain, S. K., Brooks, M. W., King, J. E., Elenbaas, B., Sabatini, D. M., DeCaprio, J. A., and Weinberg, R. A. (2002). Enumeration of the simian virus 40 early region elements necessary for human cell transformation. *Mol Cell Biol* 22, 2111-2123.
- Halicka, H. D., Huang, X., Traganos, F., King, M. A., Dai, W., and Darzynkiewicz, Z. (2005). Histone H2AX phosphorylation after cell irradiation with UV-B: relationship to cell cycle phase and induction of apoptosis. *Cell Cycle* 4, 339-345.
- Hanahan, D., and Weinberg, R. A. (2000). The hallmarks of cancer. *Cell* 100, 57-70.
- Harada, H., Nakagawa, H., Oyama, K., Takaoka, M., Andl, C. D., Jacobmeier, B., von Werder, A., Enders, G. H., Opitz, O. G., and Rustgi, A. K. (2003). Telomerase induces immortalization of human esophageal keratinocytes without p16INK4a inactivation. *Mol Cancer Res* 1, 729-738.
- Hayflick, L. (1965). The Limited In Vitro Lifetime Of Human Diploid Cell Strains. *Exp Cell Res* 37, 614-636.
- Hennighausen, L. (2000). Mouse models for breast cancer. *Breast Cancer Res* 2, 2-7.
- Herbig, U., Jobling, W. A., Chen, B. P., Chen, D. J., and Sedivy, J. M. (2004). Telomere shortening triggers senescence of human cells through a pathway involving ATM, p53, and p21(CIP1), but not p16(INK4a). *Mol Cell* 14, 501-513.
- Herbst, R. S. (2004). Review of epidermal growth factor receptor biology. *Int J Radiat Oncol Biol Phys* 59, 21-26.
- Herbst, R. S., Fukuoka, M., and Baselga, J. (2004). Gefitinib--a novel targeted approach to treating cancer. *Nat Rev Cancer* 4, 956-965.
- Herbst, R. S., and Langer, C. J. (2002). Epidermal growth factor receptors as a target for cancer treatment: the emerging role of IMC-C225 in the treatment of lung and head and neck cancers. *Semin Oncol* 29, 27-36.
- Herrlich, P., Morrison, H., Sleeman, J., Orian-Rousseau, V., Konig, H., Weg-Remers, S., and Ponta, H. (2000). CD44 acts both as a growth- and invasiveness-promoting molecule and as a tumor-suppressing cofactor. *Ann N Y Acad Sci* 910, 106-118; discussion 118-120.
- Hirohashi, S., and Kanai, Y. (2003). Cell adhesion system and human cancer morphogenesis. *Cancer Sci* 94, 575-581.
- Ho, H. K., Pok, S., Streit, S., Ruhe, J. E., Hart, S., Lim, K. S., Loo, H. L., Aung, M. O., Lim, S. G., and Ullrich, A. (2009). Fibroblast growth factor receptor 4 regulates proliferation, anti-apoptosis and alpha-fetoprotein secretion during hepatocellular carcinoma progression and represents a potential target for therapeutic intervention. *J Hepatol* 50, 118-127.
- Ho, M. M., Ng, A. V., Lam, S., and Hung, J. Y. (2007). Side population in human lung cancer cell lines and tumors is enriched with stem-like cancer cells. *Cancer Res* 67, 4827-4833.
- Hollstein, M., Hergenhahn, M., Yang, Q., Bartsch, H., Wang, Z. Q., and Hainaut, P. (1999). New approaches to understanding p53 gene tumor mutation spectra. *Mutat Res* 431, 199-209.

## References

- Holt, J. A., Luo, G., Billin, A. N., Bisi, J., McNeill, Y. Y., Kozarsky, K. F., Donahee, M., Wang, D. Y., Mansfield, T. A., Kliewer, S. A., *et al.* (2003). Definition of a novel growth factor-dependent signal cascade for the suppression of bile acid biosynthesis. *Genes Dev* *17*, 1581-1591.
- Hu, Z., Evarts, R. P., Fujio, K., Marsden, E. R., and Thorgeirsson, S. S. (1995). Expression of fibroblast growth factor receptors flg and bek during hepatic ontogenesis and regeneration in the rat. *Cell Growth Differ* *6*, 1019-1025.
- Huang, P., Wang, C. Y., Gou, S. M., Wu, H. S., Liu, T., and Xiong, J. X. (2008). Isolation and biological analysis of tumor stem cells from pancreatic adenocarcinoma. *World J Gastroenterol* *14*, 3903-3907.
- Huang, X., Yang, C., Jin, C., Luo, Y., Wang, F., and McKeehan, W. L. (2008). Resident hepatocyte fibroblast growth factor receptor 4 limits hepatocarcinogenesis. *Mol Carcinog*.
- Huang, X., Yang, C., Luo, Y., Jin, C., Wang, F., and McKeehan, W. L. (2007). FGFR4 prevents hyperlipidemia and insulin resistance but underlies high-fat diet induced fatty liver. *Diabetes* *56*, 2501-2510.
- Hubbard, S. R., and Till, J. H. (2000). Protein tyrosine kinase structure and function. *Annu Rev Biochem* *69*, 373-398.
- Hunter, T. (2000). Signaling--2000 and beyond. *Cell* *100*, 113-127.
- Hussain, S. P., and Harris, C. C. (1999). p53 mutation spectrum and load: the generation of hypotheses linking the exposure of endogenous or exogenous carcinogens to human cancer. *Mutat Res* *428*, 23-32.
- Inagaki, T., Choi, M., Moschetta, A., Peng, L., Cummins, C. L., McDonald, J. G., Luo, G., Jones, S. A., Goodwin, B., Richardson, J. A., *et al.* (2005). Fibroblast growth factor 15 functions as an enterohepatic signal to regulate bile acid homeostasis. *Cell Metab* *2*, 217-225.
- Irby, R. B., and Yeatman, T. J. (2000). Role of Src expression and activation in human cancer. *Oncogene* *19*, 5636-5642.
- Ishikawa, T., and Fidge, N. (1979). Changes in the concentration of plasma lipoproteins and apoproteins following the administration of Triton WR 1339 to rats. *J Lipid Res* *20*, 254-264.
- Itahana, K., Bhat, K. P., Jin, A., Itahana, Y., Hawke, D., Kobayashi, R., and Zhang, Y. (2003). Tumor suppressor ARF degrades B23, a nucleolar protein involved in ribosome biogenesis and cell proliferation. *Mol Cell* *12*, 1151-1164.
- Jaakkola, S., Salmikangas, P., Nylund, S., Partanen, J., Armstrong, E., Pyrhonen, S., Lehtovirta, P., and Nevanlinna, H. (1993). Amplification of fgfr4 gene in human breast and gynecological cancers. *Int J Cancer* *54*, 378-382.
- Jang, J. H., Shin, K. H., and Park, J. G. (2001). Mutations in fibroblast growth factor receptor 2 and fibroblast growth factor receptor 3 genes associated with human gastric and colorectal cancers. *Cancer Res* *61*, 3541-3543.
- Jeffers, M., LaRochelle, W. J., and Lichtenstein, H. S. (2002). Fibroblast growth factors in cancer: therapeutic possibilities. *Expert Opin Ther Targets* *6*, 469-482.
- Jeggo, P. A. (2005). Genomic instability in cancer development. *Adv Exp Med Biol* *570*, 175-197.
- Jelinek, D. F., Andersson, S., Slaughter, C. A., and Russell, D. W. (1990). Cloning and regulation of cholesterol 7 alpha-hydroxylase, the rate-limiting enzyme in bile acid biosynthesis. *J Biol Chem* *265*, 8190-8197.
- Jezequel, P., Campion, L., Joalland, M. P., Millour, M., Dravet, F., Classe, J. M., Delecroix, V., Deporte, R., Fumoleau, P., and Ricolleau, G. (2004). G388R mutation of the FGFR4 gene is not relevant to breast cancer prognosis. *Br J Cancer* *90*, 189-193.
- Jiang, W. G., Davies, G., Martin, T. A., Parr, C., Watkins, G., Mason, M. D., and Mansel, R. E. (2006). Expression of membrane type-1 matrix metalloproteinase, MT1-MMP in human breast cancer and its impact on invasiveness of breast cancer cells. *Int J Mol Med* *17*, 583-590.

## References

- Kan, M., Wu, X., Wang, F., and McKeehan, W. L. (1999). Specificity for fibroblast growth factors determined by heparan sulfate in a binary complex with the receptor kinase. *J Biol Chem* 274, 15947-15952.
- Kaye, F. J. (2002). RB and cyclin dependent kinase pathways: defining a distinction between RB and p16 loss in lung cancer. *Oncogene* 21, 6908-6914.
- Keen, N., and Taylor, S. (2004). Aurora-kinase inhibitors as anticancer agents. *Nat Rev Cancer* 4, 927-936.
- Kim, N. W., Piatyszek, M. A., Prowse, K. R., Harley, C. B., West, M. D., Ho, P. L., Coviello, G. M., Wright, W. E., Weinrich, S. L., and Shay, J. W. (1994). Specific association of human telomerase activity with immortal cells and cancer. *Science* 266, 2011-2015.
- Knudsen, E. S., and Knudsen, K. E. (2008). Tailoring to RB: tumour suppressor status and therapeutic response. *Nat Rev Cancer*.
- Kok, T., Hulzebos, C. V., Wolters, H., Havinga, R., Agellon, L. B., Stellaard, F., Shan, B., Schwarz, M., and Kuipers, F. (2003). Enterohepatic circulation of bile salts in farnesoid X receptor-deficient mice: efficient intestinal bile salt absorption in the absence of ileal bile acid-binding protein. *J Biol Chem* 278, 41930-41937.
- Kondapaka, S. B., Fridman, R., and Reddy, K. B. (1997). Epidermal growth factor and amphiregulin up-regulate matrix metalloproteinase-9 (MMP-9) in human breast cancer cells. *Int J Cancer* 70, 722-726.
- Kouhara, H., Hadari, Y. R., Spivak-Kroizman, T., Schilling, J., Bar-Sagi, D., Lax, I., and Schlessinger, J. (1997). A lipid-anchored Grb2-binding protein that links FGF-receptor activation to the Ras/MAPK signaling pathway. *Cell* 89, 693-702.
- Koziczak, M., and Hynes, N. E. (2004). Cooperation between fibroblast growth factor receptor-4 and ErbB2 in regulation of cyclin D1 translation. *J Biol Chem* 279, 50004-50011.
- Krepelova, A., Baxova, A., Calda, P., Plavka, R., and Kapras, J. (1998). FGFR2 gene mutation (Tyr375Cys) in a new case of Beare-Stevenson syndrome. *Am J Med Genet* 76, 362-364.
- Kruger, M., Moser, M., Ussar, S., Thievensen, I., Luber, C. A., Forner, F., Schmidt, S., Zanivan, S., Fassler, R., and Mann, M. (2008). SILAC mouse for quantitative proteomics uncovers kindlin-3 as an essential factor for red blood cell function. *Cell* 134, 353-364.
- Kumar, R., Mandal, M., Lipton, A., Harvey, H., and Thompson, C. B. (1996). Overexpression of HER2 modulates bcl-2, bcl-XL, and tamoxifen-induced apoptosis in human MCF-7 breast cancer cells. *Clin Cancer Res* 2, 1215-1219.
- Kurosu, H., and Kuro, O. M. (2009). The Klotho gene family as a regulator of endocrine fibroblast growth factors. *Mol Cell Endocrinol* 299, 72-78.
- Kyo, S., Nakamura, M., Kiyono, T., Maida, Y., Kanaya, T., Tanaka, M., Yatabe, N., and Inoue, M. (2003). Successful immortalization of endometrial glandular cells with normal structural and functional characteristics. *Am J Pathol* 163, 2259-2269.
- Lafleur, M. A., Drew, A. F., de Sousa, E. L., Blick, T., Bills, M., Walker, E. C., Williams, E. D., Waltham, M., and Thompson, E. W. (2005). Upregulation of matrix metalloproteinases (MMPs) in breast cancer xenografts: a major induction of stromal MMP-13. *Int J Cancer* 114, 544-554.
- Land, H., Parada, L. F., and Weinberg, R. A. (1983). Tumorigenic conversion of primary embryo fibroblasts requires at least two cooperating oncogenes. *Nature* 304, 596-602.
- Lapierre, P., Hajoui, O., Homberg, J. C., and Alvarez, F. (1999). Formiminotransferase cyclodeaminase is an organ-specific autoantigen recognized by sera of patients with autoimmune hepatitis. *Gastroenterology* 116, 643-649.
- Lee, Y. T. (1983). Breast carcinoma: pattern of metastasis at autopsy. *J Surg Oncol* 23, 175-180.

## References

- Li, J. J., and Li, S. A. (2006). Mitotic kinases: the key to duplication, segregation, and cytokinesis errors, chromosomal instability, and oncogenesis. *Pharmacol Ther* *111*, 974-984.
- Liang, Y., and Hyder, S. M. (2005). Proliferation of endothelial and tumor epithelial cells by progesterin-induced vascular endothelial growth factor from human breast cancer cells: paracrine and autocrine effects. *Endocrinology* *146*, 3632-3641.
- Lin, A. W., Barradas, M., Stone, J. C., van Aelst, L., Serrano, M., and Lowe, S. W. (1998). Premature senescence involving p53 and p16 is activated in response to constitutive MEK/MAPK mitogenic signaling. *Genes Dev* *12*, 3008-3019.
- Lin, D., Feng, J., and Chen, W. (2008). Bcl-2 and caspase-8 related anoikis resistance in human osteosarcoma MG-63 cells. *Cell Biol Int* *32*, 1199-1206.
- Lingle, W. L., Lukasiewicz, K., and Salisbury, J. L. (2005). Deregulation of the centrosome cycle and the origin of chromosomal instability in cancer. *Adv Exp Med Biol* *570*, 393-421.
- Liu, H., Dibling, B., Spike, B., Dirlam, A., and Macleod, K. (2004). New roles for the RB tumor suppressor protein. *Curr Opin Genet Dev* *14*, 55-64.
- Liu, J., Yang, G., Thompson-Lanza, J. A., Glassman, A., Hayes, K., Patterson, A., Marquez, R. T., Auersperg, N., Yu, Y., Hahn, W. C., *et al.* (2004). A genetically defined model for human ovarian cancer. *Cancer Res* *64*, 1655-1663.
- Liu, W., Li, J., and Roth, R. A. (1999). Heregulin regulation of Akt/protein kinase B in breast cancer cells. *Biochem Biophys Res Commun* *261*, 897-903.
- Llovet, J. M., and Bruix, J. (2008). Molecular targeted therapies in hepatocellular carcinoma. *Hepatology* *48*, 1312-1327.
- Lowe, S. W., and Lin, A. W. (2000). Apoptosis in cancer. *Carcinogenesis* *21*, 485-495.
- Lukas, C., Falck, J., Bartkova, J., Bartek, J., and Lukas, J. (2003). Distinct spatiotemporal dynamics of mammalian checkpoint regulators induced by DNA damage. *Nat Cell Biol* *5*, 255-260.
- Lundberg, A. S., Hahn, W. C., Gupta, P., and Weinberg, R. A. (2000). Genes involved in senescence and immortalization. *Curr Opin Cell Biol* *12*, 705-709.
- Lundberg, A. S., Randell, S. H., Stewart, S. A., Elenbaas, B., Hartwell, K. A., Brooks, M. W., Fleming, M. D., Olsen, J. C., Miller, S. W., Weinberg, R. A., and Hahn, W. C. (2002). Immortalization and transformation of primary human airway epithelial cells by gene transfer. *Oncogene* *21*, 4577-4586.
- Maandag, E. C., van der Valk, M., Vlaar, M., Feltkamp, C., O'Brien, J., van Roon, M., van der Lugt, N., Berns, A., and te Riele, H. (1994). Developmental rescue of an embryonic-lethal mutation in the retinoblastoma gene in chimeric mice. *Embo J* *13*, 4260-4268.
- Macdonald, D., Aguiar, R. C., Mason, P. J., Goldman, J. M., and Cross, N. C. (1995). A new myeloproliferative disorder associated with chromosomal translocations involving 8p11: a review. *Leukemia* *9*, 1628-1630.
- Machide, M., Hashigasako, A., Matsumoto, K., and Nakamura, T. (2006). Contact inhibition of hepatocyte growth regulated by functional association of the c-Met/hepatocyte growth factor receptor and LAR protein-tyrosine phosphatase. *J Biol Chem* *281*, 8765-8772.
- MacKenzie, K. L., Franco, S., Naiyer, A. J., May, C., Sadelain, M., Rafii, S., and Moore, M. A. (2002). Multiple stages of malignant transformation of human endothelial cells modelled by co-expression of telomerase reverse transcriptase, SV40 T antigen and oncogenic N-ras. *Oncogene* *21*, 4200-4211.
- Malumbres, M., and Barbacid, M. (2001). To cycle or not to cycle: a critical decision in cancer. *Nat Rev Cancer* *1*, 222-231.

## References

- Mander, A., Hodgkinson, C. P., and Sale, G. J. (2005). Knock-down of LAR protein tyrosine phosphatase induces insulin resistance. *FEBS Lett* 579, 3024-3028.
- Manes, T., Zheng, D. Q., Tognin, S., Woodard, A. S., Marchisio, P. C., and Languino, L. R. (2003). Alpha(v)beta3 integrin expression up-regulates cdc2, which modulates cell migration. *J Cell Biol* 161, 817-826.
- Maniatis, J. S. E. F. T. (1989). *Molecular cloning: a laboratory manual*, 2nd edn (New York: Cold Spring Harbor: Cold Spring Harbor Laboratory).
- Martin, G. S. (2001). The hunting of the Src. *Nat Rev Mol Cell Biol* 2, 467-475.
- Mason, I. (2007). Initiation to end point: the multiple roles of fibroblast growth factors in neural development. *Nat Rev Neurosci* 8, 583-596.
- Masumoto, N., Nakano, S., Fujishima, H., Kohno, K., and Niho, Y. (1999). v-src induces cisplatin resistance by increasing the repair of cisplatin-DNA interstrand cross-links in human gallbladder adenocarcinoma cells. *Int J Cancer* 80, 731-737.
- Maton, A., Jean Hopkins, Charles William McLaughlin, Susan Johnson, Maryanna Quon Warner, David LaHart, Jill D. Wright (1993). *Human Biology and Health* (Englewood Cliffs, New Jersey, USA: Prentice Hall).
- McArdle, L., Rafferty, M. M., Satyamoorthy, K., Maelandsmo, G. M., Dervan, P. A., Herlyn, M., and Easty, D. J. (2005). Microarray analysis of phosphatase gene expression in human melanoma. *Br J Dermatol* 152, 925-930.
- Meek, D. W. (1999). Mechanisms of switching on p53: a role for covalent modification? *Oncogene* 18, 7666-7675.
- Meijer, D., Sieuwerts, A. M., Look, M. P., van Agthoven, T., Foekens, J. A., and Dorsers, L. C. (2008). Fibroblast growth factor receptor 4 predicts failure on tamoxifen therapy in patients with recurrent breast cancer. *Endocr Relat Cancer* 15, 101-111.
- Meuwissen, R., Linn, S. C., Linnoila, R. I., Zevenhoven, J., Mooi, W. J., and Berns, A. (2003). Induction of small cell lung cancer by somatic inactivation of both Trp53 and Rb1 in a conditional mouse model. *Cancer Cell* 4, 181-189.
- Michaloglou, C., Vredeveld, L. C., Soengas, M. S., Denoyelle, C., Kuilman, T., van der Horst, C. M., Majoor, D. M., Shay, J. W., Mooi, W. J., and Peeper, D. S. (2005). BRAFE600-associated senescence-like cell cycle arrest of human naevi. *Nature* 436, 720-724.
- Mittnacht, S. (1998). Control of pRB phosphorylation. *Curr Opin Genet Dev* 8, 21-27.
- Miyagishi, M., and Taira, K. (2002). U6 promoter-driven siRNAs with four uridine 3' overhangs efficiently suppress targeted gene expression in mammalian cells. *Nat Biotechnol* 20, 497-500.
- Mondello, C., Chiesa, M., Rebuzzini, P., Zongaro, S., Verri, A., Colombo, T., Giulotto, E., D'Incalci, M., Franceschi, C., and Nuzzo, F. (2003). Karyotype instability and anchorage-independent growth in telomerase-immortalized fibroblasts from two centenarian individuals. *Biochem Biophys Res Commun* 308, 914-921.
- Morimoto, Y., Ozaki, T., Ouchida, M., Umehara, N., Ohata, N., Yoshida, A., Shimizu, K., and Inoue, H. (2003). Single nucleotide polymorphism in fibroblast growth factor receptor 4 at codon 388 is associated with prognosis in high-grade soft tissue sarcoma. *Cancer* 98, 2245-2250.
- Morrison, R. S., Yamaguchi, F., Bruner, J. M., Tang, M., McKeehan, W., and Berger, M. S. (1994). Fibroblast growth factor receptor gene expression and immunoreactivity are elevated in human glioblastoma multiforme. *Cancer Res* 54, 2794-2799.
- Munger, K. (2002). The role of human papillomaviruses in human cancers. *Front Biosci* 7, d641-649.
- Munger, K., Basile, J. R., Duensing, S., Eichten, A., Gonzalez, S. L., Grace, M., and Zacny, V. L. (2001). Biological activities and molecular targets of the human papillomavirus E7 oncoprotein. *Oncogene* 20, 7888-7898.

## References

- Muthuswamy, S. K., Gilman, M., and Brugge, J. S. (1999). Controlled dimerization of ErbB receptors provides evidence for differential signaling by homo- and heterodimers. *Mol Cell Biol* *19*, 6845-6857.
- Myлона, E., Giannopoulou, I., Fasomytakos, E., Nomikos, A., Magkou, C., Bakarakos, P., and Nakopoulou, L. (2008). The clinicopathologic and prognostic significance of CD44+/CD24(-/low) and CD44-/CD24+ tumor cells in invasive breast carcinomas. *Hum Pathol* *39*, 1096-1102.
- Nadal, A., Marrero, P. F., and Haro, D. (2002). Down-regulation of the mitochondrial 3-hydroxy-3-methylglutaryl-CoA synthase gene by insulin: the role of the forkhead transcription factor FKHRL1. *Biochem J* *366*, 289-297.
- Nagi, C., Guttman, M., Jaffer, S., Qiao, R., Keren, R., Triana, A., Li, M., Godbold, J., Bleiweiss, I. J., and Hazan, R. B. (2005). N-cadherin expression in breast cancer: correlation with an aggressive histologic variant--invasive micropapillary carcinoma. *Breast Cancer Res Treat* *94*, 225-235.
- Naidu, K. A., Fang, Q., Naidu, K. A., Cheng, J. Q., Nicosia, S. V., and Coppola, D. (2007). P53 enhances ascorbyl stearate-induced G2/M arrest of human ovarian cancer cells. *Anticancer Res* *27*, 3927-3934.
- Natarajan, A., Wagner, B., and Sibilio, M. (2007). The EGF receptor is required for efficient liver regeneration. *Proc Natl Acad Sci U S A* *104*, 17081-17086.
- Neumeister, P., Albanese, C., Balent, B., Grealley, J., and Pestell, R. G. (2002). Senescence and epigenetic dysregulation in cancer. *Int J Biochem Cell Biol* *34*, 1475-1490.
- Nevins, J. R. (2001). The Rb/E2F pathway and cancer. *Hum Mol Genet* *10*, 699-703.
- Nicholes, K., Guillet, S., Tomlinson, E., Hillan, K., Wright, B., Frantz, G. D., Pham, T. A., Dillard-Telm, L., Tsai, S. P., Stephan, J. P., *et al.* (2002). A mouse model of hepatocellular carcinoma: ectopic expression of fibroblast growth factor 19 in skeletal muscle of transgenic mice. *Am J Pathol* *160*, 2295-2307.
- Nicoletti, I., Migliorati, G., Pagliacci, M. C., Grignani, F., and Riccardi, C. (1991). A rapid and simple method for measuring thymocyte apoptosis by propidium iodide staining and flow cytometry. *J Immunol Methods* *139*, 271-279.
- Noblitt, L. W., Bangari, D. S., Shukla, S., Knapp, D. W., Mohammed, S., Kinch, M. S., and Mittal, S. K. (2004). Decreased tumorigenic potential of EphA2-overexpressing breast cancer cells following treatment with adenoviral vectors that express EphrinA1. *Cancer Gene Ther* *11*, 757-766.
- O'Brien, C. A., Pollett, A., Gallinger, S., and Dick, J. E. (2007). A human colon cancer cell capable of initiating tumour growth in immunodeficient mice. *Nature* *445*, 106-110.
- O'Neill, C. F., Urs, S., Cinelli, C., Lincoln, A., Nadeau, R. J., Leon, R., Toher, J., Mouta-Bellum, C., Friesel, R. E., and Liaw, L. (2007). Notch2 signaling induces apoptosis and inhibits human MDA-MB-231 xenograft growth. *Am J Pathol* *171*, 1023-1036.
- Ong, S. E., and Mann, M. (2006). A practical recipe for stable isotope labeling by amino acids in cell culture (SILAC). *Nat Protoc* *1*, 2650-2660.
- Ong, S. H., Guy, G. R., Hadari, Y. R., Laks, S., Gotoh, N., Schlessinger, J., and Lax, I. (2000). FRS2 proteins recruit intracellular signaling pathways by binding to diverse targets on fibroblast growth factor and nerve growth factor receptors. *Mol Cell Biol* *20*, 979-989.
- Opitz, O. G., Suliman, Y., Hahn, W. C., Harada, H., Blum, H. E., and Rustgi, A. K. (2001). Cyclin D1 overexpression and p53 inactivation immortalize primary oral keratinocytes by a telomerase-independent mechanism. *J Clin Invest* *108*, 725-732.
- Paddison, P. J., Silva, J. M., Conklin, D. S., Schlabach, M., Li, M., Aruleba, S., Balija, V., O'Shaughnessy, A., Gnoj, L., Scobie, K., *et al.* (2004). A resource for large-scale RNA-interference-based screens in mammals. *Nature* *428*, 427-431.

## References

- Padilla-Nash, H. M., Wu, K., Just, H., Ried, T., and Thestrup-Pedersen, K. (2007). Spectral karyotyping demonstrates genetically unstable skin-homing T lymphocytes in cutaneous T-cell lymphoma. *Exp Dermatol* *16*, 98-103.
- Pai, R., Dunlap, D., Qing, J., Mohtashemi, I., Hotzel, K., and French, D. M. (2008). Inhibition of fibroblast growth factor 19 reduces tumor growth by modulating beta-catenin signaling. *Cancer Res* *68*, 5086-5095.
- Palmero, I., and Peters, G. (1996). Perturbation of cell cycle regulators in human cancer. *Cancer Surv* *27*, 351-367.
- Partanen, J., Makela, T. P., Eerola, E., Korhonen, J., Hirvonen, H., Claesson-Welsh, L., and Alitalo, K. (1991). FGFR-4, a novel acidic fibroblast growth factor receptor with a distinct expression pattern. *Embo J* *10*, 1347-1354.
- Pear, W. S., Nolan, G. P., Scott, M. L., and Baltimore, D. (1993). Production of high-titer helper-free retroviruses by transient transfection. *Proc Natl Acad Sci U S A* *90*, 8392-8396.
- Penault-Llorca, F., Bertucci, F., Adelaide, J., Parc, P., Coulier, F., Jacquemier, J., Birnbaum, D., and deLapeyriere, O. (1995). Expression of FGF and FGF receptor genes in human breast cancer. *Int J Cancer* *61*, 170-176.
- Perou, C. M., Sorlie, T., Eisen, M. B., van de Rijn, M., Jeffrey, S. S., Rees, C. A., Pollack, J. R., Ross, D. T., Johnsen, H., Akslén, L. A., *et al.* (2000). Molecular portraits of human breast tumours. *Nature* *406*, 747-752.
- Petit, A. M., Rak, J., Hung, M. C., Rockwell, P., Goldstein, N., Fendly, B., and Kerbel, R. S. (1997). Neutralizing antibodies against epidermal growth factor and ErbB-2/neu receptor tyrosine kinases down-regulate vascular endothelial growth factor production by tumor cells in vitro and in vivo: angiogenic implications for signal transduction therapy of solid tumors. *Am J Pathol* *151*, 1523-1530.
- Pietras, R. J., Fendly, B. M., Chazin, V. R., Pegram, M. D., Howell, S. B., and Slamon, D. J. (1994). Antibody to HER-2/neu receptor blocks DNA repair after cisplatin in human breast and ovarian cancer cells. *Oncogene* *9*, 1829-1838.
- Pittius, C. W., Hennighausen, L., Lee, E., Westphal, H., Nicols, E., Vitale, J., and Gordon, K. (1988). A milk protein gene promoter directs the expression of human tissue plasminogen activator cDNA to the mammary gland in transgenic mice. *Proc Natl Acad Sci U S A* *85*, 5874-5878.
- Prieur, A., and Peeper, D. S. (2008). Cellular senescence in vivo: a barrier to tumorigenesis. *Curr Opin Cell Biol* *20*, 150-155.
- Przybyłowska, K., Smolarczyk, K., Blasiak, J., Kulig, A., Romanowicz-Makowska, H., Dziki, A., Ulanska, J., and Pander, B. (2001). A C/T polymorphism in the urokinase-type plasminogen activator gene in colorectal cancer. *J Exp Clin Cancer Res* *20*, 569-572.
- Ramaswami, U., Rumsby, G., Hindmarsh, P. C., and Brook, C. G. (1998). Genotype and phenotype in hypochondroplasia. *J Pediatr* *133*, 99-102.
- Recalcati, S., Tacchini, L., Alberghini, A., Conte, D., and Cairo, G. (2003). Oxidative stress-mediated down-regulation of rat hydroxyacid oxidase 1, a liver-specific peroxisomal enzyme. *Hepatology* *38*, 1159-1166.
- Reddel, R. R. (2000). The role of senescence and immortalization in carcinogenesis. *Carcinogenesis* *21*, 477-484.
- Rich, J. N., Guo, C., McLendon, R. E., Bigner, D. D., Wang, X. F., and Counter, C. M. (2001). A genetically tractable model of human glioma formation. *Cancer Res* *61*, 3556-3560.
- Riley, D. J., Lee, E. Y., and Lee, W. H. (1994). The retinoblastoma protein: more than a tumor suppressor. *Annu Rev Cell Biol* *10*, 1-29.
- Rizki, A., Weaver, V. M., Lee, S. Y., Rozenberg, G. I., Chin, K., Myers, C. A., Bascom, J. L., Mott, J. D., Semeiks, J. R., Grate, L. R., *et al.* (2008). A human breast cell model of preinvasive to invasive transition. *Cancer Res* *68*, 1378-1387.

## References

- Roidl, A., Berger, H. J., Kumar, S., Bange, J., Knyazev, P., and Ullrich, A. (2009). Resistance to chemotherapy is associated with fibroblast growth factor receptor 4 up-regulation. *Clin Cancer Res* 15, 2058-2066.
- Roscioli, T., Flanagan, S., Kumar, P., Masel, J., Gattas, M., Hyland, V. J., and Glass, I. A. (2000). Clinical findings in a patient with FGFR1 P252R mutation and comparison with the literature. *Am J Med Genet* 93, 22-28.
- Ruhe, J. E., Streit, S., Hart, S., and Ullrich, A. (2006). EGFR signaling leads to downregulation of PTP-LAR via TACE-mediated proteolytic processing. *Cell Signal* 18, 1515-1527.
- Ruley, H. E. (1983). Adenovirus early region 1A enables viral and cellular transforming genes to transform primary cells in culture. *Nature* 304, 602-606.
- Ruohola, J. K., Viitanen, T. P., Valve, E. M., Seppanen, J. A., Loponen, N. T., Keskitalo, J. J., Lakkakorpi, P. T., and Harkonen, P. L. (2001). Enhanced invasion and tumor growth of fibroblast growth factor 8b-overexpressing MCF-7 human breast cancer cells. *Cancer Res* 61, 4229-4237.
- Russell, D. W. (2003). The enzymes, regulation, and genetics of bile acid synthesis. *Annu Rev Biochem* 72, 137-174.
- Rutland, P., Pulleyn, L. J., Reardon, W., Baraitser, M., Hayward, R., Jones, B., Malcolm, S., Winter, R. M., Oldridge, M., Slaney, S. F., and et al. (1995). Identical mutations in the FGFR2 gene cause both Pfeiffer and Crouzon syndrome phenotypes. *Nat Genet* 9, 173-176.
- Sakamoto, M., Takamura, M., Ino, Y., Miura, A., Genda, T., and Hirohashi, S. (2001). Involvement of c-Src in carcinoma cell motility and metastasis. *Jpn J Cancer Res* 92, 941-946.
- Salomon, D. S., Brandt, R., Ciardiello, F., and Normanno, N. (1995). Epidermal growth factor-related peptides and their receptors in human malignancies. *Crit Rev Oncol Hematol* 19, 183-232.
- Sandgren, E. P., Schroeder, J. A., Qui, T. H., Palmiter, R. D., Brinster, R. L., and Lee, D. C. (1995). Inhibition of mammary gland involution is associated with transforming growth factor alpha but not c-myc-induced tumorigenesis in transgenic mice. *Cancer Res* 55, 3915-3927.
- Scharenberg, C. W., Harkey, M. A., and Torok-Storb, B. (2002). The ABCG2 transporter is an efficient Hoechst 33342 efflux pump and is preferentially expressed by immature human hematopoietic progenitors. *Blood* 99, 507-512.
- Scheel, C., Schaefer, K. L., Jauch, A., Keller, M., Wai, D., Brinkschmidt, C., van Valen, F., Boecker, W., Dockhorn-Dworniczak, B., and Poremba, C. (2001). Alternative lengthening of telomeres is associated with chromosomal instability in osteosarcomas. *Oncogene* 20, 3835-3844.
- Schlessinger, J. (2000). Cell signaling by receptor tyrosine kinases. *Cell* 103, 211-225.
- Schlessinger, J., Plotnikov, A. N., Ibrahimi, O. A., Eliseenkova, A. V., Yeh, B. K., Yayon, A., Linhardt, R. J., and Mohammadi, M. (2000). Crystal structure of a ternary FGF-FGFR-heparin complex reveals a dual role for heparin in FGFR binding and dimerization. *Mol Cell* 6, 743-750.
- Seger, Y. R., Garcia-Cao, M., Piccinin, S., Cunsolo, C. L., Doglioni, C., Blasco, M. A., Hannon, G. J., and Maestro, R. (2002). Transformation of normal human cells in the absence of telomerase activation. *Cancer Cell* 2, 401-413.
- Selbach, M., and Mann, M. (2006). Protein interaction screening by quantitative immunoprecipitation combined with knockdown (QUICK). *Nat Methods* 3, 981-983.
- Serrano, M., Lin, A. W., McCurrach, M. E., Beach, D., and Lowe, S. W. (1997). Oncogenic ras provokes premature cell senescence associated with accumulation of p53 and p16INK4a. *Cell* 88, 593-602.
- Shah, R. N., Ibbitt, J. C., Alitalo, K., and Hurst, H. C. (2002). FGFR4 overexpression in pancreatic cancer is mediated by an intronic enhancer activated by HNF1alpha. *Oncogene* 21, 8251-8261.

## References

- Shay, J. W., and Bacchetti, S. (1997). A survey of telomerase activity in human cancer. *Eur J Cancer* 33, 787-791.
- Shay, J. W., Pereira-Smith, O. M., and Wright, W. E. (1991). A role for both RB and p53 in the regulation of human cellular senescence. *Exp Cell Res* 196, 33-39.
- Shay, J. W., and Wright, W. E. (2000). Hayflick, his limit, and cellular ageing. *Nat Rev Mol Cell Biol* 1, 72-76.
- Shay, J. W., and Wright, W. E. (2005). Senescence and immortalization: role of telomeres and telomerase. *Carcinogenesis* 26, 867-874.
- Sheridan, C., Kishimoto, H., Fuchs, R. K., Mehrotra, S., Bhat-Nakshatri, P., Turner, C. H., Goulet, R., Jr., Badve, S., and Nakshatri, H. (2006). CD44+/CD24- breast cancer cells exhibit enhanced invasive properties: an early step necessary for metastasis. *Breast Cancer Res* 8, R59.
- Sherr, C. J. (2000). Cell cycle control and cancer. *Harvey Lect* 96, 73-92.
- Sherr, C. J. (2004). Principles of tumor suppression. *Cell* 116, 235-246.
- Sherr, C. J., and McCormick, F. (2002). The RB and p53 pathways in cancer. *Cancer Cell* 2, 103-112.
- Sherr, C. J., and Weber, J. D. (2000). The ARF/p53 pathway. *Curr Opin Genet Dev* 10, 94-99.
- Shevchenko, A., Wilm, M., Vorm, O., and Mann, M. (1996). Mass spectrometric sequencing of proteins silver-stained polyacrylamide gels. *Anal Chem* 68, 850-858.
- Shibata, T., Kawano, T., Nagayasu, H., Okumura, K., Arisue, M., Hamada, J., Takeichi, N., and Hosokawa, M. (1996). Enhancing effects of epidermal growth factor on human squamous cell carcinoma motility and matrix degradation but not growth. *Tumour Biol* 17, 168-175.
- Sibilia, M., and Wagner, E. F. (1995). Strain-dependent epithelial defects in mice lacking the EGF receptor. *Science* 269, 234-238.
- Simpson, C. D., Anyiwe, K., and Schimmer, A. D. (2008). Anoikis resistance and tumor metastasis. *Cancer Lett* 272, 177-185.
- Sinal, C. J., Tohkin, M., Miyata, M., Ward, J. M., Lambert, G., and Gonzalez, F. J. (2000). Targeted disruption of the nuclear receptor FXR/BAR impairs bile acid and lipid homeostasis. *Cell* 102, 731-744.
- Skorski, T. (2002). Oncogenic tyrosine kinases and the DNA-damage response. *Nat Rev Cancer* 2, 351-360.
- Slamon, D. J., Clark, G. M., Wong, S. G., Levin, W. J., Ullrich, A., and McGuire, W. L. (1987). Human breast cancer: correlation of relapse and survival with amplification of the HER-2/neu oncogene. *Science* 235, 177-182.
- Somlo, G., Chu, P., Frankel, P., Ye, W., Groshen, S., Doroshow, J. H., Danenberg, K., and Danenberg, P. (2008). Molecular profiling including epidermal growth factor receptor and p21 expression in high-risk breast cancer patients as indicators of outcome. *Ann Oncol* 19, 1853-1859.
- Southern, E. M. (1974). An improved method for transferring nucleotides from electrophoresis strips to thin layers of ion-exchange cellulose. *Anal Biochem* 62, 317-318.
- Spinola, M., Leoni, V., Pignatiello, C., Conti, B., Ravagnani, F., Pastorino, U., and Dragani, T. A. (2005). Functional FGFR4 Gly388Arg polymorphism predicts prognosis in lung adenocarcinoma patients. *J Clin Oncol* 23, 7307-7311.
- Spinola, M., Leoni, V. P., Tanuma, J., Pettinicchio, A., Frattini, M., Signoroni, S., Agresti, R., Giovanazzi, R., Pilotti, S., Bertario, L., *et al.* (2005). FGFR4 Gly388Arg polymorphism and prognosis of breast and colorectal cancer. *Oncol Rep* 14, 415-419.
- Stadler, C. R., Knyazev, P., Bange, J., and Ullrich, A. (2006). FGFR4 GLY388 isotype suppresses motility of MDA-MB-231 breast cancer cells by EDG-2 gene repression. *Cell Signal* 18, 783-794.

## References

- Stahtea, X. N., Kousidou, O., Roussidis, A. E., Tzanakakis, G. N., and Karamanos, N. K. (2008). Small tyrosine kinase inhibitors as key molecules in the expression of metalloproteinases by solid tumors. *Connect Tissue Res* *49*, 211-214.
- Stark, K. L., McMahon, J. A., and McMahon, A. P. (1991). FGFR-4, a new member of the fibroblast growth factor receptor family, expressed in the definitive endoderm and skeletal muscle lineages of the mouse. *Development* *113*, 641-651.
- Streit, S., Bange, J., Fichtner, A., Ihrler, S., Issing, W., and Ullrich, A. (2004). Involvement of the FGFR4 Arg388 allele in head and neck squamous cell carcinoma. *Int J Cancer* *111*, 213-217.
- Streit, S., Mestel, D. S., Schmidt, M., Ullrich, A., and Berking, C. (2006). FGFR4 Arg388 allele correlates with tumour thickness and FGFR4 protein expression with survival of melanoma patients. *Br J Cancer* *94*, 1879-1886.
- Su, G., Blaine, S. A., Qiao, D., and Friedl, A. (2008). Membrane type 1 matrix metalloproteinase-mediated stromal syndecan-1 shedding stimulates breast carcinoma cell proliferation. *Cancer Res* *68*, 9558-9565.
- Sung, J. M., Cho, H. J., Yi, H., Lee, C. H., Kim, H. S., Kim, D. K., Abd El-Aty, A. M., Kim, J. S., Landowski, C. P., Hediger, M. A., and Shin, H. C. (2008). Characterization of a stem cell population in lung cancer A549 cells. *Biochem Biophys Res Commun* *371*, 163-167.
- Suzuki, T., Minagawa, S., Michishita, E., Ogino, H., Fujii, M., Mitsui, Y., and Ayusawa, D. (2001). Induction of senescence-associated genes by 5-bromodeoxyuridine in HeLa cells. *Exp Gerontol* *36*, 465-474.
- Tanaka, T., Kurose, A., Huang, X., Dai, W., and Darzynkiewicz, Z. (2006). ATM activation and histone H2AX phosphorylation as indicators of DNA damage by DNA topoisomerase I inhibitor topotecan and during apoptosis. *Cell Prolif* *39*, 49-60.
- Thussbas, C., Nahrig, J., Streit, S., Bange, J., Kriner, M., Kates, R., Ulm, K., Kiechle, M., Hoefler, H., Ullrich, A., and Harbeck, N. (2006). FGFR4 Arg388 allele is associated with resistance to adjuvant therapy in primary breast cancer. *J Clin Oncol* *24*, 3747-3755.
- Todaro, G. J., and Green, H. (1963). Quantitative studies of the growth of mouse embryo cells in culture and their development into established lines. *J Cell Biol* *17*, 299-313.
- Ullrich, A., Coussens, L., Hayflick, J. S., Dull, T. J., Gray, A., Tam, A. W., Lee, J., Yarden, Y., Libermann, T. A., Schlessinger, J., and et al. (1984). Human epidermal growth factor receptor cDNA sequence and aberrant expression of the amplified gene in A431 epidermoid carcinoma cells. *Nature* *309*, 418-425.
- Ullrich, A., and Schlessinger, J. (1990). Signal transduction by receptors with tyrosine kinase activity. *Cell* *61*, 203-212.
- van Staveren, W. C., Solis, D. Y., Hebrant, A., Detours, V., Dumont, J. E., and Maenhaut, C. (2009). Human cancer cell lines: Experimental models for cancer cells in situ? For cancer stem cells? *Biochim Biophys Acta* *1795*, 92-103.
- Vastrik, I., Kaipainen, A., Penttila, T. L., Lymboussakis, A., Alitalo, R., Parvinen, M., and Alitalo, K. (1995). Expression of the mad gene during cell differentiation in vivo and its inhibition of cell growth in vitro. *J Cell Biol* *128*, 1197-1208.
- Vietri, M., Bianchi, M., Ludlow, J. W., Mittnacht, S., and Villa-Moruzzi, E. (2006). Direct interaction between the catalytic subunit of Protein Phosphatase 1 and pRb. *Cancer Cell Int* *6*, 3.
- Vogelstein, B., Lane, D., and Levine, A. J. (2000). Surfing the p53 network. *Nature* *408*, 307-310.
- Wang, J., Cai, Y., Penland, R., Chauhan, S., Miesfeld, R. L., and Ittmann, M. (2006). Increased expression of the metastasis-associated gene Ehm2 in prostate cancer. *Prostate* *66*, 1641-1652.
- Wang, J., Stockton, D. W., and Ittmann, M. (2004). The fibroblast growth factor receptor-4 Arg388 allele is associated with prostate cancer initiation and progression. *Clin Cancer Res* *10*, 6169-6178.

## References

- Wang, J., Yu, W., Cai, Y., Ren, C., and Ittmann, M. M. (2008). Altered fibroblast growth factor receptor 4 stability promotes prostate cancer progression. *Neoplasia* 10, 847-856.
- Wang, J. Y., Knudsen, E. S., and Welch, P. J. (1994). The retinoblastoma tumor suppressor protein. *Adv Cancer Res* 64, 25-85.
- Wang, K., Wang, K., Li, W., Huang, T., Li, R., Wang, D., Shen, B., and Chen, X. (2009). Characterizing Breast Cancer Xenograft Epidermal Growth Factor Receptor Expression by Using Near-Infrared Optical Imaging. *Acta Radiol*, 1-9.
- Wang, S. E., Xiang, B., Guix, M., Olivares, M. G., Parker, J., Chung, C. H., Pandiella, A., and Arteaga, C. L. (2008). Transforming growth factor beta engages TACE and ErbB3 to activate phosphatidylinositol-3 kinase/Akt in ErbB2-overexpressing breast cancer and desensitizes cells to trastuzumab. *Mol Cell Biol* 28, 5605-5620.
- Wang, X., Weng, L. P., and Yu, Q. (2000). Specific inhibition of FGF-induced MAPK activation by the receptor-like protein tyrosine phosphatase LAR. *Oncogene* 19, 2346-2353.
- Wang, Z. H., Ding, M. X., Yuan, J. P., Jin, M. L., Hao, C. F., Chew-Cheng, S. B., Ng, H. K., and Chew, E. C. (1999). Expression of bcl-2 and Bax in EGFR-antisense transfected and untransfected glioblastoma cells. *Anticancer Res* 19, 4167-4170.
- Warmuth, M., Damoiseaux, R., Liu, Y., Fabbro, D., and Gray, N. (2003). SRC family kinases: potential targets for the treatment of human cancer and leukemia. *Curr Pharm Des* 9, 2043-2059.
- Wasco, M. J., Pu, R. T., Yu, L., Su, L., and Ma, L. (2008). Expression of gamma-H2AX in melanocytic lesions. *Hum Pathol*.
- Weinberg, R. A. (1995). The retinoblastoma protein and cell cycle control. *Cell* 81, 323-330.
- Weng, L. P., Yuan, J., and Yu, Q. (1998). Overexpression of the transmembrane tyrosine phosphatase LAR activates the caspase pathway and induces apoptosis. *Curr Biol* 8, 247-256.
- White, K. E., Cabral, J. M., Davis, S. I., Fishburn, T., Evans, W. E., Ichikawa, S., Fields, J., Yu, X., Shaw, N. J., McLellan, N. J., *et al.* (2005). Mutations that cause osteoglophonic dysplasia define novel roles for FGFR1 in bone elongation. *Am J Hum Genet* 76, 361-367.
- Wilkie, A. O., Patey, S. J., Kan, S. H., van den Ouweland, A. M., and Hamel, B. C. (2002). FGFs, their receptors, and human limb malformations: clinical and molecular correlations. *Am J Med Genet* 112, 266-278.
- Woo, K. J., Yoo, Y. H., Park, J. W., and Kwon, T. K. (2005). Bcl-2 attenuates anticancer agents-induced apoptosis by sustained activation of Akt/protein kinase B in U937 cells. *Apoptosis* 10, 1333-1343.
- Wright, W. E., and Shay, J. W. (2001). Cellular senescence as a tumor-protection mechanism: the essential role of counting. *Curr Opin Genet Dev* 11, 98-103.
- Wu, X., Ge, H., Gupte, J., Weizmann, J., Shimamoto, G., Stevens, J., Hawkins, N., Lemon, B., Shen, W., Xu, J., *et al.* (2007). Co-receptor requirements for fibroblast growth factor-19 signaling. *J Biol Chem* 282, 29069-29072.
- Xie, M. H., Holcomb, I., Deuel, B., Dowd, P., Huang, A., Vagts, A., Foster, J., Liang, J., Brush, J., Gu, Q., *et al.* (1999). FGF-19, a novel fibroblast growth factor with unique specificity for FGFR4. *Cytokine* 11, 729-735.
- Xue, W., Zender, L., Miething, C., Dickins, R. A., Hernando, E., Krizhanovsky, V., Cordon-Cardo, C., and Lowe, S. W. (2007). Senescence and tumour clearance is triggered by p53 restoration in murine liver carcinomas. *Nature* 445, 656-660.
- Yoshida, B. A., Sokoloff, M. M., Welch, D. R., and Rinker-Schaeffer, C. W. (2000). Metastasis-suppressor genes: a review and perspective on an emerging field. *J Natl Cancer Inst* 92, 1717-1730.
- Yu, C., Wang, F., Jin, C., Huang, X., and McKeehan, W. L. (2005). Independent repression of bile acid synthesis and activation of c-Jun N-terminal kinase (JNK) by activated hepatocyte fibroblast growth factor receptor 4 (FGFR4) and bile acids. *J Biol Chem* 280, 17707-17714.

## References

- Yu, C., Wang, F., Jin, C., Wu, X., Chan, W. K., and McKeehan, W. L. (2002). Increased carbon tetrachloride-induced liver injury and fibrosis in FGFR4-deficient mice. *Am J Pathol* *161*, 2003-2010.
- Yu, C., Wang, F., Kan, M., Jin, C., Jones, R. B., Weinstein, M., Deng, C. X., and McKeehan, W. L. (2000). Elevated cholesterol metabolism and bile acid synthesis in mice lacking membrane tyrosine kinase receptor FGFR4. *J Biol Chem* *275*, 15482-15489.
- Yu, J., Boyapati, A., and Rundell, K. (2001). Critical role for SV40 small-t antigen in human cell transformation. *Virology* *290*, 192-198.
- Zheng, L., and Lee, W. H. (2001). The retinoblastoma gene: a prototypic and multifunctional tumor suppressor. *Exp Cell Res* *264*, 2-18.
- Zheng, X., Jiang, F., Katakowski, M., Zhang, Z. G., Lu, Q. E., and Chopp, M. (2009). ADAM17 promotes breast cancer cell malignant phenotype through EGFR-PI3K-AKT activation. *Cancer Biol Ther* *8*.
- Zhu, J., Woods, D., McMahon, M., and Bishop, J. M. (1998). Senescence of human fibroblasts induced by oncogenic Raf. *Genes Dev* *12*, 2997-3007.
- Zongaro, S., de Stanchina, E., Colombo, T., D'Incalci, M., Giulotto, E., and Mondello, C. (2005). Stepwise neoplastic transformation of a telomerase immortalized fibroblast cell line. *Cancer Res* *65*, 11411-11418.
- Zou, L., Zhang, P., Luo, C., and Tu, Z. (2006). Mad1 suppresses bladder cancer cell proliferation by inhibiting human telomerase reverse transcriptase transcription and telomerase activity. *Urology* *67*, 1335-1340.

# Curriculum Vitae

## PERSÖNLICHE DATEN

**Name:** Nina Seitzer  
**Geburtsdatum:** 01. Oktober 1980 in Eggenfelden/Rottal Inn  
**Anschrift:** Planegger Str. 79, 81241 München  
**Nationalität:** deutsch  
**Familienstand:** verheiratet

## AUSBILDUNG

### **Seit August 2005:**

Max-Planck Institut für Biochemie: Abteilung für Molekulare Biologie  
Doktorarbeit: *Investigation of the Impact of Tumor Suppressors and Promoters on Oncogenesis*

### **Mai 2005:**

Universität Regensburg: **Diplom in Biologie** an der Fakultät III für vorklinische Medizin und Biologie

### **August 2004-April 2005:**

Universitätsklinikum Regensburg: Abteilung für Labormedizin und klinische Chemie  
Diplomarbeit: *Untersuchungen zur RNAi und Überexpression von ABC-Transportern*

### **September 2000 – Juni 2004:**

Universität Regensburg: Studium der Biologie an der Fakultät III für vorklinische Medizin und Biologie

## SCHULBILDUNG

**Juni 2000:** Allgemeine Hochschulreife, Note 1,7  
**August 1991 – Juli 2000:** König Karlmann Gymnasium Altötting  
**August 1987 – Juli 1991:** Volksschule Neuötting

## WEITERE WISSENSCHAFTLICHE KENNTNISSE

### **Februar 2007:**

Ludwig-Maximilians-Universität München: Lehrstuhl für Chemie/Pharmazie, Praktikumsbetreuung

### **Februar 2006:**

Ludwig-Maximilians-Universität München: Lehrstuhl für Chemie/Pharmazie, Praktikumsbetreuung

### **November 2005:**

Max-Planck-Institut für Biochemie: Fortbildung zur Vermittlung der Sachkunde für Projektleiter und Beauftragte für biologische Sicherheit nach dem Gentechnikgesetz

### **January 2003 – September 2003:**

BioGents, Regensburg: Studentische Hilfskraft

## MEETINGS UND KONFERENZEN

International Congress/Munich 2008: Integrative Cancer Genomics 2008  
Spetses International Summer School 2007: Regeneration, Stem Cells and Cancer

## **AUSLANDSAUFENTHALTE**

### **November 2003:**

Departamento Microbiología del Suelo y Sistemas Simbióticos, Granada, Spanien  
Praktikum im Zuge einer Kooperation mit der Universität Regensburg, Lehrstuhl Genetik

### **March 2003:**

Tenerife, Spanien  
Praktikum der Universität Regensburg, Lehrstuhl Botanik

## **PUBLIKATIONEN UND PATENTE**

**Nina Seitzer**, Thomas Mayr, Sylvia Streit and Axel Ullrich  
*A Single Nucleotide Difference in the Mouse Genome Accelerates Breast Cancer Progression*  
Cancer Res. 2010 Jan 15;70(2):802-12. Epub 2010 Jan 12.

Markus Reschke, Ingvar Ferby, Ewa Stepniak, **Nina Seitzer**, David Horst, Erwin F. Wagner and Axel Ullrich

*Mig-6 is a Negative Regulator of EGFR Signalling in Hepatocytes and Human Hepatocellular Carcinoma*  
Hepatology. 2009 Nov 13. [Epub ahead of print]

**Nina Seitzer** and Axel Ullrich  
*The knockdown of p53 and Rb partially displays an inartificial in vitro model of oncogenesis*  
Manuscript in Preparation

**Nina Seitzer**, Philipp Mertins,..., Axel Ullrich  
*A SILAC-based screen of the FGFR4 interactome in vivo and in vitro*  
Manuscript in Preparation

43589P EP: Axel Ullrich, Thomas Mayr, **Nina Seitzer**, Sylvia Streit  
*FGFR4 Arg388 Cancer Model*  
Patent in Revision

0204-3956 ZMSG: Axel Ullrich, **Nina Seitzer**  
*Human Cancer Model*  
Pending Patent